THE EFFECTS OF PARTICLE PRECIPITATION ON THE IONOSPHERE IN THE SOUTH ATLANTIC ANOMALY REGION

THESIS
Submitted in fulfilment of the
requirements for the Degree of
DOCTOR OF PHILOSOPHY
of Rhodes University

by

RAYMOND HAGGARD

December 1994

Contents

Abstract

The first ground based observations of aeronomic phenomena in the South Atlantic Anomaly Region are presented. These data show that enhancements in foF2 and foE can be directly attributed to precipitated electron energy fluxes in the Anomaly Region. The regular occurrence of particle induced sporadic-E ionization is also presented together with the first measurable 391.4 nm airglow radiation of about 16 R.

The first comprehensive survey of energy fluxes carried by energetic particles using satellites is also presented for both daytime and nighttime as well as the seasonal fluctuations. We found that the nocturnally precipitated electron energy fluxes varied between 1×10^{-4} and 38×10^{-4} erg $cm^{-2}s^{-1}$, depending upon magnetic activity and season, whereas the daytime precipitated electron energy fluxes tended to vary between 1×10^{-3} and 8×10^{-3} erg $cm^{-2}s^{-1}$, with a tendency to decrease during magnetically active periods.

Electron density and temperature contours as well as NO^+ and O^+ ions contours for nighttime are also presented.

The main conclusion of the study is that precipitating electrons provide a significant and sometimes dominant source of ionization in the ionosphere over the South Atlantic Anomaly Region.

Acknowledgements

This type of project depends on the co-operation and assistance of a number of people.

Firstly, Jörg Lichtenberg, who assisted with the design and building of the portable ionosonde used in the initial stages of the project. The South African Airforce and the erstwhile Antarctic Section of the Department of Transport for the use of their vessels and the co-operation of the late Captain Funk. The Atmosphere Explorer-C Team for the data tapes and Messrs Anthony Kesterton and John Goetsch for their assistance in reading and deciphering the satellite data tapes.

My grateful thanks to Barbara Jordan for word processing assistance, ably assisted by Paul Nathanson, whose expert knowledge of Latex saved many hours of frustration.

To Allon Poole, my surrogate supervisor, a big thank you for your invaluable comments on the draft copy of the thesis.

To my original supervisor, who influenced me most, a big thank you. The late Jack Gledhill encouraged, cajoled, shaped my thinking, but above all provided the resources and somehow managed to always obtain the elusive data needed to complete the project.

Finally, my sincere thanks to my late parents for their initial assistance and to my wife and daughter for their patience, understanding and much more.

Preface

Declaration of originality

Chapter 1 is a brief resumé of the work done in the field of charged particle-precipitation up to 1976.

Chapter 2 deals with the aircraft flights and cruises of the supply vessel R.S.A. in the region of interest during the periods 1974 to 1977.

The author designed and built the transmitter and the stable variable frequency oscillator used in the ionosonde to collect the data. The antennae used on the Hercules C130 aircraft as well as those on board the research ship were designed, constructed and installed by the author. The planning of the research trips and the routes taken were decided by the author in conjunction with the Captains of the research vessels.

All the data used in this chapter was personally collected by the author who also reduced and interpreted all the ionogrammes. The data analysis was also carried out by the author.

Chapters 3 and 4 deal with the Atmosphere Explorer-C. Data as supplied by NASA. The manipulation and analysis of the data was conducted by the author. Jack Gledhill assisted with the mathematics involvement in mapping the data point to a constant 300 km height and an 1SML data package - graph plotting facilities on the 1901T - were used to reproduce the contour maps.

Chapter 5 covers the ISAAC campaign which was planned in conjunction with Prof Gledhill bearing in mind the results of my research and that of other workers in the field. Unfortunately I could not accompany the ship during the ISAAC cruise period but did design, build and install the antennae systems on board the SA Agulhas used by the Barry Research Chirpsounder, which was modified by Mr Geoff Evans who also ran the equipment and collected the data during the ISAAC cruise. The reduction interpretation and analysis of all the data used was the sole work of the author, only the electron energy spectra deduced from the electron density profiles were calculated using Prof. Gledhill's programme.

Chapter 6 is a brief resumé of the major findings achieved by the author as a result of research reported in this dissertation.

List of figures

List of tables

Chapter 1

Introduction

1.1 Trapping of Charged Particles in the Geomagnetic Field

Birkeland (1908) first showed experimentally that electrons could be trapped in a dipolar magnetic field and Störmer (1955) confirmed this theoretically. Since then the phenomenal development of plasma physics has made clear the conditions of such trapping and the details of particle motion in the magnetic field (Northrop, 1963). Briefly, the component of velocity perpendicular to the field lines causes the electron, or other charged particle, to travel in a circle round a line, revolving at an angular frequency depending on the magnetic field strength and the charge/mass ratio of the particle. The component of velocity along the line of force is responsible for motion in that direction.

The magnetic field of the earth may be reasonably well represented by that of a dipole, for distances closer to the earth than about 6 earth radii. It is customary to refer to individual lines of force by the distance, in earth radii, at which they cross the magnetic equatorial plane. This is illustrated in Fig. 1.1 in the case of the line labelled L = 4. Mc Ilwain (1961) has extended the meaning of this parameter so that it can be applied to distorted fields, as in the case of the actual geomagnetic field. Fig. 1.2 from Hess (1968), shows the path of a trapped particle. The motion consists of rotation round a line of force and longitudinal motion along it. Since the magnetic field is stronger nearer to the earth, the radius of the circle decreases and the pitch angle (the angle between the velocity of the particle and the field line) increases, until it reaches 90° at a point known as the "mirror point", at which the direction of motion along

the line reverses; this happens again at the other end of the trajectory, so that the particle may be thought of as "bouncing" between the two mirror points. These occur at the same total intensity of the magnetic field.

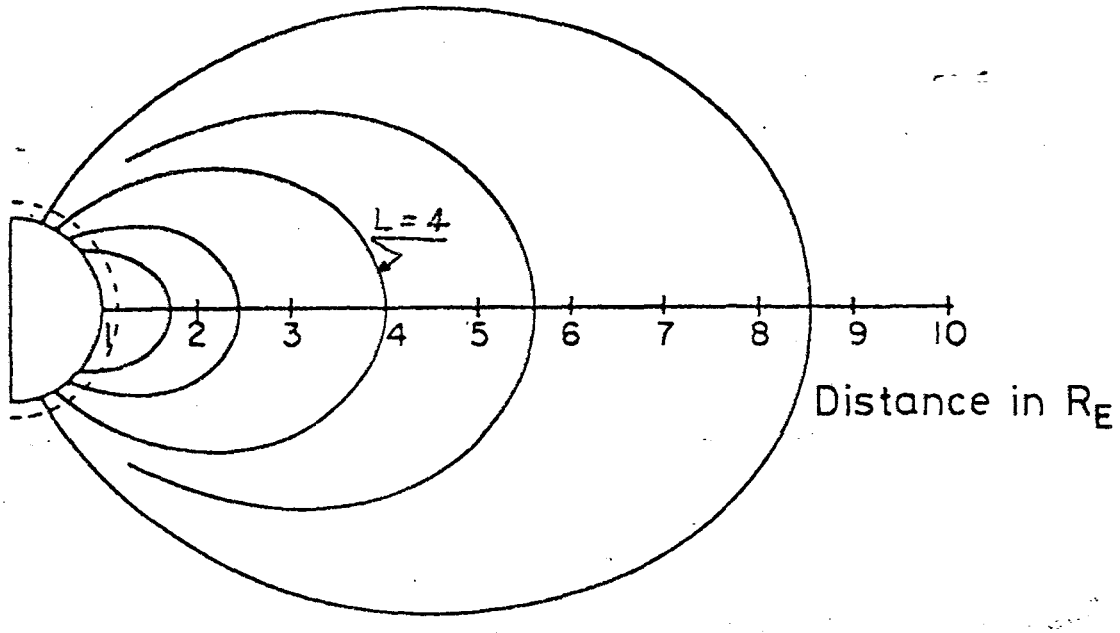

Figure 1.1: Magnetic field lines of a dipole, also illustrating the McIlwain parameter L for labelling field lines.

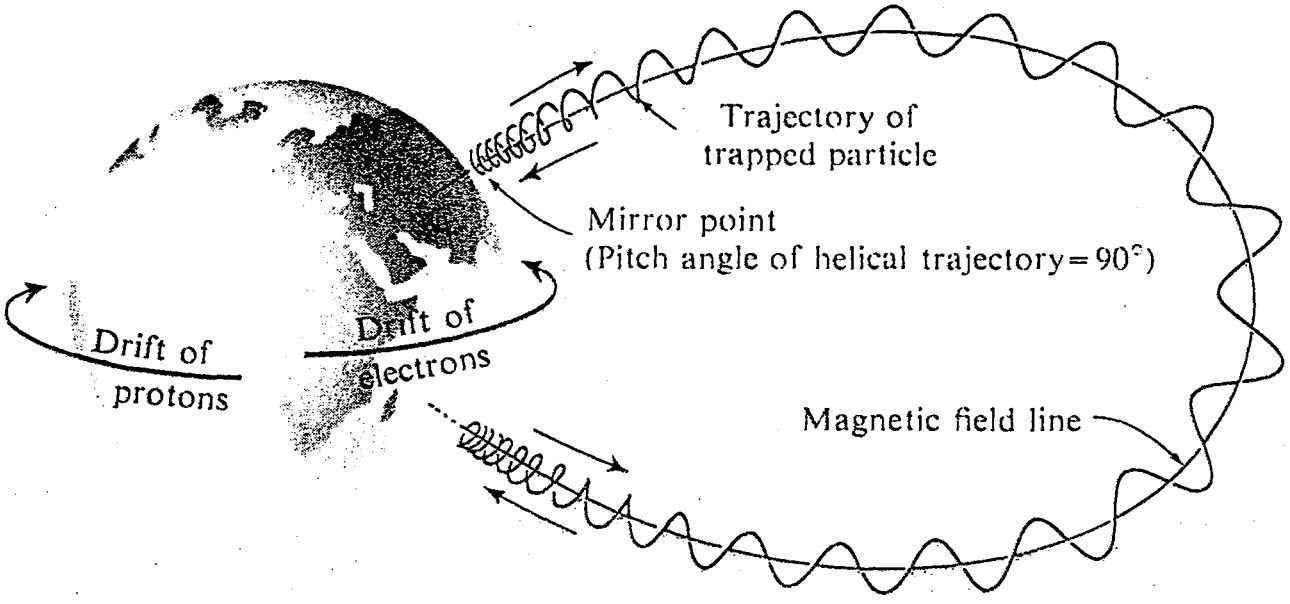

Figure 1.2: Motion of charged particles in a dipole field (From Hess, 1968).

There is a third component of the motion of trapped particles. This is due to a combination of the effects of the variation of the magnetic field strength between the inner and outer points on the orbit round the field lines, curvature of the lines of force and the gravitational force acting on the particle. These result in a "drift" of the particles, electrons going eastward and positively charged particles westward, as shown in Fig. 1.2. The times taken to complete the different cycles are in general energy-dependent, but typically the gyration round the lines of force takes a time of the order of microseconds, the north-south bouncing motion requires a few seconds and the drift motion needs times of the order of several minutes to an hour or so to complete a circuit of the earth.

1.2 The South Atlantic Anomaly

It has been known for a long time that the geomagnetic field magnitude, at constant height, shows its minimum value at a point near the coast of Brazil. Fig. 1.3 from Chapman and Bartels (1940) shows a map of the total field intensity for the epoch 1922. The contours shown in Fig. 1.3 are in decimal fractions of a gauss, where 1 gauss equals 10^{-4}T. Although the details have changed, the general configuration is much the same today. The point at about 20°S; 40°W is the spot where the total field has its minimum value anywhere on the surface of the earth. The region round it, especially that within the 0.3 gauss (0.3×10^{-4}T) contour, is referred to as the South Atlantic Geomagnetic Anomaly.

At the antipodes, 20°N; 140°E, the field strength is seen to be about 0.38 gauss, much larger than the 0.25 gauss at the Brazilian end. Thus, although it is possible to represent the geomagnetic field to a first approximation by a dipole, it is necessary to shift the dipole away from the centre of the earth in the direction of south-east Asia in order to give the minimum near Brazil. It is the requirement that the mirror points occur at the same total intensity that produces the phenomenon. The minimum in the intensity in the South Atlantic Geomagnetic Anomaly results in charged particles trapped in the field descending into the upper atmosphere there to reach their mirror points, if their pitch angles at the equator are small enough. In fact, the critical pitch angle can easily be calculated below which particles *must* descend into the dense atmosphere in the Brazilian sector. Particles with pitch angles less than this critical value are said to be in the "loss cone," since collisions with molecules in the atmosphere knock them off their trajectories and they are then lost to the trapped population.

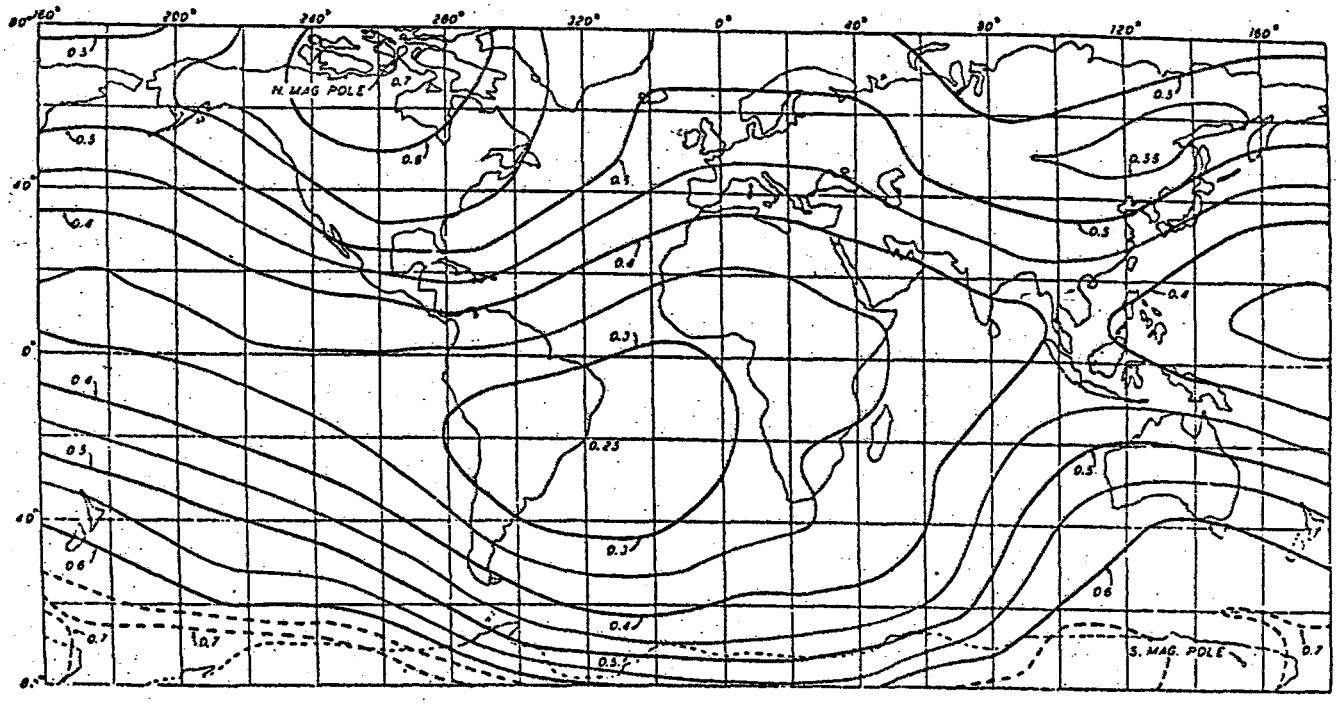

Figure 1.3: The South Atlantic Geomagnetic Anomaly shown on a map of total field intensity for 1922. (From Chapman and Bartels, 1940)

It is usual nowadays to refer to the region where the motion of charged particles is determined by the geomagnetic field as the "magnetosphere". The high-energy part of the trapped particle population is referred to as the "radiation belts", having first been discovered by J A van Allen in 1958 (van Allen 1959).

The first experimental demonstration that radiation belt particles actually do penetrate to heights of 300 km and less was due to Ginzburg *et al.* (1962). They had a geiger counter telescope on the "second Soviet space ship" in 1959. Fig. 1.4 shows the counting rates of this telescope, from their paper cited above. The most obvious feature is the region of high counting rate lying roughly between 15° and 45°S and 0° and 60°W, close to, but not exactly coinciding with, the geomagnetic anomaly in Fig. 1.3. There is also a second region to the south-east of this one. The height of the satellite was about 320 km and a later one, the "third cosmic space ship", passed through at about 200 km. It also detected high energy particles over the South Atlantic, though in a different pattern from that shown in Fig. 1.4. Nowhere else were such high counting rates encountered, as Fig. 1.4 shows, though the orbits of these early satellites did not take them into the auroral zones, where high counting rates are also recorded at low altitudes.

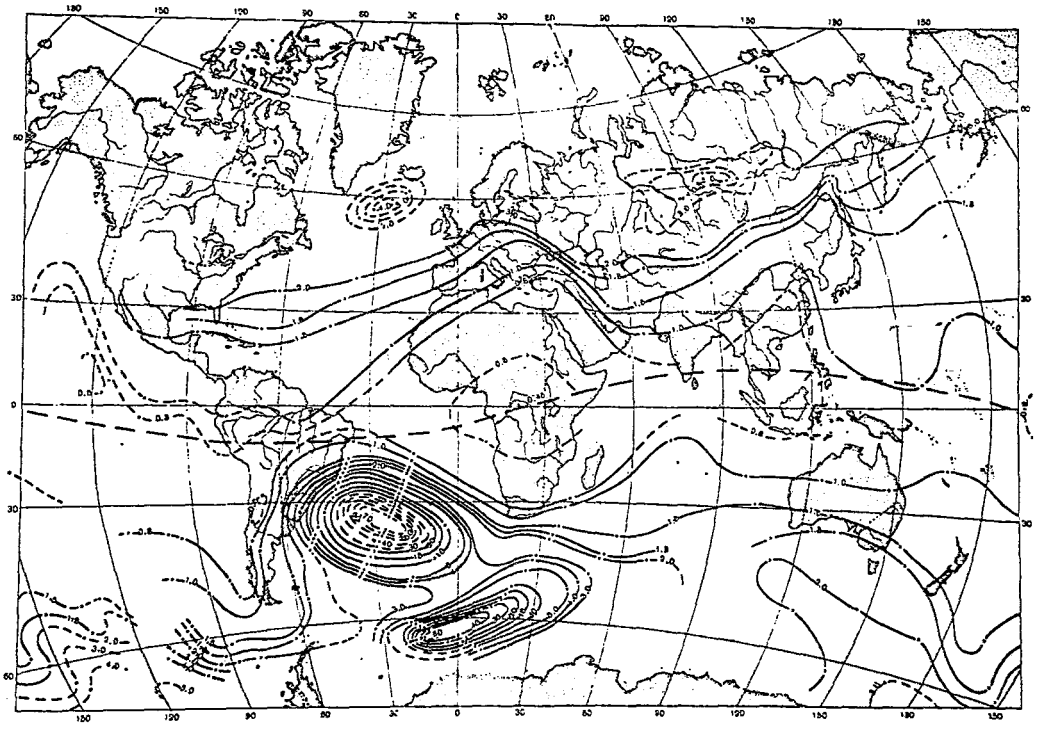

Figure 1.4: Regions of high particle counting rate observed by the Geiger counter telescope on the second Soviet space ship (From Ginzburg *et al.*, 1962)

These early experiments were followed by others, by both Russian and American groups, that demonstrated the reality and relative constancy in position of the region of particle penetration off the Brazilian coast, though the more southernly one was not usually found. The former region became known as the "South Atlantic Radiation Anomaly", and later as simply the "South Atlantic Anomaly".

1.3 The Ionosphere

Fluxes of energetic particles at heights of the order of 300 km and less would be expected to ionize molecules in the atmosphere and so produce perturbations in the ionosphere there.

Solar ultraviolet radiation impinging on the upper atmosphere ionizes some of the neutral molecules and atoms there to produce free electrons. These are removed again by recombination and diffusion, the principal loss processes. The number of free electrons per unit volume at any given height and time is the result of the competition of these production and loss processes. It is usually referred to as the "electron density". As the sun sets the production rate decreases, and so the electron density falls also. During the night there is no solar radiation and recombination

and diffusion continue to decrease the electron density. This would go on throughout the night were it not for perturbations, due for example, to winds, that may even cause temporary increases. At sunrise the solar photoionization rate increases rapidly and so does the electron density.

The ability of the ionosphere to reflect radio waves back to earth, and so make possible its use in international HF radio communication, depends on the electron density. There is a maximum frequency that can be reflected, which depends on the electron density and the angle of incidence of the radio waves on the ionospheric layer reflecting them. Below 90 km such free electrons, accelerated by the electric field of the radio wave, suffer collisions with molecules of air and so wave energy is converted to thermal energy of atmospheric gases. Radio waves are therefore attenuated in passing through the D-region of the ionosphere, between 60 and 90 km above the earth's surface. Above this lies the E-region, between 90 and 150 km, and above that the F-region, which may be split into two parts, the F1- and F2- regions, during the day. The structure of the ionosphere is illustrated in Fig. 1.5 for a typical day at mid-latitude.

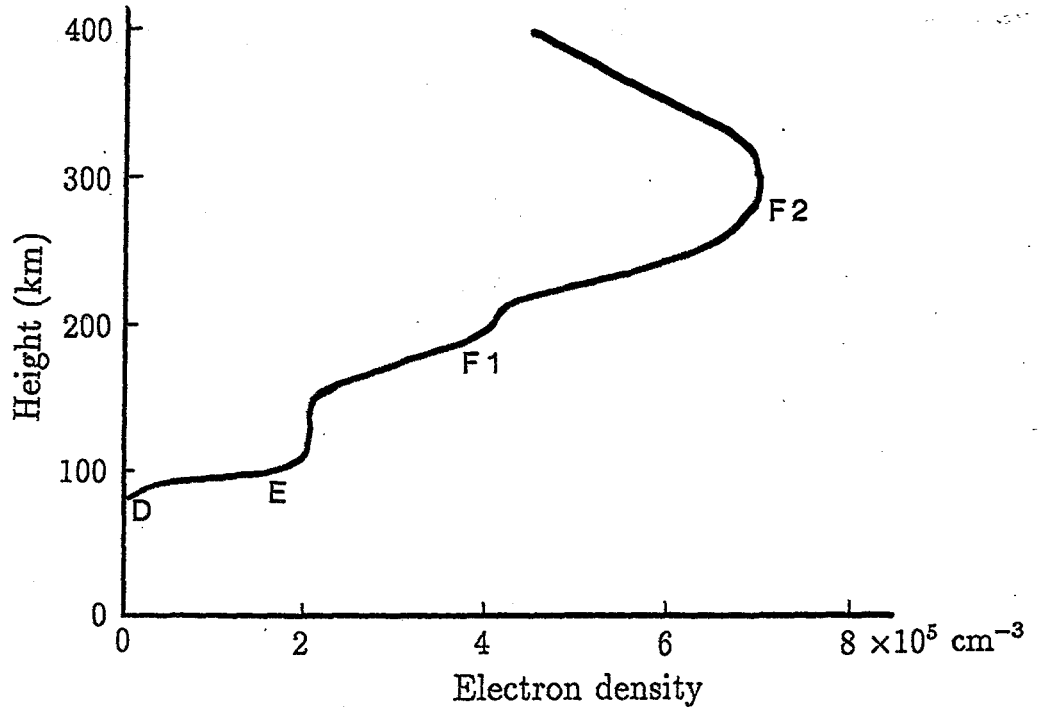

Figure 1.5: Structure of the ionosphere at mid-latitude on a typical day.

The ionosphere is investigated by means of an ionosonde, a type of radar in which the frequency is increased continuously, typically from about 0.5 MHz to 15 or 20 MHz. As the frequency of the radio waves increase they progress further into the ionosphere and a greater electron density is required to reflect these higher frequency waves. The records usually take the form of

graphs of time-delay between the transmission and reception versus frequency, often recorded automatically on film. Such a record is called an ionogramme. Fig. 1.6 shows a typical ionogramme recorded at Grahamstown. The ordinates, marked "virtual height", are calculated on the assumption that the signal travels at the free-space speed of light at all times. In fact, the plasma slows the signal down so that the virtual heights are greater than the true heights of reflection. By means of a computer it is possible to deduce the true heights from an ionogramme and so to construct a graph of electron density versus true height, usually called an "N(h) profile".

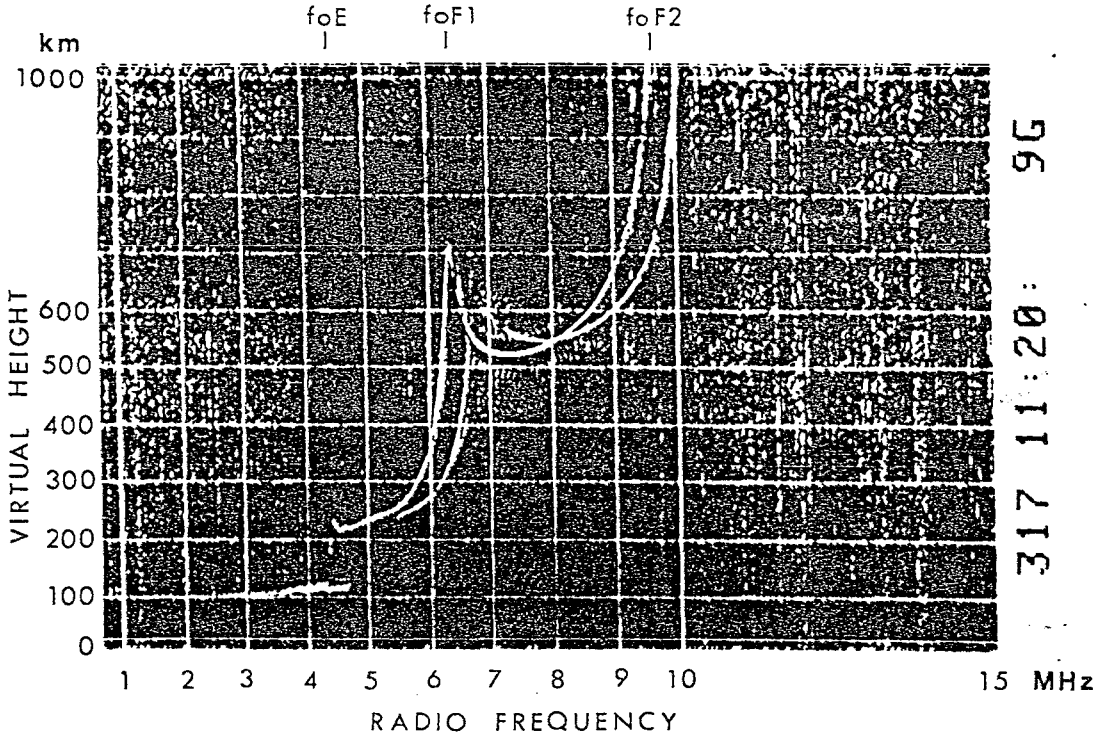

Figure 1.6: A typical mid-latitude ionogramme recorded at Grahamstown using a Barry Research VOS 1 ionosonde.

At the lower end of the frequency scale in Fig. 1.6 the radio frequency is about 0.6 MHz. It increases towards the right, with frequency marks automatically recorded at intervals of 1 MHz to 10 MHz and ends at 15 MHz. Below 2.6 MHz there is no signal reflected from the E-region, due to the absorption in the D-region. This, the lowest frequency seen on an ionogramme, is called the minimum frequency f_{min}. At 2.6 MHz a reflection is seen at a delay corresponding to the virtual height of 100 km, from the E-region. This minimum virtual height of the ordinary wave E trace taken as a whole is known as h'E. The signal penetrates the E-region at about 4.4 MHz and then is returned from the higher F1-region at a minimum virtual height h'F of about 220 km. It is evident that the trace on the ionogramme is a double one. This is because

the earth's magnetic field causes the plasma to be birefringent, so that a single incident signal returns as two with different delays. These waves are known as magneto-ionic or, preferably, magnetoelectronic component waves. The trace showing penetration at the lower frequency is the "ordinary ray", the other being the "extraordinary ray", by analogy with crystal optics. Since the ordinary ray is simpler to interpret in terms of electron density, it is the one ordinarily scaled. The penetration frequency of the ordinary ray through the E-region is called the "critical frequency of the E-region for the ordinary ray", abbreviated to foE. The critical frequency is the highest frequency at which the layer reflects and transmits equally and is usually identified on the ionogramme by the retardation present when the layer is thick, showing a sudden change to a higher reflection level. It is reasonably simple to convert this to the maximum electron density in the E-region and, as above, to find the true height at which this occurs. Similarly, at 6.3 MHz in Fig. 1.6, the ordinary ray penetrates the F1 region at the critical frequency of the F1- region for the ordinary ray foF1 and is then returned from yet a higher region, the F2 region. The decrease in retardation of the signal above foF1 is due to the dependence of the delay on the frequency of the radio wave compared with the penetration frequency of the lower layer through which it passes. The F2 trace shows a minimum virtual height h'F2 of about 520 km, which is much larger than the true height of reflection at this frequency of about 7.3 MHz. Finally the ordinary ray passes through the F2-maximum into space above a foF2 of 9.6 MHz, where foF2 is the critical frequency of the F2-region for the ordinary ray. When referring to the critical frequencies of the extraordinary ray the subscript o is replaced with an x.

During the nighttime the F-region is not split into F1 and F2 portions and its critical frequency is then denoted by foF. During many nights, and often during daytime also, traces appear at E-region heights and disappear again after a while. These reflections, which are often very intense, come from ionized regions which may or may not lie directly overhead. They are called "sporadic-E" traces and there are several different mechanisms responsible for the ionization that reflects the radio waves.

Due to absorption of the ordinary ray critical frequency one has to use the extraordinary ray critical frequency to obtain the ordinary ray critical frequency by utilising the gyrofrequency f_B. The gyrofrequency is the natural resonance frequency of the electrons about a magnetic field of strength B. The relationship between the critical frequencies fo, fx and the gyrofrequency f_B is given by

$$f^2x - f^2o = fxf_B$$
$$fx - fo = \frac{fxf_B}{fo + fx} = \frac{f_B}{fo/fx + 1}$$

From experimental results, it is known that for the F region when fo and fx are both large compared with f_B then fo/fx is approximately equal to one and

$$fx - fo \approx \frac{1}{2}f_B$$

For critical frequencies near the gyrofrequency the ordinary and extraordinary ray separation becomes slightly larger than one-half of the gyrofrequency. Experimental data has shown that the ordinary and extraordinary separation increases to 0,62 of the gyrofrequency as the ordinary ray critical frequency fo, approaches the gyrofrequency, f_B. Whilst one must exercise caution during times of rapid change in the ionosphere, since the lateral deviation of the ordinary and extraordinary components can lead to large departures from the usual critical-frequency separation (Beynon and Brown, 1957).

1.4 Ionization by Precipitating Charged Particles

In the auroral zones, where the solar particles are funnelled by the earth's magnetic field down into an oval area which surrounds each of the earth's magnetic poles from about 60° to 70° magnetic latitude. Electrons and protons from the magnetosphere penetrate to heights as low as 100 km and produce the aurora by exciting atmospheric molecules to higher energy levels. When they return to lower levels many do so by emitting photons. Amongst the wavelengths usually observed are 630.0 nm and 557.7 nm, from excited oxygen atoms, and 391.4 nm from excited N_2^+. The precipitating particles also ionize the atmospheric gases, producing irregular enhancements in the ionosphere which can be observed by radio methods, the so-called "radio aurora".

Since large fluxes of charged particles were observed at ionospheric heights in the South Atlantic Anomaly as discussed previously and reported by Gledhill (1976), the question arose as to whether effects similar to those seen in the auroral zones would be observable in the Anomaly. The high-energy particles shown in Fig. 1.4 would deposit most of their energy in the D-region and thus cause more absorption of radio waves in the Anomaly than at similar latitudes

elsewhere. The effects observed in the auroral zones are, however, produced by electrons and protons of much lower energies, usually in the range 1 - 20 keV. Unfortunately, measurements of particles with these energies in the Anomaly could not be made, because the high-energy particles penetrated the spacecraft walls and produced such a large background of spurious counts in the low-energy spectrometers as to swamp completely the desired energy ranges. When Gledhill (1976) surveyed the efforts that had been made to observe such particles and their aeronomic effects, he was forced to conclude that little had been achieved up to that time. Fortunately, Rhodes's observational campaign in the South Atlantic Anomaly region using conventional pulse ionosondes and photometers from aboard the various research and supply vessels sailing in or near the region had just started. A satellite had also just commenced making measurements that would go a long way to solving the above lack of information. The work reported here is an attempt to report the progress made in our knowledge of the South Atlantic Anomaly region since Gledhill's review article in 1976.

Chapter 2

Observations of the Ionosphere

The precipitating electron or ion fluxes in the energy range of principal aeronomic importance to this dissertation, below 40 keV, would be expected to produce their main effects in the E- and F- regions of the ionosphere. These effects would be manifested in the form of increased ionization during both day and night in the E- and F- regions as well as the emission of the 391.4 nm radiation of the N_2^+ ion, excited by electron impact. Accordingly, a portable ionosonde was designed and built with which to probe the ionosphere in the South Atlantic Region.

2.1 Airborne Observations

A great deal of time was spent designing and building a dual purpose instrument, that is, one which could be used on board ship or aircraft, as well as the associated antenna systems, especially for use on the aircraft where size and safety criteria imposed severe limitations on the antenna system used. The completed system was installed in a C130 Hercules Aircraft and on the evening of October 15, 1974, the first research flight was undertaken to approximately 48°S; 1°E. These were the first ionospheric data to be recorded by bottomside ionosondes over the South Atlantic Ocean. Fig. 2.1 shows the flight paths taken. The flight path *A* was undertaken on the afternoon of the 14th October, 1974 to a point approximately 43°S; 26°E, where the aircraft circled with ever decreasing height for 2 hours. Unfortunately, the ionosonde interfered with other research equipment on board and the attempts at obtaining research ionogrammes had to be abandoned. However,the flight was used to test the antennae systems and equipment. However, flight path *B* was allocated primarily for ionospheric research. This flight took place

on the 15th October 1974 and ionogrammes were taken every 10 minutes, or approximately every 90 km, up to about 44°S; 6°E. Thereafter ionogrammes were taken every minute, or about every 9 km, and likewise for the return flight. Some typical ionogrammes obtained during the flight are shown in Fig. 2.2. The approximate geographical positions are indicated on the diagrams as well as the time of day, in Universal time.

Fig. 2.2(a) exhibits sharp, well defined critical frequencies both for the ordinary and extraordinary rays as described in section 1.3. The reduction of this ionogramme produces the following values: foF2 = 3.3 MHz, fxF2 = 3.7 MHz, h'F = 270 km and f_{min} is approximately 2.2 MHz. Whether f_{min} as obtained is a true reflection of the absorption in the D-layer is extremely doubtful due to the transmitting antenna limitations. Note that the second order trace or second hop ionogramme is also visible.

Fig. 2.2(b) corresponds approximately to the turning point at 48°S; 1°E. Quite clearly the ordinary ray critical frequency is below f_{min}. Hence foF2 was obtained by assuming an inverse cube field, ie., near field, and taking the values of the magnetic field at the earth's surface from data collected by the Hermanus Magnetic Observatory during an earlier voyage of the motor vessel RSA to Sanae in 1965/66. Thus the field at 300 km could be calculated and the gyrofrequency, f_B obtained, from which foF2's were computed from fxF2 by subtracting half the gyrofrequency as explained in section 1.3. Fig. 2.2(c) was taken on the return flight and clearly exhibits spread F condition, i.e., densely ionized patches which are not overhead continuing to reflect at frequencies above the critical frequency. Clearly, the reflecting layer is inhomogeneous and oblique echoes are received as well - this is often referred to as tilts in the ionosphere.

The ordinary ray critical frequencies obtained during the flight of the C130 aircraft, as well as those obtained from the fixed stations of Grahamstown and Hermanus are plotted as a function of frequency versus local solar time in Fig. 2.3. Error bars have been included and the solid line for the aircraft represents the most probable value of foF2. The broken line and the dash, dot, dot line represents Grahamstown and Hermanus respectively. The lower values of foF2 obtained in the beginning of the flight are as yet unexplained, but as can be seen there is a marked decrease in foF2 as the flight proceeded further south compared to those of Grahamstown and Hermanus. Both Halley Bay and Sanae records exhibit total black out conditions for this period, whilst no other stations were operational during this time in the area of interest.

The magnetic K_p index, as recorded at Hermanus for the period under consideration is indicated

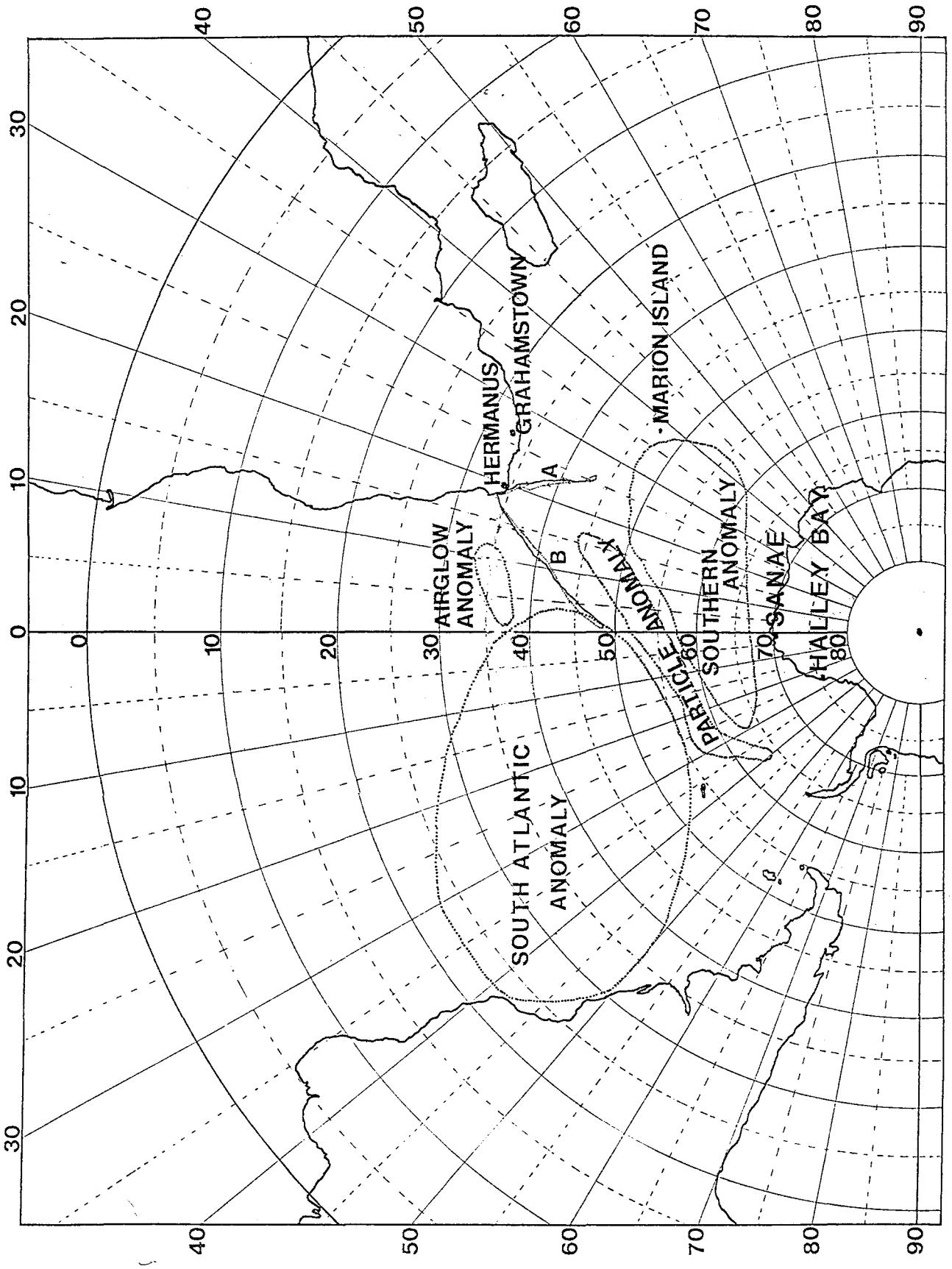

Figure 2.1: The South Atlantic Ocean, showing anomalous areas previously reported and the flight paths taken.

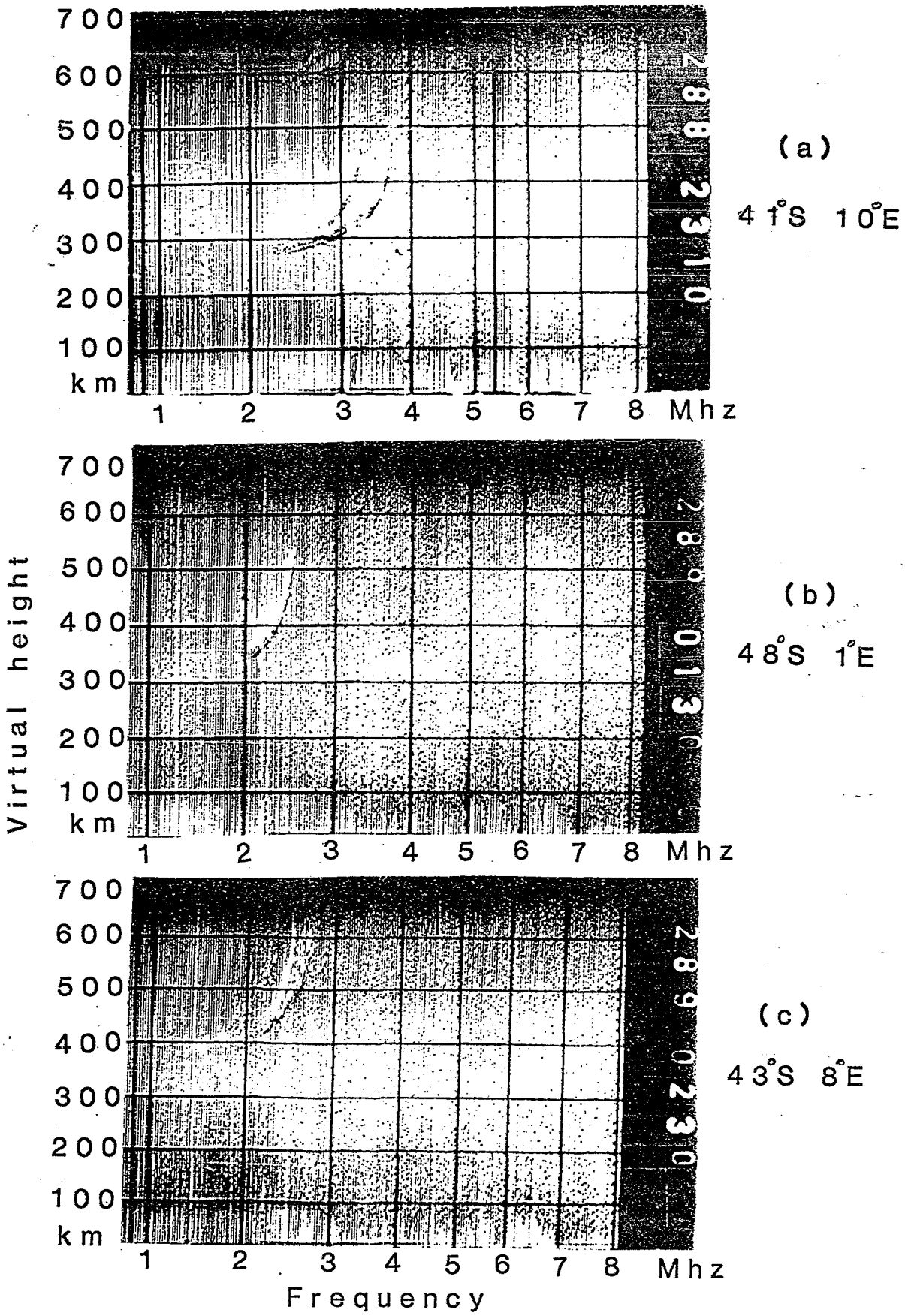

Figure 2.2: Typical ionogrammes obtained during the flight, indicating the approximate geographical positions and time of day in UT.

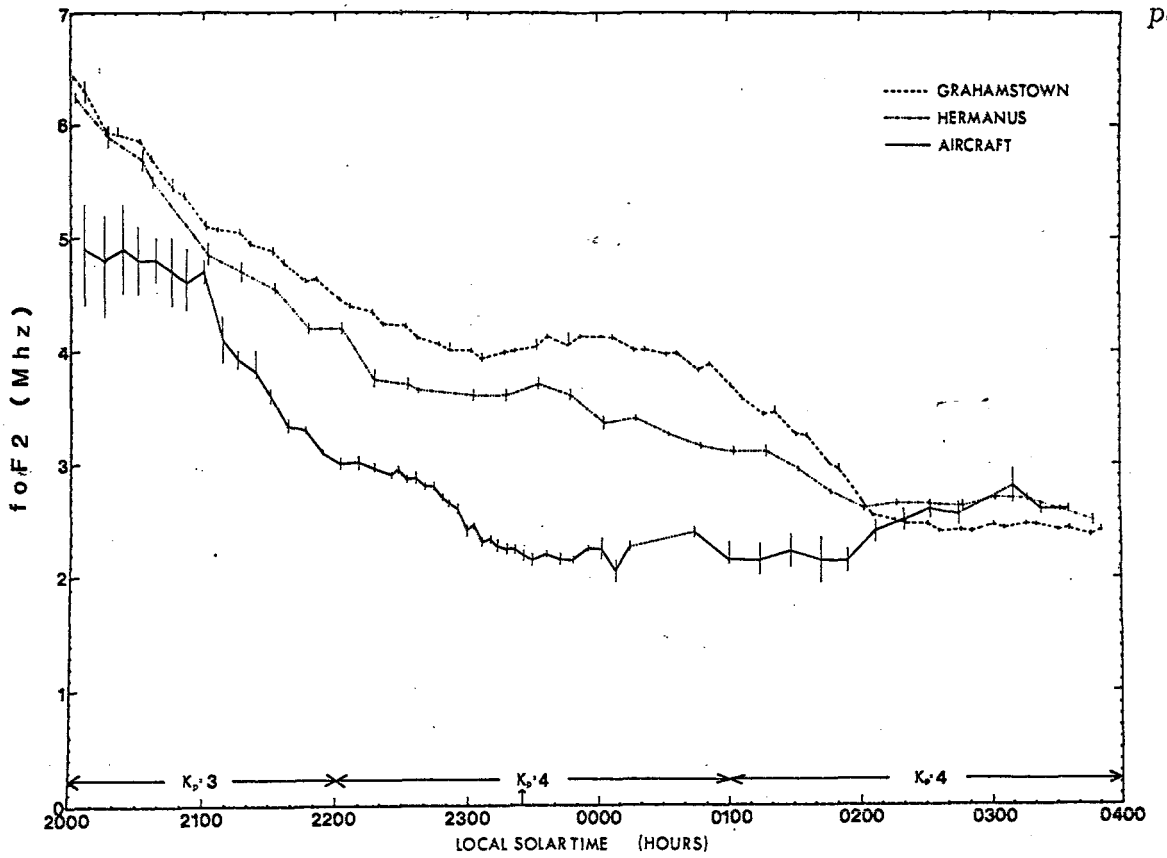

Figure 2.3: The ordinary ray F-region critical frequencies obtained during the flight versus local solar time (solid line). Also shown are the values for Grahamstown (broken line) and Hermanus (dash, dot, dot line).

for each three hourly interval in Fig. 2.3, where K_p is the planetary 3 hourly index designed to measure solar particle radiation by its magnetic effects, specifically to meet the needs of research workers in the ionospheric field. The overall magnetic character of the day was 1.0, hence the field was moderately disturbed and particle precipitation could have been possible, although airglow data from Sutherland and that obtained on the flight showed no particular enhancement.

The virtual heights, h'F, obtained on board the aircraft and at Grahamstown and Hermanus are shown in Fig. 2.4 as a plot in km versus local solar time. The increase in the virtual height of the F-layer as obtained on board the aircraft is immediately noticeable compared to the graph for Grahamstown and Hermanus. The error bars descending from the graph indicate the minimum possible values of h'F, whereas those spanning the curve represent the maximum possible range of h'F.

Disturbances in the F2 region are of two kinds. Usually the critical frequency of the layer foF2 decreases sharply and the virtual height h'F2 increases, as is the case in this study. These changes are entirely consistent with the heating of the F region by energy loss from the precipitated electrons. The second kind of disturbance the F2 region can experience is

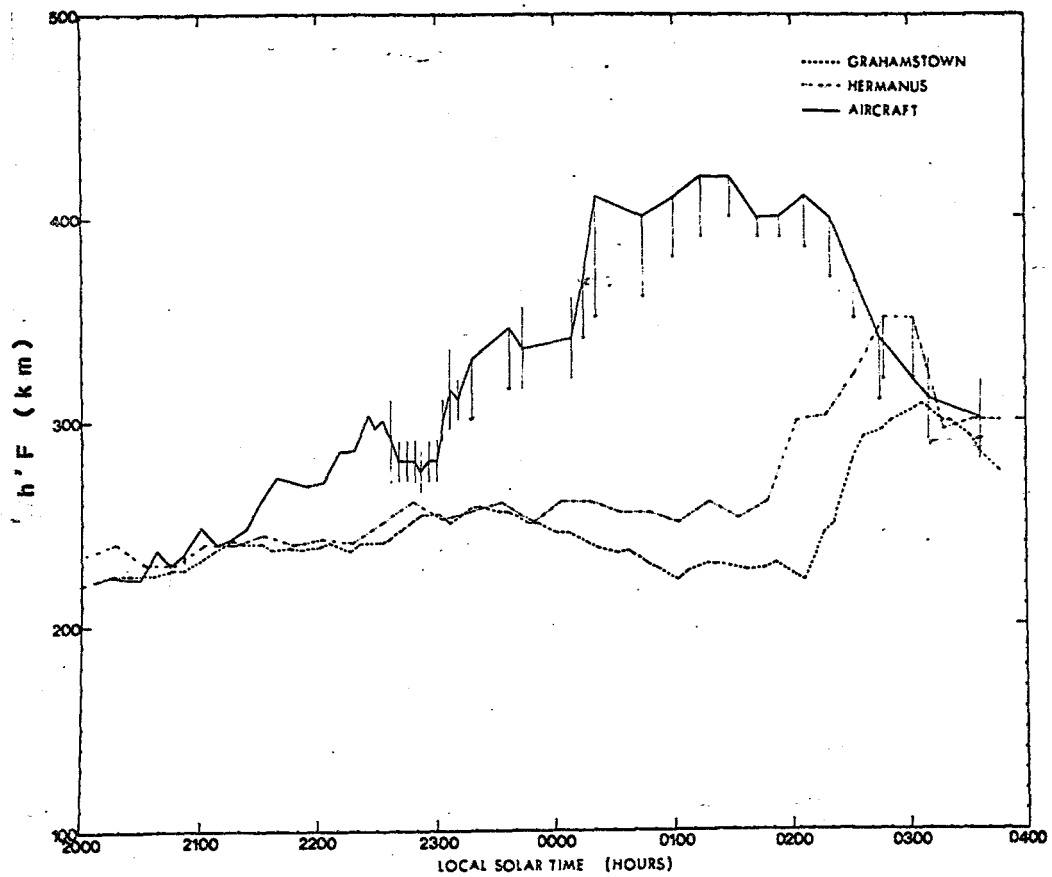

Figure 2.4: The virtual heights of the F-region obtained during the flight versus local solar time (solid line), as well as those of Grahamstown (broken line) and Hermanus (dash, dot, dot line).

one in which the critical frequency of the layer foF2 increases and the virtual height h'F2 decreases. This behaviour is consistent with the precipitating electrons losing their energy both by ionizing the molecules in the F2 region and by emission of heat due to collisions. The type of disturbance produced would depend on the energy spectrum and the flux of the incoming electrons. Under some circumstances the heating effect would predominate, whilst under others the extra ionization would be the principle effect [Rees (1963), Gledhill and van Rooyen (1963) and Maeda (1965)].

Thus it is seen that the results obtained here would support the first mechanism in that foF2 decreases sharply and the virtual height h'F2 increases. Further, the high f_{min} values or total black out recorded at Halley Bay and Sanae, indicating absorption in the D-region, are all entirely consistent with the heating of the F region by energy lost from precipitated electrons as they descend to the D-region.

These results encouraged us to continue our endeavours to make ground based (bottomside) ionospheric observations in the South Atlantic Region. The presence of the South Atlantic Anomaly (Gledhill, 1976) suggests that unusual phenomena may be expected there. Satellites have recorded relatively large particle fluxes in the area at low altitudes (Ginzburg *et al.* (1962))

and Greenspan and Stone (1964) recorded a pronounced airglow enhancement in the region about 35°S; 6°E, during a voyage to Gough and Bouvet Islands in 1962. This is all summarised in Fig. 2.5.

2.2 Shipborne Observations

The South African Research Ship RSA passes through this region on its way to and from Gough Island and Tristan da Cunha. By arrangement with the South African Department of Transport, a vertical incidence ionosonde was operated on board the vessel during the voyages in October/November, 1975; August/September, 1976 and October/November, 1977. The courses followed on these three voyages are indicated in Fig. 2.5. The history of these voyages and observations is given in Table 2.1.

Location	Observations	First Voyage 1975	Second Voyage 1976	Third Voyage 1977
Cape Town - Gough Island	Every 15 minutes	4 to 10 October	14 to 19 August	14 to 19 October
At Gough Island	Every 15 min. when possible	13 Oct. to 2 November		19 Oct. to 1 November
Gough Island - Cape Town	Every 15 minutes	3 to 9 November	30 Aug. to 4 September	2 to 7 November

Table 2.1 History of voyages and observation periods.

The courses followed by the RSA during the voyages to and from Gough Island and Tristan da Cunha hardly deviate from the geomagnetic latitude 34°S, which corresponds to a value of 1.75 of McIlwain's parameter L (McIlwain, 1961). Thus the observations recorded during the courses followed by the RSA might be expected to show up the longitudinal dependence of phenomena due to precipitated particles, if such existed.

Fig. 2.6 shows the contours of constant McIlwain's parameter L at 300 km as well as the location of Gough Island.

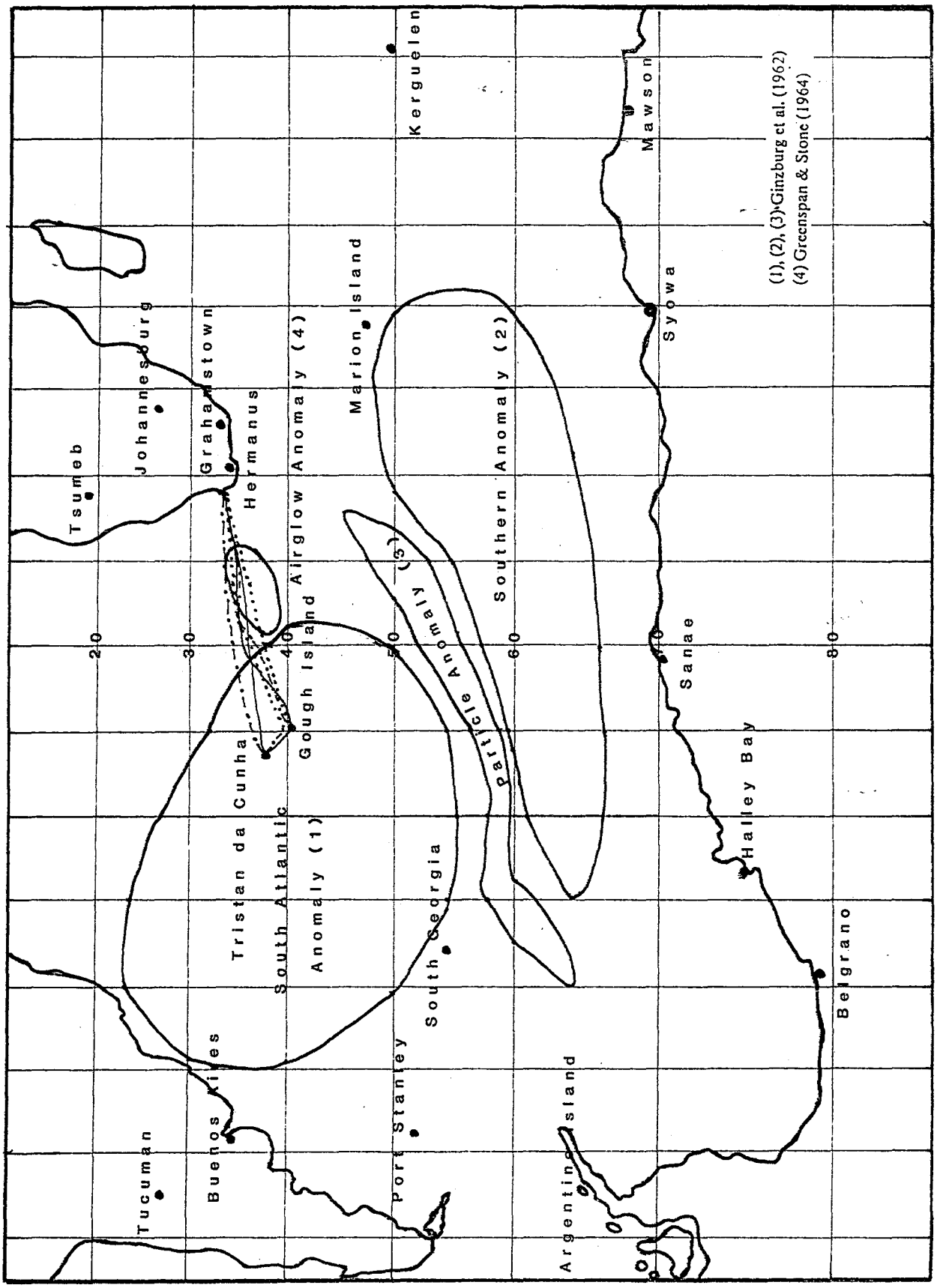

Figure 2.5: The South Atlantic Region, showing anomalous areas previously reported and the routes taken by the RSA in 1975(−), 1976 (···) and 1977(---).

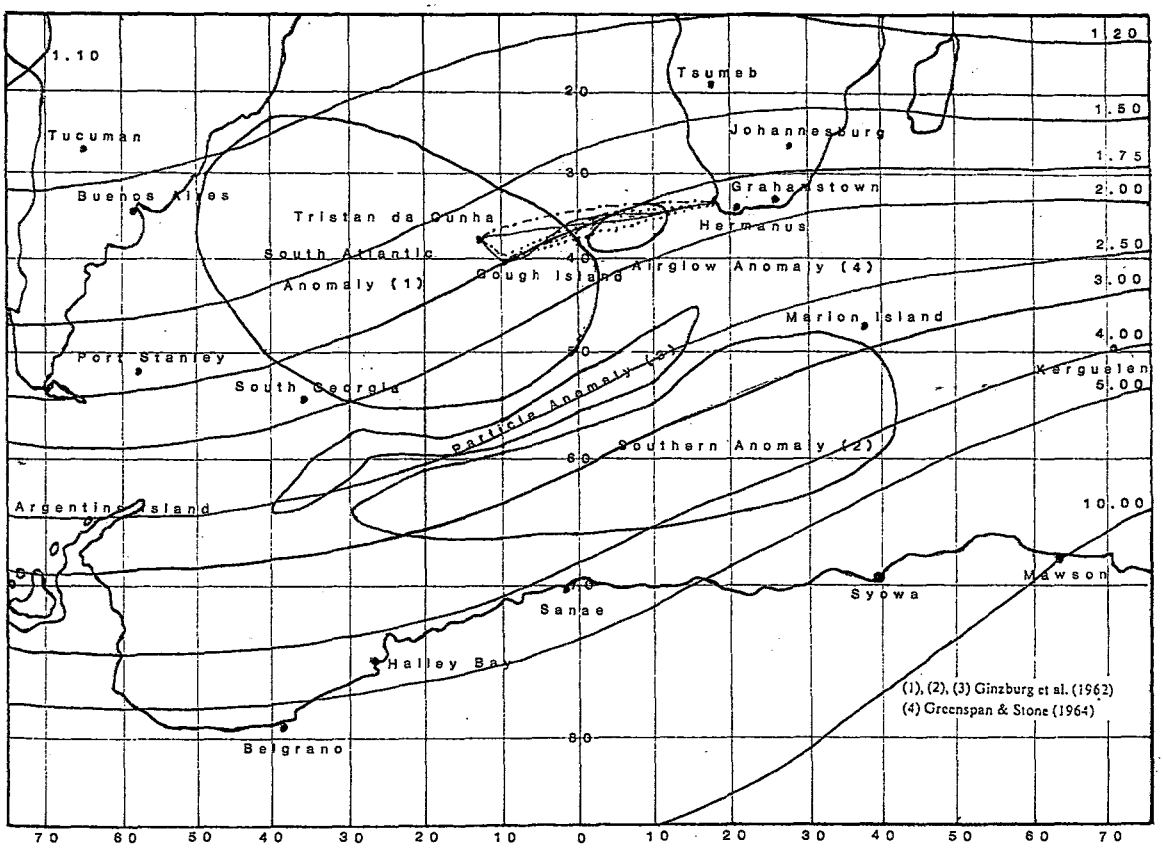

Figure 2.6: Map showing contours of constant McIlwain's parameter L at 300 km above ground level.

2.3 The F-region Ionosphere

In Fig. 2.7 the values of foF2 recorded on board the RSA with those recorded at Grahamstown are compared for the corresponding local time during the return voyage from Tristan da Cunha in 1975. The geographic longitude of the ship at noon each day is shown at the top of the figure. It is very striking that the values of foF2 over the South Atlantic west of the Greenwich meridian exceed those at Grahamstown by as much as 5 MHz.

Similar graphs were prepared for the other five voyages, but the results are more clearly displayed by plotting ΔfoF2, i.e., foF2 observed on board the RSA minus foF2 observed at Grahamstown at the same local time. These values are shown in the following six figures for the six voyages through the region between Cape Town and the islands of Gough and Tristan da Cunha. In all six figures the values are shown as functions of local solar time. The geographic longitudes at the top of each figure always have the islands on the left hand side and Cape Town on the right, i.e., from west to east. The K_p-indices are indicated along the abscissa.

Fig. 2.8 and Fig. 2.9 show the results of the outward and return voyages during 1975 respectively. In both figures it is seen that foF2 over the ship was abnormally high compared with that at Grahamstown during both the outward and return voyages during 1975, especially

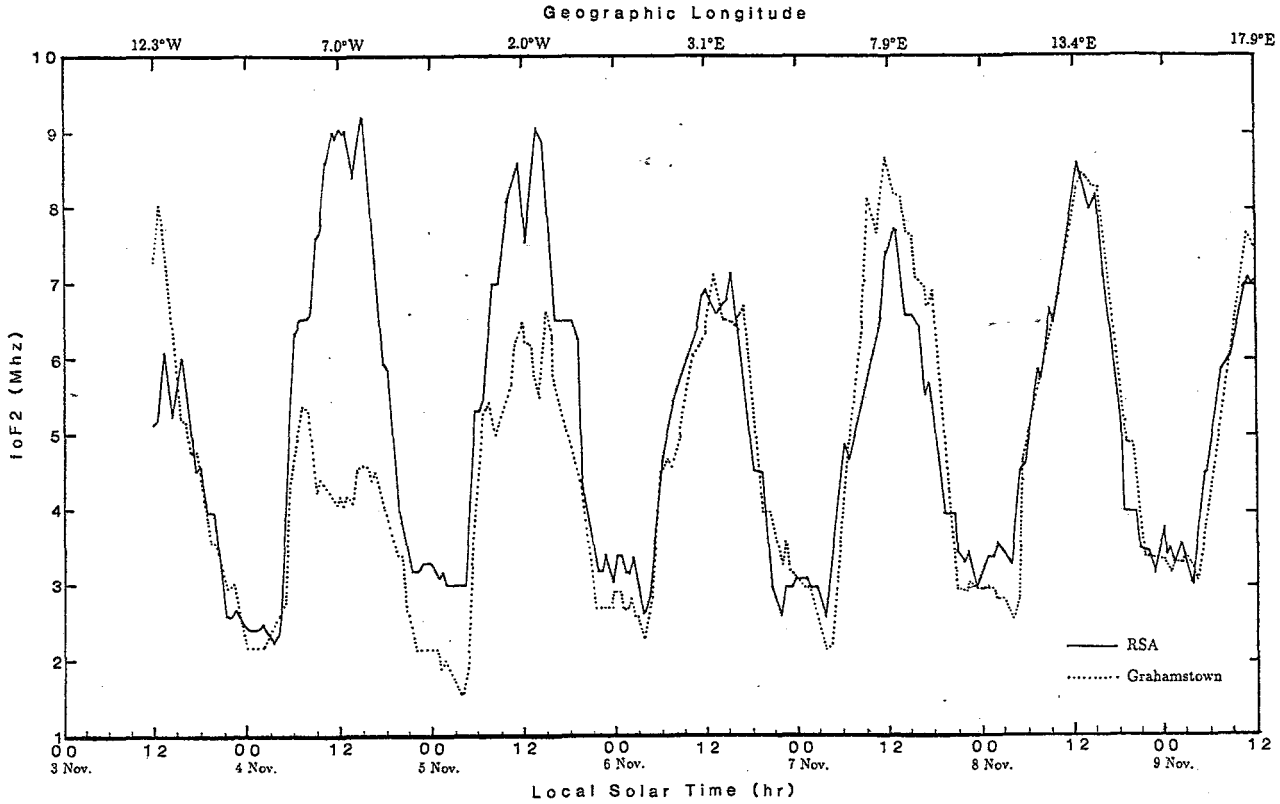

Figure 2.7: Values of foF2 versus local solar time observed on the RSA and at Grahamstown during the return voyage, 1975.

during the daylight hours. The region concerned lies between 9°W and 0°W on both voyages so that it lies to the west of the "Airglow Anomaly" found by Greenspan and Stone (1964). Unfortunately, the highest values of the planetary magnetic K_p-index coincide with the passage of the ship through the same region in both directions, so that it is not possible to draw any definite conclusions from the abnormal behaviour, since the magnetic field was moderately disturbed. O'Brien (1964) found that precipitation is generally more intense during magnetic storms as measured by the planetary magnetic disturbance index K_p. Thus, caution must be exercised in labelling this region in the South Atlantic as the "Haggard Anomaly".

Figures 2.10 and 2.11 are the difference plots for the voyages of 1976. As can be seen high values were observed between 7° West and 14° East during the daylight hours on most days on both the outward and return voyages. The differences are much less, however the K_p-indices are also lower than during the 1975 voyages indicating rather quiet magnetic conditions during the 1976 voyages.

Figures 2.12 and 2.13 are the difference plots for the voyages of 1977 to and from the islands of Gough and Tristan da Cunha. On the outward voyage it is noticed that foF2 monitored on board ship between the longitudes of about 0° West to 10° West, was abnormally high for the

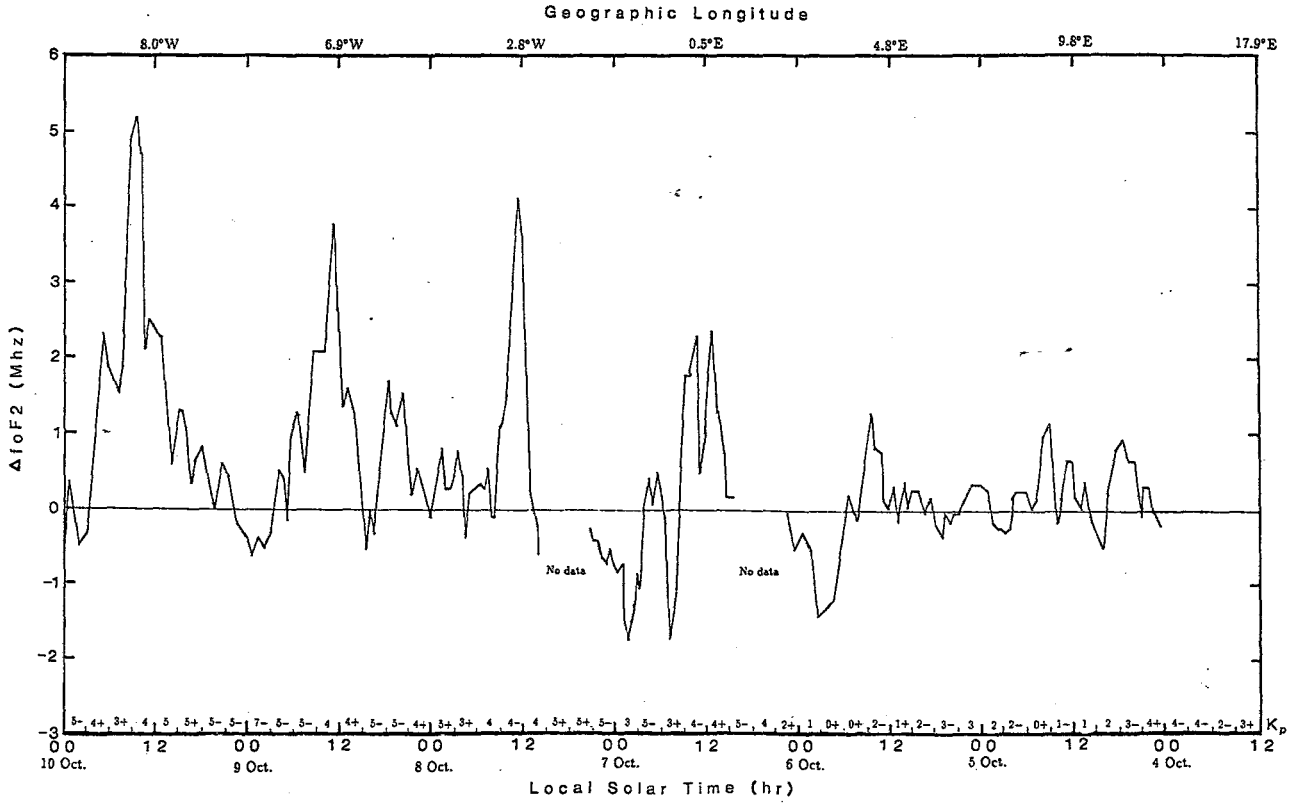

Figure 2.8: Δ foF2 values between the RSA and Grahamstown, for the outward voyage during 1975, versus local solar time.

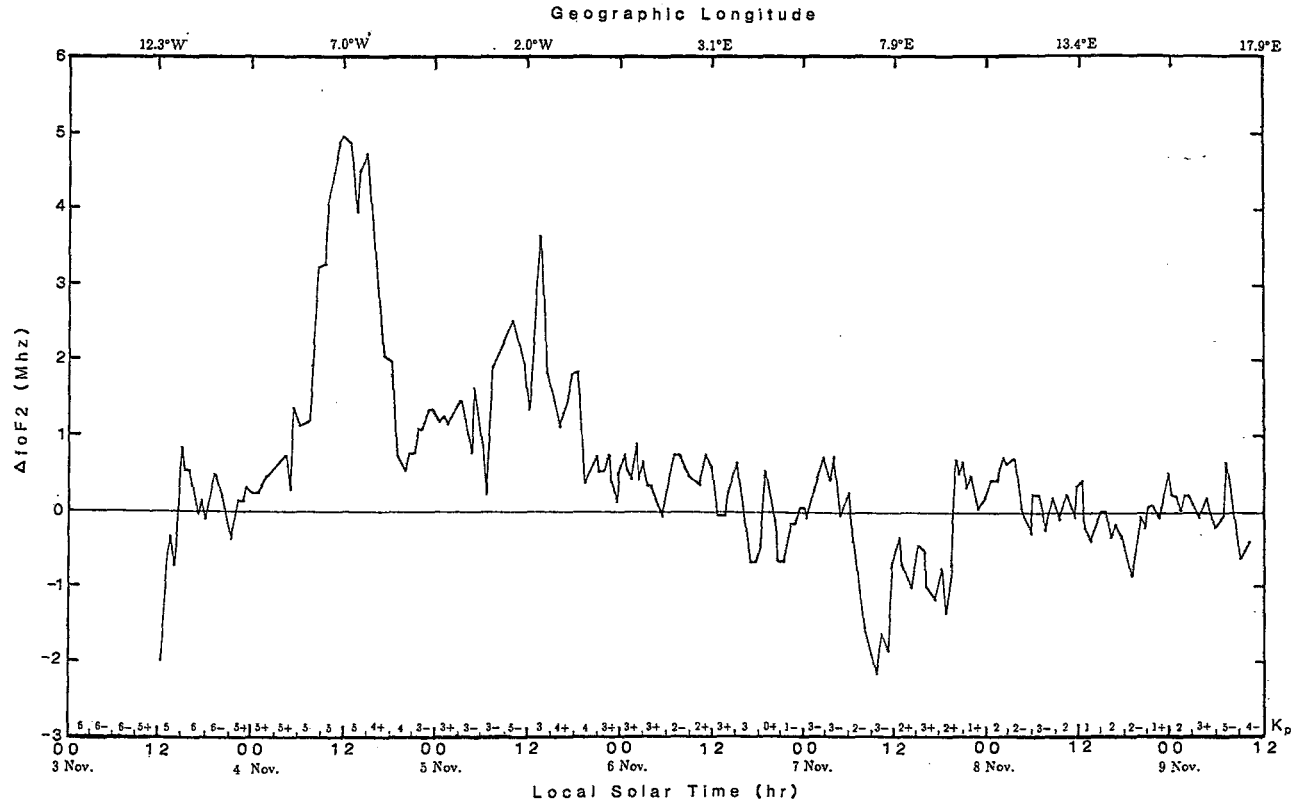

Figure 2.9: Δ foF2 values between the RSA and Grahamstown, for the return voyage during 1975, versus local solar time.

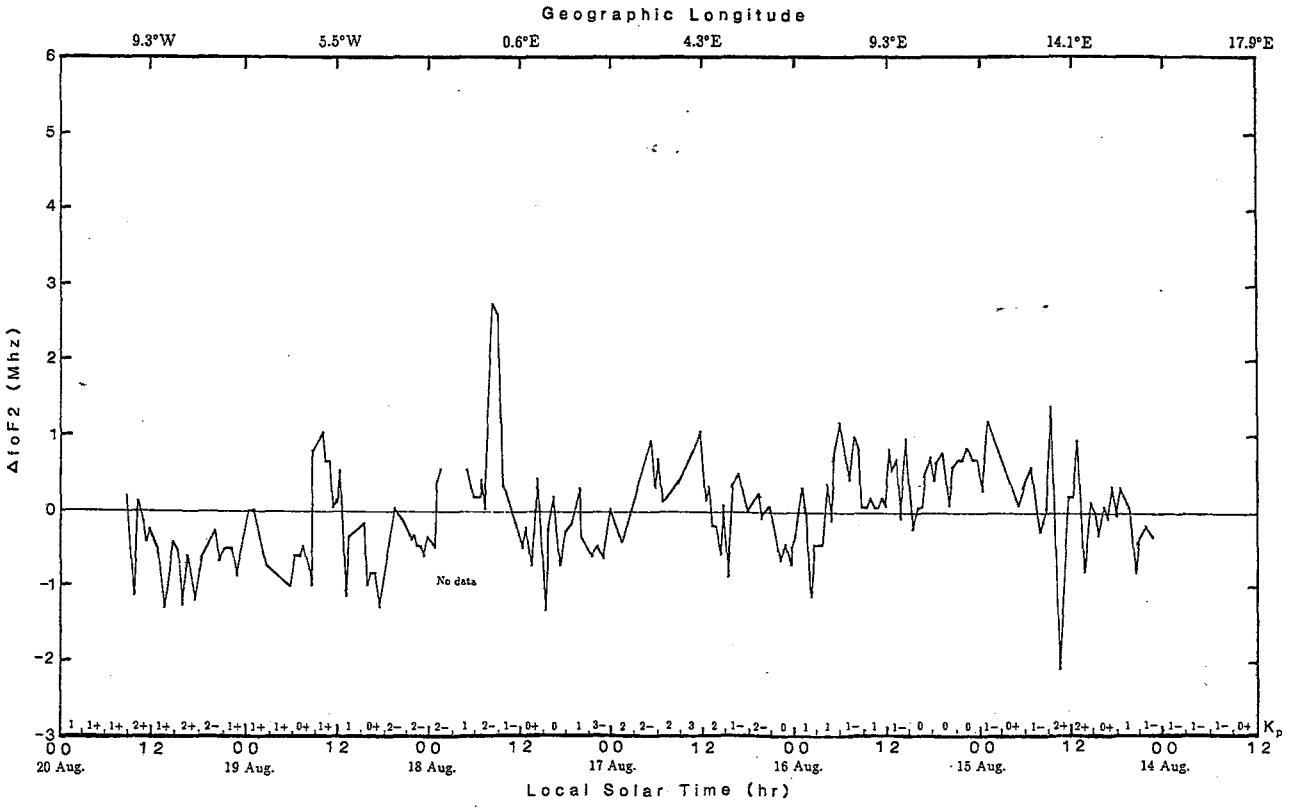

Figure 2.10: Δ foF2 values between the RSA and Grahamstown, for the outward voyage during 1976, versus local solar time.

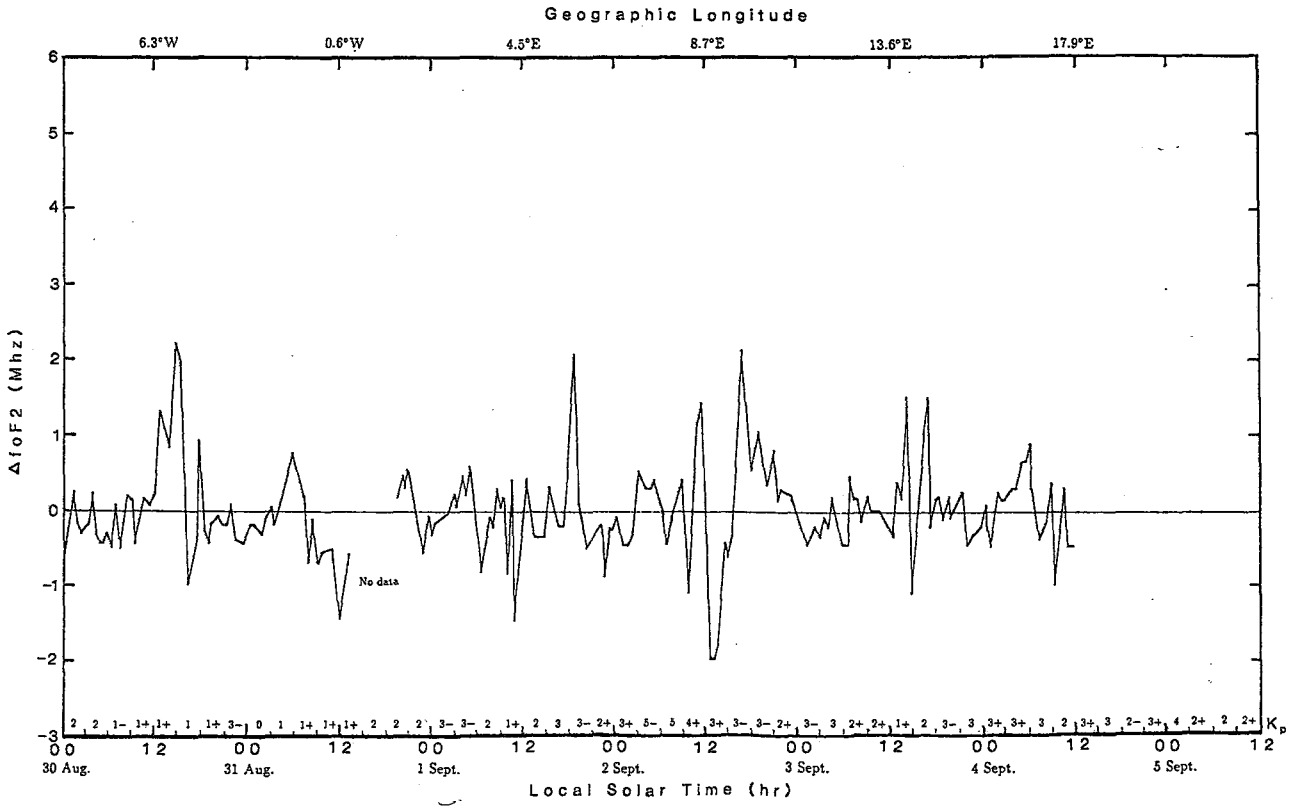

Figure 2.11: Δ foF2 values between the RSA and Grahamstown, for the return voyage during 1976, versus local solar time.

daylight hours compared with that as measured at Grahamstown, whereas East 0° West the differences are much less. Once more the highest values of the magnetic K_p index coincided with the region where the difference frequencies were greatest. During the return voyage high values of difference frequency were again observed between 7° West and 14° East during the daylight hours on most days. The difference is much less than for the outward voyage, however the magnetic K_p-indices are lower during the return voyage compared to the K_p values of the outward voyage.

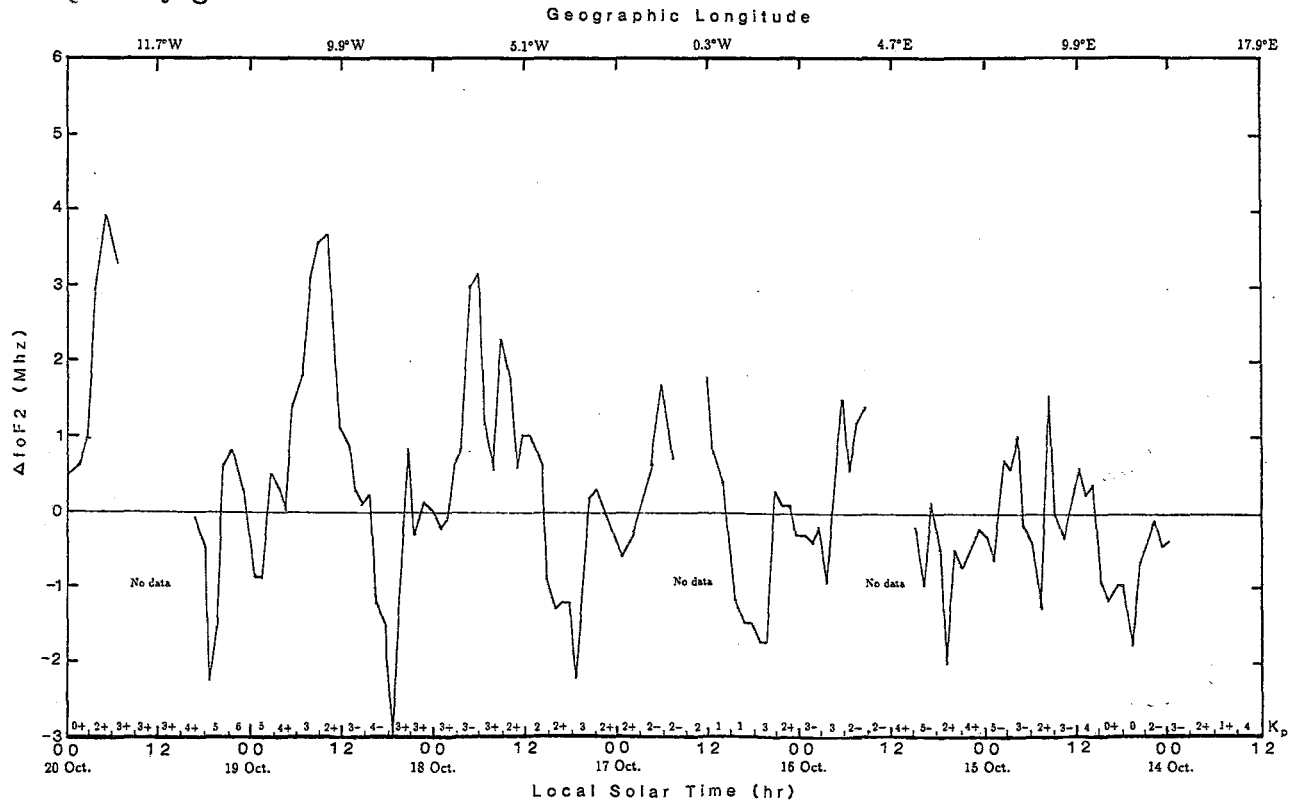

Figure 2.12: Δ foF2 values between the RSA and Grahamstown, for the outward voyage during 1977, versus local solar time.

Greenspan and Stone (1964) observed enhancement of both 557.7 nm (OI) and 427.8 nm (N_2^+) emission in the region shown in Fig. 2.5 in the vicinity of 35°S; 6°E. Van der Walt *et al.* (1966), making observations from an aircraft following the route taken by Greenspan and Stone, also observed an enhanced emission of the 557.7 nm line at about 38° South, 1° West in both flight directions. The region where large deviations in ΔfoF2 were recorded lies close to that in which maximum intensity of electron precipitation has been predicted by Torr *et al.* (1975).

Although no particle type sporadic-E was observed on any of the voyages reported here, what was very prevalent was an additional intermediate layer between the normal E layer and the F1 layer. This E2-layer was more noticeable during periods of enhanced magnetic activity. Where

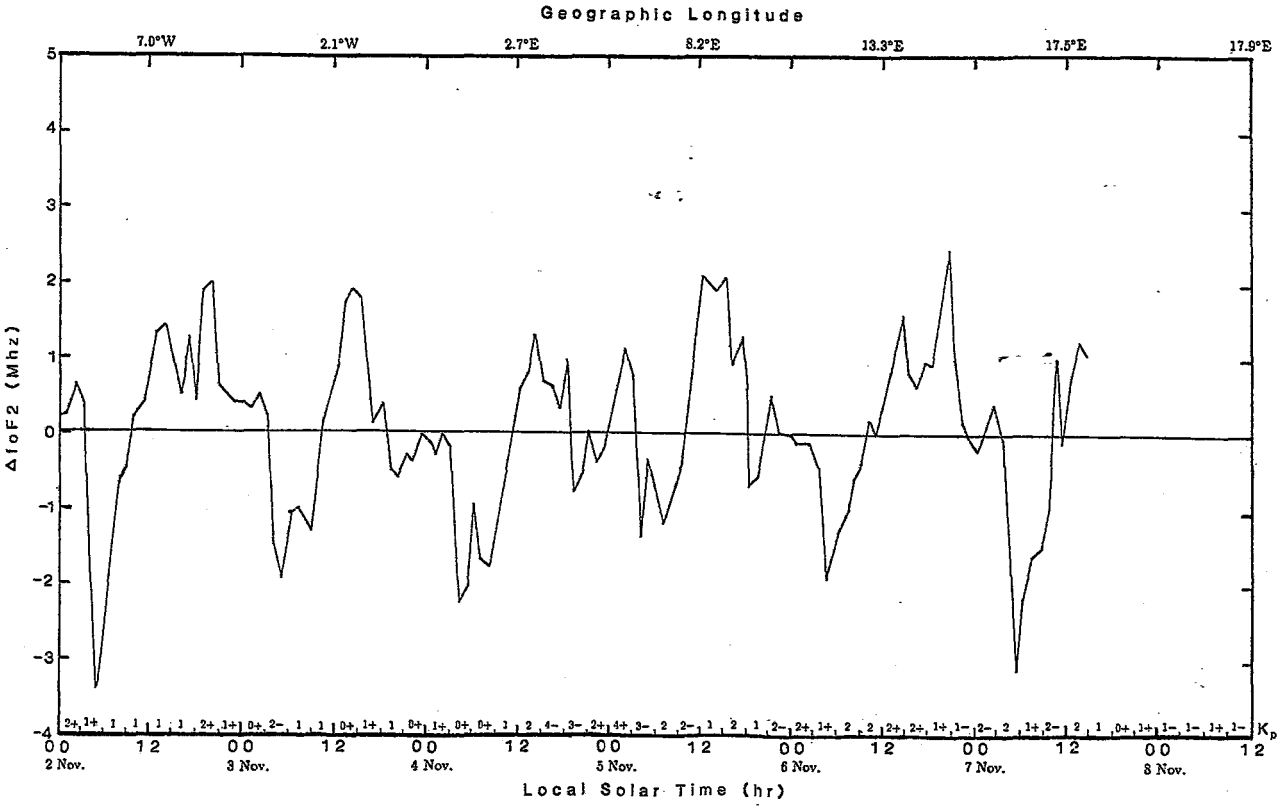

Figure 2.13: Δ foF2 values between the RSA and Grahamstown, for the return voyage during 1977, versus local solar time.

data was available from South American stations, no noteworthy effects were recorded.

Next, the results obtained whilst the RSA was at anchor at Gough Island (40.4° S; 9.9° W) were analysed. During 1975 reliable results are available for this 21 day sojourn but unfortunately during the 1976 visit no data is available due to offloading of cargo and equipment failure. In 1977 ionospheric soundings for a 14 day period were made.

A careful analysis of all the data for these two periods in 1975 and 1977 were made and median values calculated for ordinary ray critical frequencies of the E, F1 and F2 layers as well as the minimum frequency at which an echo could be detected, f_{min}. These results are represented graphically in Figures 2.14 (1975) and 2.15 (1977). The number of values represented by each point is indicated on both diagrams in the legend. The planetary magnetic three-hour range K_p-indices for the 1975 period were also analysed and 157 of the 168 possible three-hourly periods were 3 or less and only 11 exceeded 3, the maximum value being 7-. For the 1977 period 94 of the possible 112 three-hourly periods were 3 or less whilst 18 exceeded 3, the maximum value being 7+. On the whole, 1977 was slightly more active magnetically than 1975. The geomagnetic three-hourly range indices K_p for each day of the two observation periods are shown in Table 2.2. The Southern Hemisphere magnetic three-hour range indices, K_s, were also considered for these periods and found to agree closely with the K_p-indices.

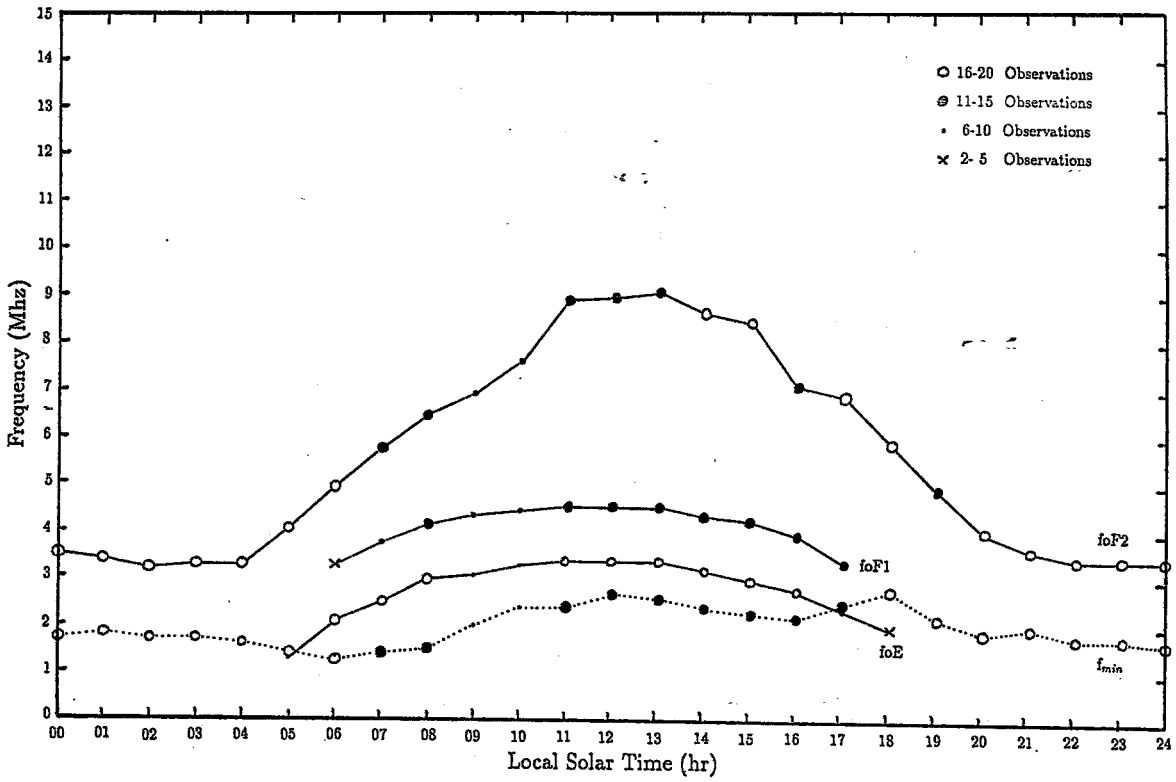

Figure 2.14: Median values of ionospheric parameters observed at Gough Island during the period 13 October and 2 November, 1975.

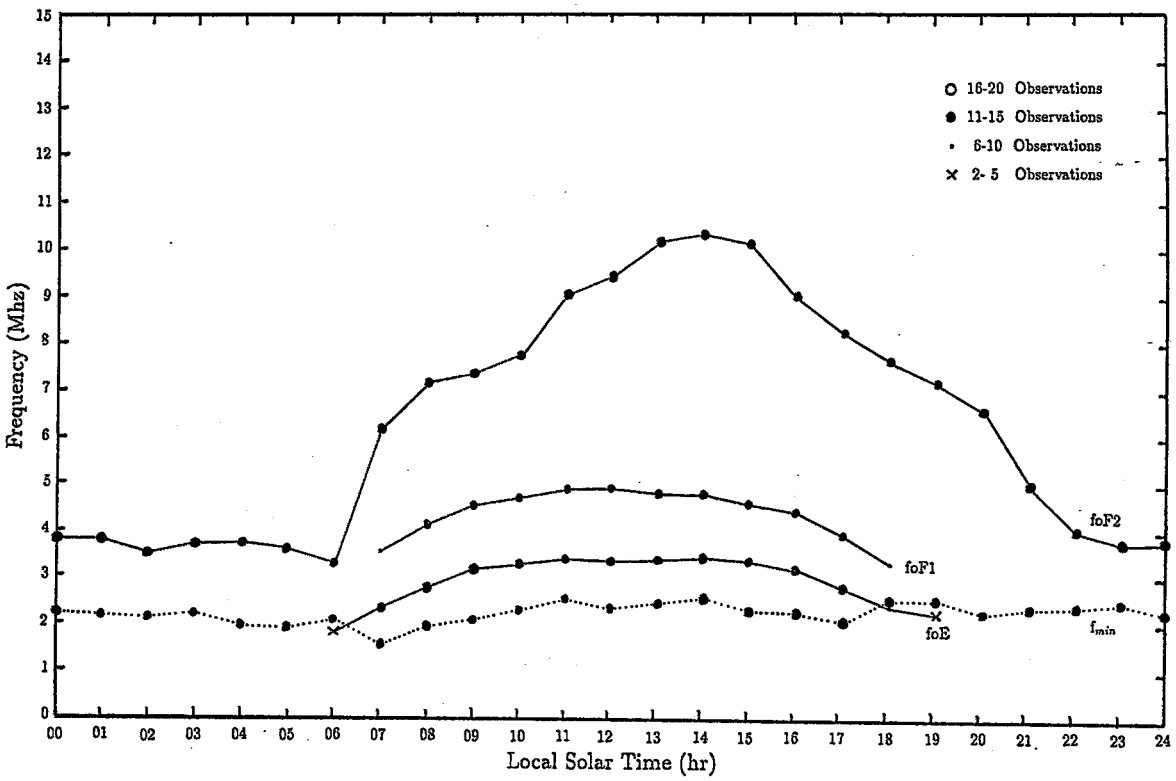

Figure 2.15: Median values of ionospheric parameters observed at Gough island during the period 19 October and 1 November, 1977.

Date	1	2	3	4	5	6	7	8	SUM
13 Oct'75	1	3−	3−	1	2	2−	2−	2	15−
14 Oct'75	1+	0+	3	3	2+	3−	2	2+	17
15 Oct'75	1	2−	1+	2+	1−	1−	1−	1	9+
16 Oct'75	2+	2−	2−	3	2	2	4−	2−	18
17 Oct'75	3+	2	2−	2+	2+	2−	1	1+	16−
18 Oct'75	0	1	1−	1	2+	2−	2	1−	9+
19 Oct'75	0	0+	0+	1−	1	1	2−	1+	6+
20 Oct'75	2−	1+	1−	1−	1	1−	1	3−	10−
21 Oct'75	3+	2	1	2−	0+	0+	0+	2	11
22 Oct'75	2	2−	2−	1+	1	1−	2−	2+	12+
23 Oct'75	3	3	1−	1+	1	0+	1+	1+	12
24 Oct'75	2+	2+	2−	1−	1−	0+	0+	0+	9−
25 Oct'75	1−	1−	1+	1+	1+	1−	0+	0+	7−
26 Oct'75	2	0+	1	1	1−	3−	1	2	11−
27 Oct'75	3	3−	1+	0+	0+	1−	0+	0+	9
28 Oct'75	2−	0+	1−	2−	2−	2	4−	4−	15+
29 Oct'75	3	4−	4	1+	0+	1−	1+	3	17+
30 Oct'75	3−	2	2+	2+	1+	2−	2−	3+	17+
31 Oct'75	3	4	5+	3	1−	3	3	1+	23+
1 Nov'75	1+	1+	2−	2+	2−	1	1−	3+	13+
2 Nov'75	2+	3	2	3+	4−	4	7−	6	31
19 Oct'77	6	5	4+	3+	3+	3+	2+	0+	28
20 Oct'77	0	1+	1+	2	2+	3	1+	2+	14−
21 Oct'77	3−	0+	1	1	1−	1+	1+	2	10+
22 Oct'77	4−	4	5	3	3	3+	3−	4−	28+
23 Oct'77	3−	3−	2−	1−	0	0+	2	2−	12−
24 Oct'77	2+	2	1+	1+	1+	1	1+	2−	12+
25 Oct'77	2−	0+	1−	0+	0	1+	2	2	8+
26 Oct'77	1−	2+	2−	1	0+	1−	1	3	11−
27 Oct'77	4	3+	3+	6+	6−	5	7−	7−	41
28 Oct'77	6	7+	5+	3−	3+	3+	4+	2	34+
29 Oct'77	2+	2	1	3−	4−	2+	1	2−	17−
30 Oct'77	1+	1	2−	2	2+	4	2	2−	16
31 Oct'77	2	2−	2−	2−	1	1	2	1+	12+
1 Nov'77	1+	0+	1+	1	1	1−	1+	2+	9+

Table 2.2 Geomagnetic three-hourly range indices K_p for the two observation periods.

It was found that during 1975, 159 of the intervals were 3 or less and only 9 exceeded 3, where the maximum value was found to be 5+, while for the 14 day period in 1977, 95 were 3 or less and 18 exceeded 3, with a maximum value of 6. Comparing the median values of 1975 with the median values of 1977 a great similarity between the two years can be seen with the exception of the post noon median foF2 values. A marked increase during 1977 of the afternoon median foF2 values is immediately evident. At noon the difference between the median foF2 values for 1975 and 1977 is 0.4 MHz and this steadily increases to a maximum difference of 2.5 MHz at 20:00 local solar time. Thereafter the differences between the 2 periods of observations decreases. Fig. 2.16 illustrates the similarities and differences between the median foF2 values for the two periods more clearly, where the dashed line refers to 1975 observations and the solid line to the 1977 observations of foF2. This can be ascribed to the increased magnetic character of the 1977 period of observations. Also, during 1975 the observation were almost at sunspot minimum since March 1976 is the minimum for solar cycle 20. Looking at the relative sunspot numbers for the two periods it was found that the 1975 period had a mean Zurich, R_z, value of 7.4, while during the 1977 period the mean R_z value was 38.4, a factor of five times larger than the 1975 period of observations.

To illustrate the consistency in the behaviour of the F2 layer under the foregoing conditions for the two periods, plots of the upper and lower quartiles of foF2 together with the median values for both periods of observations have been included. These are shown in Fig. 2.17.

Data from 16 ground based "surrounding" stations were available for the periods of interest to this study. Although some stations exhibited a distinct lack of useful data for both periods it was possible to calculate confident median values for the 1975 period. For the 1977 period the median values are less reliable, since the period of observations was for 14 days only.

The median values of foF2 at Gough Island for October/November 1975 are plotted together with those for the surrounding permanent ionosphere observatories at Tucuman (26.9°S; 65.4°W), Grahamstown (33.3°S; 26.5°E), Buenos Aires (34.5°S; 58.5°W), Marion Island (46.9°S; 37.9°E), Port Stanley (51.7°S; 57.8°W), South Georgia (54.3°S; 36.5°W) and Sanae (70.3°S; 2.4°W) are shown in Fig. 2.18. It is noticeable that foF2 at Gough Island exceeds those at all the other stations, with the exception of Tucuman and Buenos Aires, during the daylight hours, but during the night it is greater than Marion Island and comparable with those at Grahamstown and Sanae. The night time values at the remaining observatories tend to be much higher.

The minimum foF2 values of Tucuman and to a lesser extent that of Buenos Aires at about

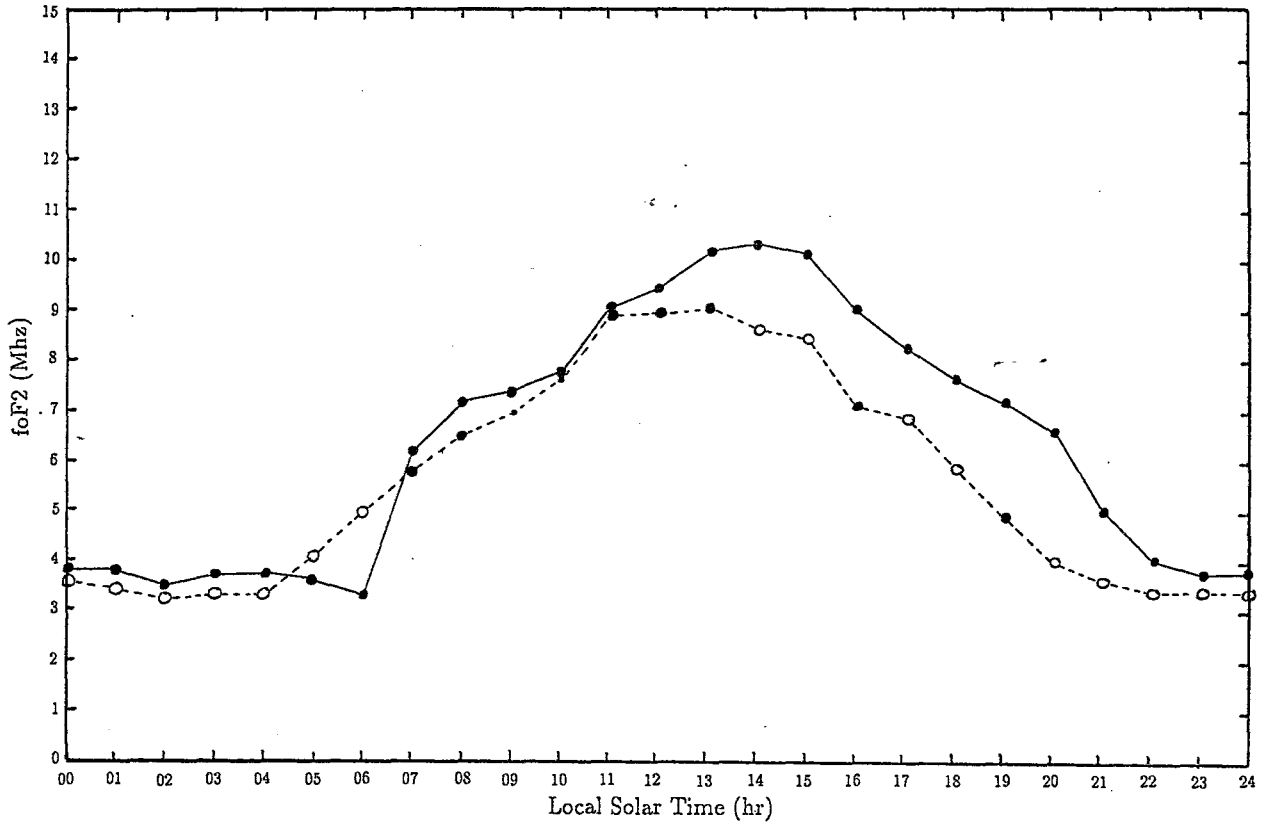

Figure 2.16: Median foF2 values at Gough Island during the 1975 (dashed line) and 1977 (solid line) observation periods.

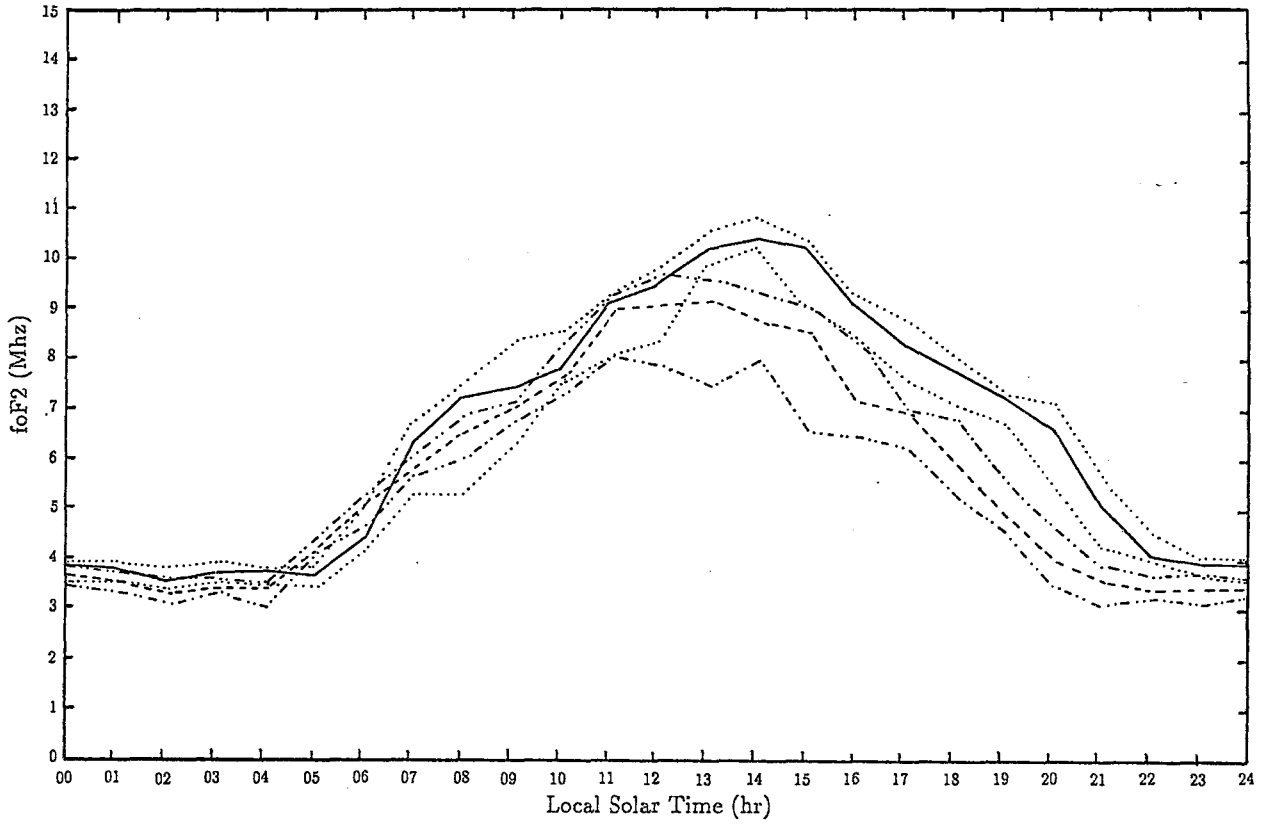

Figure 2.17: Median, upper and lower quartiles of foF2 values at Gough Island during the 1975 (dashed line) and 1977 (solid line) observation periods.

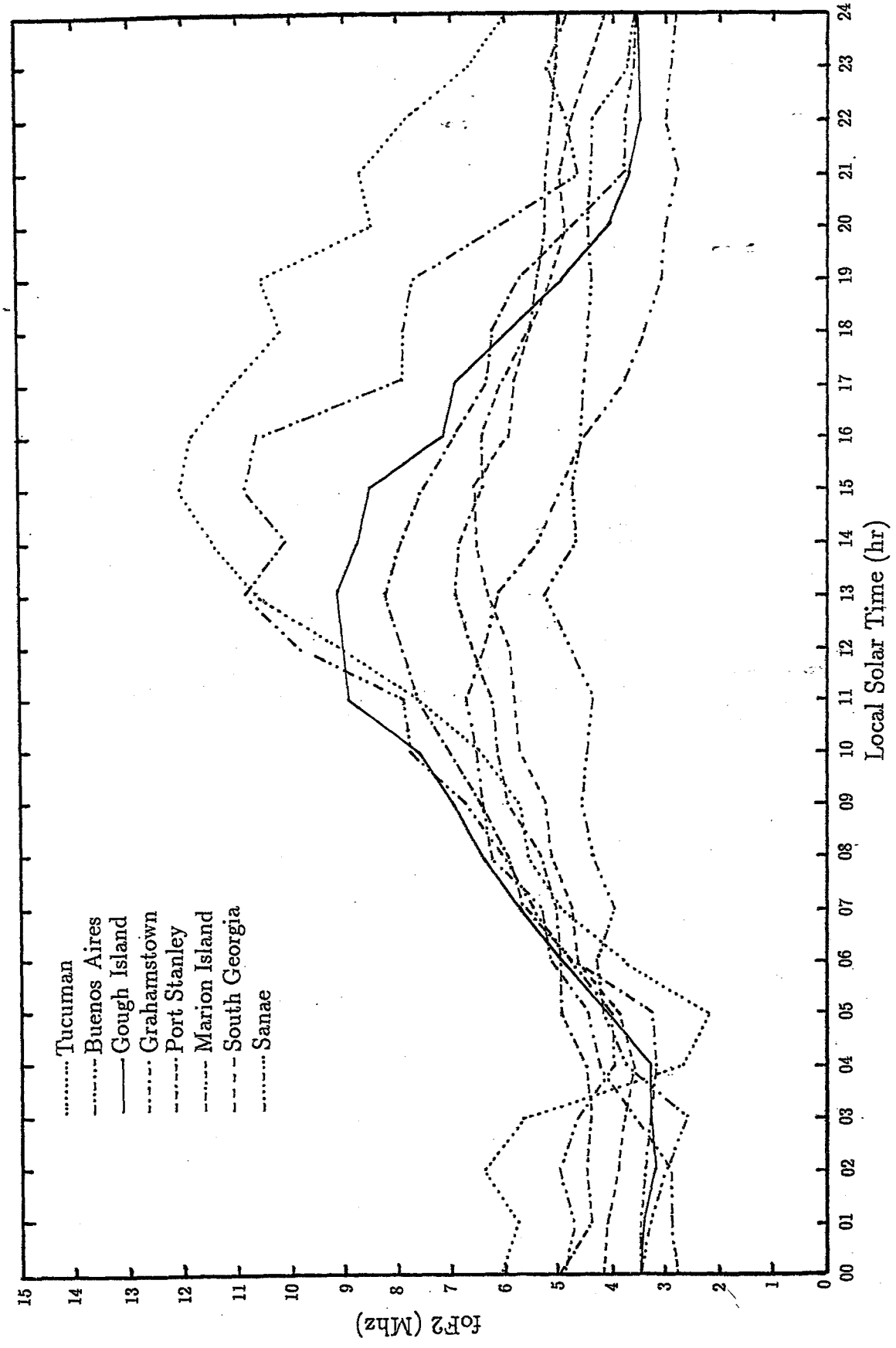

Figure 2.18: Comparison of median foF2 values at seven selected stations for the 1975 observation period together with those from Gough Island.

sunrise as well as their enhanced foF2 values in the afternoon could be ascribed to their proximity to the equatorial anomalous region. The equatorial anomaly produces enhanced foF2 near 20° geomagnetic south, which corresponds to approximately 30° geographic south, in the afternoon. (De Mendonca, 1965). The equivalent graph for the period of observation during 1977 is shown in Fig. 2.19. As can be seen, Figures 2.18 and 2.19 exhibit similar properties.

Fig. 2.20 shows the magnetic field intensity at 300 km for the region of interest as well as the observatories used in this study. As can be seen only Buenos Aires and Tucuman lie closer to the area of minimum magnetic field intensity than Gough Island as indicated by the contours of constant magnetic field intensity (B) at 300 km. (Stassinopoulos, 1970).

The following five graphs are an attempt to find some form of correlation between the maximum median foF2 and various physical phenomena or properties for the fifteen permanent observatories shown in Fig. 2.20 and Gough Island.

Fig. 2.21 shows geomagnetic longitude plotted against maximum median foF2 to investigate any possible interdependence between the critical frequency and geomagnetic longitude as suggested by Greenspan and Stone, 1964, Torr *et al.*, 1975 and the results obtained during the voyages between South Africa and Gough Island. From the diagram the conclusion may be reached that the closer one is to the zone marked South Atlantic Anomaly in Fig. 2.20, the greater the enhancement in foF2. Superimposed on all these graphs is the least squares fit line and the correlation coefficient r^2 for the plotted data.

Seeking an explanation for the enhancement of foF2 at Gough Island, the maximum median values versus magnetic dip (Fig. 2.22), and the B field at 300 km altitude (Fig. 2.23) were plotted. Likewise, plots of maximum median values versus the McIlwain's parameter L at 300 km (Fig. 2.24) and the great circle distance from minimum magnetic field intensity B (Fig. 2.25) as determined by Muzzio *et al.* (1966) were prepared. Figures 2.23 and 2.25 are both highly suggestive of a spatial dependence of foF2 upon position relative to the centre of the South Atlantic Magnetic Anomaly.

The 1975 maximum median values of foF2, foF1 and foE are plotted against geographic latitude for Johannesburg (26.1°S), Tucuman (26.9°S), Grahamstown (33.3°S), Hermanus (34.4°S), Buenos Aires (34.5°S), Gough Island (40.4°S), Marion Island (46.9°S), Kerguelen (49.4°S), Port Stanley (51.7°S), South Georgia (54.3°S), Argentine Islands (65.2°S), Mawson (67.6°S), Syowa (69.0°S), Sanae (70.3°S), Halley Bay (75.5°S) and Belgrano (77.9°S) in Fig. 2.26. The variation

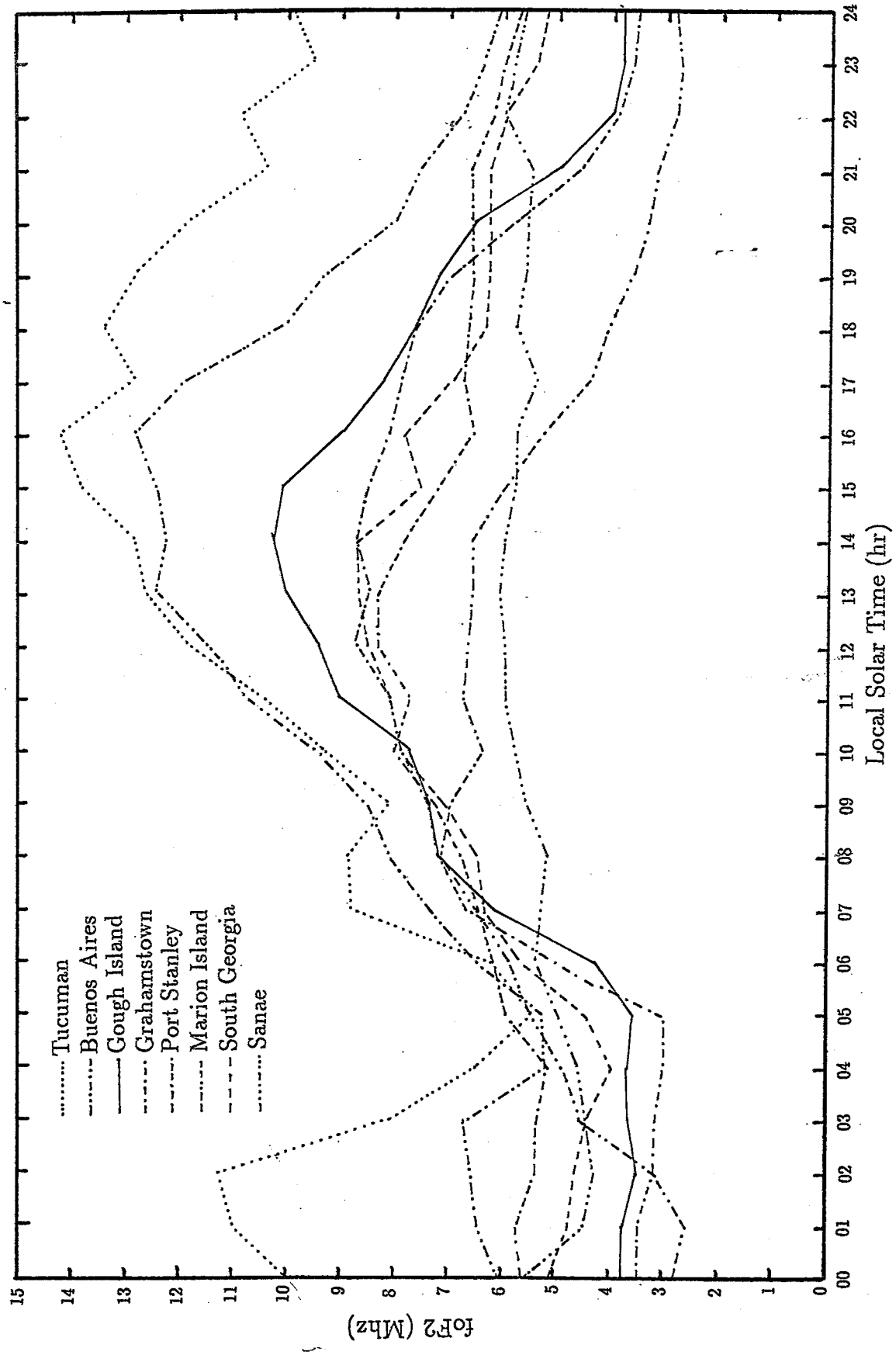

Figure 2.19: Comparison of median foF2 values at the seven selected stations for the 1977 observation period together with those from Gough Island.

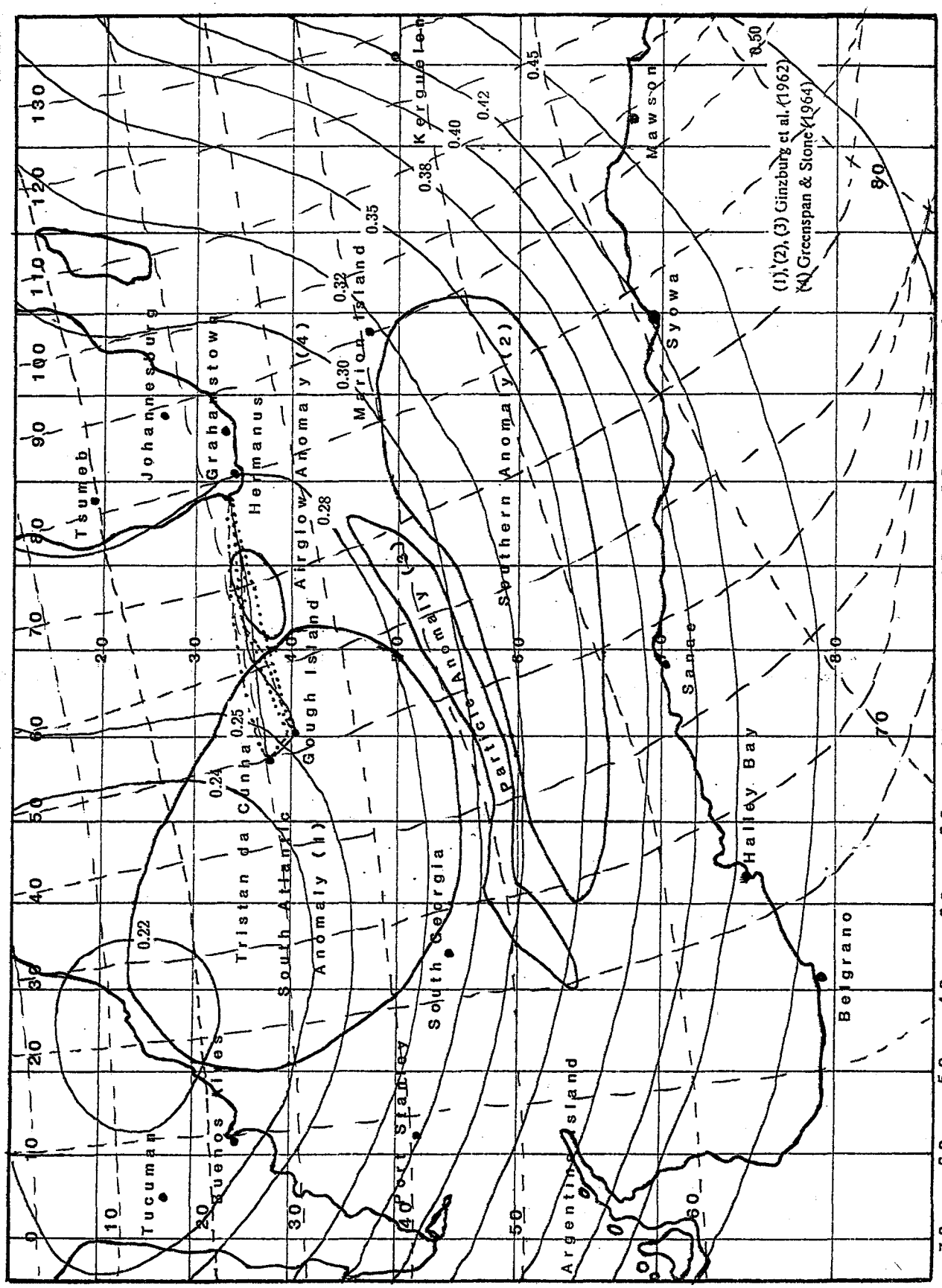

Figure 2.20: Map showing the contours of magnetic field intensity B (in gauss, where a G is 10^{-4}T) at 300 km, as well as the surrounding permanent observatories. The dashed lines shown correspond to the geomagnetic co-ordinates.

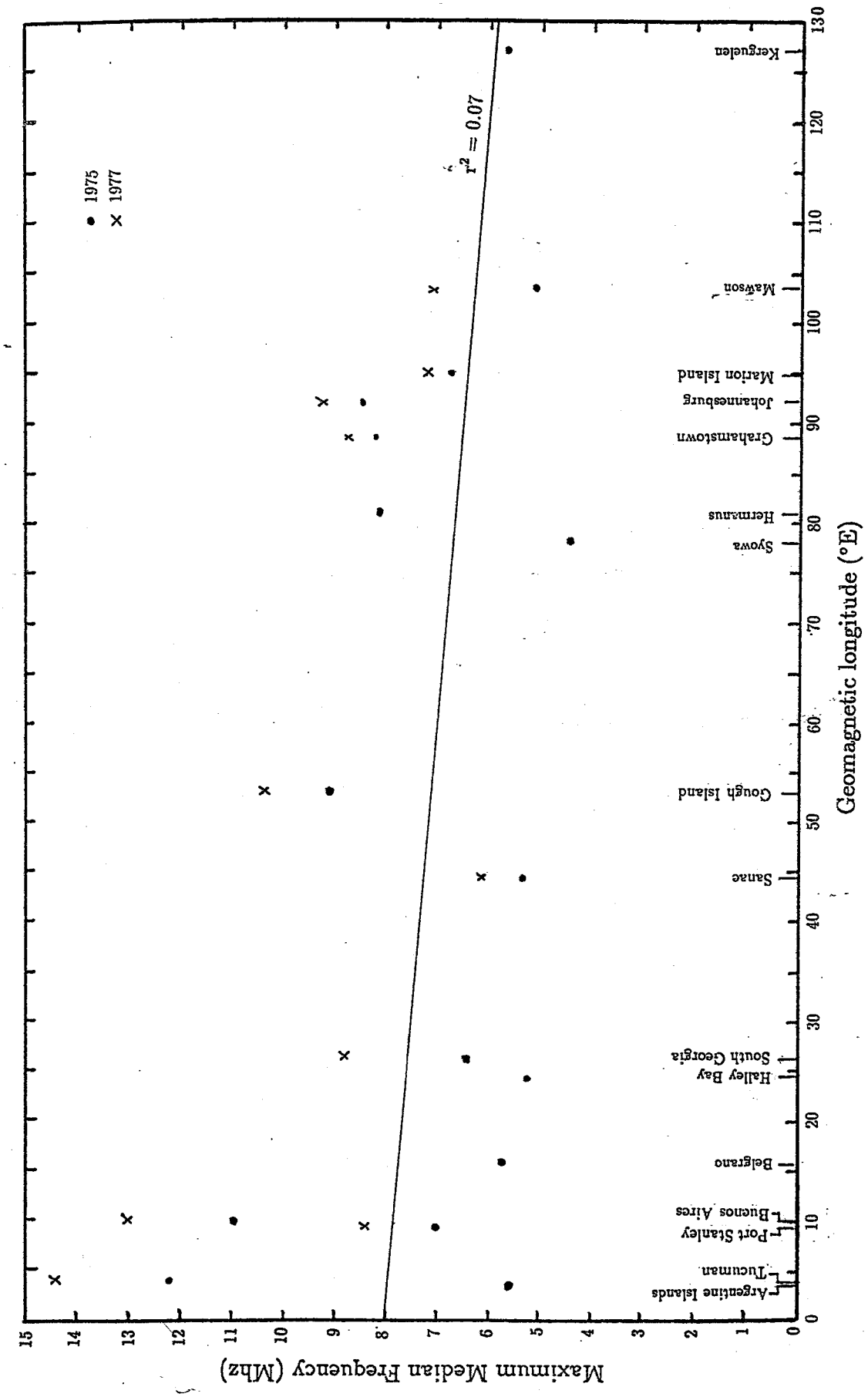

Figure 2.21: Maximum median foF2 values versus geomagnetic longitude in degrees East for the 15 permanent surrounding observatories and Gough Island.

is surprisingly regular, with the exception of foF2 at Gough Island, which deviates from the straight line shown by about 1.5 MHz. Tucuman and Buenos Aires exhibit a similar deviation of 3.6 MHz and 3.0 MHz respectively which could be due to the previously mentioned equatorial anomaly.

Kerguelen (70.3°E), Mawson (62.9°E) and Syowa (39.6°E) all lie below the straight line but then these three stations are all far away from the South Atlantic Anomaly in the eastern sector. Belgrano, which lies above the straight line, suffered from a paucity of numerical values, the maximum count being 5 for any particular hour with an average count of 2 or 3.

A superposition of the 1977 maximum median foF2 values and geographic latitude for those stations for which data are available reinforces the findings for the 1975 data, as shown in Fig. 2.27. The 1977 data should be treated rather cautiously as the median count during the 1977 period is only for 14 days. It should also be borne in mind that the magnetic field was more active during the 1977 period.

Fig. 2.28 shows a superposition of the 1975 and 1977 maximum median values of foF2, foF1 and foE plotted against the geomagnetic latitude of the preceding surrounding permanent observatories. There is a marked similarity between Figures 2.27 and 2.28, suggesting that the latitudinal position of Gough Island relative to the centre of the Anomaly region is of cardinal importance.

Hence it may not be just a coincidence that Gough Island is also the only station which lies inside the zone marked "South Atlantic Anomaly" in Fig. 2.5. Most workers who have made satellite-borne observations over the South Atlantic have reported increases in the electron density in the South Atlantic Anomaly zone (Gledhill, 1976 and the references contained therein), suggesting that the precipitating electrons which penetrate to the lower atmosphere in the area of minimum magnetic field intensity are swept south eastwards by atmospheric winds and dispersed in the South Atlantic Anomaly region. This influx of precipitated electrons increases the electron density which leads to enhanced foF2 values.

More specifically Gledhill and Hoffman (1981) have reported the results of a four-year survey of electron precipitation, using data from the satellite Atmosphere Explorer-C. They found that the flux of positive ions at 300 km, in the energy range 0.2 to 26 keV, to be insignificant, but they showed that there was a considerable downward flux of electrons in that energy range. Vampola and Gorney (1983) have reported similar measurements of electrons in the range 36

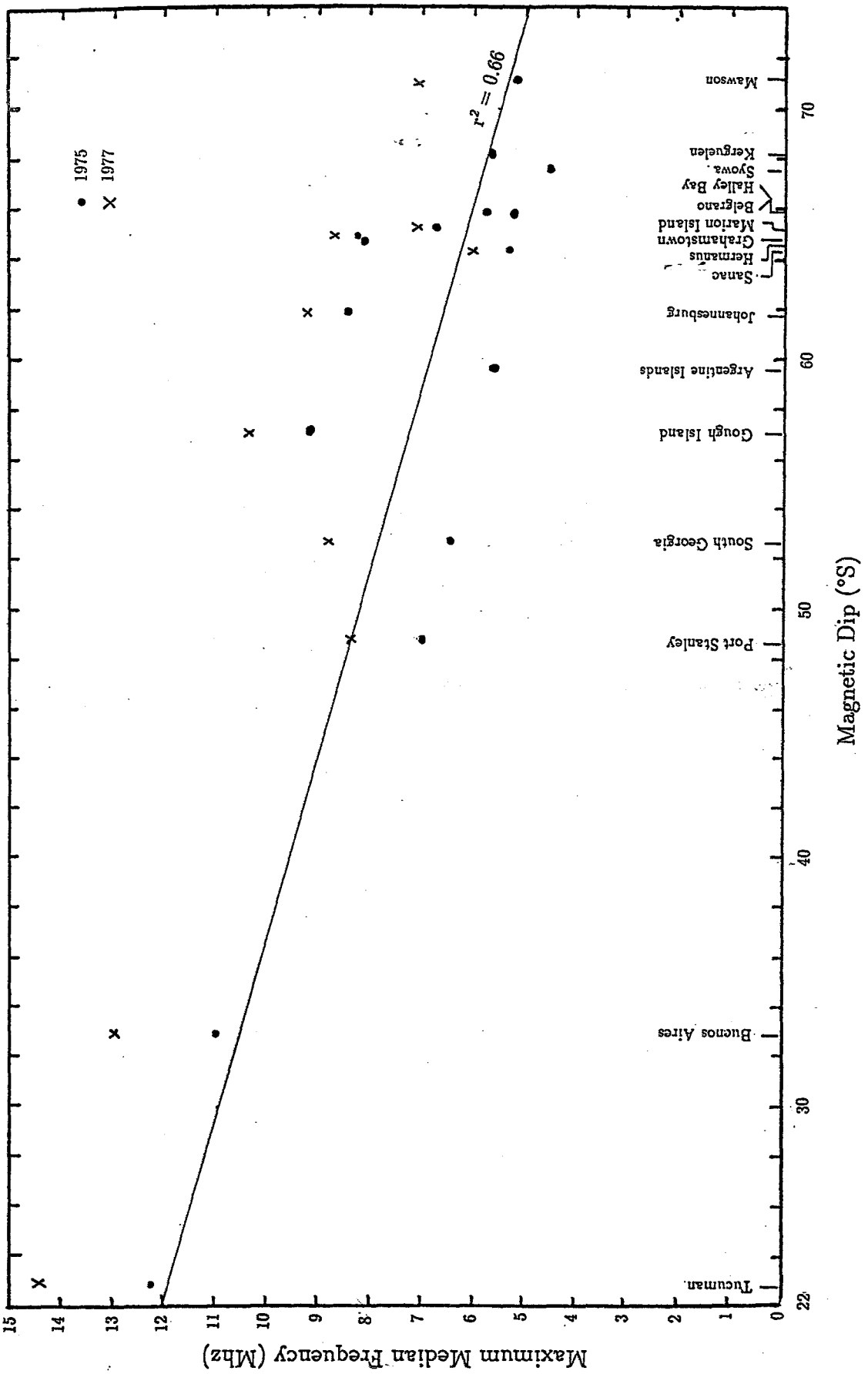

Figure 2.22: Maximum median foF2 values versus magnetic dip in degrees South from the equator for the 15 permanent surrounding observatories and Gough Island.

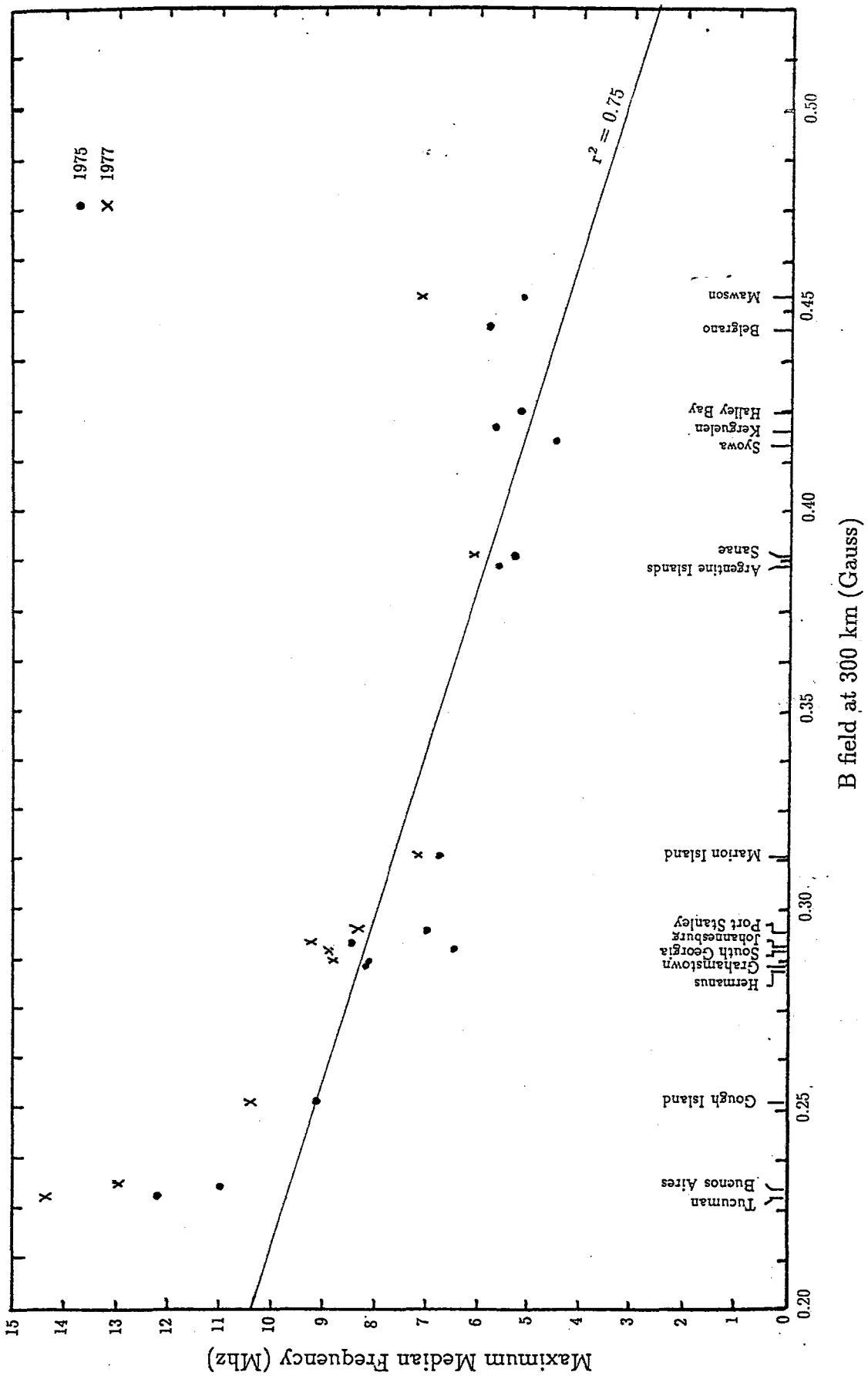

Figure 2.23: Maximum median foF2 values versus the magnetic field intensity B at 300 km altitude in gaussian units for the 15 permanent surrounding observatories and Gough Island.

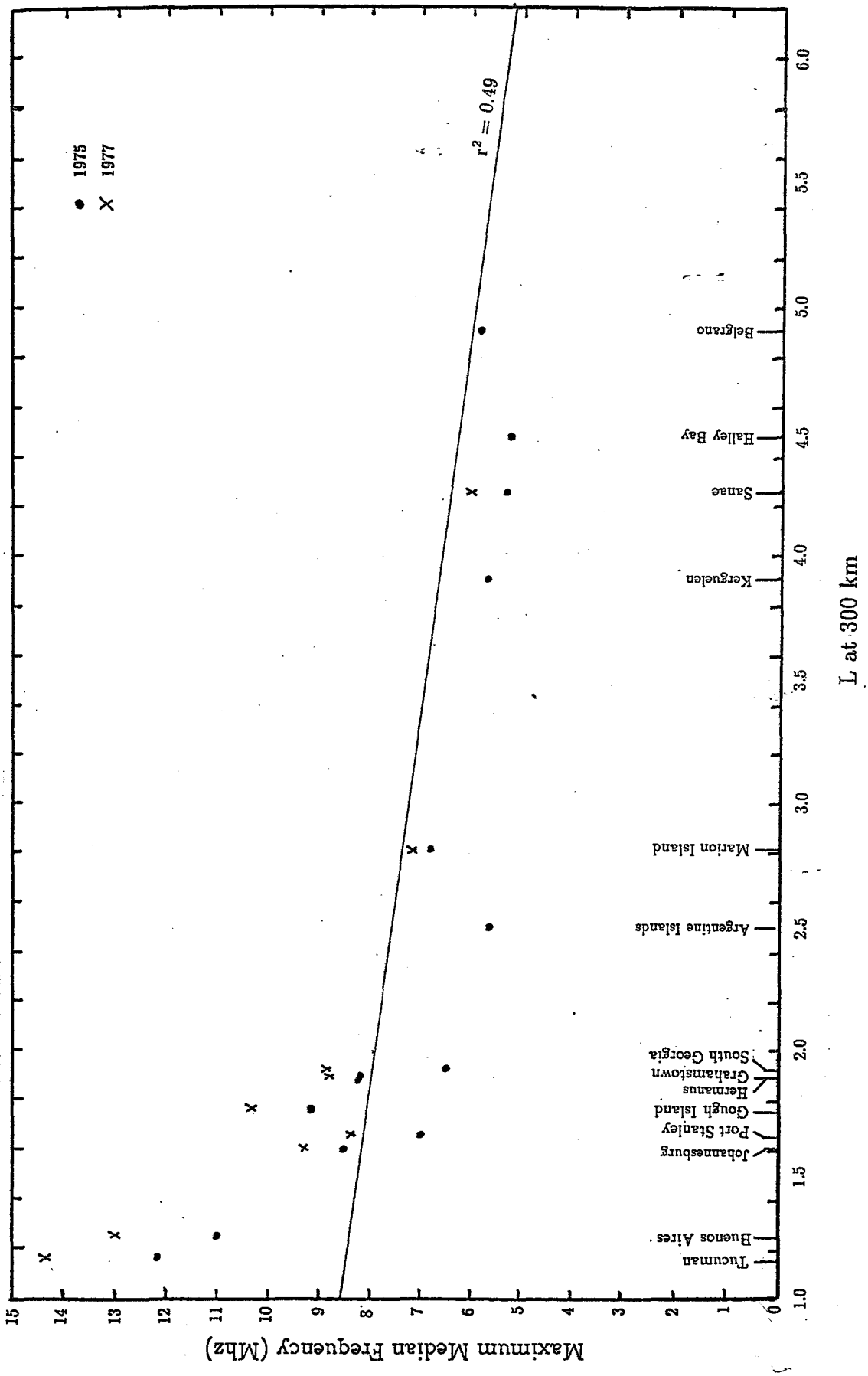

Figure 2.24: Maximum median foF2 values versus McIlwain parameter L at 300 km for the 15 permanent surrounding observatories and Gough Island.

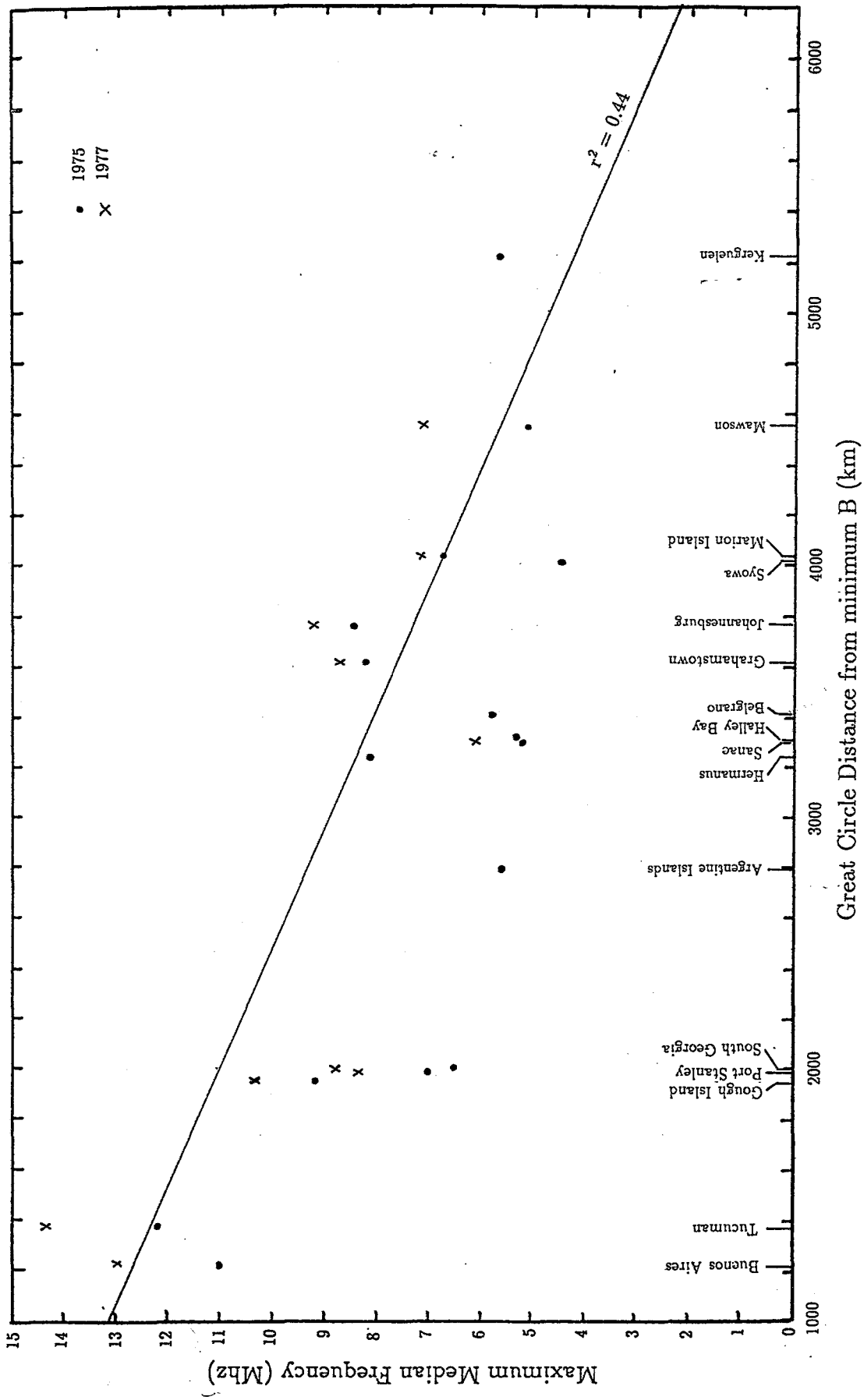

Figure 2.25: Maximum median foF2 values versus great circle distance in km from minimum B for the 15 permanent surrounding observatories and Gough Island.

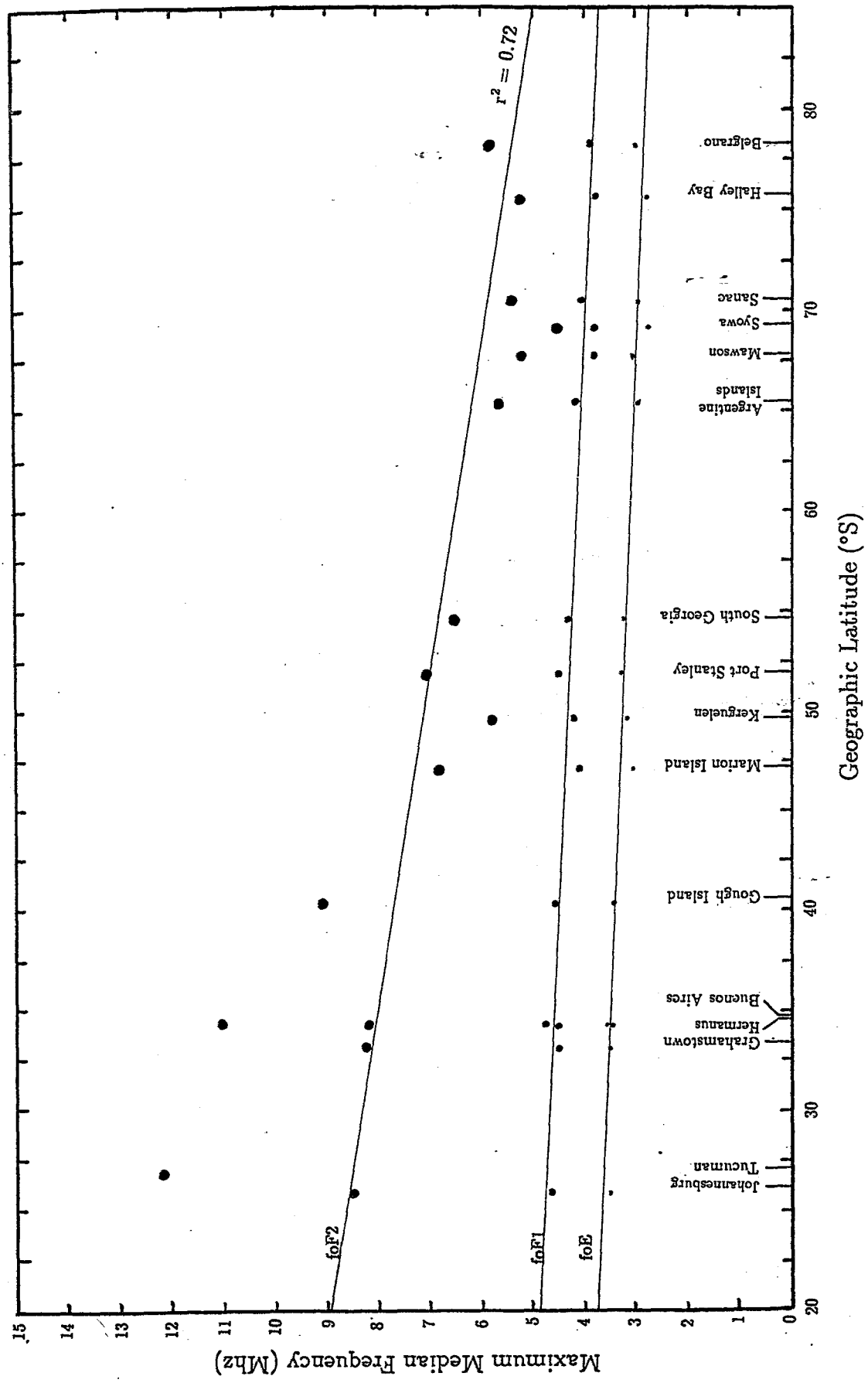

Figure 2.26: Maximum median foF2, foF1 and foE values versus geographic latitude in degrees south for the 15 permanent surrounding observatories and Gough Island.

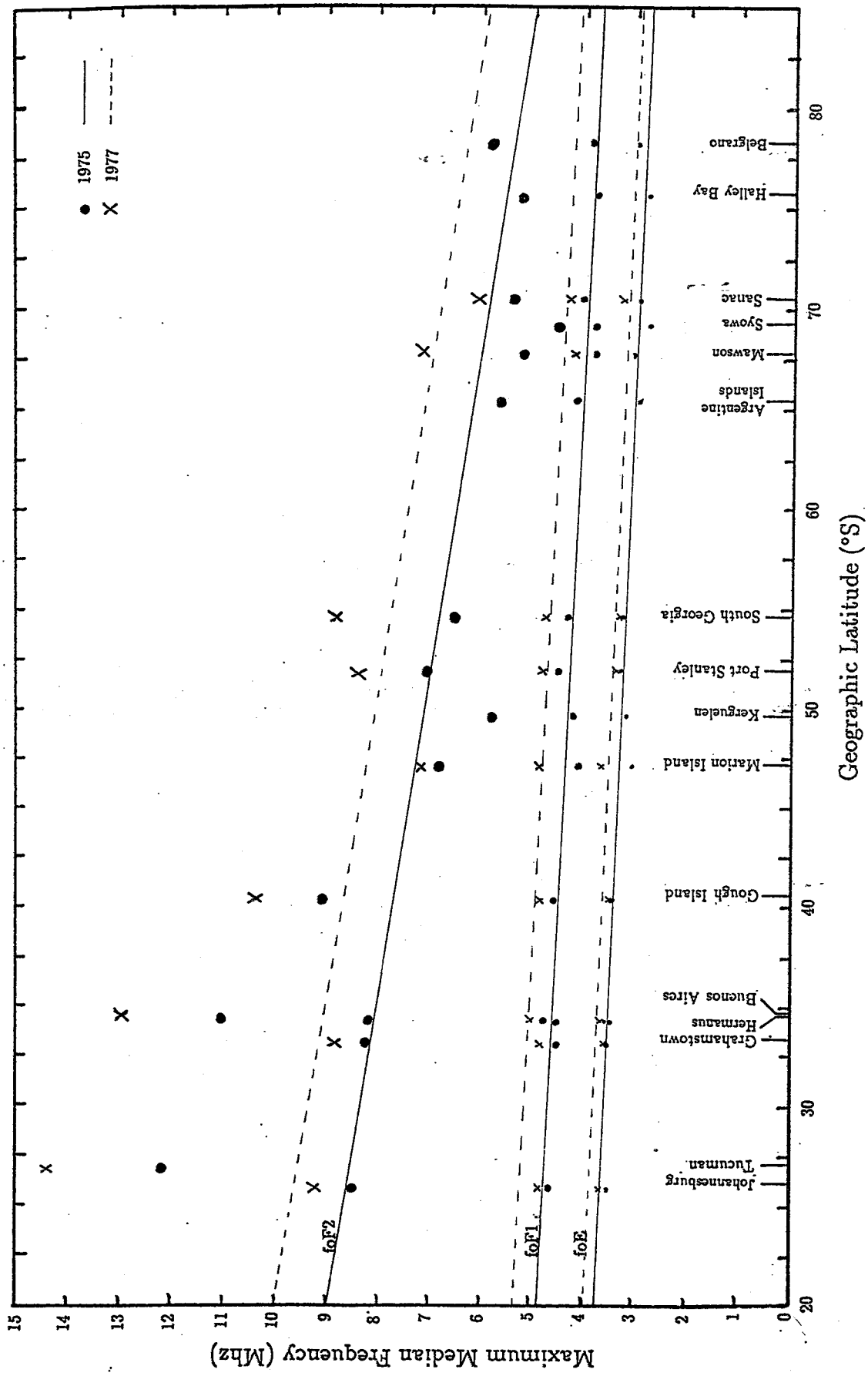

Figure 2.27: The 1977 maximum median foF2, foF1 and foE values superimposed on the 1975 values versus geographic latitude in degrees south for the 15 permanent surrounding observatories and Gough Island.

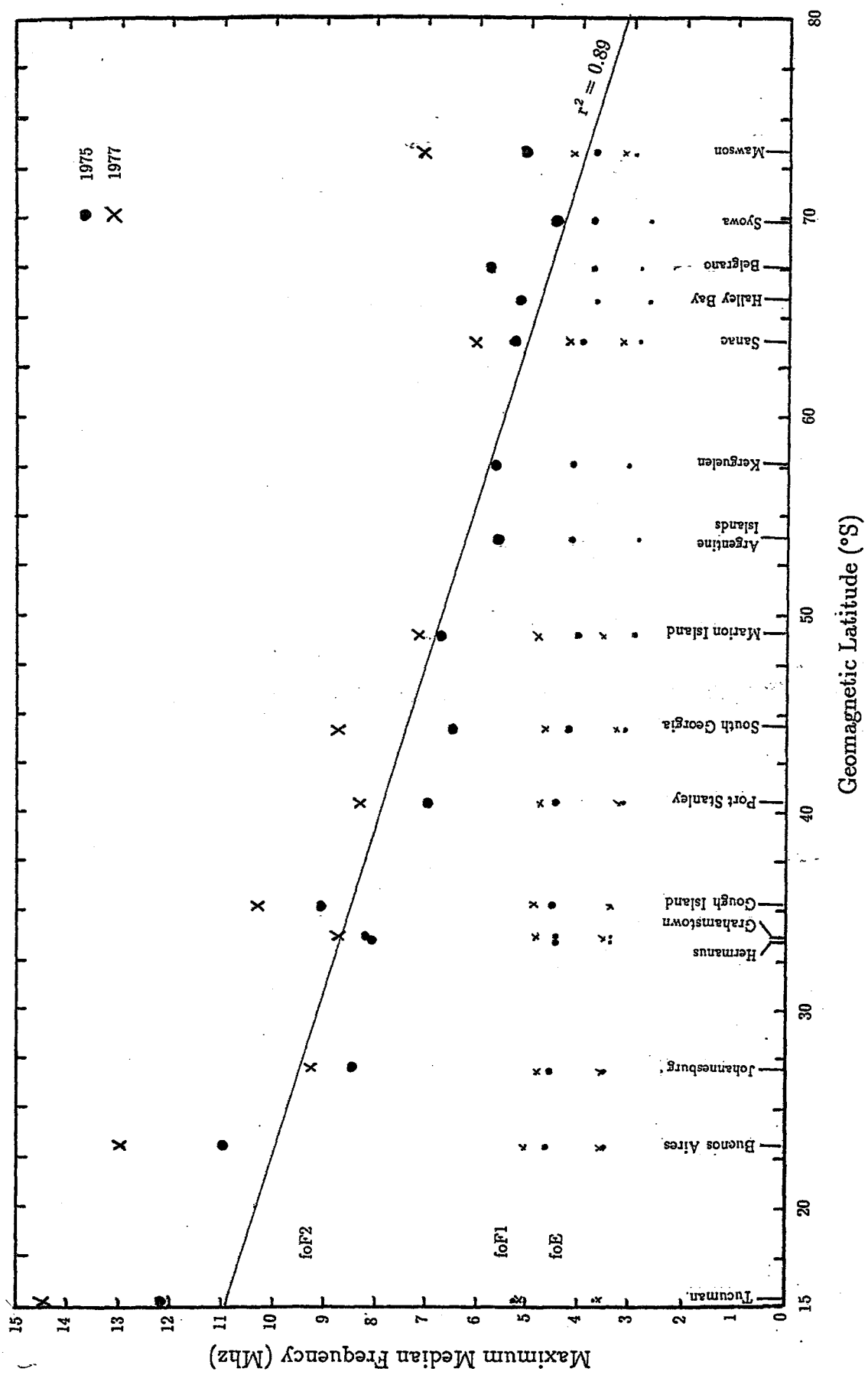

Figure 2.28: The maximum median foF2, foF1 and foE values for 1975 and 1977 versus geomagnetic latitude in degrees south for the 15 permanent observatories and Gough Island.

to 317 keV, from the satellite S 3-2. Gough Island (40.4° S; 9.9° W; L = 1.7) lies in the region of most intense electron precipitation, according to the findings of Gledhill and Hoffman (1981) and of Vampola and Gorney (1983).

2.4 The E-region Ionosphere

The E-region is the part of the ionosphere directly affected by precipitating electrons in the energy range above 1 keV and it is also more amenable to quantitative treatment than the more irregular F- region. It is speculated that the enhancement of foF2 of Gough Island was possibly due to particle precipitation. With this in mind, it was decided to investigate the E-region more fully.

Unfortunately, the antenna system on the research ship RSA did not permit observations of the ionosphere below 1.2 MHz, so that no experimental information on nighttime E-region ionization could be obtained. The value 1.2 MHz was the lowest f_{min} value observed on any of the ionogrammes recorded during the voyage. The satellite measurements of electron fluxes reported by Gledhill and Hoffman (1981) refers to nighttime only. The measurements of Vampola and Gorney (1983) are means for all hours of the day and night, however, they refer to energies so high that most of their effects occur below the E-layer peak.

Good ionogrammes were nevertheless available for the daytime E-region, from which the critical frequency foE could be determined with satisfactory precision. It was therefore decided to examine these for anomalous variation of the daytime foE with solar zenith angle, in order to look for any extra ionization which might be attributed to the precipitating electrons.

It is well known that foE varies regularly with solar zenith angle χ. Plots were thus prepared of foE versus $\cos\chi$ and $(\text{foE})^2$ versus $\cos\chi$ as shown in Figures 2.29 and 2.30, where the latter plot was to provide a better straight line fit to the data. Muggleton (1972) showed that a linear relationship of the form

$$(\text{foE})^2 = A\cos^n\chi$$

existed between the critical frequency of the E-layer and solar zenith angle where the value of n had a world value of about 0.6. This value of n for the Gough Island data was found to be $n = 0.529$ as inferred from Fig. 2.31.

Chapman (1931) proposed the use of a function $\text{Ch}(x,\chi)$ as an E-region describing function

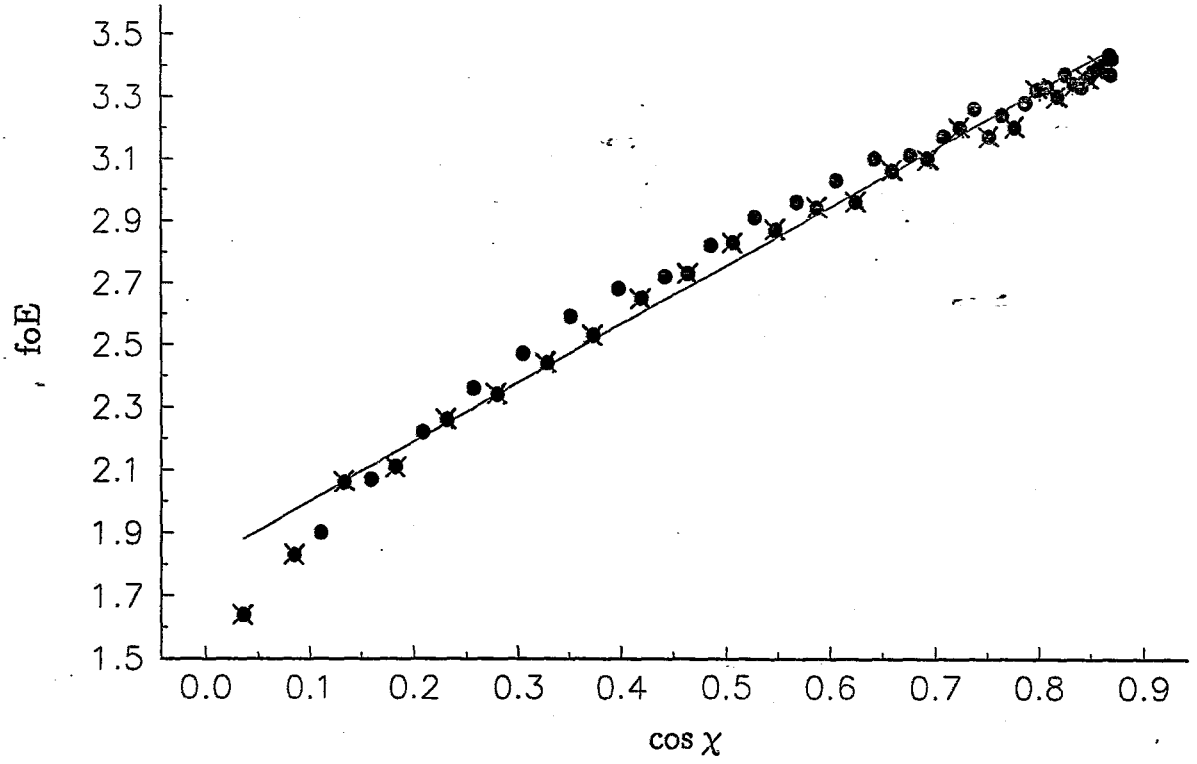

Figure 2.29: Plot of foE versus $\cos\chi$ for mean quarter- hourly values over the 21 day period, 13 October to 3 November 1975 at Gough Island, where the crosses denote morning values and the circles afternoon values.

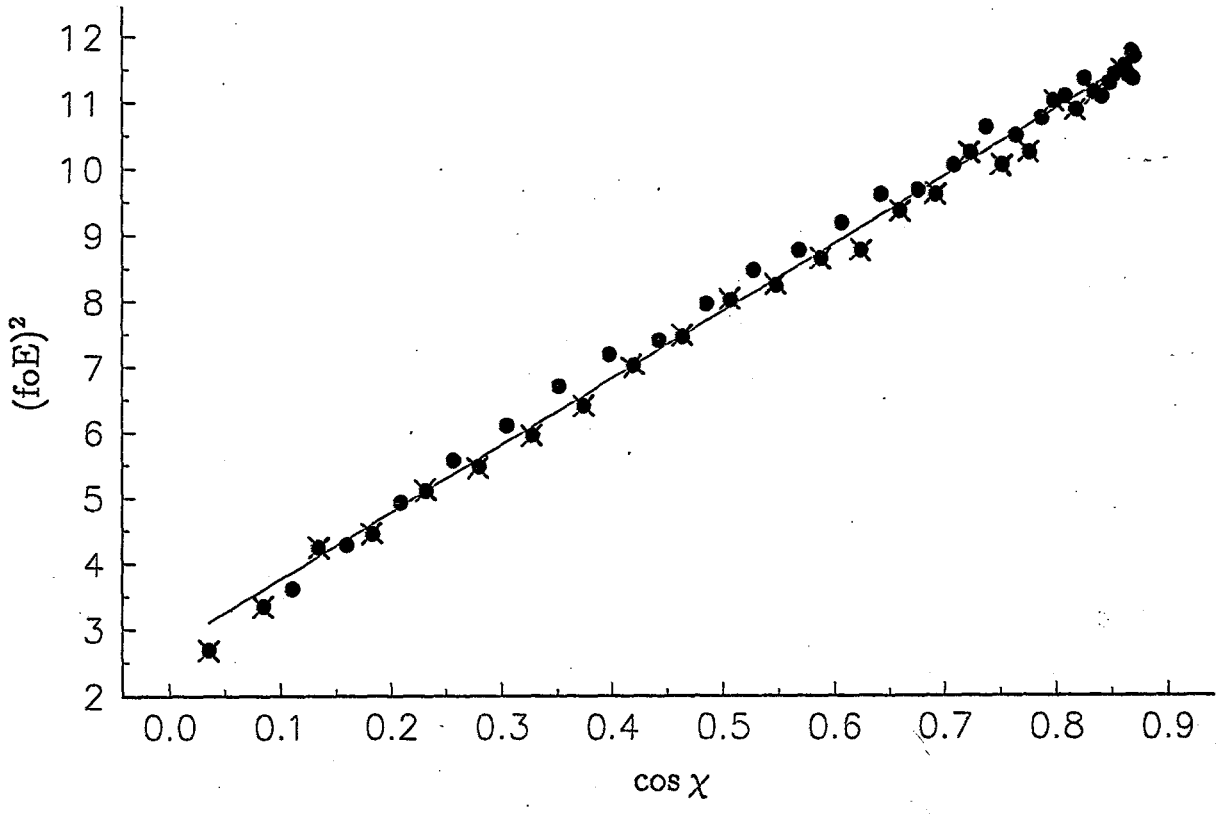

Figure 2.30: Plot of $(\text{foE})^2$ versus $\cos\chi$ for mean quarter-hourly values over the 21 day period. 13 October to 3 November 1975 at Gough Island, where the crosses denote morning values and the circles afternoon values.

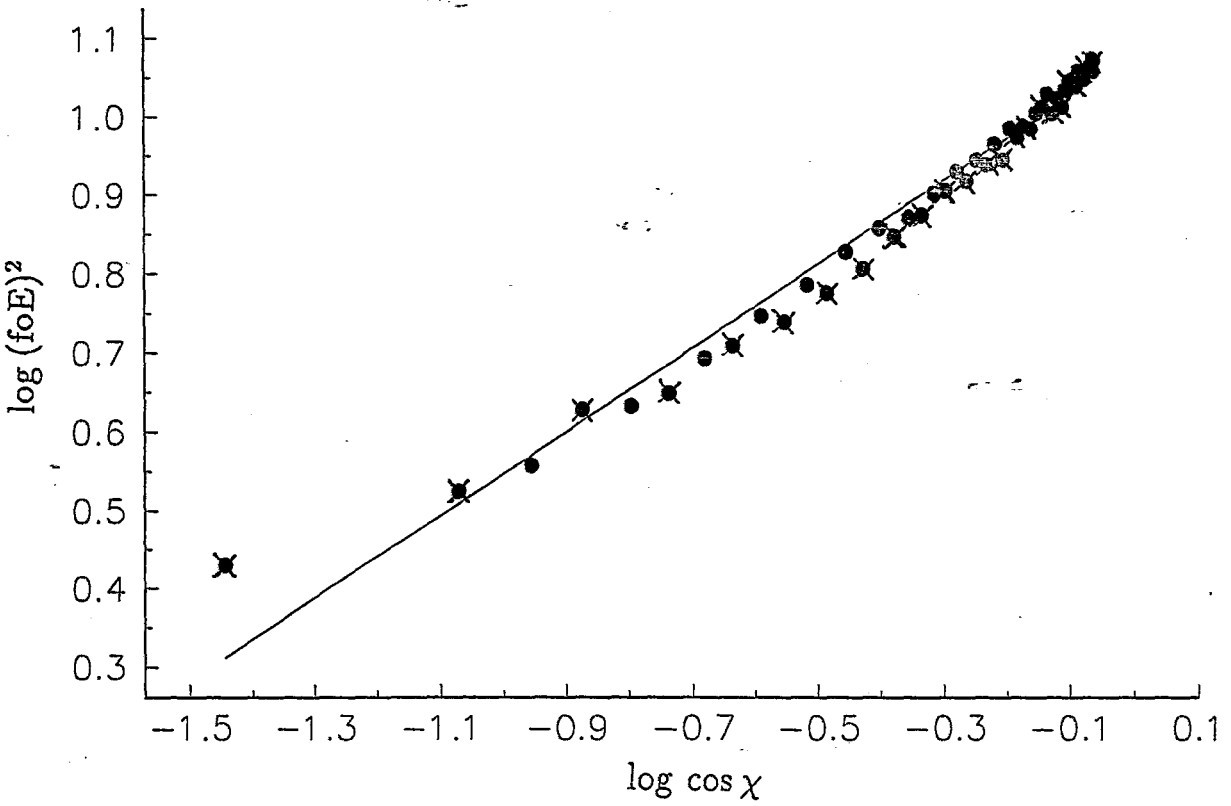

Figure 2.31: Plot of log $(\text{foE})^2$ versus log $\cos\chi$ for mean quarter-hourly values over the 21 day period, 13 October to 3 November 1975 at Gough Island, where the crosses denote morning values and the circles afternoon values.

where x is a parameter dependent on the scale height H and the layer height h, known as the Chapman grazing incidence function (Chapman, 1931; Wilkes, 1954).

Briefly, the need for the Chapman function arises because the basic theory of electron production rate assumes a plane-stratified isothermal atmosphere. The solar zenith angle χ is simply related to the electron production rate as $\sec\chi$ which is just the inverse of $\cos\chi$, where the electron production rate q at height h and solar zenith angle χ is given by

$$q = q_0 \exp(1 - z - e^{-z}\sec\chi),$$

where q_0 is the maximum rate of electron production occurring at height h_0 when the sun's rays are vertical and where $z = (h - h_0)/H$, where H is the scale height of the ionized atmosphere. This relationship is generally sufficient for low and medium values of χ. For the higher range of values ($\chi > 70°$) and also to take into account the sphericity of the earth and its atmosphere the $\sec\chi$ term is replaced by the Chapman function $\text{Ch}(x,\chi)$ which remains finite for $\chi \geq 90°$. The fact that $\text{Ch}(x,\chi)$ remains finite for $\chi \geq 90°$ is an important consideration, since the values of χ in this study extended to 104°. The Chapman grazing incidence function is thus defined as

$$\text{Ch}(x,\chi) = x\sin x \int_0^x \exp\{x(1 - \sin\chi/\sin\lambda)\}\csc^2\lambda d\lambda,$$

where λ is the scale height gradient.

Since χ and H are not independent of h, it was decided to plot log foE versus log Ch(x, χ). The resultant graph normally yields a good straight line with a slope that is usually about -0.35 instead of the value -0.25 appropriate for an isothermal Chapman layer. The difference may be attributed to the influence of the temperature gradient in the E-region (Rishbeth and Garriott, 1959). Fig. 2.32 shows the graph of log (foE) versus log Ch(x, χ) for the mean quarter-hourly values of foE over the 21 day stay at Gough Island, where $x = 800$ has been used in computing the Chapman function, which corresponds to a scale height of approximately 8 km at 110 km altitude (cf. CIRA, 1972).

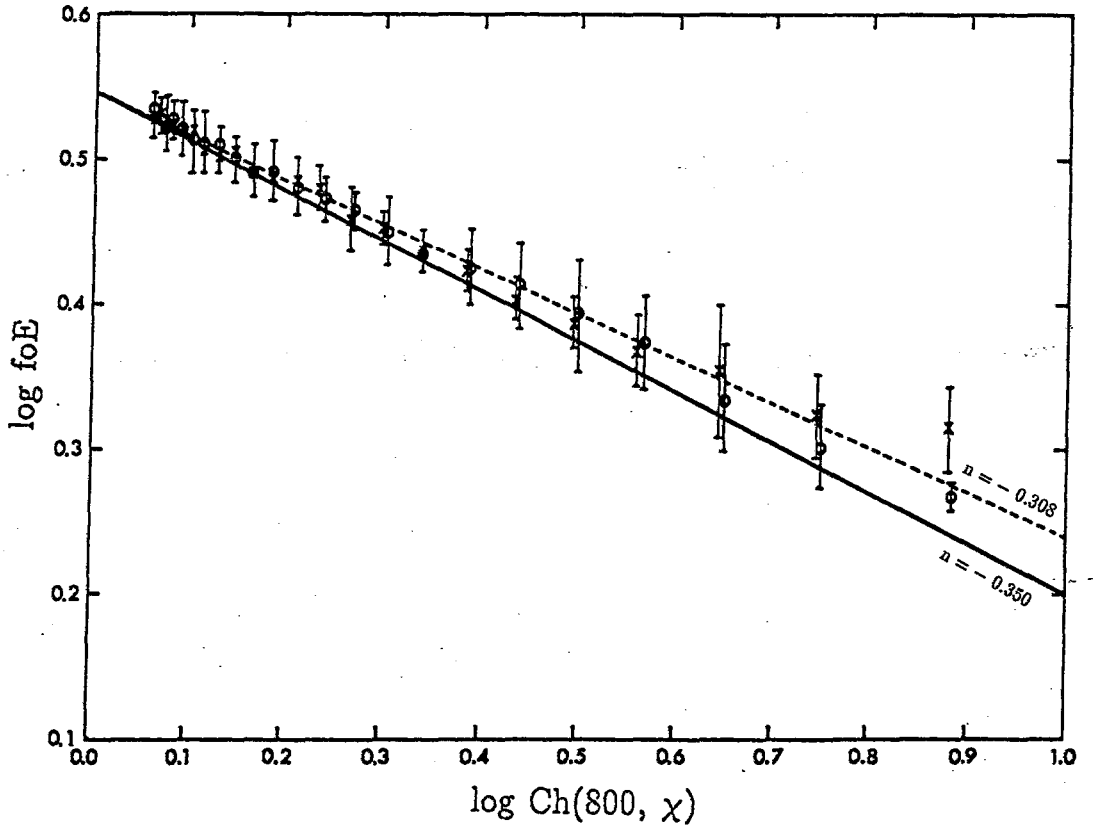

Figure 2.32: Plot of log foE versus log Ch(800, χ) for mean quarter-hourly values over the 21 day period, 13 October to 3 November 1975 at Gough Island, where the crosses denote morning values and the circles afternoon values.

The crosses denote morning values and the circle afternoon values. The error bars show the standard deviations of the means, i.e., $\left(\sum d_i^2/n(n-1)\right)^{1/2}$. There is a reasonably linear relationship for log Ch(x, χ) less than 1, corresponding to solar zenith angles smaller than 85°. The least-squares-fitted straight line, shown dashed, has a slope of -0.308 ± 0.008 and the intercept on the log foE axis is 0.546 ± 0.004. The antilog of 0.546 will yield the value of solar zenith angle $\chi = 0$, that is when the sun is overhead.

For comparison purposes sufficiently complete and reliable data for foE during the same 21 day period from nine stations in the vicinity of the South Atlantic Anomaly was obtained. Their locations are shown in Fig. 2.33. The data from these stations were plotted, Fig. 2.34, to determine the slopes and intercepts of the best-fitting straight lines on the log foE versus log $\mathrm{Ch}(x, \chi)$ graphs. The results are tabulated in Table 2.3, from whence it is clear that the slope of the Gough Island graph is anomalously low for its latitude. The standard deviations of the slopes and intercepts were calculated by the usual formulae for a least-squares straight line fit (Meyer, 1975)

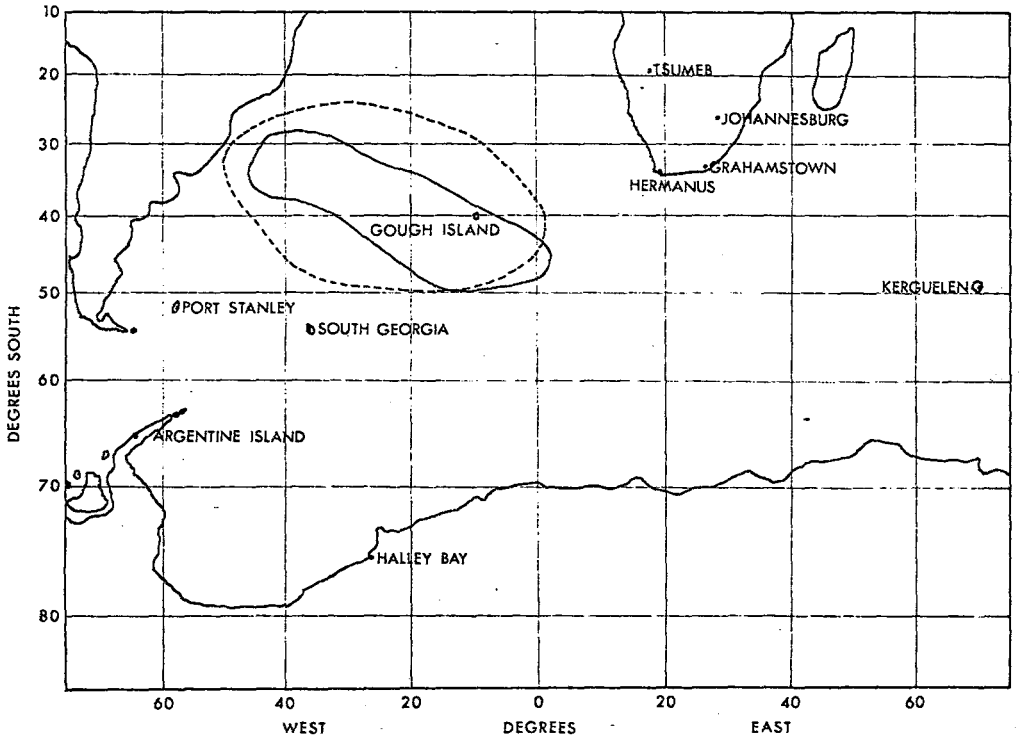

Figure 2.33: Locations of the 10 stations, which contributed to the E-region analysis, with respect to the South Atlantic Anomaly. Contours indicating the regions of precipitation of high energy (- - -) and low energy (—) electrons are from Gledhill and Hoffman (1981).

If the E-region were predominantly solar controlled a reasonably smooth variation of these slopes and intercepts with geographic latitude λ would be expected. The plot of foE versus $\cos\chi$ or log foE versus log $(\cos\chi)$ for stations at different latitudes for the same solar zenith angle yields an approximately straight line graph. Noting from Table 2.3 that the slope n decreases with increasing latitude, plots of slope n versus geographic latitude λ were prepared as well as slope n versus $\cos\lambda$. To determine the power of $\cos\lambda$ which yielded the best straight line fit a plot of log (slope n) versus log $(\cos\lambda)$ was prepared which showed that the best straight-line fit was proportional to $\cos^{0.177}\lambda$.

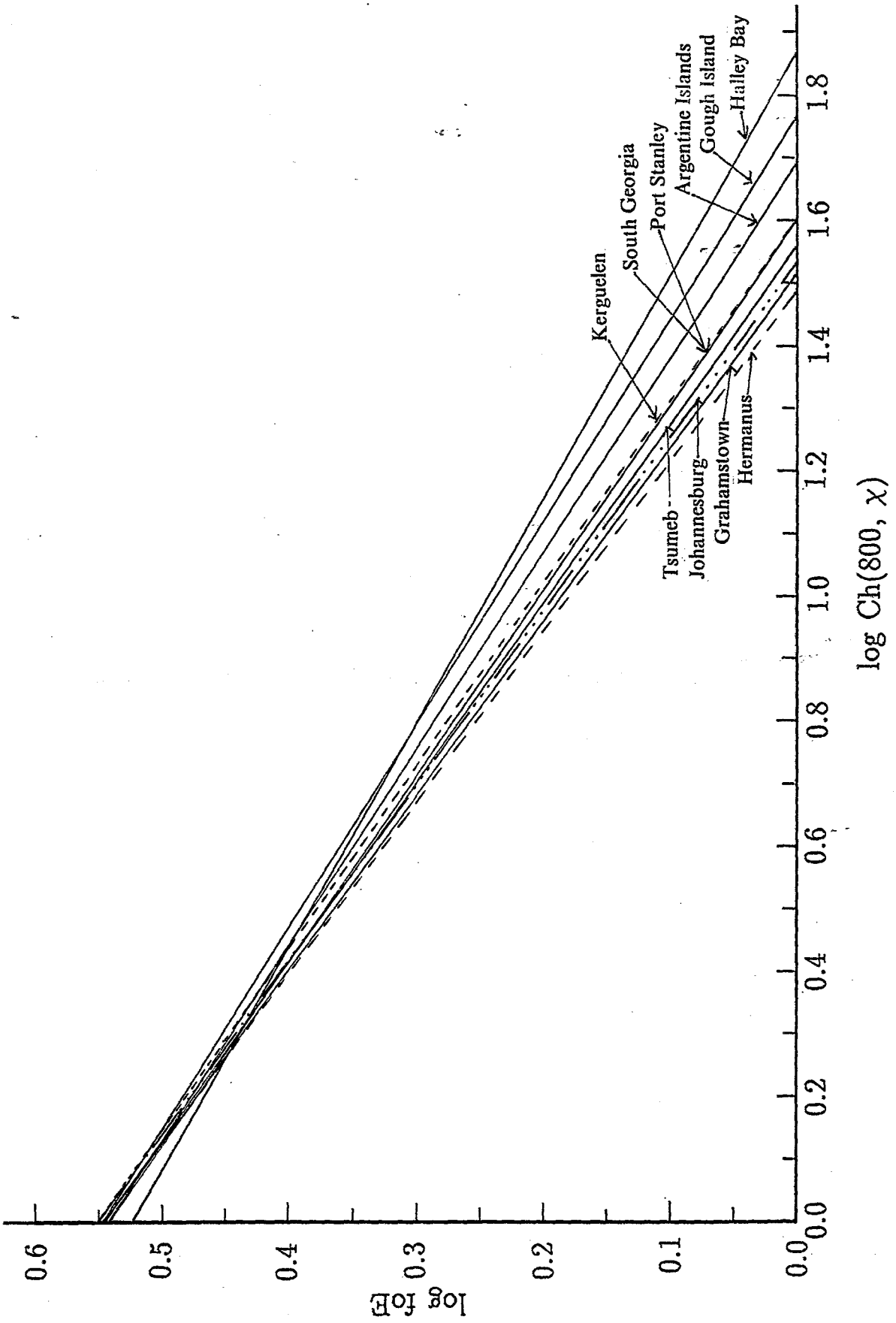

Figure 2.34: Plot of log foE versus log Ch(800, χ) for the 9 comparison stations and Gough Island for the period 13 October to 3 November 1975.

The slopes from Table 2.3 and their estimated standard deviations are plotted against $\cos^{0.177}\lambda$ in Fig. 2.35. The magnitude of the slopes are shown here, although all are in fact negative. This diagram clearly shows the anomalous behaviour of the Gough Island results. The points for the nine comparison stations are all within one standard deviation of the weighted least-squares straight line, where each point has been weighted inversely as the square of its standard deviation, $w_j = \frac{1}{\sigma^2_{B_j}}$, but the slope for Gough Island lies more than 5 times its standard deviation below the line. Thus, there is more than a 99% confidence level that the slope is anomalous (Meyer, 1975). This smaller slope is what would be expected if there was an extra source of ionization at Gough Island. The effect of this extra source of ionization would be to raise the values of foE, especially at large solar zenith angles where the solar photo-ionization rate is relatively smaller, and so to decrease the slope of the line on the log foE versus log $\mathrm{Ch}(x,\chi)$graph below the value it would have in the absence of the additional source of ionization.

Station	Lat.	Long.	Slope	Intercept
Tsumeb	19.2°S	17.7°E	0.349±0.041	0.545±0.011
Johannesburg	26.1°S	28.1°E	0.358±0.015	0.548±0.004
Grahamstown	33.3°S	26.5°E	0.358±0.004	0.544±0.002
Hermanus	34.4°S	19.2°E	0.366±0.041	0.544±0.018
Gough Island	40.4°S	9.9°W	0.308±0.008	0.546±0.004
Kerguelen	49.4°S	70.2°E	0.333±0.013	0.534±0.005
Port Stanley	51.7°S	57.9°W	0.342±0.028	0.551±0.012
South Georgia	54.3°S	36.5°W	0.347±0.023	0.551±0.010
Argentine Islands	63.3°S	64.3°W	0.324±0.011	0.541±0.005
Halley Bay	75.5°S	26.6°W	0.280±0.024	0.523±0.014

Table 2.3 Data for the nine comparison stations and for Gough Island.

Since Gough Island lies within the South Atlantic Anomaly, an area identified by Ginzburg *et al.* (1962) as a position of maximum high energy electron fluxes and also since Gough Island lies close to the position of maximum low energy electron fluxes observed by Gledhill and Hoffman (1981), as shown in Fig. 2.33, it seems possible that ionization by these low energy electrons may be partly responsible for the extra ion production.

The magnitude of the extra ionization rate necessary to maintain the observed electron density

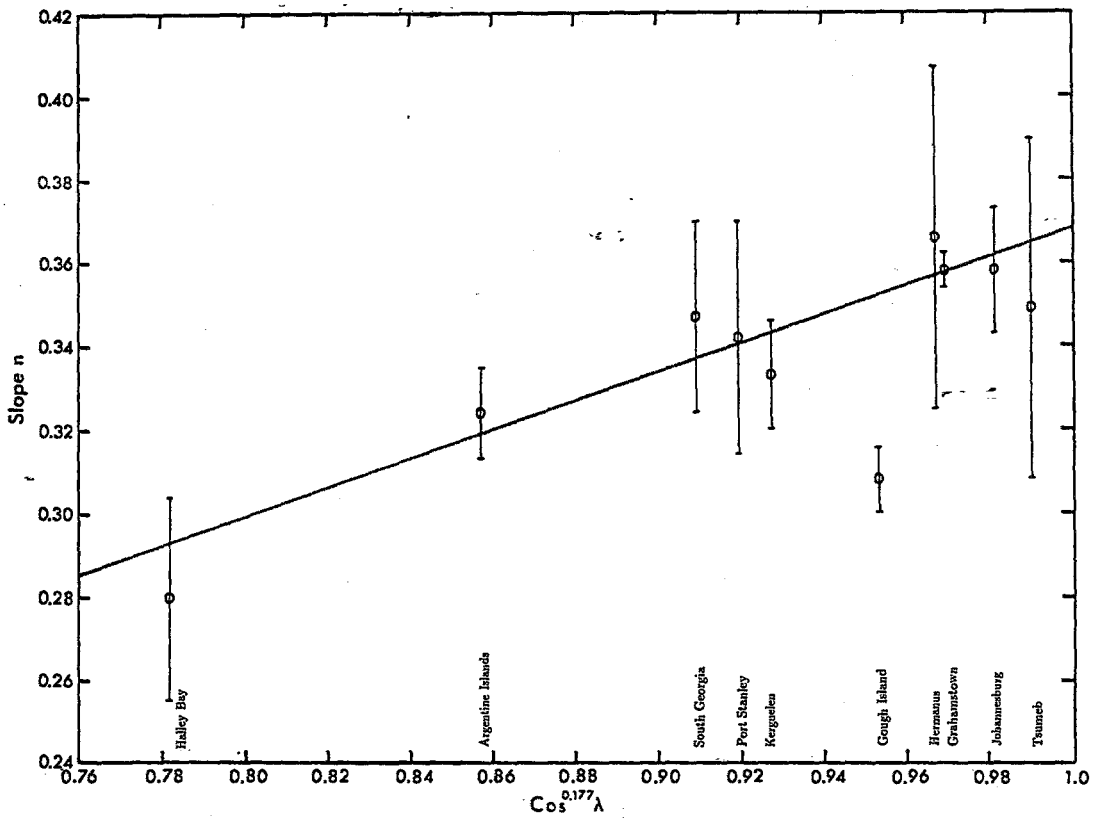

Figure 2.35: The magnitudes of the slopes of log foE versus log Ch(800, χ) graphs for the 10 stations for the 21 day period. The abscissa is $\cos^{0.177}\lambda$ (see text), where λ is the geographic latitude. The error bars denote estimated standard deviations of the slopes.

at Gough Island may be estimated as follows. We assume that, in the absence of the extra source, the "unperturbed" slope at the Gough Island graph would be that corresponding to its latitude read off the regression line in Fig. 2.35, namely $-$ 0.352. Assuming that its standard deviation, which is largely instrumental in origin, would be the same as that of the observed value, namely 0.008. There is also a small dependence of the intercepts on the latitude, and the "unperturbed" value for Gough Island was read off from a corresponding graph of intercept versus $\cos\lambda$ in Fig. 2.36, where intercept versus $\cos\lambda$ yielded a better straight line fit than intercept versus $\cos^{0.177}\lambda$. This changed the intercept marginally from 0.546 to 0.544 $\pm$ 0.004. The continuous straight line in Fig. 2.32 gives the "unperturbed" relationship. With this intercept and slope it is easy to calculate the "unperturbed" value of foE for each quarter hour. This is denoted by foE_u. These values of foE_u are for the same solar zenith angles as for the observed values of foE, but using the new value of the slope, viz $-$ 0.352.

The difference in frequency ΔF, between the observed value of foE and the "unperturbed" value of foE_u is graphically illustrated in Fig. 2.37, which indicates an approximately constant extra input into the ionosphere in the vicinity of Gough Island. The additional production rate required to yield the larger values of foE observed at Gough Island are then calculated.

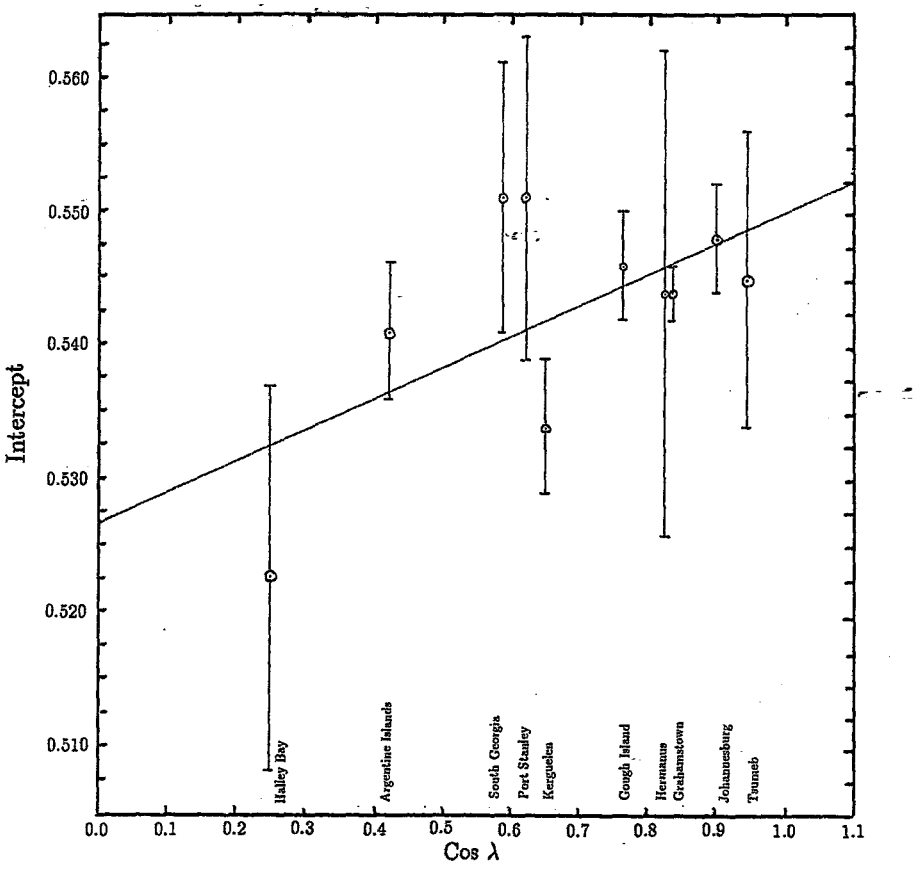

Figure 2.36: The plot of intercept versus cos λ for the 10 stations during the 21 day period of the study.

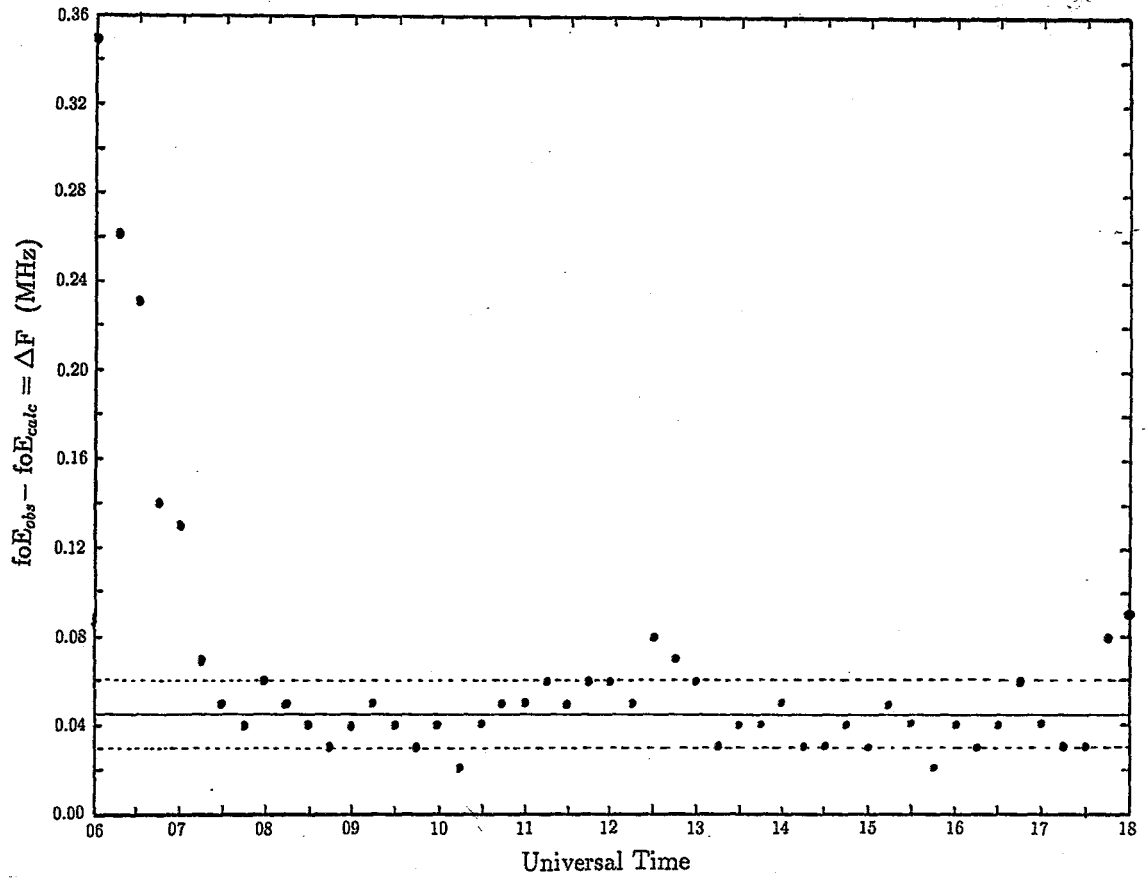

Figure 2.37: The difference frequency ΔF versus universal time for the 21 day period whilst the RSA was at Gough Island.

For simplicity it is assumed that the ionization at the E-layer maximum is in the steady state and that the loss rate follows the simple square law, so that

$$q_u \doteq \alpha N_u^2$$

gives q_u, the unperturbed rate of production of electron-ion pairs per cm^3 per second. Here α is the effective recombination coefficient for the height at which the maximum occurs. The peak electron density of the unperturbed layer is then given by the usual formula.

$$N_u = 1.24 \times 10^4 (foE_u)^2 \text{ cm}^{-3}$$

N-h profiles were computed from the hourly ionogrammes observed at Gough Island and so the median true height h of the E-layer peak was determined for each hour. Values of α were found from the expression (Gledhill, 1986)

$$\log \alpha = 67.01 - 67.16 \log h + 15.22 (\log h)^2$$

where α is in cm^3s^{-1} and h in km.

The observed values of foE were converted to the corresponding ionization rates q_o, in a similar way. The extra production rates could then be found for each quarter hour as

$$\Delta q = q_o - q_u \text{ cm}^{-3}\text{s}^{-1}$$

The differences which are dealt with are small. Near noon the total ionization rate was of the order of 4000 $cm^{-3}s^{-1}$ whereas the values of Δq were typically 200 - 400 $cm^{-3}s^{-1}$. Near sunrise and sunset, where the solar photo-ionization rate was much smaller, Δq reached a level of more than 50% of the total rate. The standard deviations of the calculated values of Δq were often larger than Δq itself in the middle part of the day. Nevertheless, all the calculated values of Δq were positive, ranging from 50 to 394 $cm^{-3}s^{-1}$, with considerable scatter. The mean of all the values have been taken, weighted inversely as the squares of their standard deviations, to obtain some idea of the magnitude of the extra production rate required to explain the observed behaviour of foE. This was found to be 151 $\pm$ 37 $cm^{-3}s^{-1}$. There is, of course, no reason why this should be constant throughout the day, and this is merely a rough estimate of the extra ionization rate needed. Fig. 2.38 graphically illustrates the difference or extra production rate

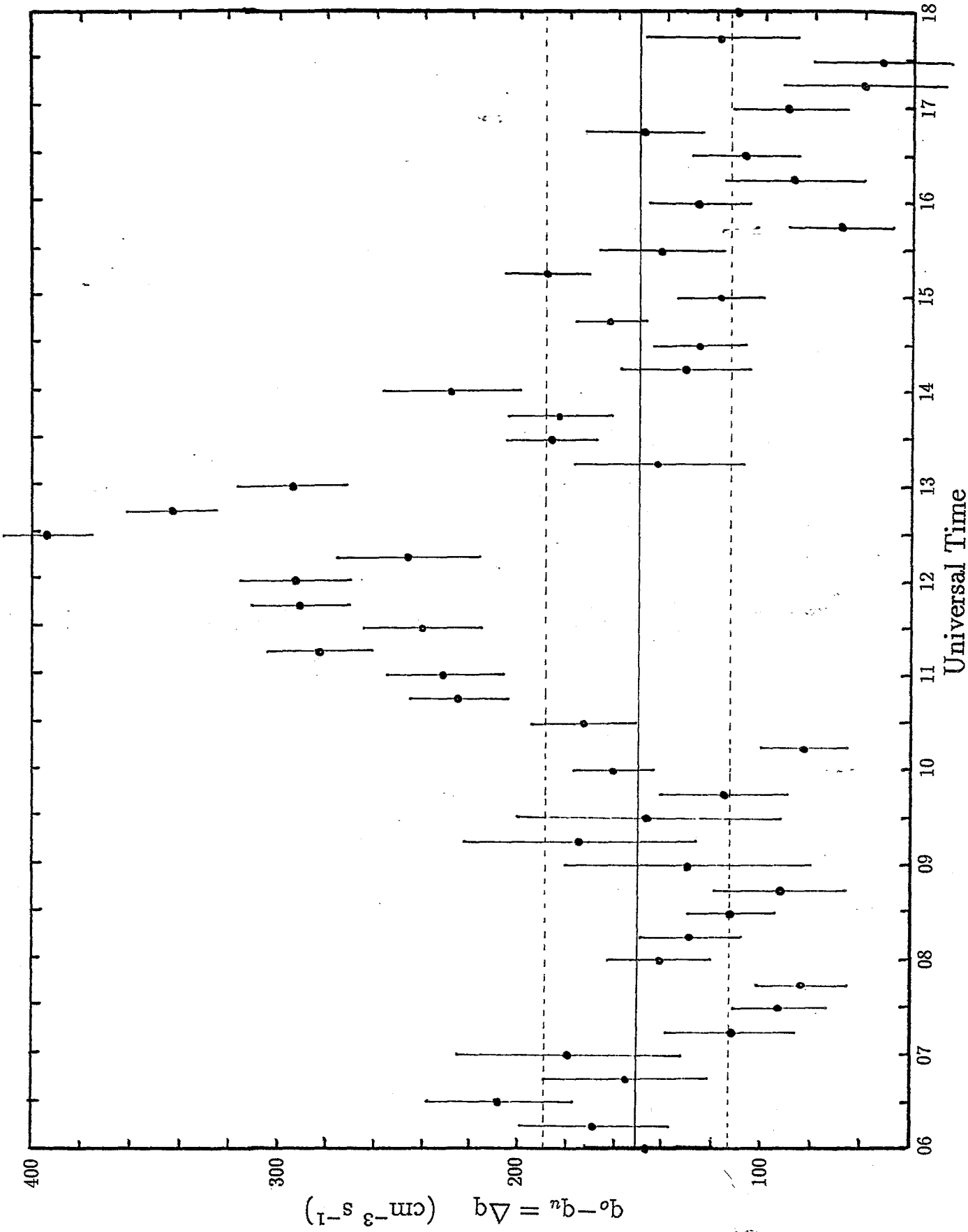

Figure 2.38: The difference in ionization rates Δq versus universal time for the 21 day period during which the RSA was at Gough Island.

Δq versus universal time. The large Δq values at around midday are enhanced by the fact that foE is a maximum at that time and the Δq relation is dependent on foE to the fourth power.

The most obvious source of the extra ionization is electron precipitation, in view of the geographical situation of Gough Island in the South Atlantic Anomaly. Although Gledhill and Hoffman (1981) measured the spectra of precipitating electron fluxes only during the night, Torr *et al.* (1976), using data from the same detectors on the same satellite, examined both day-time and night-time fluxes, but only outside the Anomaly. They found that the day-time flux was an order of magnitude greater than that at night. There seems to be no obvious reason why this should not be true inside the Anomaly region also. The night-time flux observed by Gledhill and Hoffman (1981) has therefore been increased by a factor of 10. Assuming it to be isotropic, as reported by Torr *et al.* (1976), the flux for the total downcoming spectrum was found to be

$$7.2 \times 10^5 \; E^{-1} \; \mathrm{cm^{-2}s^{-1}\,keV^{-1}},$$

where E is in keV. Although this was based on measurements in the range 0.2 to 26 kev, the assumption that it can be extended to 30 keV has been made. Above this energy the spectrum due to Vampola and Gorney (1983) has been used, which corresponds to a downward flux of $4.2 \times 10^5 E^{-2.27}$ $\mathrm{cm^{-2}s^{-1}\,keV^{-1}}$, assuming it to be isotropic. The contribution from this flux does not exceed 1% of the total ionization rate due to electron precipitation in the height range where the peak occurs.

The ionization rate as a function of height, due to this composite spectrum, was calculated by using the modification of the method due to Rees (1963) described by Wulff and Gledhill (1974) and extended by Gledhill (1984). The CIRA (1972) mean model atmosphere and the magnetic dip angle appropriate to Gough Island, 57° have been used. The maximum ionization rate was found to be 165 $\mathrm{cm^{-3}s^{-1}}$ at 101 km. This value lies close to the figure of 151 $\mathrm{cm^{-3}s^{-1}}$ found from the ionogrammes and is well within the standard deviation of the latter. In view of the very approximate nature of the assumptions that have been made in deriving both values, especially the day/night ratio of precipitating fluxes, and of the marginal nature of most of the values of Δq, this agreement must be regarded as fortuitous. Nevertheless, the present study does show that the ionization due to electron precipitation is of the appropriate magnitude to account for the anomalous behaviour of foE at Gough Island.

Chapter 3

Atmosphere Explorer-C

3.1 High Energy Particle Fluxes at Ionospheric Heights

It has been believed since the discovery of the radiation belts in 1958 (van Allen, 1959) that a very important loss mechanism for otherwise trapped particles is by their interaction with the upper atmosphere in the region of the South Atlantic magnetic anomaly, where the mirror points reach their lowest height on any drift shell.

Various estimates have been made in the past of the location and magnitude of the flux of particles at ionospheric heights and predictions have been made of their possible aeronomic effects, but most of the experimental evidence is inconclusive and indirect.

The total intensity of the geomagnetic field reaches its lowest value anywhere on the earth's surface at a point not far south-west of Rio de Janeiro, Brazil, about 25°S; 45°W as shown in Fig. 3.1 [Vernov *et al.* (1967)]. Even at great heights, the minimum does not depart very far from this position; at an altitude of 3000 km it is at approximately 15°S; 40°W. Trapped and quasi-trapped magnetospheric particles mirror at a fixed value of the total magnetic intensity, depending only on their pitch angles in the equatorial plane, unless they interact with low frequency electromagnetic waves or collide with other particles. Thus they descend further into the atmosphere over the South Atlantic than they do anywhere else, as they drift along a given L shell as shown by Torr *et al.* (1975) in Fig. 3.2. This precipitation zone is identified as the South Atlantic Anomaly and these particles are the unique non-solar ionizing agent in the Anomaly.

The first experimental observations of such particles at ionospheric heights were made with

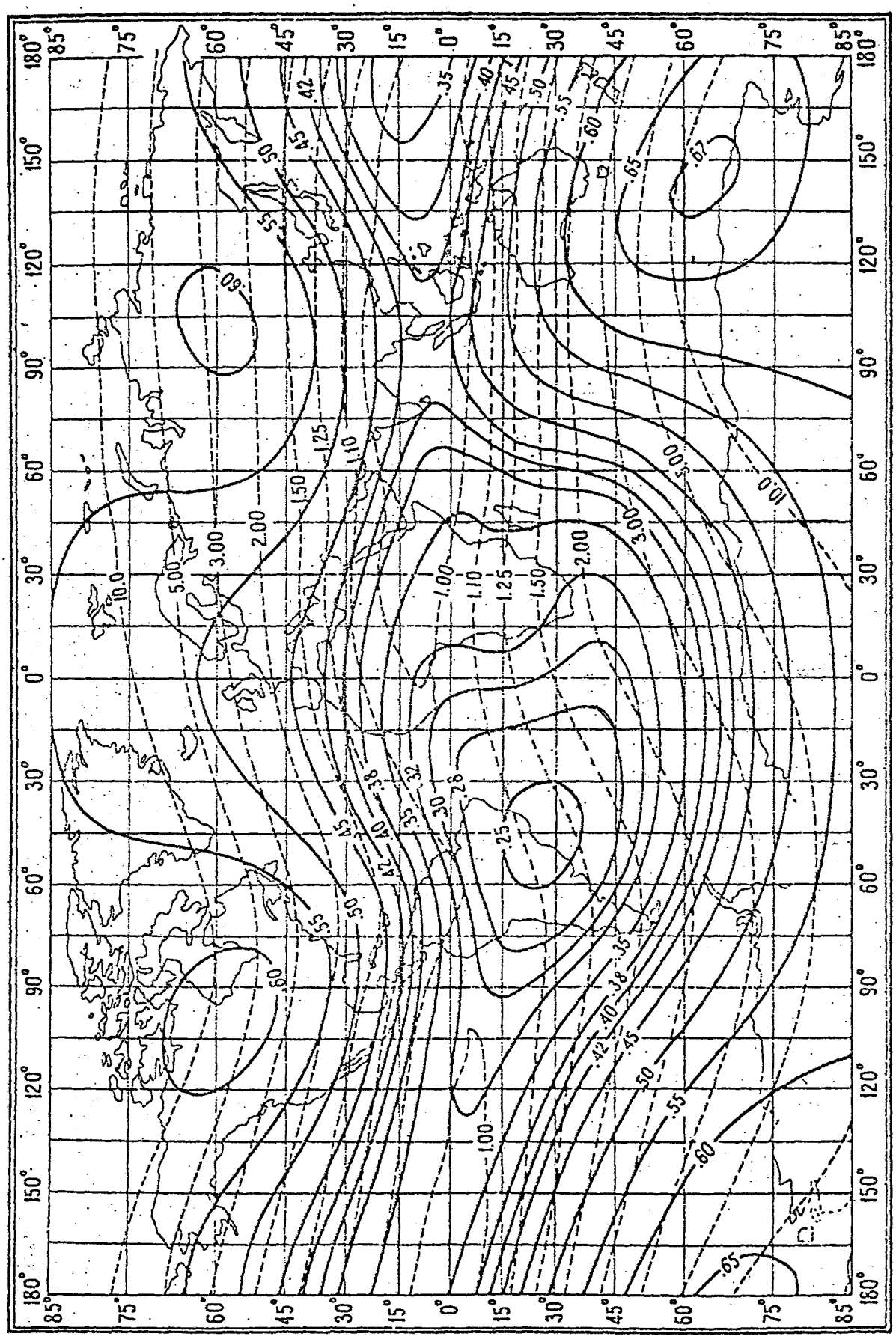

Figure 3.1: The geomagnetic field. Continuous lines are contours of constant magnetic field intensity B at ground level; dashed lines are contours of constant L at ground level. (From Vernov *et al.*, 1967)

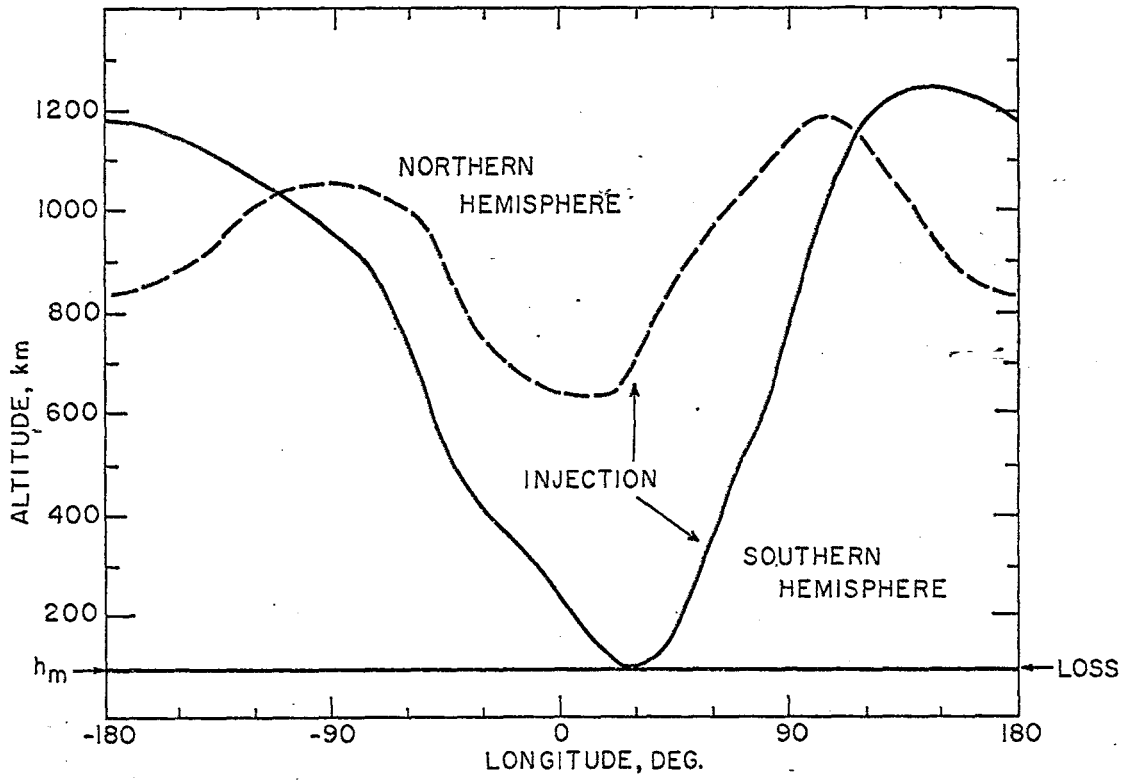

Figure 3.2: Mirror heights of particles mirroring at about 1000 km over North America on L = 1,8 as a function of longitude in the northern and southern hemispheres (From Torr *et al.*, 1975).

some of the earliest satellites. Fig. 3.3 shows measurements made by Ginzburg *et al.* (1962) from a Soviet satellite at about 320 km in August 1960. The counting rate maxima of the Geiger counter telescope at about 35°S; 25°W and 62°S; 0°E are the most prominent features of the map. The particles were thought to be electrons with energies greater than 8 MeV, but later work suggested that there was contamination from X-ray photons.

Since that time many satellites have passed repeatedly through the Anomaly and found similar maxima in counting rate, though not always in the same places. The measurements have been difficult to interpret however because the instruments used were primarily designed to measure the fluxes of particles in the auroral regions, whose energies tend to be less than about 30 keV and fluxes to be greater than those in the Anomaly by two orders of magnitude or more.

The more energetic particles in the Anomaly penetrate the spacecraft directly, so increasing the counting rates of directional charged particle detectors by an omnidirectional additional background. This is usually so intense that the responses of the instruments bear little relation to the directional fluxes which they purport to measure. X-ray astronomers, attempting to measure very small, directional fluxes of X-rays, have encountered the same problem when their spacecraft were in the South Atlantic region (Holt, 1974).

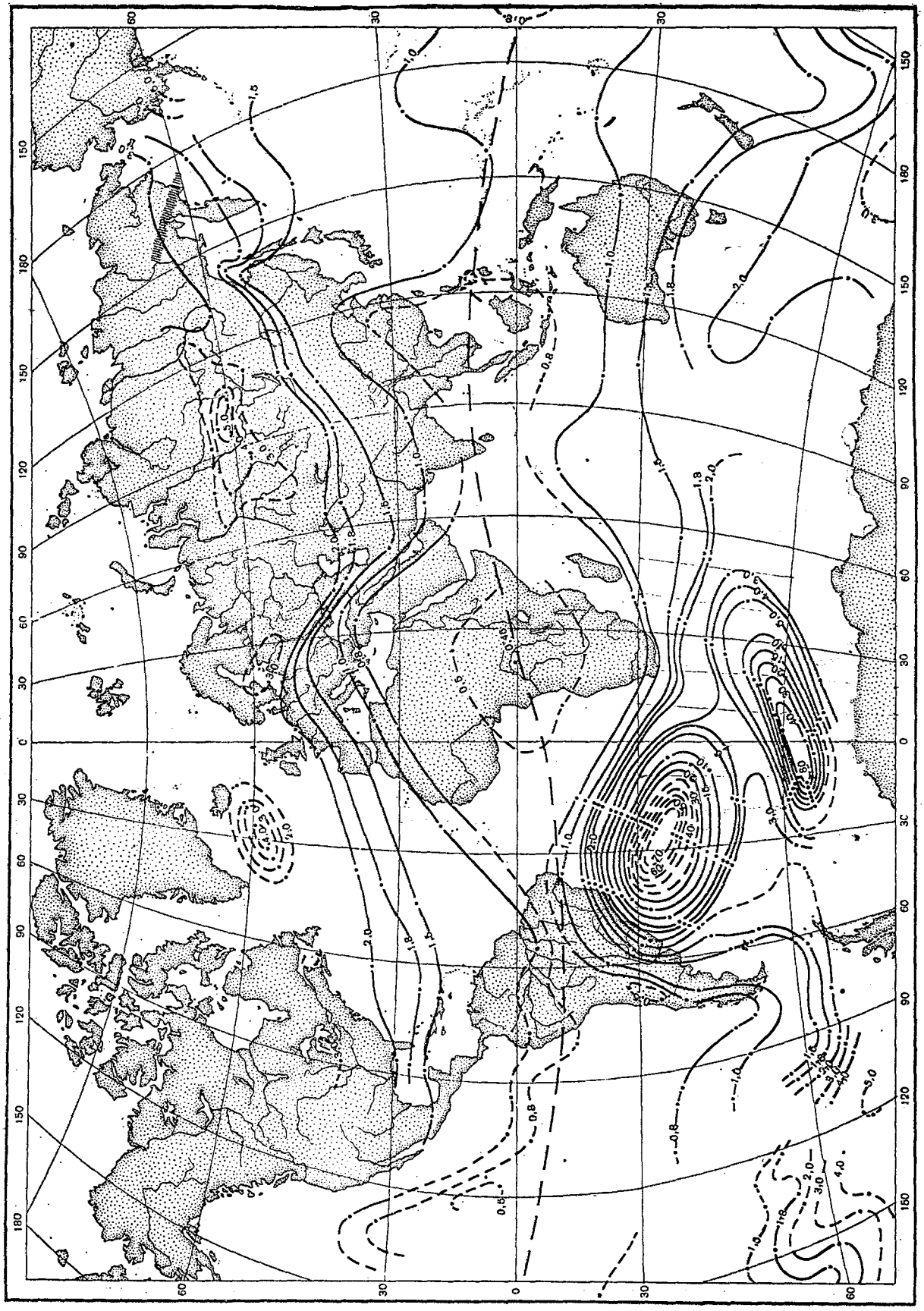

Figure 3.3: Regions of high particle counting rate observed by the Geiger counter telescope on the second Soviet space ship (From Ginzburg *et al.*, 1962)

The difficulties were compounded by the detonation over Johnston Island, in the Pacific Ocean, of the "Starfish" high-altitude nuclear device by the United States of 9 July 1962. This injected large fluxes of fission electrons, which had a very hard spectrum and persisted for several years at low L values. There were also several higher altitude nuclear explosions at higher L values carried out by the Soviet Union during the latter part of 1962. For these reasons, the early measurements of particle fluxes in the South Atlantic Anomaly, which were reviewed by Vernov *et al.* in 1967, cannot be regarded as representative of normal conditions.

In his review of particle precipitation at mid-latitudes, Paulikas (1975) concluded that there were still no reliable measurements of fluxes in the Anomaly itself. One of the main reasons was the large number of parameters involved: latitude, longitude, L value, magnetic field intensity, altitude, energy, pitch angle, local time, season, magnetic activity, etc. By the time the data from one satellite have been sorted out into the appropriate bins, there are so few values in each bin that the statistics are very poor indeed, even from what would be a large data base for many other purposes. Gledhill (1976) came to a similar conclusion when reviewing aeronomic effects in the Anomaly.

3.2 Low Energy Particle Fluxes at Ionospheric Heights

In an attempt to remedy the position somewhat, Torr *et al.* (1975) predicted the electron fluxes in the Anomaly, basing their figures on a continuous, isotropic injection model and using the measurements made by Armstrong (1965) to estimate the absolute values. Later, however Torr *et al.*,(1976) reported global averages of energy fluxes carried by electrons and protons in the range 0.2 to 26 keV, observed by the Atmosphere Explorer-C satellite. Although they mentioned the increase in background counting rate due to "MeV electrons", they did not give any estimates of the energy fluxes in the Anomaly itself. Comparison with their earlier paper (Torr *et al.*, 1975) suggests that the maximum fluxes in the Anomaly would be about an order of magnitude greater than those outside it.

In 1974, the Antarctic and Southern Hemisphere Aeronomy Year (ASHAY), was established with a view to determining what types of effects actually take place and where they are most likely to be observable in the South Hemisphere. It was decided that if the results of this preliminary study were favourable, then it would propose to carry out co-ordinated measurements between ground-based stations, ships and satellites in the most appropriate area of the South

Atlantic Ocean during the International Magnetospheric Study (IMS) period 1976 - 1978.

As part of the ASHAY International Southern Hemisphere programme, measurements were made in the Anomaly by Atmosphere Explorer-C during two periods of co-operative observation during 1976. I was fortunate to be elected Data Coordinator for the ASHAY Working Group and thus managed to obtain a printout of data obtained by Atmosphere Explorer-C during these periods.

The measurements of charged particles at altitudes of about 300 km and lower at midlatitudes is difficult, because the energy fluxes are small and also because of the difficulty of operating satellites at such low altitudes.

These difficulties were resolved with the launching on December 15, 1973 of the Atmosphere Explorer-C satellite, which is equipped with low-energy charged particle detectors designed to measure electron and proton energy fluxes in the energy range 0.2 to 26 keV. The Atmosphere Explorer-C orbits can be changed from elliptical to circular orbit and the perigee can be decreased to low altitudes, limited only by the inability of the instrumentation to operate in a high density environment (Dalgarno *et al.*, 1973).

3.3 Observations

Briefly, the satellite contains three detectors, two measuring protons and electrons from 0.2 to 26 keV in 16 logarithmic steps which are scanned in one second, and one measuring 5 keV electrons continuously. Angular distributions were measured by utilizing the satellite in the spinning mode. Each low-energy charged particle detector consisted of a cylindrical electrostatic analyser for species and energy selection and a spiraltron electron multiplier for particle detection. Further instrumental details can be found in the paper by Hoffman, R.A. et al., (1973).

Additional sensors were employed on Atmosphere Explorer-C to provide measurements for aeronomy studies. Amongst these was the cylindrical electrostatic probe. The primary purpose of this device was to provide accurate measurements of electron temperature with a high spatial resolution. An additional role was to measure the electron and ion concentrations encountered along the orbits of Atmosphere Explorer-C. (Brace *et al.*, 1973)

The magnetic ion-mass spectrometer was used to provide data on the concentration ratios,

H^+ : He^+, N^+ : O^+, and N_2^+ : NO^+ : O_2^+, to the retarding-potential analyser which, in turn, used this information to provide accurate absolute values for the total concentrations in the 1 to 4, 14 to 16, and 28 to 32 amu mass ranges. In this complementary manner, the two instruments supplied absolute ion concentrations of which the accuracy is limited only by the spectrometer's ability to measure the concentration ratios and the analyser's ability to measure the concentrations of the sum of these ions. (Hoffman, J.H. *et al.*, 1973).

The results obtained during March 25 - April 2, 1976 and June 19 - July 4, 1976, i.e. ASHAY periods I and II will be discussed. The observations obtained during the two periods have been combined to give a larger data base.

The altitude range of the satellite in the region of interest was from 277 to 310 km, with an average altitude of 299 km, which corresponds to the F-layer of the ionosphere.

Data for the period between 20:00 and 00:30 local time, corresponding to 00:00 ± 4 h Universal Time has been used.

Sources of contamination have been discussed by Hoffman *et al.* (1974) and Torr *et al.* (1976). The main sources of contamination in the South Atlantic Anomaly are the "MeV electrons" of Torr *et al.* (1976). These authors corrected for the effects of the high energy electrons and also of "Scattered UV Photons" by noting that the proton channel showed no spectral response in the energy channels below 7 keV. The low energy proton channels were therefore used as background monitors of the contaminations due to these sources and their counts were subtracted from the other channels for both electrons and protons.

Since the spectral responses were not available, the uncorrected data from the electron and proton channels, are presented here. The *total* proton or ion channel response was subtracted from the electron channel, since the contamination cannot exceed this value. Since penetrating radiation would affect all channels in the same way, the mean counting rate of the ion channels would give the background counting level. The electron and ion detectors are next to each other on the satellite and have identical geometry, thus it is reasonable to assume that both detectors would record the same background counting rates. Hence, if the mean counting rate of the ion channels is subtracted from the mean counting rate of each electron channel, the corrected rate for electrons would be obtained. Therefore, the uncorrected electron fluxes represent maximum possible values, while the corrected ones represent minimum possible values.

The values for the energy fluxes carried by precipitated electrons and protons discussed in this

section were obtained by summing the fluxes in all channels from 0.2 to 26 keV, counting only those occasions when the particles observed were moving downward at the location concerned.

3.4 Results and Discussion

For the purpose of this analysis, the South Atlantic region was divided into 240 bins, each 5° in latitude and longitude, from 20°to 70°South and from 65° West to 55° East.

Averages of precipitated electron and proton energy fluxes and electron densities and temperatures as well as the NO^+ and O^+ ion concentrations were computed for each bin. Whenever a particular bin was void of observations an average value was assigned to that bin by taking the mean of all the surrounding bins, so as not to disrupt the contours. The average number of observations for precipitated electron and proton energy fluxes was 7 per bin, while the average for electron densities and temperatures as well as the ion concentrations was 17 per bin.

During ASHAY period I the three hourly K_p indices varied from 2– to 7, whereas the K_p indices only varied from 0+ to 4– for ASHAY period II for the orbits considered in this analysis; the former period included the events of March 26 and April 1, 1976. Hence, to obtain some measure of uniformity, these disturbances have been excluded by limiting the analysis to data which excluded K_p greater than 4+.

Fig. 3.4 shows the contours of uncorrected precipitated electron energy fluxes, which range from 0.5 to 30 $\times 10^{-4}$ ergs $cm^{-2}s^{-1}$ (1×10^{-3} ergs $cm^{-2}s^{-1} = 1\ \mu Wm^{-2}$). A well defined maximum of 27×10^{-4} ergs $cm^{-2}s^{-1}$ occurs off the Brazilian coast at about 33° S; 47°W, and another maximum in the South Eastern region near 57°S; 23°E is evident, where the peak value is 30×10^{-4} ergs $cm^{-2}s^{-1}$. A band of minimum flux running across the South Atlantic from about 60°S; 60°W to 25°S; 40°E is also noticeable.

In Fig. 3.5 the contours for apparent precipitated proton energy fluxes are presented, these range from 0.5 to 15 $\times 10^{-4}$ ergs $cm^{-2}s^{-1}$. Again, a maximum of 15×10^{-4} ergs $cm^{-2}s^{-1}$ off the Brazilian coast at about 37°S; 32°W is noticed, as well as an area of more intense proton precipitation in the South Eastern sector.

The distribution of electron and proton fluxes differ markedly from those proposed by Torr *et al.* (1975) on theoretical grounds; their predicted maximum of precipitated electron flux at altitudes of 200 km was centred on approximately 48°S; 15°W.

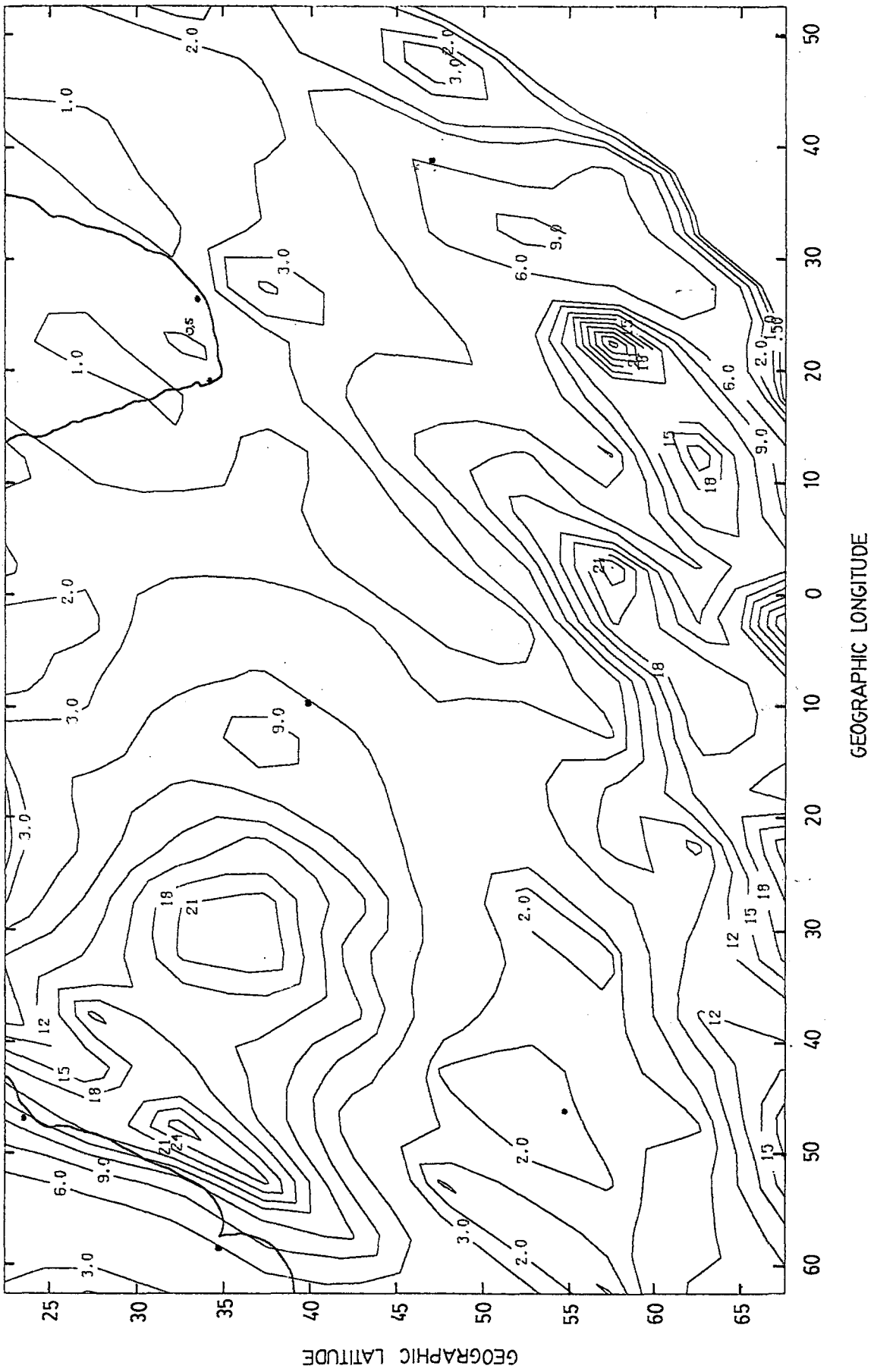

Figure 3.4: Contours of uncorrected precipitated electron energy fluxes at 300 km in the range 0.2 to 26 keV, in units of 10^{-4} ergs $cm^{-2}s^{-1}$.

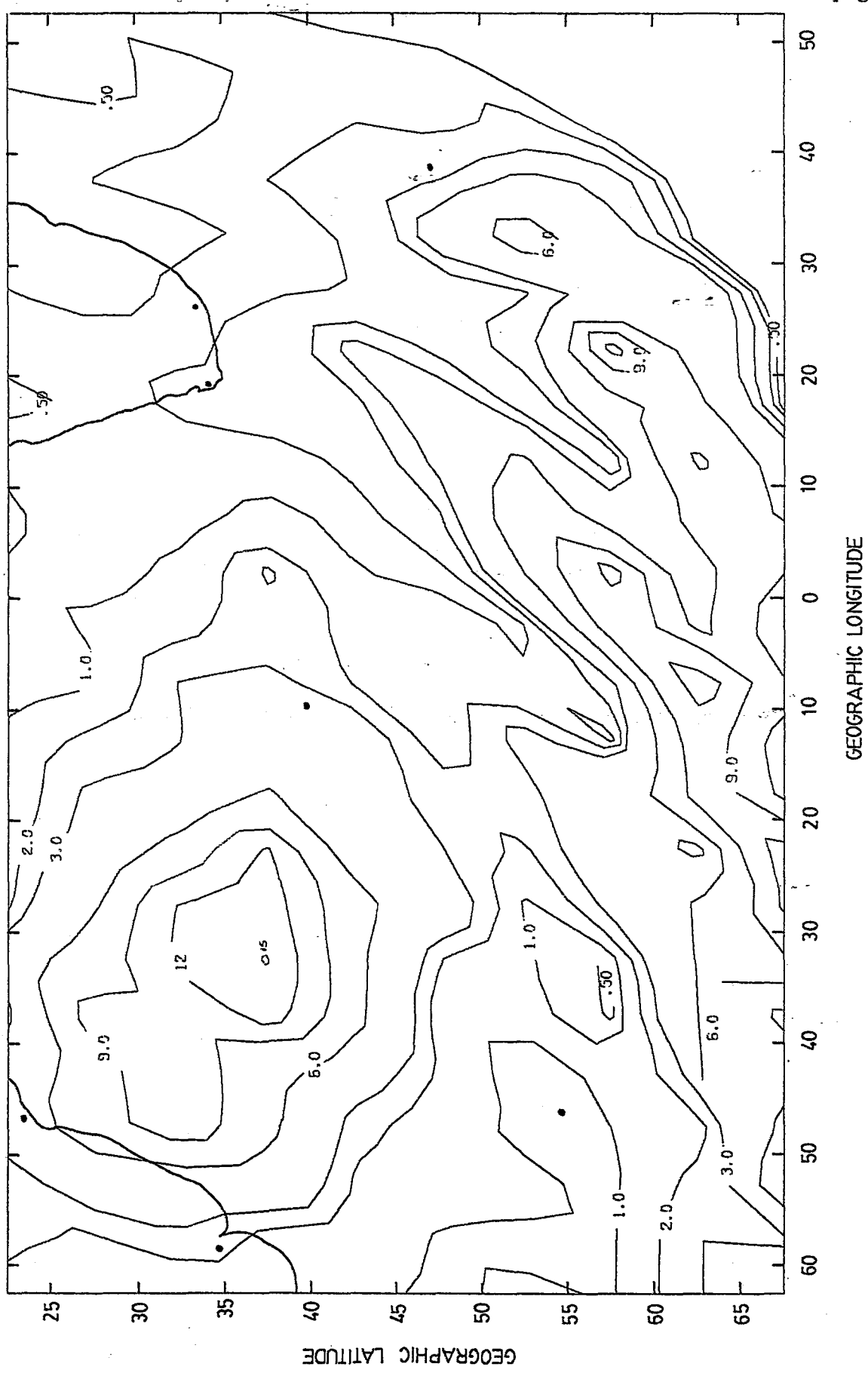

Figure 3.5: Contours of apparent precipitated proton energy fluxes at 300 km in the range 0.2 to 26 keV, in units of 10^{-4} ergs $cm^{-2}s^{-1}$.

Ginzburg *et al.* (1962) reported relatively large particle fluxes in the South Atlantic region for very high energy particles. A comparison of the contours presented here with their results shows that the maxima of the contours presented here roughly correspond to their "South Atlantic" or Brazilian Anomaly, and the "Southern Anomaly". This suggests strongly that both the proton and the electron channels are counting high-energy penetrating radiation as a strong background.

Fig. 3.6 shows the corrected precipitated electron energy fluxes, obtained by subtracting the apparent proton energy fluxes of Fig. 3.5 from the electron values in Fig. 3.4. The maximum off the Brazilian coast persists, though its value has been reduced to 18×10^{-4} ergs $cm^{-2}s^{-1}$, but the large subsidiary maximum at 35°S; 30°W has almost disappeared, suggesting that it was largely due to the background. The peak at 57°S; 23°E also persists, but has been halved in size. Examination of the data shows this to be a recurrent peak, not due to merely a few high points. It is seen that the maximum flux in the anomaly is an order of magnitude greater than that outside it, where the average values agree with those found by Torr *et al.* (1976) in their general survey.

In the following diagram Fig. 3.7, contours of electron density have been plotted. The contours range from 1×10^4 to 1×10^5 cm^{-3}. The most prominent feature of the electron density map is that, in general, it exhibits areas of minimum electron density, where Fig. 3.6 shows maximum fluxes of energy carried by precipitated electrons. This is contrary to previously reported observations made by several observers (Willmore and Henderson, (1965); Knudsen, (1968); Knudsen and Sharp, (1968); etc.). In fact, in both anomalous areas regions of minimum electron densities are found for the periods under observation. It is also evident that maxima of electron density seem to coincide with minimum precipitated electron energy flux, e.g. in the region 45°- 55°S; 30°- 40°W and in the vicinity of South Africa.

Fig. 3.8 is a contour map representing the electron temperatures, where the contours range from 650 to 2600 K. The electron temperatures exhibit a minimum off the East coast of Brazil increasing towards the South Eastern sector. These contours agree fairly well with the nighttime temperature distribution for 300 km presented by Spenner and Plugge (1978) using electron temperature data from AEROS-A. The temperature distribution is, in general, consistent with the production of heat in the plasmapause region and the consequent heat flow towards the equator. In this figure the strong heat flux into the atmosphere near the plasmapause, which increases the electron temperature towards $L \approx 4$, is easily seen.

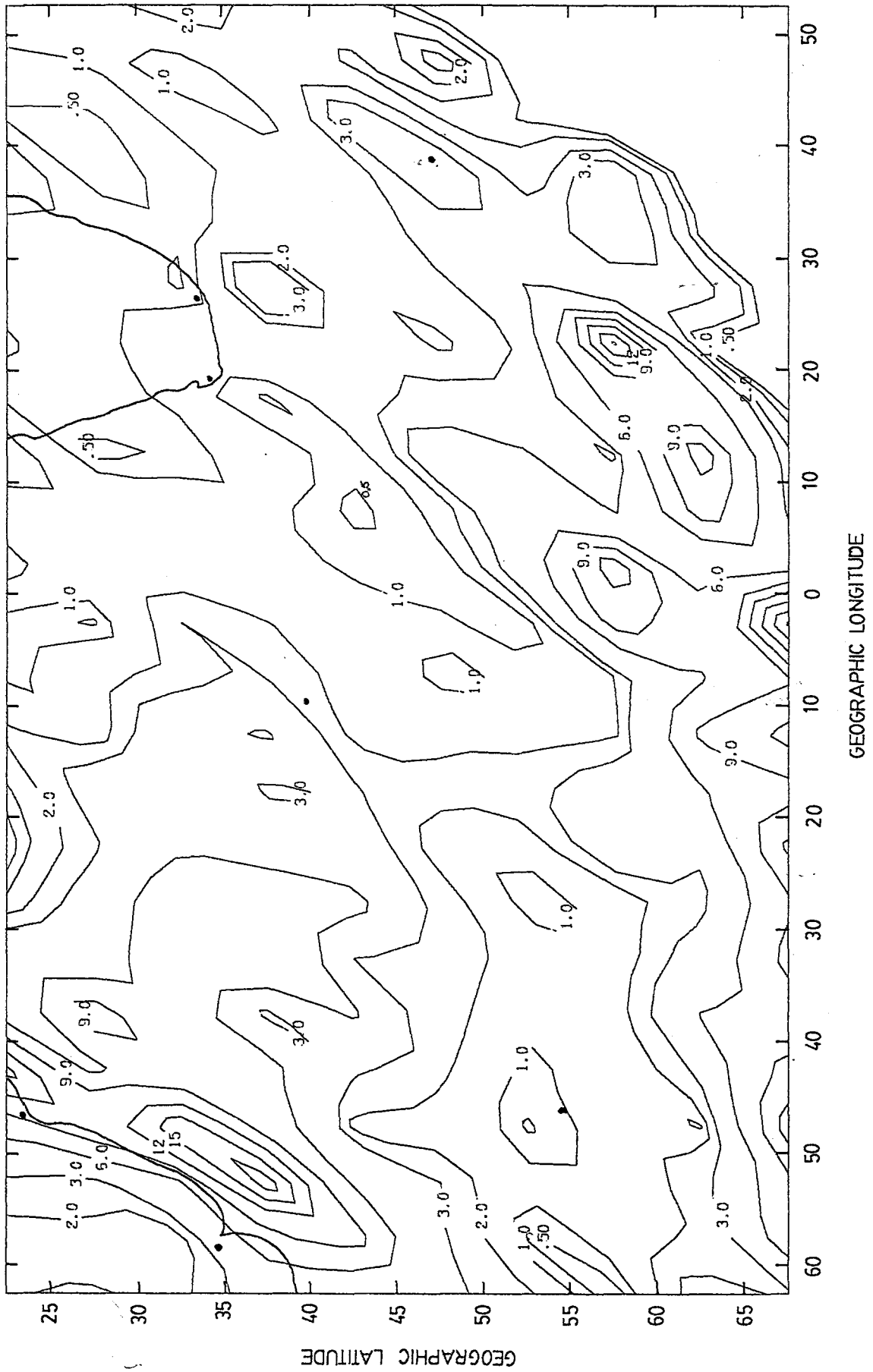

Figure 3.6: Contours of corrected precipitated electron energy fluxes at 300 km in the range 0.2 to 26 keV, in units of 10^{-4} ergs $cm^{-2}s^{-1}$.

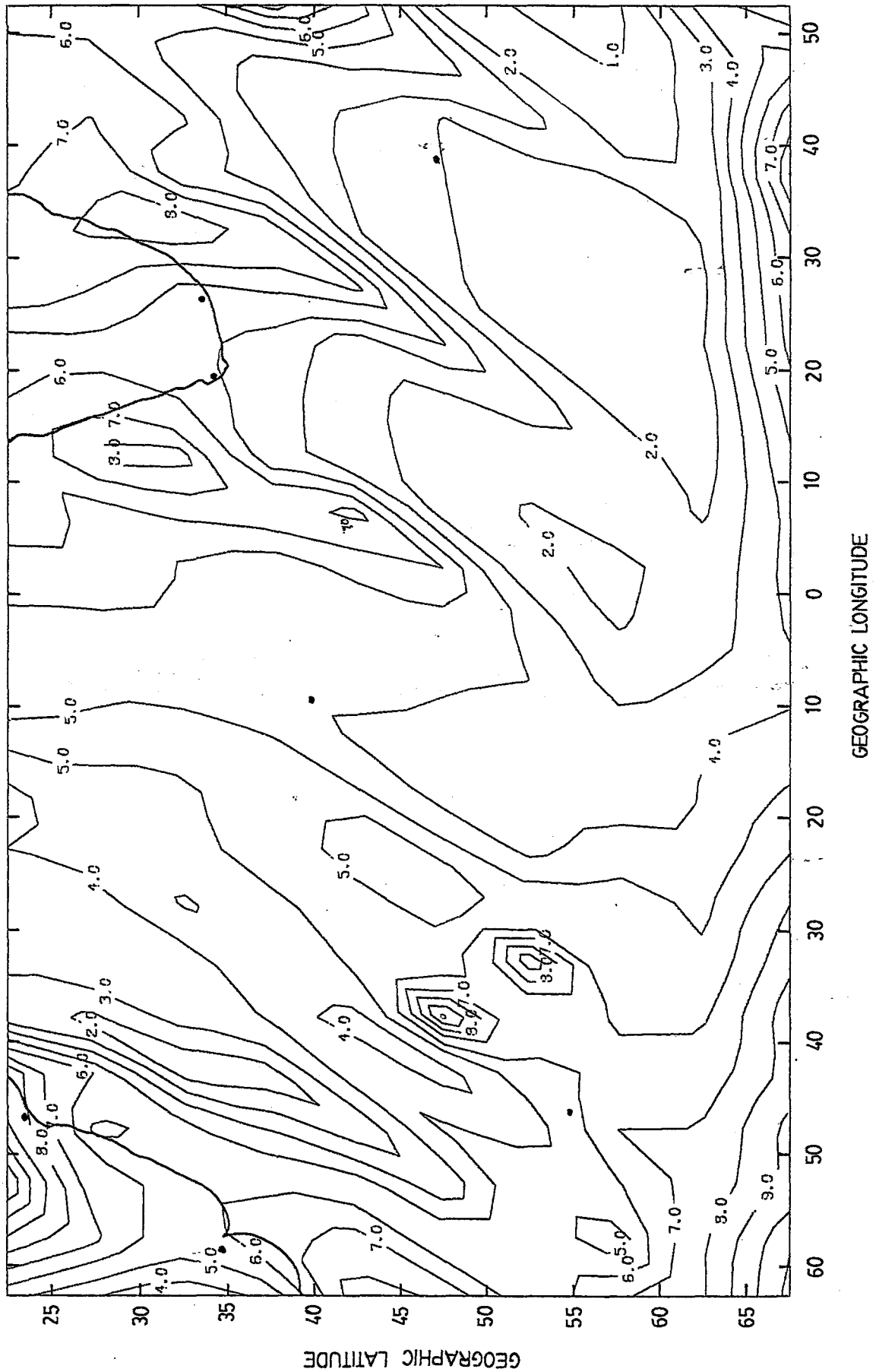

Figure 3.7: Contours of electron density at 300 km in the range 0.2 to 26 keV, in units of 10^4 cm^{-3}.

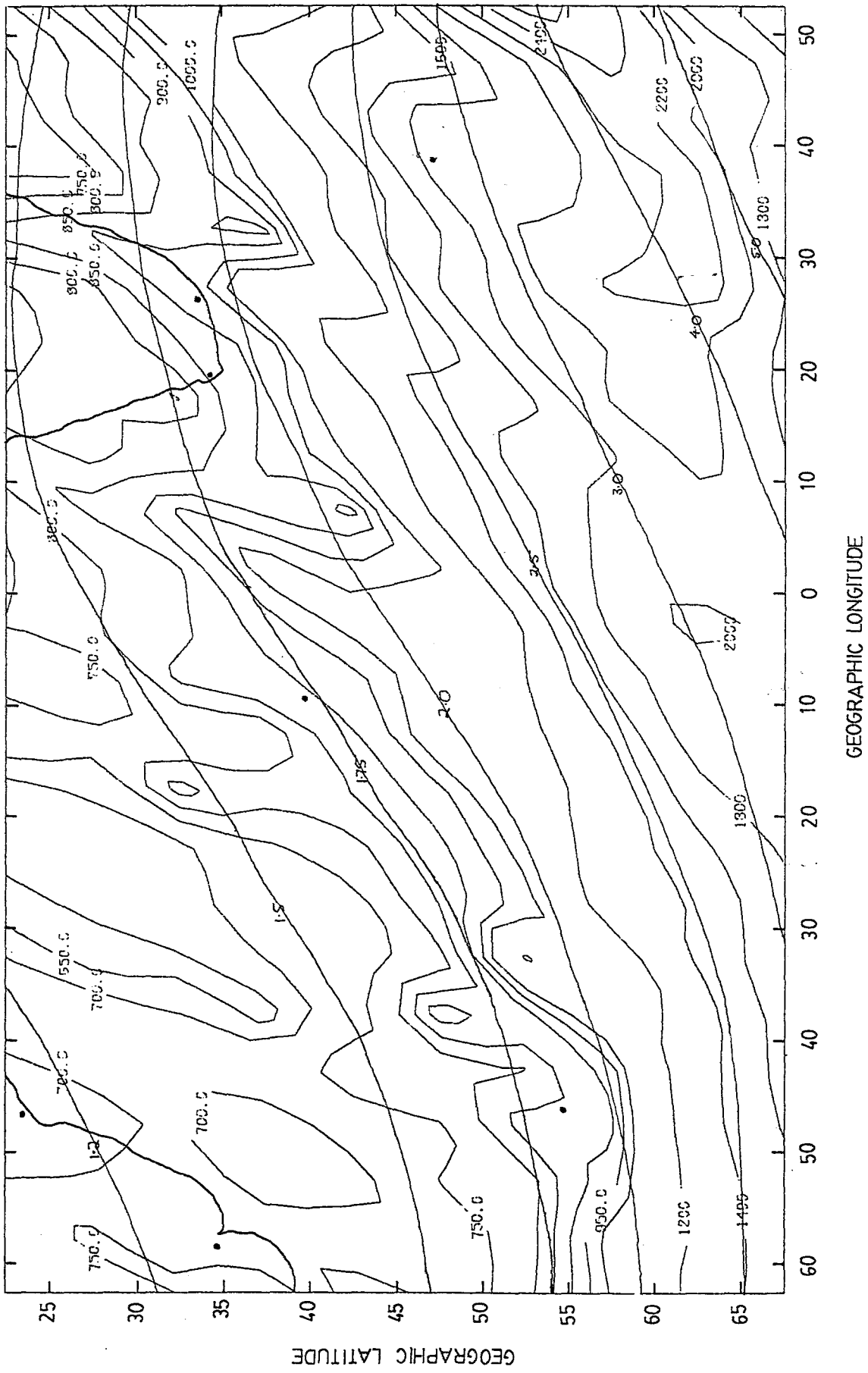

Figure 3.8: Contours of electron temperature at 300 km in the range 0.2 to 26 keV, in degrees Kelvin, with lines of constant L at 300 km superimposed.

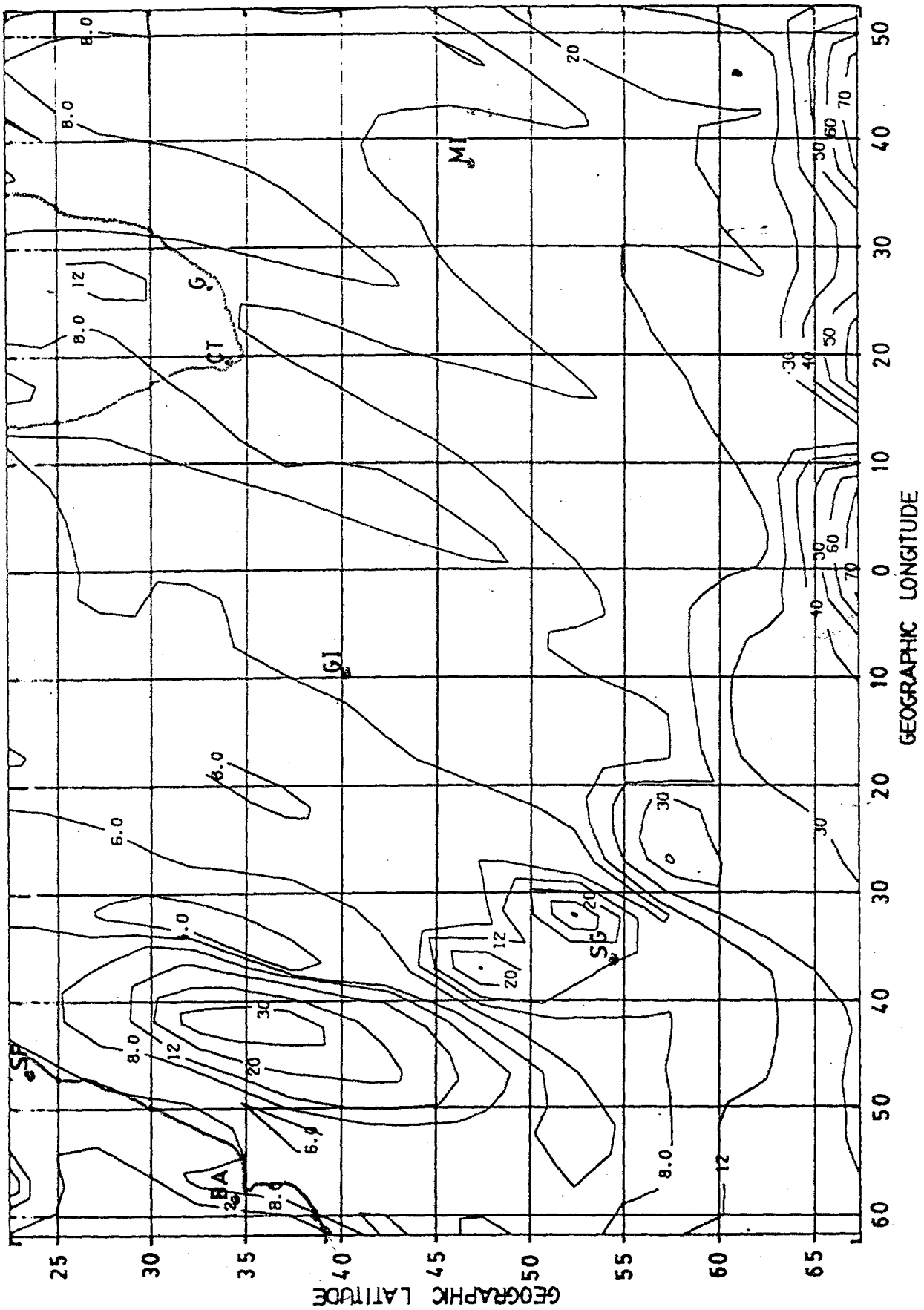

Figure 3.9: Contours of atomic nitric oxide NO^+ at 300 km, in units of 10 cm^{-3}.

The next diagram, Fig. 3.9, shows the concentration of atomic nitric oxide, NO^+, where the contours range from 40 to 700 cm^{-3}. A well defined maximum of 300 cm^{-3} occurs off the Brazilian coast at about 35°S; 42°W, and another round about 50°S; 35°W. Also clearly visible is a band of maximum concentration in the Southern most portion of the Eastern sector. Thus, in general, it can be seen that areas of maximum NO^+ concentrations coincide with areas of minimum precipitated electron and proton energy fluxes and likewise areas of minimum NO^+ ion concentrations coincide with areas of maximum precipitated electron and proton energy fluxes. The same is also true when the NO^+ ion concentrations are compared with electron densities.

In Fig. 3.10 the concentration of atomic oxygen, O^+, contours have been plotted. The contours range from 8 to 90 $\times 10^3$ cm^{-3}. Two well defined minima areas are exhibited centred on about 35°S; 42°W and 57°S; 25°E. This is contrary to previous observations of increased oxygen concentrations over the South Atlantic Anomaly (Raitt *et al.*, 1965). However, since these observations were all recorded at night, the results obtained are to be expected, since the O^+ ion concentrations decay rapidly after sunset. A comforting feature of the O^+ ion concentrations is that they exhibit similar maxima and minima to the electron densities, since above 180 km $nO(^+) \simeq n(e)$ (Holmes *et al.*, 1965).

Fig. 3.11 exhibits contours of the ratio of NO^+ ion concentrations to O^+ ion concentrations (NO^+/O^+) and range from 2 to 40 $\times 10^{-3}$. Once more a well defined maximum is found off the Brazilian coast-centred on 35°S; 42°W, and a lesser maximum in the South Eastern sector. Also note that the maxima and minima areas are opposite to the electron densities maxima and minima.

In the following figure, Fig. 3.12, the same ratio as for the previous figure but this time for values of $K_p > 4+$ are presented. The contours now range from 2 to 90 $\times 10^{-3}$ and very large areas of maxima are seen to occur in the South Eastern sector. An interesting observation is that for large K_p values the contours are in fairly close agreement with the electron temperature contours.

3.5 Conclusions

The results show that the energy precipitated by electrons in the Brazilian and Southern Ocean regions is on the average an order of magnitude greater than that observed outside the South

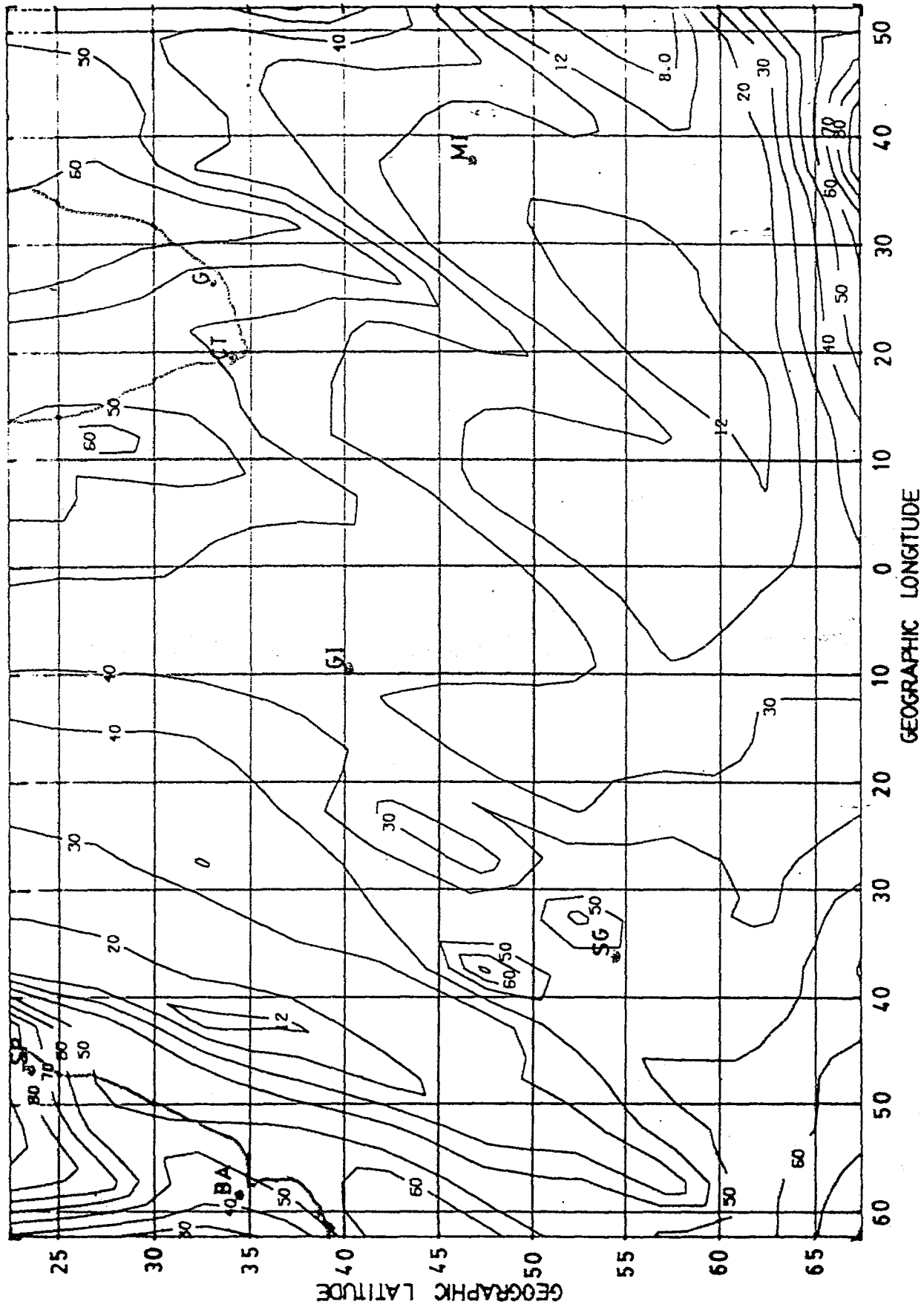

Figure 3.10: Contours of atomic oxygen O^+ at 300 km. in units of 10^3 cm^{-3}.

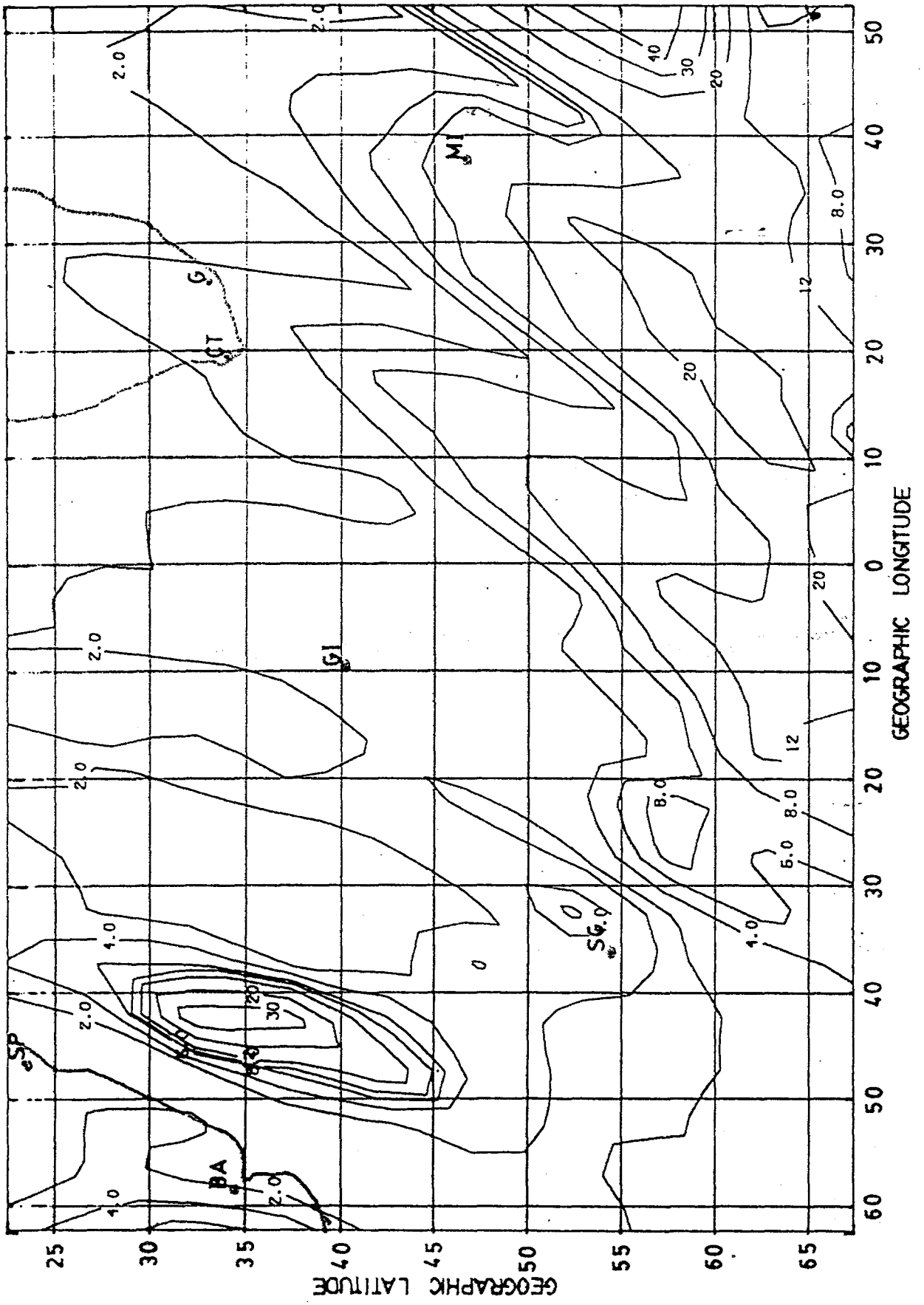

Figure 3.11: Contours of the ratio NO^+/O^+ ion concentrations at 300 km, in units of 10^{-3}.

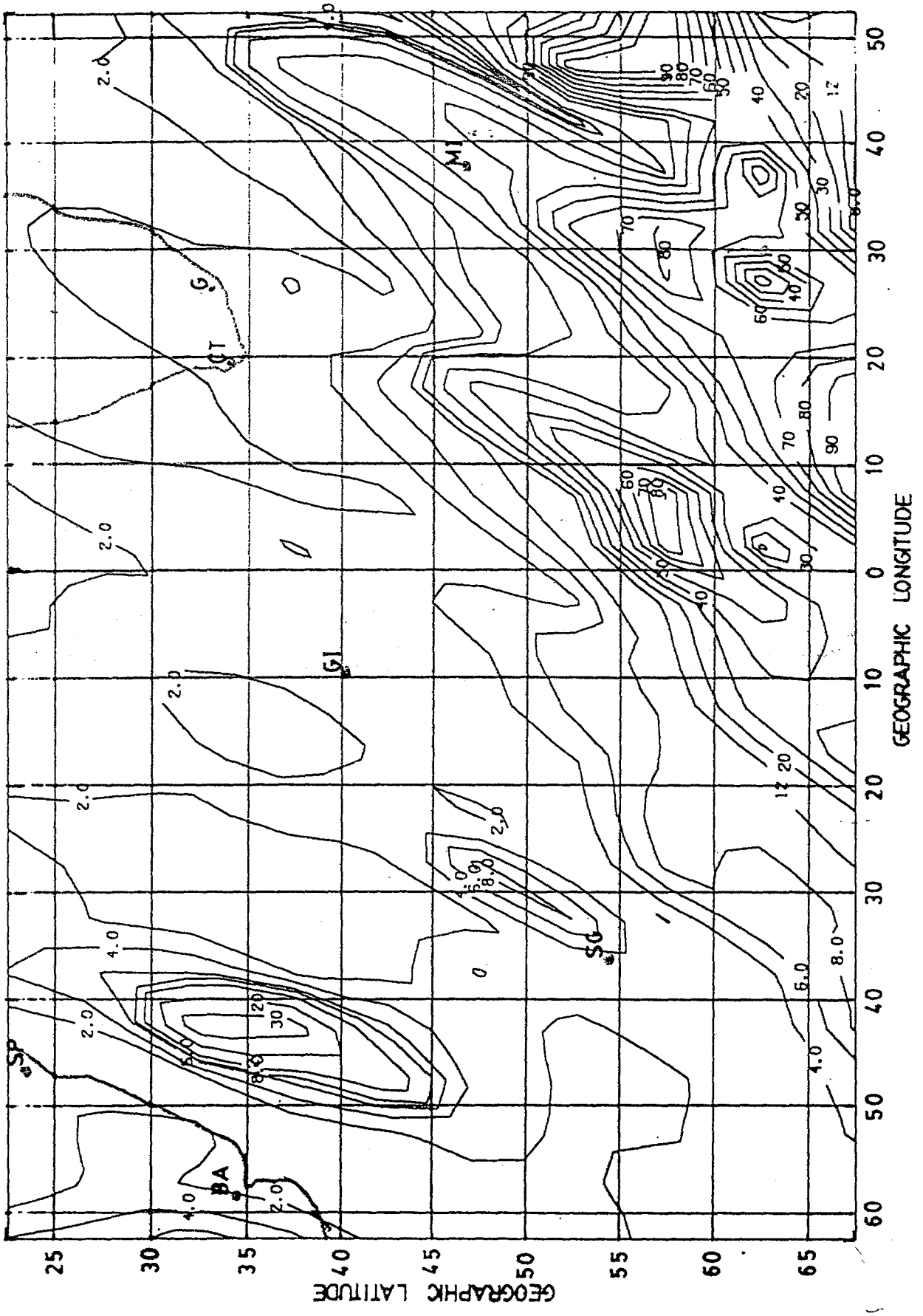

Figure 3.12: Contours of the ratio NO^+/O^+ ion concentrations at 300 km for values of $K_p > 4+$, in units of 10^{-3}.

Atlantic, as reported by Torr *et al.* (1975) on the basis of a theoretical study.

There appears to be a persistent maximum in low-energy electron precipitation, roughly parallel to the South American coast, and another, broader region centred about 60°S; 15°E. There is a band of minimum flux, running across the South Atlantic from about 60°S; 60°W to 25°S; 40°E.

Generally it is found that regions of maximum precipitated electron energy fluxes and electron densities correspond to the maximum median values of foF2 as recorded in Chapter 2 and at the observatories used in this dissertation.

Nighttime electron temperatures appear to vary fairly uniformly from over 2000 K near the plasmapause over the Southern Indian Ocean to a minimum of about 700 K near the South American coast.

The minimum in electron density running from 25°S; 35°W to 45°S; 50°W is a persistent feature which is reminiscent of the mid-latitude trough at first sight. However, its non-alignment with lines of constant L and the absence of any sign of a maximum in electron temperature suggest that its origin is entirely different and is probably associated with the maximum of electron precipitation a few degrees to the west of it.

In general, the maximum NO^+ ion concentrations coincide with minimum precipitated electron and proton energy fluxes and vice versa. Whereas the NO^+ ion concentrations and O^+ ion concentrations exhibit similar maxima and minima to the electron densities.

The increase in NO^+ ion concentrations is far greater than the increase in O^+ ion concentrations for large values of K_p. Consequently, the NO^+/O^+ ratio is markedly affected by an increase in magnetic activity.

Voss and Smith (1980) have reviewed the available measurements of particle fluxes at mid-latitudes during the nighttime. They have shown that precipitation takes place in fairly well-defined zones which follow L shells (Fig. 3.13). They found that the low- latitude zone centred on $L = 1.4$ consists of electrons with energies < 20 keV and pitch angles near 90°. For $K_p \approx 5$ the precipitated energy flux is about 5×10^{-4} erg $cm^{-2}s^{-1}$. The mid-latitude zone at about $L = 2.6$, on the other hand, consists mainly of protons with energies in the range 10 to 100 keV, which carry about 5×10^{-3} erg $cm^{-2}s^{-1}$ and have pitch angles within about 10° of 90°. These are thought to be precipitated from the ring current by ion-cyclotron interactions. The positions of the maxima of precipitation in the Anomaly predicted by Voss and Smith agree well

with those usually observed. These authors do not, however, make any quantitative estimate of the intensity of precipitation in the Anomaly. No experimental evidence has been put forward that the particle precipitation in the Southern Anomaly near 60° S; 0° E are in fact mainly protons .

Two rocket experiments of interest in the vicinity of the Anomaly have been reported.

Prangé and Crifo (1977) launched a rocket from Mar del Plata, Argentina (38° S; 58° W) at 01:30 LT on 13 December 1972. The vehicle reached a height of 380 km at $L = 1.32$ and carried electrostatic particle spectrometers for electrons and protons. Unfortunately, owing to a malfunction, no electron data are available. The proton detector encountered *upward moving* field-aligned beams of positive ions, which were thought to be O^+ (Fig. 3.14). These were found to coincide with increases in the flux of trapped electrons with energies greater than 40 keV. The energies of the ions were in the range 0.15 to 33 keV and the upward energy flux was 2×10^{-2} erg $cm^{-2}s^{-1}sr^{-1}$ at maximum (Prangé, 1978). There was, regrettably, no means of identifying the positive ions definitely as O^+.

Kelley *et al.* (1977) launched a rocket from Natal, Brazil (6°S; 35° W), which lies very near the equator, at 19:40 LT pm 18 November 1973. Their pitch angle distributions (Fig. 3.15) showed trapped electrons and, in addition, a northward-directed field-aligned flux of electrons. The energy spectra of these escaping electrons (Fig. 3.16) showed that the fluxes returning from the northern hemisphere were an order of magnitude less and were what would be expected from backscatter, by the atmosphere at the northern end of the field line, of the observed northward fluxes. The protons observed showed only a slightly anisotropic distribution, with a small excess travelling northwards.

It is clear that little is known, from actual measurements, of electron and proton fluxes in the Anomaly, especially in the two regions of maximum flux. The earlier satellite observations were so contaminated by the high-energy background that they show only that there are usually two such regions in which relatively large fluxes of charged particles are found at F-region heights: the Brazilian or South Atlantic Anomaly, centred about 35° S; 25° W and the region around 60° S; 0° E, which shall be called the Southern Anomaly following the Russian group (Ginzburg et al., 1962). Measurements of the fluxes of very high energy particles are not affected much by the background. Kurnosova (1976) has reviewed some flux measurements of electrons and protons with energies of several hundred MeV, including some in the Brazilian (South Atlantic) and Southern Anomalies by the satellite Kosmos 443, which show a distribution remarkably

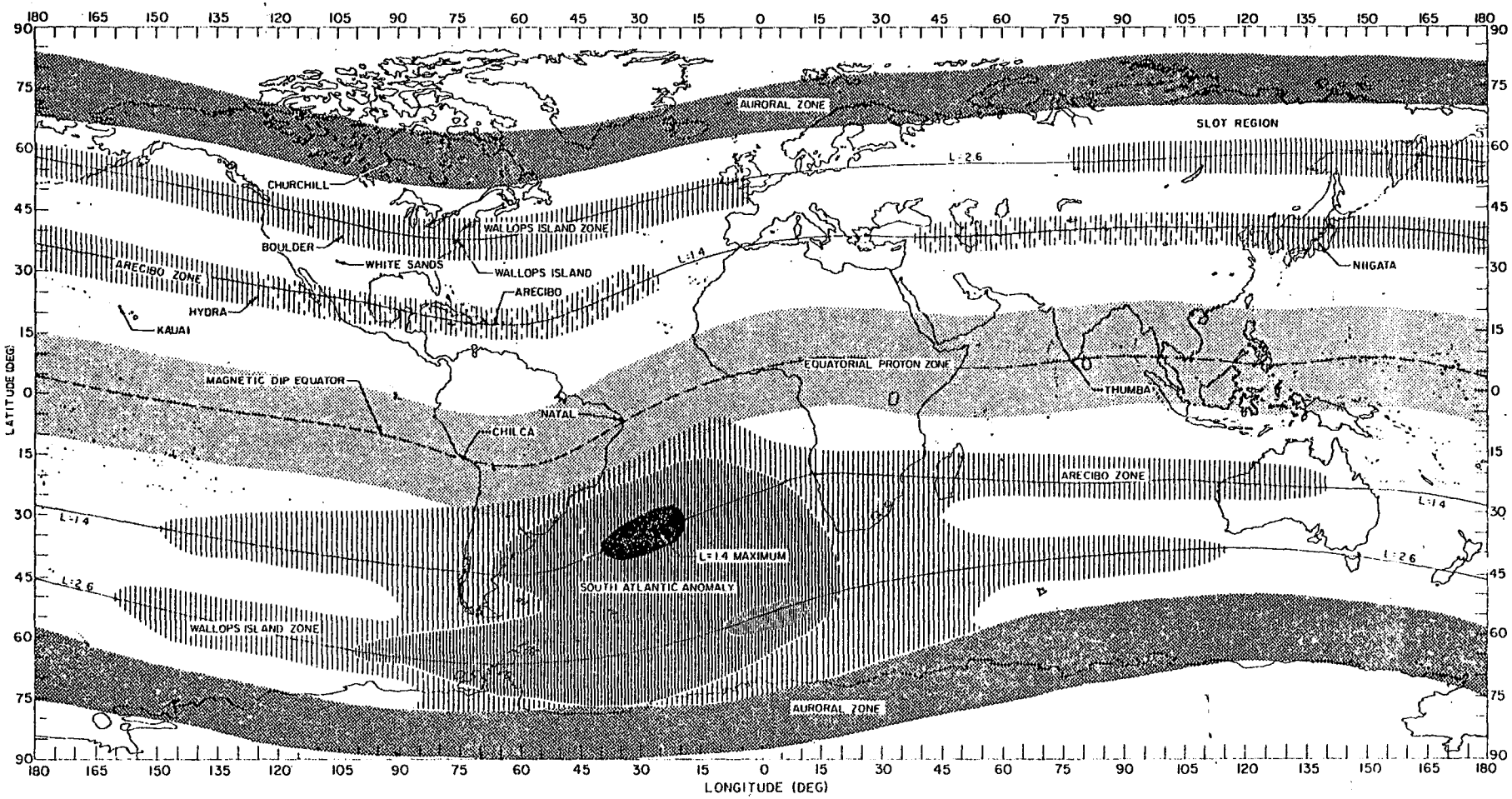

Figure 3.13: Precipitation zones according to Voss and Smith (1979).

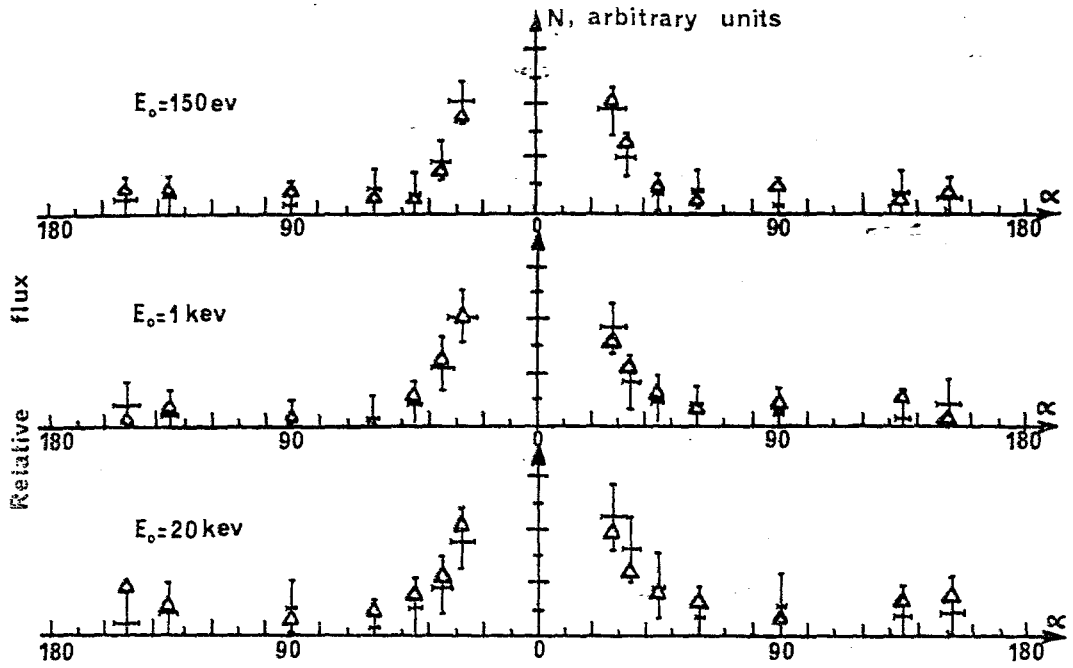

Figure 3.14: Pitch angles of positive ions observed by Prange and Crifo (1979).

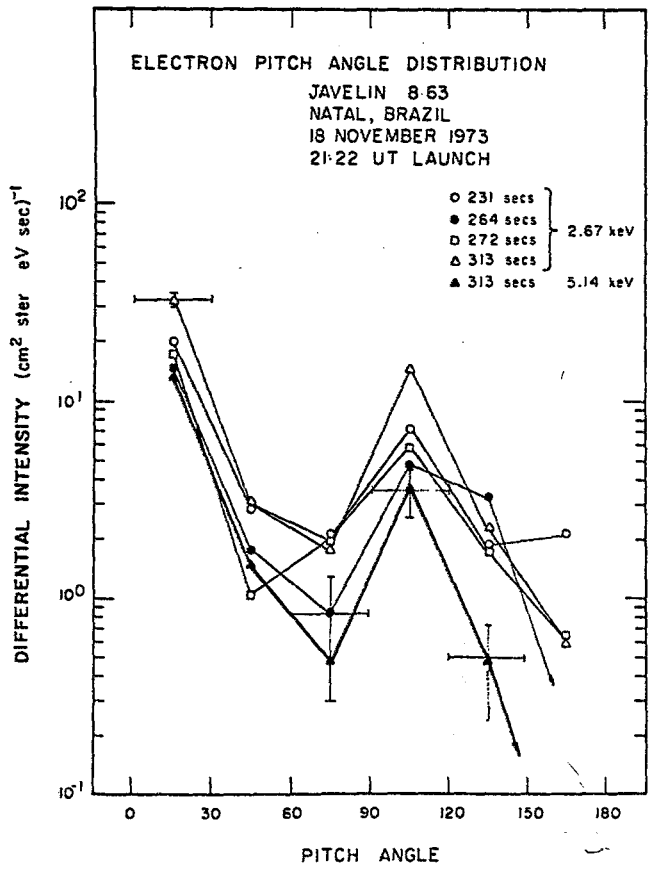

Figure 3.15: Pitch angles of electrons near the magnetic equator (Kelley *et al.*, 1977)

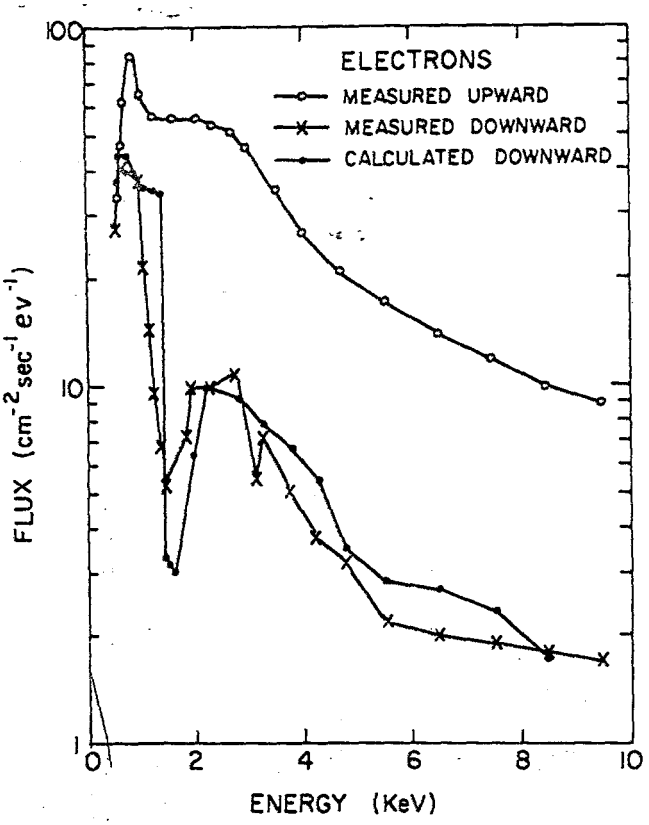

Figure 3.16: Energy spectra of electrons observed by Kelley *et al.* (1977).

like the early one in Fig. 3.3. These fluxes are, however, too small to make much contribution to ionization.

Gledhill and Hoffman (1981) using nighttime Atmosphere Explorer-C data spanning 4 years around sunspot minimum show that the Brazilian (South Atlantic) Anomaly centred on 35°S; 30° W is very stable in its location, but that the region between South Africa and Antarctica (60°S; 10°E), the Southern Anomaly, is very variable in both intensity and position. (Fig. 3.17).

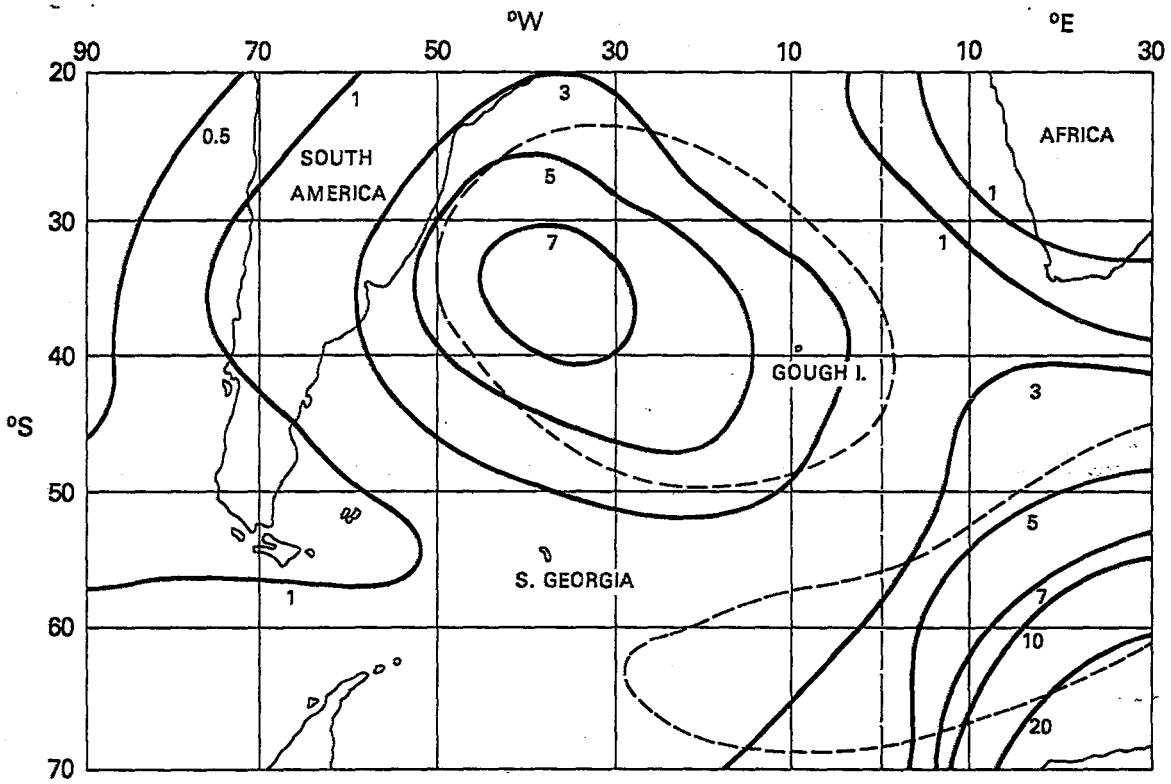

Figure 3.17: Contours of equal apparent downward electron energy flux (0.2 - 26 keV) over the South Atlantic, 1974-1977. Units are 10^{-3} erg $cm^{-2}s^{-1}$. $K_p \leq 3$. Dashed lines represent regions of high energy particle fluxes observed by Ginzburg *et al.*, (1962). From Gledhill and Hoffman (1981).

Chapter 4

Precipitated Particle Energy Fluxes

4.1 Estimates of Ionization due to Precipitated Particles in the Anomaly

Despite the lack of measurements *in situ*, the fluxes observed outside the Anomaly may be used to estimate those inside it. Since there are few daytime measurements available, the estimates shall be confined to the nighttime.

The average values of the total energy flux at 250 to 300 km found by Torr *et al.* (1976) with Atmosphere Explorer-C are shown as a function of invariant latitude in Fig. 4.1. Values are given for the energy carried by electrons during the night and during the day and by protons at night. From the figure it can be seen that, for both the latitude of the South Atlantic Anomaly ($\Lambda = 32°$S; $L = 1.4$) and that of the Southern Anomaly ($\Lambda = 52°S; L = 2.6$), the daytime electron energy flux is about 2×10^{-3} erg cm^{-2}s^{-1}, the nighttime flux about 4×10^{-4} erg cm^{-2}s^{-1} and the nighttime proton energy flux about 1×10^{-4} erg cm^{-2}s^{-1}. If the tenfold increase in the Anomaly deduced from the figures of Torr *et al.* (1975) and confirmed by this dissertation are accepted as typical, then the corresponding nighttime electron energy fluxes in the most intense regions of the South Atlantic and Southern Anomalies would be about 4×10^{-3} erg cm^{-2}s^{-1}, which compares well with those actually observed during the two ASHAY periods in 1976 of about 2×10^{-3} erg cm^{-2}s^{-1} found in this study and illustrated in Fig. 3.6. Fig. 4.2 shows typical energy spectra of these electrons, observed by Torr *et al.* (1976). The portions of the electron spectra above 2 keV can be fitted with straight lines corresponding to power law exponents of about -1. The data can alternatively be represented by an exponential

spectrum, $700e^{-E/15}$ $cm^{-2}s^{-1}sr^{-1}$ keV^{-1}. Since the Rhodes group have developed rapid methods for estimating the ionization produced by electrons with exponential spectra, the latter is used here (Wulff and Gledhill, 1974; Gledhill, 1984). Torr *et al.* (1976) state that the pitch angle distributions were isotropic. Hence the above may be multiplied by π, to estimate the flux isotropic over the downward hemisphere, and by 10 to allow for the intensification in the Anomaly, obtaining $2 \times 10^4 e^{-E/15}$ $cm^{-2}s^{-1}$ keV^{-1}. This corresponds to a flux of 3.7×10^{-3} erg $cm^{-2}s^{-1}$, in good agreement with the figure of 4×10^{-3} erg $cm^{-2}s^{-1}$ found above.

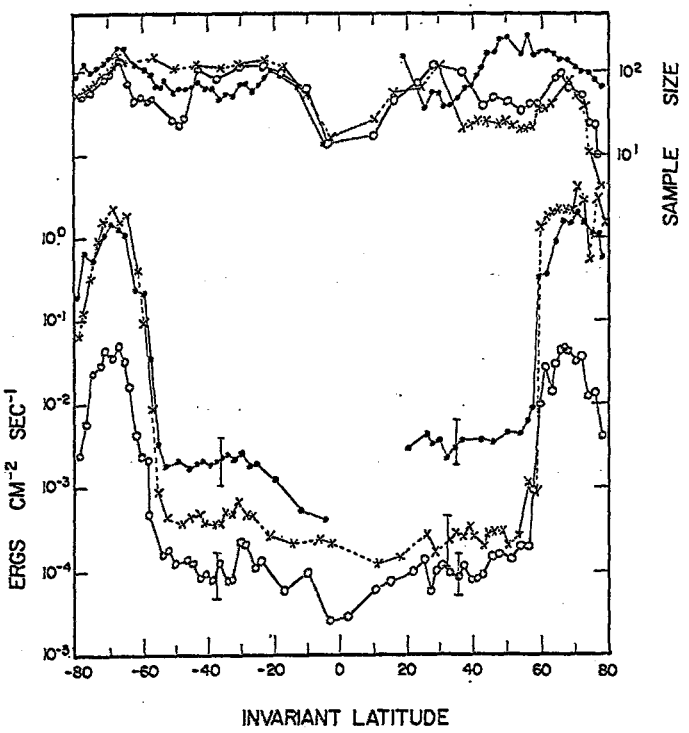

Figure 4.1: The total energy flux between 250 and 300 km altitude as a function of invariant latitude: (●—●) electrons, daytime; (—x- - -) electrons, nighttime; (o—o) protons, nighttime. The error bars indicate the probable uncertainties. The three uppermost curves show the sample size for each invariant latitude bin. From Torr *et al.* (1976)

This spectrum would produce maximum ionization at about 96 km with about 2400 electrons per cm^3 with a corresponding critical frequency (foE) of the E-region of just below 0.5 MHz. There would be appreciable ionization at least down to 85 km, in the upper D-region which would be increased by the portion of the spectrum above 26 keV. The low-energy portion, below 2 keV, which have been neglected, would deposit its energy in the F-region above 140 km. Since the F-region is very sensitive to dynamic effects such as neutral winds it is hardly possible to make a general estimate of the effects of this energy input.

Whereas Torr *et al.* (1976) show a fairly uniform distribution of energy flux between latitudes

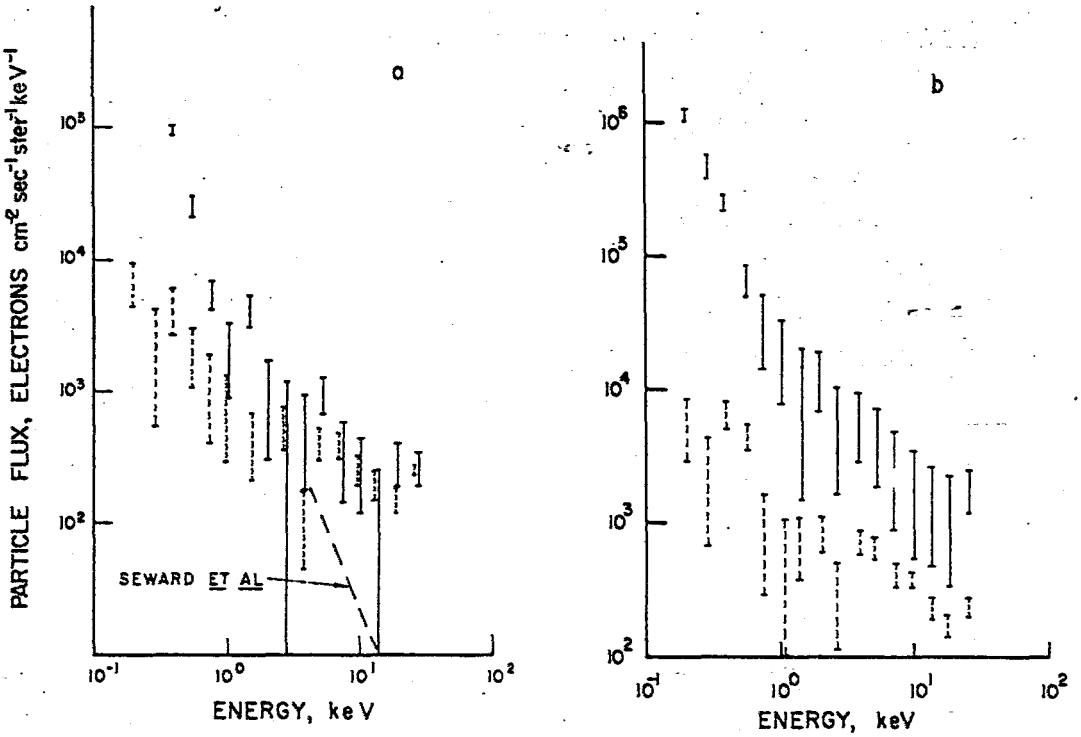

Figure 4.2: Spectra of electrons and protons observed by Torr *et al.* (1976).

20°S and 60°S (Fig. 4.1), Voss and Smith (1980) find separate zones of precipitation, with definite minima between them. Their low-latitude and mid- latitude zones agree well in position with the South Atlantic and Southern Anomalies, as has already been noted. Unlike Torr *et al.*, (1976), they find that the pitch angle distributions are by no means isotropic, but peak near 90° at all altitudes. Thus at any height most of the particles are mirroring or nearly so. The resulting ionization is almost constant with height from about 200 km down to a cut-off height, below which it decreases rapidly. For the electrons in the low-latitude zone this cut-off is at about 100 km, while for the protons in the mid-latitude zone it is at about 130 km.

It is not easy to estimate the effects of these fluxes drifting into the Anomaly. Presumably the cut-off height would be lowered because of the decreasing magnetic field at a fixed height, but the exponential increase of neutral atmospheric density would limit this change to a few kilometres. A complex calculation is needed to estimate the effects more closely (Voss and Smith, 1977). Nevertheless, the value of 5×10^{-4} erg cm^{-2}s^{-1} for the energy precipitated in the low-latitude zone found by Voss and Smith (1977) is very similar to the 4×10^{-4} erg cm^{-2}s^{-1} found by Torr *et al.*, (1976) and, in the absence of more detailed calculations,it may be concluded that the observations of Voss and Smith (1979) are not inconsistent with the formation in the South Atlantic Anomaly of an E-layer like that deduced above from the figures given by Torr *et al.*

(1976). The height may be a little greater on account of the flat pitch angle distribution. The greater energy carried by protons in the mid-latitude zone according to Voss and Smith (1979), namely 5×10^{-3} erg $cm^{-2}s^{-1}$, and the greater cut-off height, consistent with the larger ionization cross sections of atmospheric constituents for proton impact, suggest that the E-layer in the Southern Anomaly would be higher and more dense than that in the South Atlantic anomaly.

4.2 Observations of Ionization in the Anomaly D-region

We would expect ionization in the D-region to be produced by the higher-energy part of the electron spectrum in the South Atlantic Anomaly, and perhaps not so much by the protons in the Southern Anomaly, on account of the larger cross-sections, which would remove most of the particles before they penetrate to D-region depths. D-region ionization has two easily observable affects: an increase in the absorption of radio waves passing through it and an increase in the phase velocity along the earth-ionosphere waveguide of VLF waves propagating in it.

Abdu *et al.* (1973) and Trivedi *et al.* (1973) have made measurements with a 30 MHz riometer at Atibaia, Brazil (23°S; 45°W). The instrument was switched between two Yagi antennae, one directed vertically upwards and the other at 45° to the vertical, pointing westwards. Fig. 4.3 shows one of their records. In each of the two events arrowed, the absorption appears first on the westward-directed antenna. Abdu *et al.* (1973) interpret this as evidence that the particles responsible were electrons, which drift from west to east. The time delays involved are too long to be accounted for in this way unless an arbitrary electric field is assumed to exist, however, which rather reduces the conviction of the argument.

The VLF propagation method is sensitive to small changes in the height of the upper boundary of the waveguide, i.e. the lower part of the D-region. Cavalieri *et al.* (1974) have calculated that a uniform lowering of the boundary by only 1 km over the 5600 km path from the 16 kHz transmitter GBR at Rugby, England, to Baltimore, Maryland, United States of America, would produce a phase advance of 2.9 μs, easily measurable with modern atomic frequency standards. Unfortunately, changes in the vertical gradient of ionization density at the lower edge of the D-region amount in effect to changes in the width of the waveguide also and can either advance or retard the phase. Also, variations in the waveguide width cause differences in the propagation times of different modes to the receiver, thus producing, by interference,

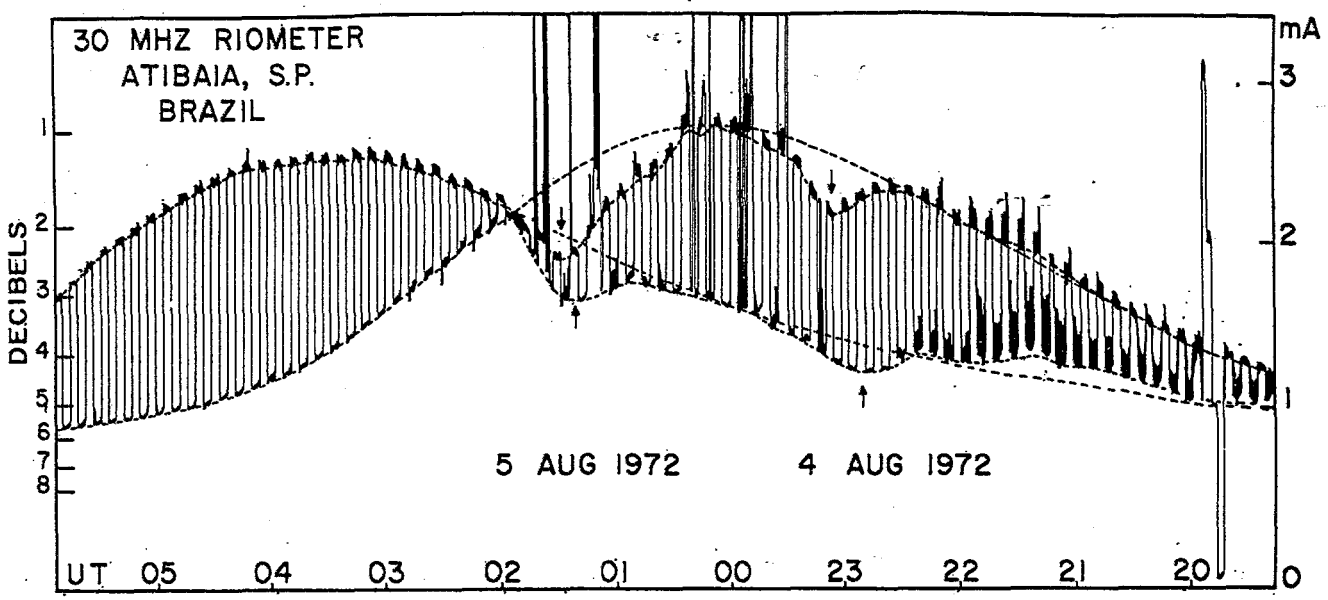

Figure 4.3: 30 MHz riometer recordings. From Abdu *et al.* (1973). The broken smooth curve represents the variation of the unabsorbed cosmic noise intensity. The upper curve represents the westward looking antenna, whilst the vertical antenna is represented by the lower curve.

apparent changes of phase which are not simply related to the height of the reflecting region. (Svennesson and Westerlund, 1979). Thus the interpretation of such measurements is open to question, unless comparison can be made with similar paths which do not pass through the Anomaly and unless a great deal is known about conditions along the whole propagation path.

Several groups, especially those in Brazil, have made regular recordings of the phase and amplitude of the signals from various VLF transmitters for some years. The results have, however, not been as fruitful as one might hope as far as the study of the Anomaly is concerned. Mendes *et al.* (1970) adopted a method due to Westerlund *et al.* (1969) to show that the VLF phase and amplitude changes observed near the centre of the magnetic anomaly during polar cap absorption (PCA) and solar proton events agreed with the values of VLF phase changes calculated from the proton fluxes observed by satellites. This is rather surprising in view of the general belief that protons are not important ionizing agents at these low latitudes during such events.

Gough (1975) recorded the phase of the 22.3 kHz signal from North West Cape, Australia, as received at São Paulo, Brazil. The propagation path (Fig. 4.4) passed through both the Southern and the South Atlantic Anomalies. Unfortunately, it also passed through the auroral

zone in the vicinity of Enderby Land, Antarctica. Because there was only a short period, less than two hours each day, when the whole path was either illuminated or in darkness, Gough considered only the difference in phase delay between these two extremes ie, the whole path illuminated or the whole path in darkness. He found two maxima in the correlation coefficient of this quantity with the planetary magnetic index A_p, one coinciding with the day of observation and the other delayed by 3 or 4 days. Similar correlations for the phase of the signal from NLK, in Washington State, USA, the path of which passed through the South Atlantic Anomaly but not the auroral zone (Fig. 4.4), showed only the delayed maximum. He therefore attributed this delayed maximum to the effect of the Anomaly and preceded to show that, on this assumption, there is no evidence of enhanced D-region ionization in the Anomaly, since only the NWC path which passes through the auroral zone exhibited a direct correlation peak with increased magnetic index A_p.

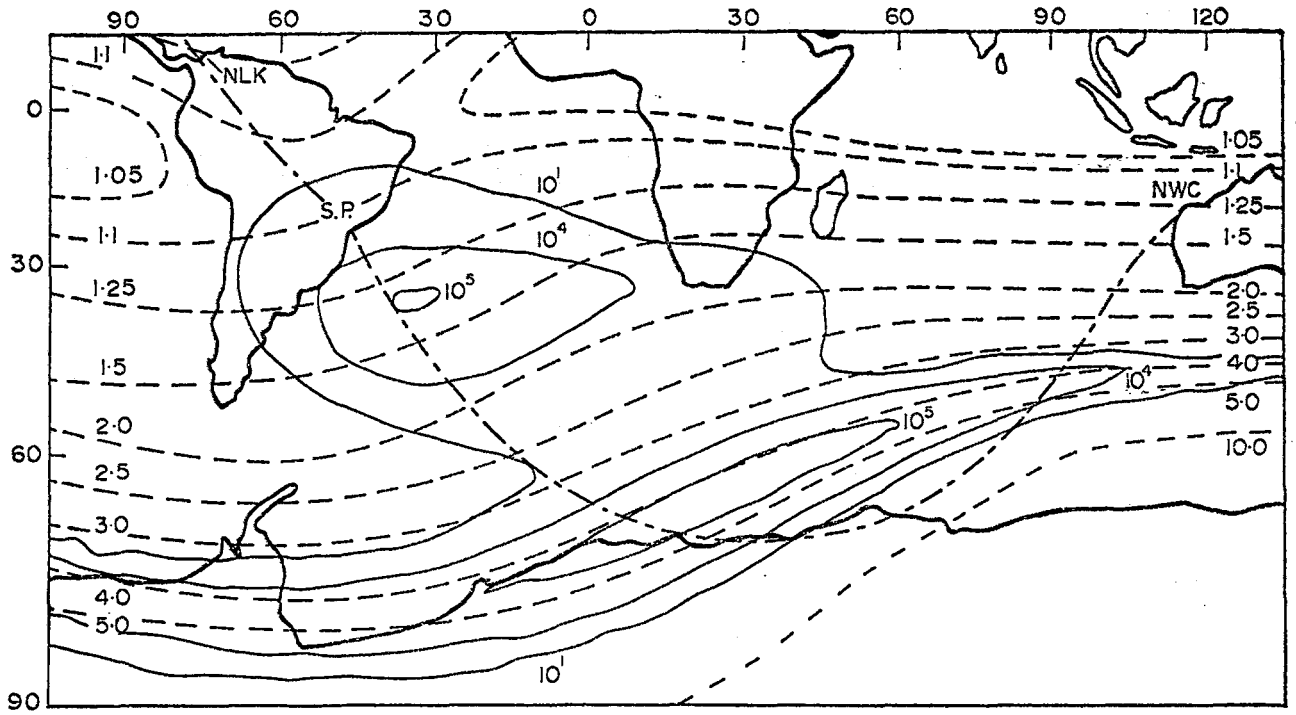

Figure 4.4: Paths of VLF waves observed by Gough (1975).

Doherty (1971) reported that rapid simultaneous phase and amplitude fluctuations were observed much more frequently on the Nantucket (Massachusetts) - Jupiter (Florida) path than on paths in the Aleutian Islands and suggested that this might be because the midpoint of the former path lies in the conjugate region to the South Atlantic Anomaly.

Thus, the meagre evidence which exists for particle produced ionization in the D-region in the

Anomaly is inconclusive at present.

4.3 Observations of Ionization in the Anomaly E-region

The E-layer at a height just below 100 km, with a critical frequency of about 0.5 MHz, which was predicted above, may indeed exist as a regular feature of the South Atlantic Anomaly; at present nothing is known of the E-region in the Southern Anomaly.

Abdu and Rai (1974) reported the frequent occurrence of a low-lying sporadic E-layer, at 90-95 km, during the night over Cachoeira Paulista, Brazil (23°S; 45°W). They observed a "regularly" ionized layer with a critical frequency in the range 0.3 to 0.6 MHz. Simultaneous riometer recordings at 30 MHz showed absorption of the expected magnitude. The authors stated their belief that this was good proof of the production of ionization by particle precipitation in the South Atlantic Anomaly. Later, Abdu and Batista (1977) found that sporadic E layers occur much more frequently at Cachoeira Paulista than at any other station at comparable latitudes (Fig. 4.5). They also reported that auroral type sporadic E is observed at Cachoeira Paulista, but the ionogrammes published by Batista and Abdu (1977) appear rather to be a spread type of flat sporadic E (Fig. 4.6). This may, nevertheless, be produced by precipitated particles, especially by fluxes with flat pitch angle distributions like those observed by Voss and Smith (1979).

After a tour of South American ionosphere stations W.R. Piggott (private communication, 1976) ventured that in his opinion particle E is often seen at many stations there, but is not reported as such because it is generally believed to be confined to the auroral and sub-auroral regions. A study of these ionogrammes would be rewarding.

Abdu *et al.* (1979) have reported a re-analysis of rocket observations made by several groups during the total solar eclipse of 12 November 1966 at Cassino, Brazil (32°S; 52°W). By solving the time-dependent continuity equations for the important ion species in the region 75-110 km, with a solar illumination function calculated from the circumstances of the eclipse, they showed that it was necessary to add an ion production rate which could be ascribed to particles. It is difficult to estimate the residual radiation from the solar corona during totality of an eclipse and this, together with uncertainties in the rate coefficients of the ionic reactions and the possible effects of those which were neglected, must cast some doubt on this interpretation. All that can be said is that the analysis is consistent with the presence of an ionizing source during totality,

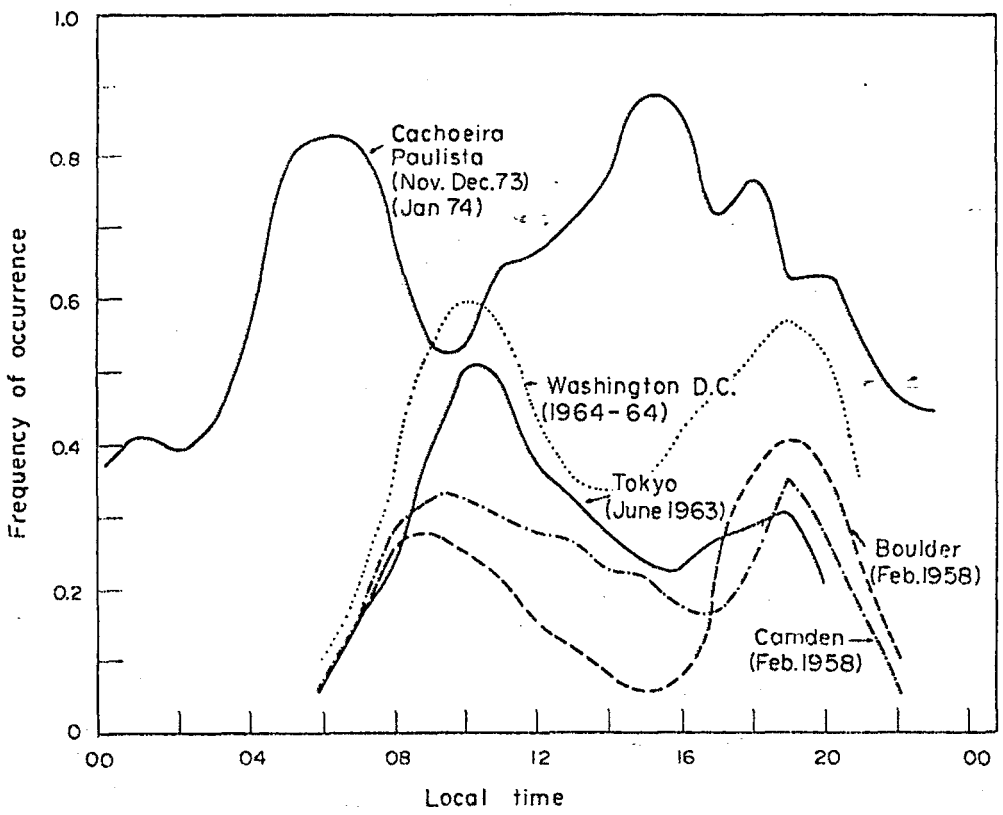

Figure 4.5: Frequency of occurrence of sporadic-E layer, from Abdu and Batista (1977).

over and above the residual solar radiation assumed by these authors. It has not been shown that the fluxes and spectra of electrons necessary to produce the extra ionization are consistent with estimates of those likely to be found at the western edge of the South Atlantic Anomaly.

In the second chapter an attempt was made to present the case of a source of extra ionization, for the daytime E-layer as being due to particle precipitation. Yet again, this is speculative in nature. The analysis of Atmosphere Explorer-C data for the nighttime is far more convincing yielding the right sort of numbers for the fluxes and spectra of electrons required to maintain an E-layer at night. Unfortunately, shipborne ionosondes are limited by the length of antenna available and consequently have f_{min} values greater than 1 MHz and thus the "regular" nighttime E-layer with an approximate critical frequency (foE) of 0.5 MHz is not seen in this remote and inaccessible location.

4.4 Observations of Ionization in the Anomaly F-region

There have been many, and often conflicting, reports of phenomena in the F-region of the Anomaly. King *et al.* (1964) reported spread F, local increases in electron density and "thin sheets of ionization" over the South Atlantic, observed by the satellite Alouette 1. Rothwell

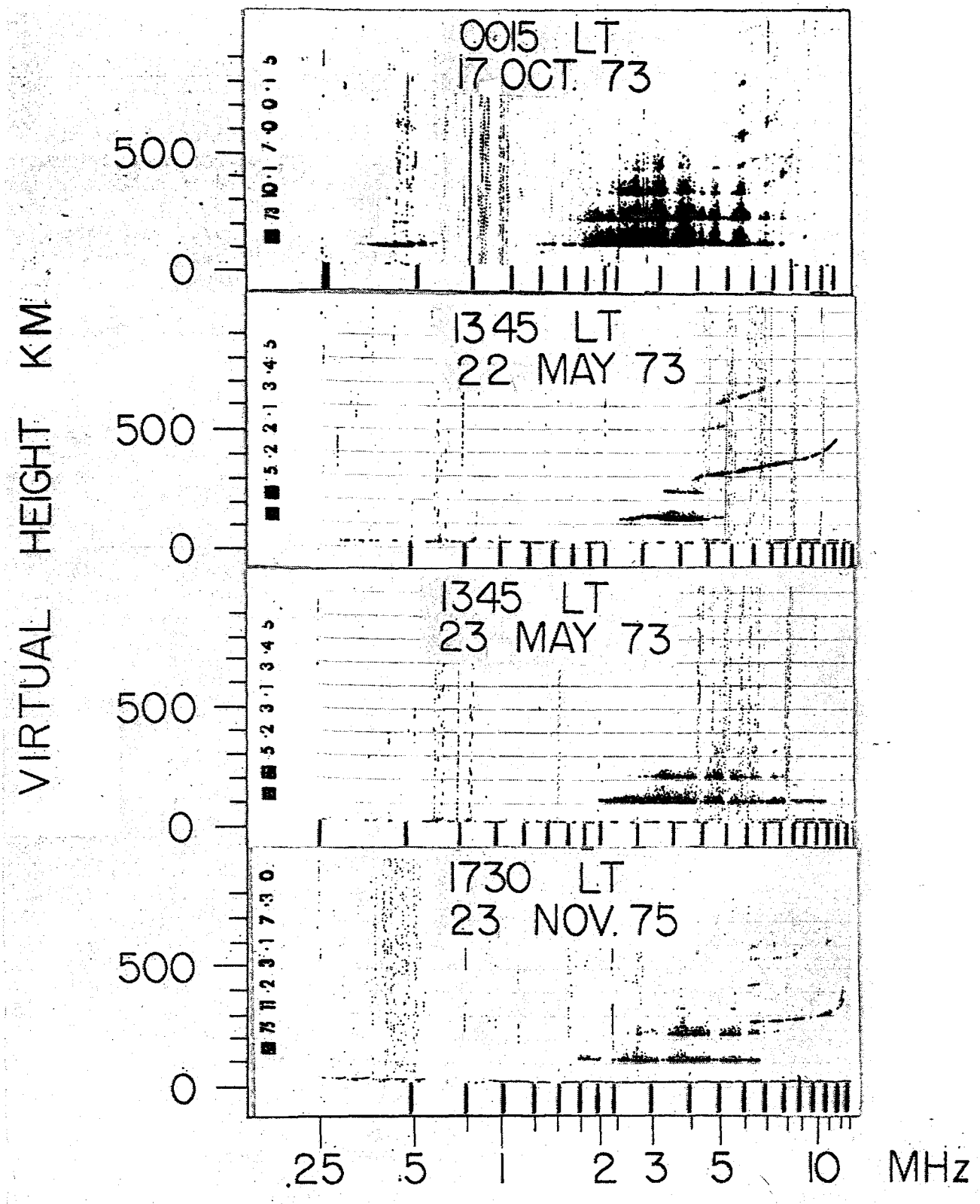

Figure 4.6: Examples of the so called auroral type sporadic E as observed at Cachoeira Paulista. From Batista and Abdu (1977).

(1964) found similar maxima and minima with Ariel 1. Gledhill and Torr (1966) showed that a high correlation existed between fluxes of electrons with energies above 40 keV in the conjugate area to SANAE, Antarctica, (70°S; 2°W) and F-region disturbances at that station. Gledhill *et al.* (1967) found a greater frequency of F-region disturbance at SANAE than at any other station near the same shell, L = 4, and Torr and Torr (1967) demonstrated that the F-region is more variable in the Anomaly than at any other mid-latitude location. Knudsen and Sharp (1968) found very variable ionization maxima at 300 km in the Anomaly. Haggard and Gledhill (1976) have shown that the median values of the daily maxima of foE, foF1 and FoF2 at Gough Island (40°S; 10°W) all lie above the straight lines connecting the corresponding points for other stations surrounding the South Atlantic, when plotted against geographic latitude (Fig. 2.26). Measurements made with the swept-frequency impedance probe on the Japanese satellite TAIYO (Oya *et al.*, 1979) also show increased ionization at heights of about 300 km in the South Atlantic Anomaly.

This dissertation has shown that in general *minima* of electron density at about 300 km coincide with *maxima* in precipitated energy carried by electrons at night, and *vice versa*. This is in conflict with some of the observations reported above and with the total electron content measurements by de Mendonca (1965), who observed a marked *increase* of electron content in the South Atlantic Anomaly, but Kauffmann *et al.* (1976) reported a pronounced *decrease* in total electron content in the same region, by a factor of 2 to 3 from 53°W to 40°W at 21°S, during the eastward movement of the ATS-6 satellite. Massambani (1978) found, during the movement of the same satellite westwards, that the decay of the plasma density at night was faster in the east than in the west. He suggested that this may be due to the replacement of ionization on the westward side of the Anomaly by electron precipitation.

Measurements of ion concentrations by Sharp *et al.* (1966) showed that, at longitudes which passed through the South Atlantic Anomaly, there were pronounced differences between the ion density on opposite sides of the equator. They found the excess ionization in the southern hemisphere to coincide in location with large fluxes of trapped electrons with energies greater than 0.24 MeV (Fig. 3.24). At longitudes outside the Anomaly this was not so. Although these measurements were made in 1963, when there were still large fluxes of "Starfish" electrons present, it would be surprising if there was not a corresponding asymmetry with the smaller, less energetic fluxes now existing there.

By now it must be clear that there are few actual measurements in the South Atlantic Anomaly

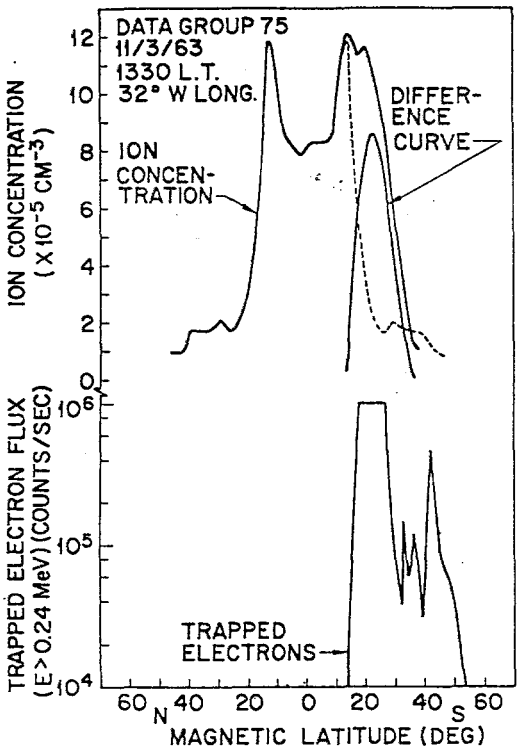

Figure 4.7: Ionization at longitudes passing through the South Atlantic Anomaly. From Sharp *et al.* (1966).

which are not open to suspicion in one way or another, and fewer still in the Southern Anomaly.

It is worth noting that the observation of the occurrence of ionization minima close to electron precipitation maxima in the previous chapter, the rapid fluctuations observed by other workers (Dachev, 1976; Oya *et al.*, 1979), the phenomena noted by King *et al.* (1964) and Rothwell (1964), and especially the upward fluxes of oxygen ions (Prangé and Crifo, 1977) and electrons (Kelley *et al.*, 1977) all suggest strongly that electric fields play a much more important part than has previously been suspected in determining the configuration of the ionosphere in the South Atlantic Anomaly. This is an aspect which deserves experimental and theoretical study in the near future.

4.5 Atmosphere Explorer-C Data: 1973-1978

Although many satellites have passed repeatedly through the South Atlantic Anomaly, very few values for the fluxes and energy spectra of electrons or positive ions in the energy range below 30 keV have been published.

The reason is primarily the high ratio of background counting rate to signal, due to the presence of high energy radiation belt particles which penetrate the space craft and the detectors, they

also produce bremsstrahling which may add to the background. The fluxes of low energy particles are 2-4 orders of magnitude less than those in the auroral zones for which most detectors have been designed, so that the statistics are poor and it has been considered unprofitable to attempt to extract information about the low-energy particles from the data.

I was most fortunate in obtaining copies of the Atmosphere Explorer-C data tapes in 1988 which contained six years of precipitating electron and proton flux data, albeit in sometimes shambolic coded bits.

Atmosphere Explorer-C passed through the Anomaly several times each day for more than six years and telemetry form the low energy particle experiment (LEE) was recorded on many of these orbits.

With this extensive data base it has proved possible to correct for the effects of the penetrating background radiation and to produce estimates of the spectra and fluxes.

The vast mass of data from the low energy particle experiment detectors on Atmosphere Explorer-C is available in the form of 15 second averages of the total energy flux apparently carried by electrons and ions, respectively, summed over all 16 energy channels in the range 0.2 to 26 keV. It requires considerable effort, many man months, and several hundreds of hours of computer time to extract detailed spectral information from the original telemetry records. If, however, it is now assumed that the ion channels always provide a measure of the background, it is only necessary to multiply the apparent ion energy flux by a constant factor, to take account of the different efficiencies of the detectors for ions and electrons at different energies, and to subtract this from the apparent energy flux carried by electrons to obtain a corrected electron energy flux with the effects of the penetrating radiation removed.

If it should happen that there is a measurable ion spectrum at any time, this method will over correct the electron values so that the original uncorrected electron energy flux will represent a maximum and the corrected one a minimum value, even under these circumstances.

As a test of this assumption Fig. 4.8 from Gledhill and Hoffman (1981) is shown, which summarizes data from three successive passes of the satellite through the anomaly on March 28, 1976.

The apparent energy flux carried by electrons is almost always greater than that in the ion channels. It is readily shown that the constant factor mentioned earlier is 1.19. By taking running means over 11 points it is shown that when the electron energy flux is corrected by

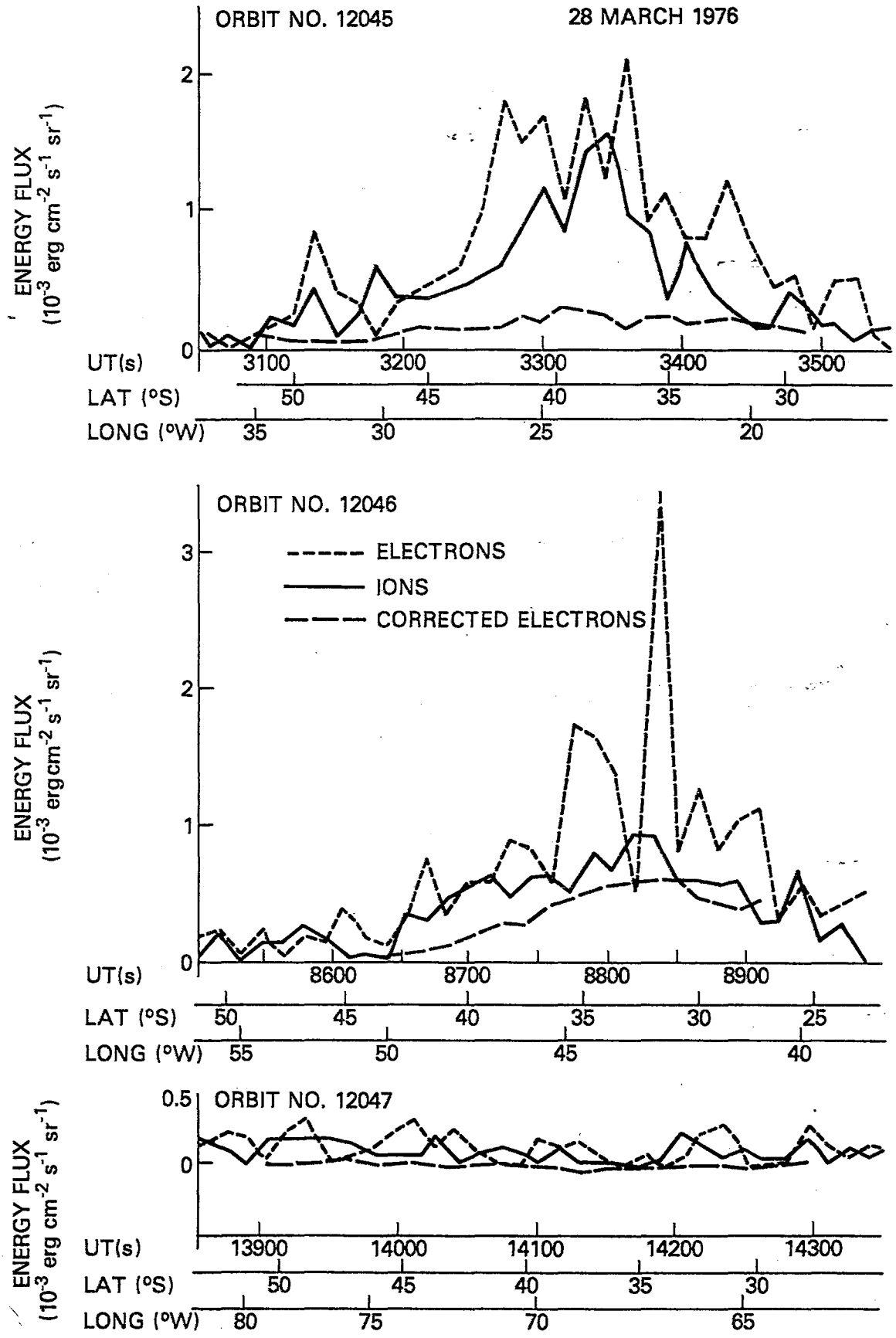

Figure 4.8: Apparent downward electron, ion and corrected electron directional energy flux for three successive orbits on March 28, 1976. Orbit 12045 and 12046 passed through the South Atlantic Anomaly but orbit 12047 lay to the west of it. From Gledhill and Hoffman (1981).

subtracting 1.19 times the ion energy flux from the electron energy flux, the resulting corrected energy flux increases towards the middle of the anomaly between 30°S and 35°S. Orbit 12047 shows a case where there was no significant electron or ion flux and the corrected electron energy flux averages zero. This orbit, however lies considerably to the west of the anomaly where only small fluxes would be expected. Note that the values may change rather dramatically in a few seconds. The much smoother nature of the corrected electron energy flux curves is, of course, due to taking the running means in the calculations of the points.

The data bank was searched for all times when Atmosphere Explorer- C was passing over the South Atlantic Ocean, at heights between 250 and 500 km, during the period January 1, 1973 to December 31, 1977, thus covering 5 years around sunspot minimum.

Whenever the satellite was in the specified volume and measurement of apparent electron and ion energy fluxes were available, the line of magnetic force on which observations were made was followed up or down to a standard level of 300 km by a complicated mapping procedure. The data were sorted into bins of latitude and longitude and the fluxes were averaged in each bin after eliminating data contaminated by scattered UV photons, MeV electrons and also sun spikes.

In all 180000 seconds of observations, representing one spectrum per second have been incorporated. 72% of the data base was for low magnetic activity ($K_p \leq 3$) and the remaining 28% for moderate magnetic activity ($3 \leq K_p \leq 6$) and 56% of the data was for the daytime while 44% was for the nighttime.

The bins finally used were 20° in longitude and 10° in latitude, with smaller bins the fluctuations were unacceptably high and structure due to single orbits with unusually large or small fluxes could be distinguished, despite the large data base.

4.6 Precipitated Electron Energy Fluxes

Fig. 4.9 shows the contours of daytime corrected precipitated electron energy fluxes for low magnetic activity, $K_p \leq 3$. The contours range form 0,63 to 4,20 $\times 10^{-3}$ erg $cm^{-2}s^{-1}$. A well defined maximum occurs off the East coast of Brazil at about 45°S; 50°W and another maximum in the South Eastern region, with a band of minima in between. Fig. 4.10 represents the nighttime corrected precipitated electron energy fluxes for the same conditions and period

as Fig. 4.9. Here the maximum value of the contour in the South Atlantic Anomaly region is 0,85 $\times 10^{-3}$ erg $cm^{-2}s^{-1}$. The ratio of daytime to nighttime precipitated electron energy fluxes is found to be 5 (five), which is half the value advocated by Torr *et al.* (1976).

The average number of observations for the daytime electron energy fluxes was 205 per bin whilst the average per bin for the nighttime values was 211 observations. Thus these contours are presented with a great deal of confidence. Further, they represent the minimum possible values since the data selection criteria used in this dissertation is over-discriminatory.

These daytime precipitated electron energy fluxes represent the first comprehensive study of the daytime precipitated electron energy fluxes. Previously, values for the daytime were used by increasing the nighttime values by an order of magnitude.

Observations during moderate magnetic activity viz, $3 < K_p \leq 6$ are also available. Here the average number of observations for the daytime and nighttime was 75 and 64 observations per bin respectively. These results are shown in Fig. 4.11 for the daytime and Fig. 4.12 for the nighttime. The maximum contour level in the South Atlantic Anomaly Region is $3,15 \times 10^{-3}$ erg $cm^{-2}s^{-1}$ during the daytime with a minimum value in the South West sector of $0,67 \times 10^{-3}$ erg $cm^{-2}s^{-1}$. The maximum contour level in the South Atlantic Anomaly Region during the nighttime is $2,25 \times 10^{-3}$ erg $cm^{-2}s^{-1}$ with a minimum value corresponding to $0,25 \times 10^{-3}$ erg $cm^{-2}s^{-1}$ to the south of it. The ratio of daytime to nighttime precipitated electron energy fluxes is thus seen to be much lower during moderately disturbed magnetic conditions, viz 1.4 as opposed to 5 previously found for quiet conditions - a 72% *decrease.*

The most remarkable and feature of these results is that for moderately active magnetic conditions the daytime value of precipitated electron energy fluxes is 25% *less* than during quiet magnetic conditions. However, the nighttime values show an *increase* of 165%. The nighttime results are consistent with those obtained by Voss and Smith (1980) but contrary to Gledhill and Hoffman (1981). The decrease in precipitated electron energy fluxes during the daytime is rather surprising and puzzling.

Table 4.1 represents the data for low magnetic activity, where the data has been separated into various seasonal groupings. Firstly, the approximate position of the maximum contour level within the anomaly region is given followed by the average maximum value of precipitated electron energy flux. This is followed by the minimum average value outside the anomaly. The next two columns give the average number of observations per 20° longitude by 10° latitude bin

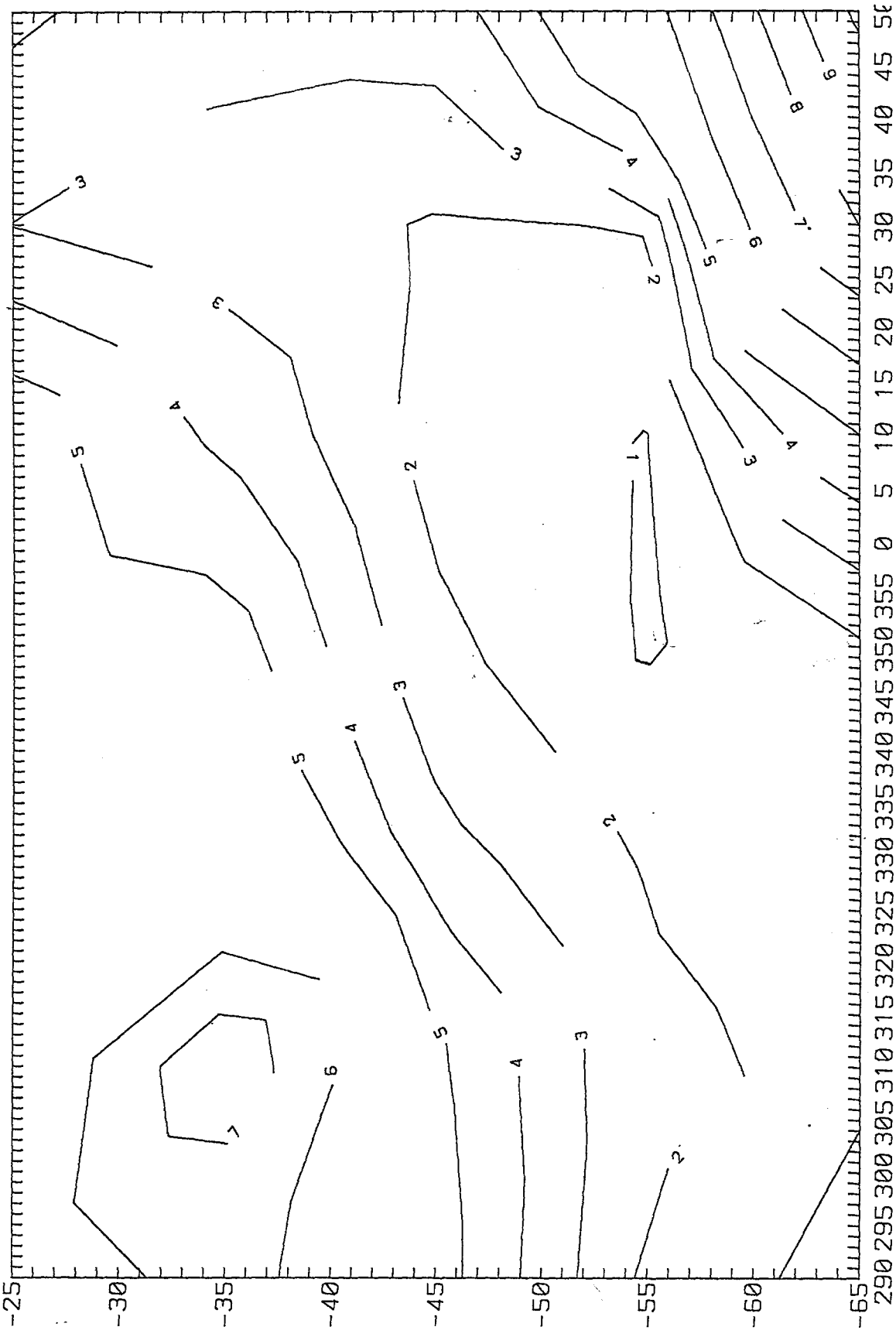

Figure 4.9: Contours of daytime corrected precipitated electron energy fluxes at 300 km in the range 0.2 to 26 keV in units of 10^{-3} erg $cm^{-2}s^{-1}$. $K_p \leq 3$.

Figure 4.10: Contours of nighttime corrected precipitated electron energy fluxes at 300 km in the range 0.2 to 26 keV in units of 10^{-3} erg $cm^{-2}s^{-1}$. $K_p \leq 3$.

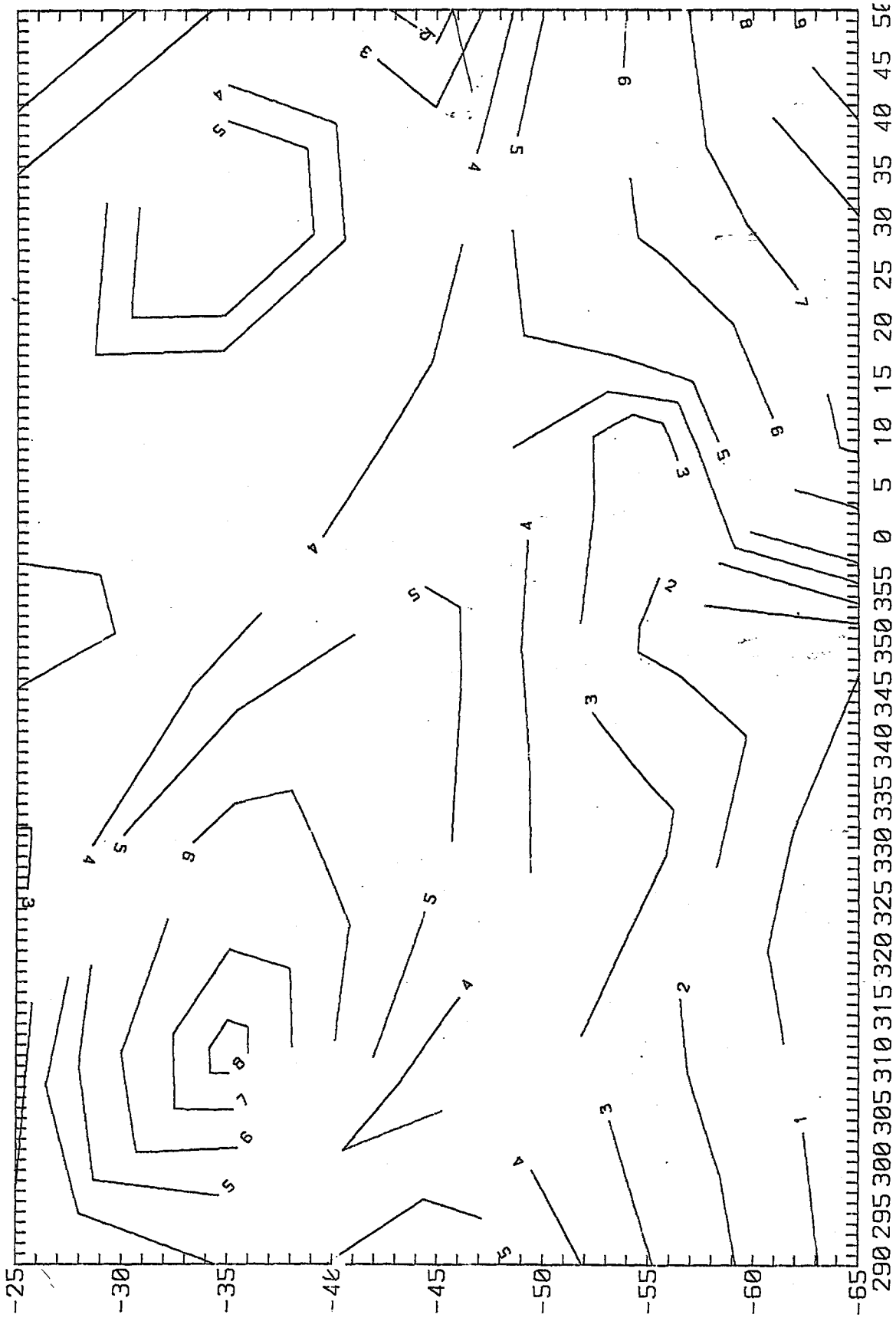

Figure 4.11: Contours of daytime corrected precipitated electron energy fluxes at 300 km in the range 0.2 to 26 keV in units of 10^{-3} erg $cm^{-2}s^{-1}$. $3 < K_p \leq 6$.

Figure 4.12: Contours of nighttime corrected precipitated electron energy fluxes at 300 km in the range 0.2 to 26 keV in units of 10^{-3} erg $cm^{-2}s^{-1}$. $3< K_p \leq 6$.

used to obtain the contour graphs, and the ratio of daytime to nighttime maximum precipitated electron energy fluxes inside the anomaly region. The last column gives the average ratio of the maximum value of precipitated electron energy fluxes inside the Anomaly Region to the minimum value of precipitated electron energy fluxes found outside the Anomaly Region. The first row of each seasonal grouping gives the daytime information, whilst the second row gives the equivalent nighttime information. The first seasonal grouping in the table gives the average values for the entire 5 year period subdivided into daytime and nighttime values. The next two seasonal groupings cover the 6 summer months and the 6 winter months, i.e. the data bank is split in half with the 6 summer months centred on mid December and the 6 winter months centred on mid June. The last 4 seasonal groupings consist of four three month periods roughly divided into 3 summer months (November, December and January), 3 autumn months (February, March and April), 3 winter months (May, June and July) and finally 3 spring months (August, September and October). Table 4.2 is similar to Table 4.1 except that it is for the moderately active magnetic periods viz, $3< K_p \leq 6$.

Period	Day or Night	Position of Anomaly Max.	Max. Value $\times 10^{-3}$erg cm^{-2}s^{-1} inside Anomaly	Min. Value $\times 10^{-3}$erg cm^{-2}s^{-1} outside Anomaly	Average number of observations per bin	Day to Night ratio inside Anomaly	Ave. ratio of max. to min. value
Average for	day	45°S; 50°W	4.20	0.63	205	5	6
the 5 years	night	35°S; 30°W	0.85	0.19	211		
6 summer months	day	35°S; 10°W	2.62	0.53	89	3	6
15 Sept.-15 Mar.	night	40°S; 70°W	0.87	0.10	41		
6 winter months	day	35°S;50°W	4.55	0.69	115	3	8
15 Mar.-15 Sept.	night	35°S; 30°W	1.66	0.14	170		
3 summer months	day	35°S; 10°W	2.66	0.54	54	12	5
Nov.,Dec.,Jan.	night	35°S; 30°W	0.23	0.06	12		
3 autumn months	day	35°S; 50°W	7.33	1.20	37	7	6
Feb.,Mar.,April	night	45°S; 30°W	1.12	0.22	49		
3 winter months	day	35°S; 50°W	7.67	0.29	63	3	22
May,June,July	night	35°S;30°W	2.40	0.17	116		
3 spring months	day	45°S; 50°W	3.76	0.51	44	6	7
Aug.,Sept.,Oct.	night	45°S; 30°W	0.64	0.09	35		

Table 4.1 Precipitated electron energy fluxes for $K_p \lesssim 3$.

Period	Day or Night	Position of Anomaly Max.	Max. Value $\times 10^{-3}$erg cm^{-2}s^{-1} inside Anomaly	Min. Value $\times 10^{-3}$erg cm^{-2}s^{-1} outside Anomaly	Average number of observations per bin	Day to Night ratio inside Anomaly	Ave. ratio of max. to min. value
Average for	day	35°S; 50°W	3.15	0.67	75	1.4	6
the 5 years	night	35°S; 30°W	2.25	0.25	64		
6 summer months	day	35°S; 30°W	0.67	0.24	37	1	4
15 Sept.-15 Mar.	night	45°S; 30°W	0.71	0.09	18		
6 winter months	day	35°S;50°W	4.97	0.45	39	1.3	13
15 Mar.-15 Sept.	night	35°S; 30°W	3.85	0.21	46		
3 summer months	day	35°S; 30°W	0.58	0.08	35	5	8
Nov.,Dec.,Jan.	night	45°S; 10°W	0.12	0.004	8		
3 autumn months	day	35°S; 30°W	2.79	0.17	20	4	13
Feb.,Mar.,April	night	45°S; 70°W	0.79	0.10	28		
3 winter months	day	35°S; 30°W	5.02	0.07	16	3	13
May,June,July	night	35°S;30°W	1.78	0.47	19		
3 spring months	day	40°S; 30°W	1.36	0.13	21	12	9
Aug.,Sept.,Oct.	night	45°S; 30°W	0.11	0.03	11		

Table 4.2 Precipitated electron energy fluxes for $3 < K_p \leq 6$.

4.7 Discussion of Results

The most obvious feature of the data pertaining to the moderately active magnetic period is the decrease in the maximum average value of the precipitated electron energy fluxes during these times. This is contrary to what would be expected and seems to indicate that those energetic particles are precipitated into the auroral zones during periods of magnetic activity exceeding $K_p = 3$. It also indicates that during periods of moderate magnetic activity the difference between precipitated energetic particles during the daytime and the nighttime are not as large as was anticipated and turned out to be very much smaller than during quiet magnetic conditions. The seasonal groupings show that for the longer periods the day/night ratio tend to one whilst the 3 month groupings tend to give larger ratios, but then the average number of observations per bin are small and the results tend to become unreliable.

The following 12 figures (Fig. 4.13 to Fig. 4.24) illustrate the observations as given in Tables 4.1 and 4.2.

These results also differ from those predicted by Torr *et al.* (1975) where the maxima occur far more westwards of their predicted maxima. The peaks of maxima obtained using the full 5 year data base as illustrated in this section agrees very well with Fig. 3.4 and Fig. 3.5 obtained using the limited data base obtained during ASHAY periods I and II. Although the daytime to nighttime ratio of precipitated electron energy fluxes is much lower for moderate magnetic activity it is however noted that the ratio of precipitated electron energy fluxes as measured in the anomaly region as opposed to the minimum energy fluxes measured outside the anomaly does increase with increased magnetic activity especially during the winter months.

The perpetual drizzle of low energy charged particles into the atmosphere over the South Atlantic Region tends to maintain the level of the nocturnal energy flux of electrons at about 1×10^{-4} to 9×10^{-4} erg $cm^{-2}s^{-1}$ for low K_p values. For moderately disturbed conditions it is found that the uppermost value increased to about 39×10^{-4} erg $cm^{-2}s^{-1}$. However, for the daytime, it is found that for both normal or low magnetic activity and moderate magnetic activity the range of electron energy flux is from about 1×10^{-3} to 5×10^{-3} erg $cm^{-2}s^{-1}$.

Thus it would appear that magnetic disturbances tend to increase the nighttime precipitation of electron fluxes and not have much effect on the daytime values. Perchance, the sun-spikes and other contamination during the daytime tends to mask any daytime enhancements in the precipitation of electron energy fluxes. Recollecting that the final precipitated electron energy

fluxes are obtained by subtracting the precipitated proton energy fluxes from the precipitated electron energy fluxes measured, could well mean that the daytime values have been overcorrected. Nevertheless, it must be remembered that the minimum possible precipitated electron energy fluxes are presented here and as such they are still the first comprehensive survey of daytime precipitated electron energy fluxes ever presented. Another noteworthy feature is that the maximum value of precipitated electron energy fluxes tended to decrease during summer for moderately active magnetic periods for both daytime and nighttime whilst the opposite is true for the winter period, especially at nighttime.

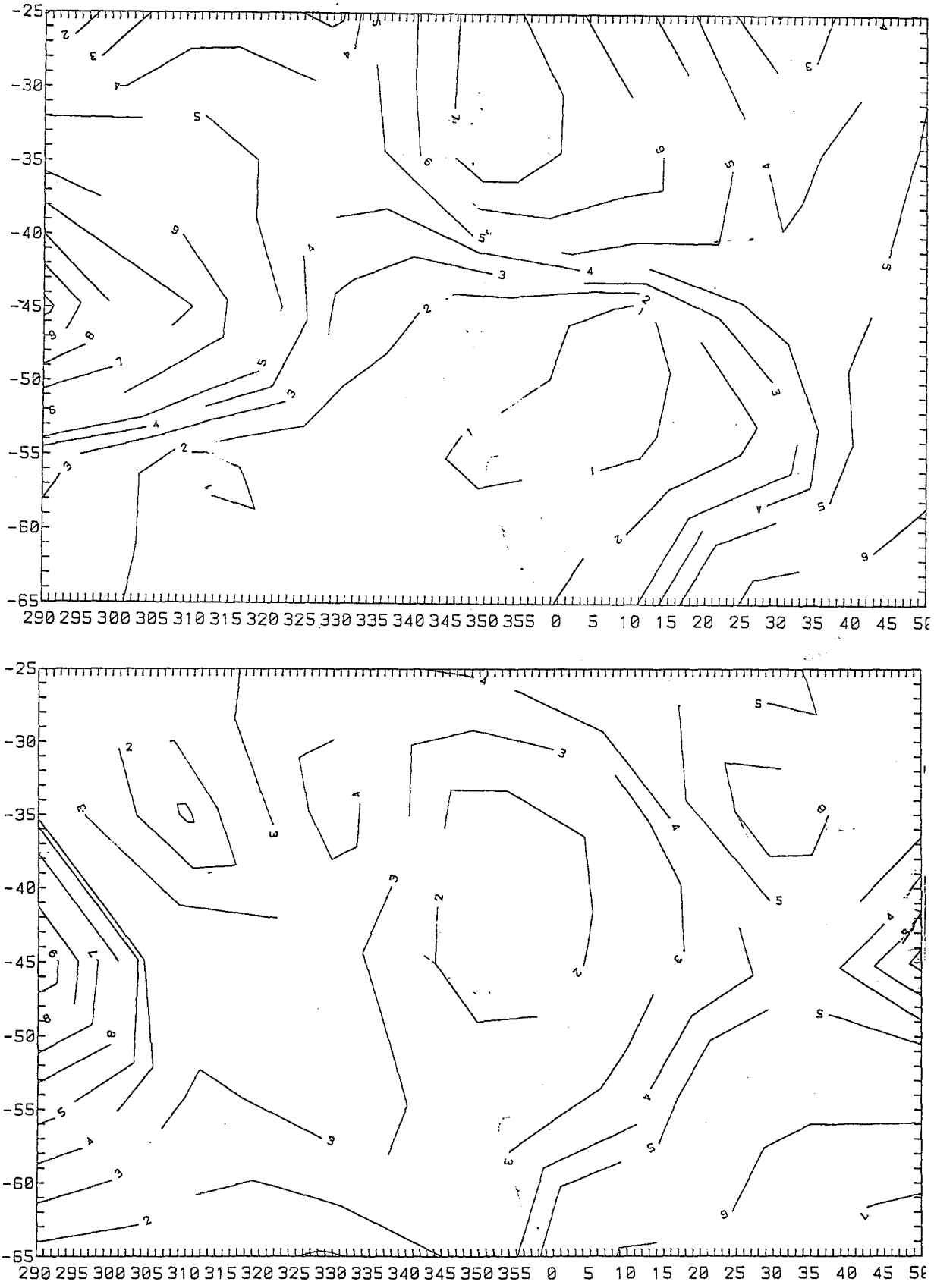

Figure 4.13: Contours of daytime corrected precipitated electron energy fluxes at 300 km in the range 0.2 to 26 keV in units of 10^{-3} erg $cm^{-2}s^{-1}$ for the 6 summer months. The upper panel is for $K_p \leq 3$ and the lower panel is for $3 < K_p \leq 6$.

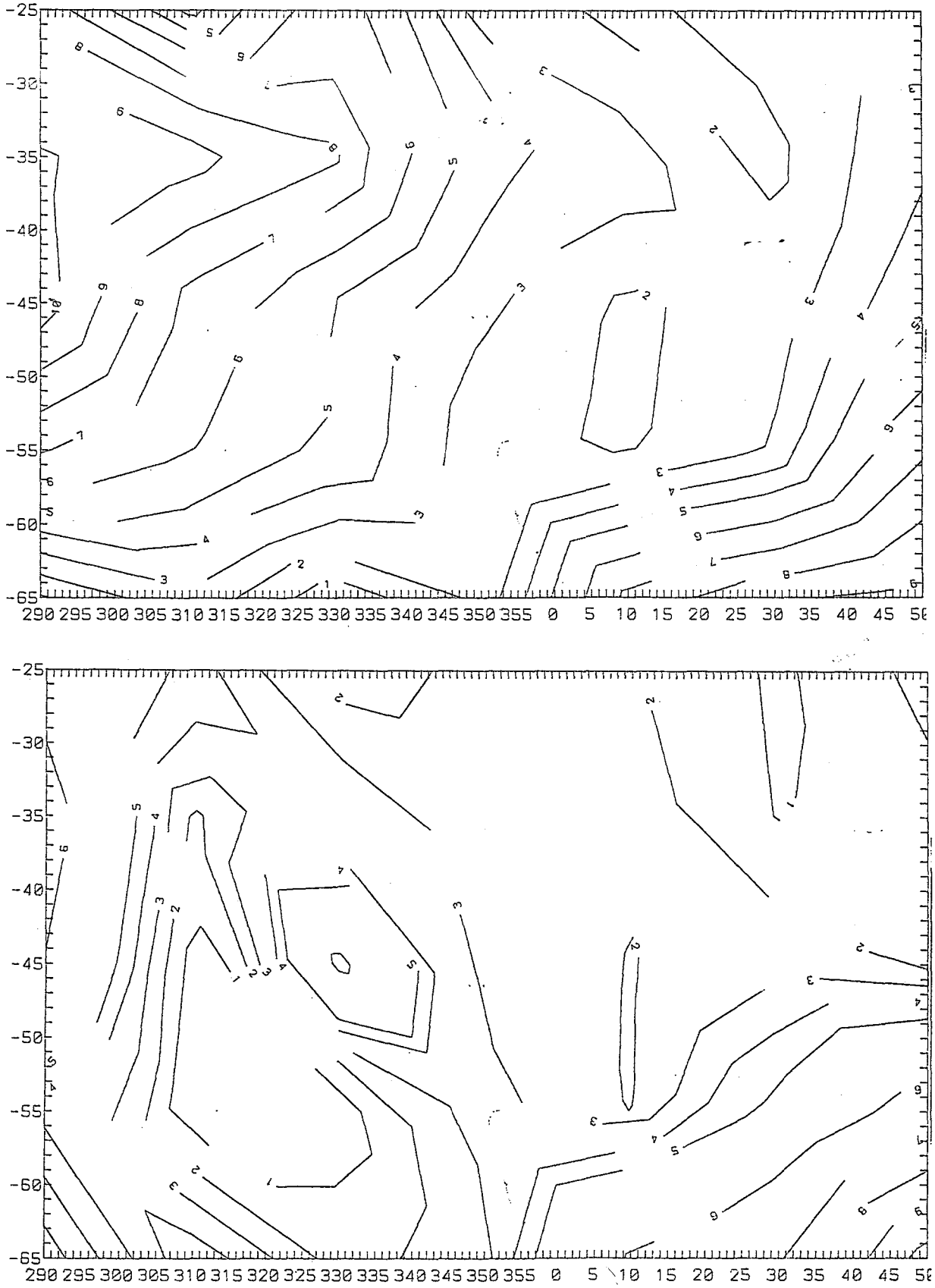

Figure 4.14: Contours of nighttime corrected precipitated electron energy fluxes at 300 km in the range 0.2 to 26 keV in units of 10^{-3} erg $cm^{-2}s^{-1}$ for the 6 summer months. The upper panel is for $K_p \leq 3$ and the lower panel is for $3 < K_p \leq 6$.

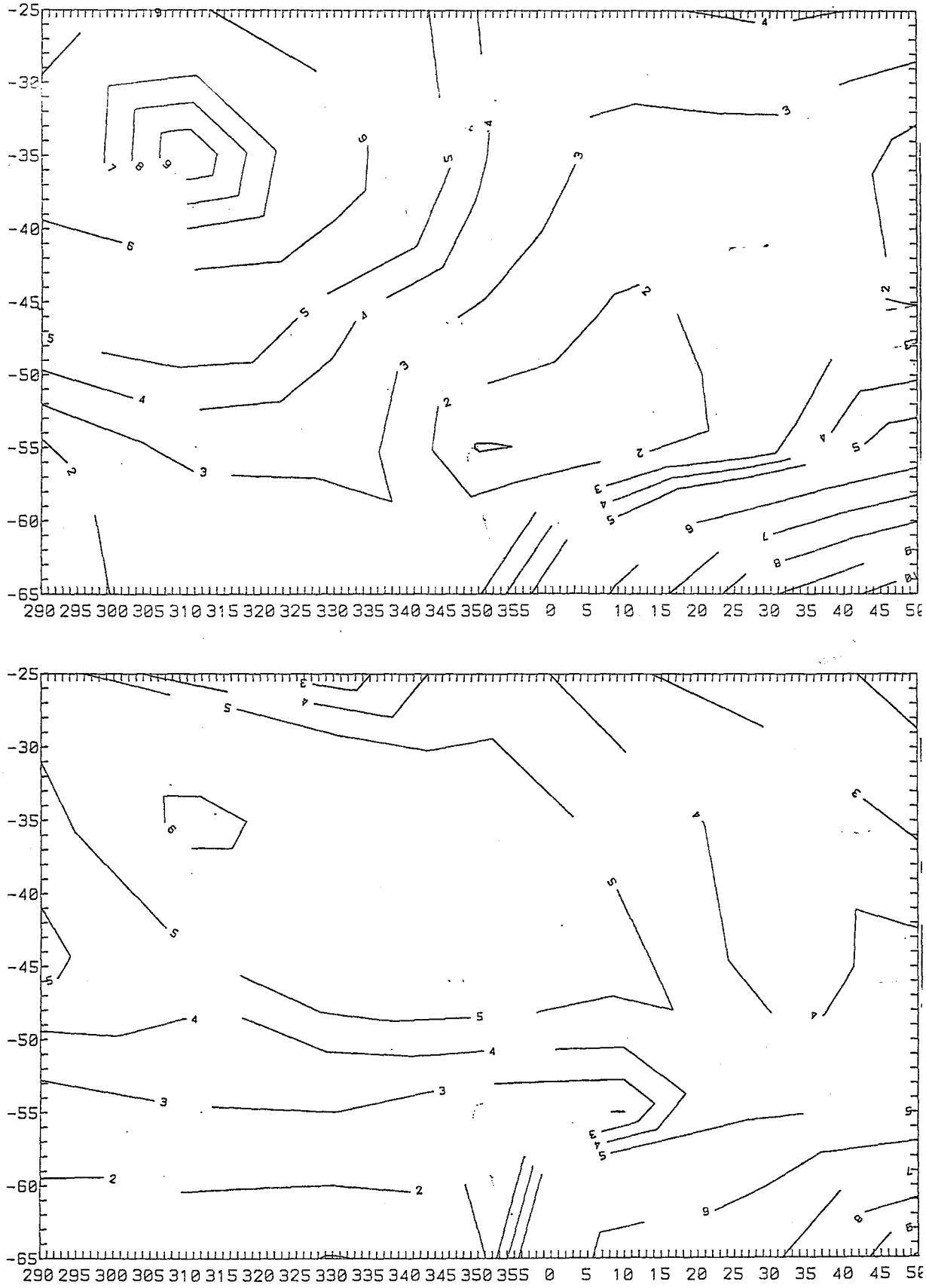

Figure 4.15: Contours of daytime corrected precipitated electron energy fluxes at 300 km in the range 0.2 to 26 keV in units of 10^{-3} erg $cm^{-2}s^{-1}$ for the 6 winter months. The upper panel is for $K_p \leq 3$ and the lower panel is for $3 < K_p \leq 6$.

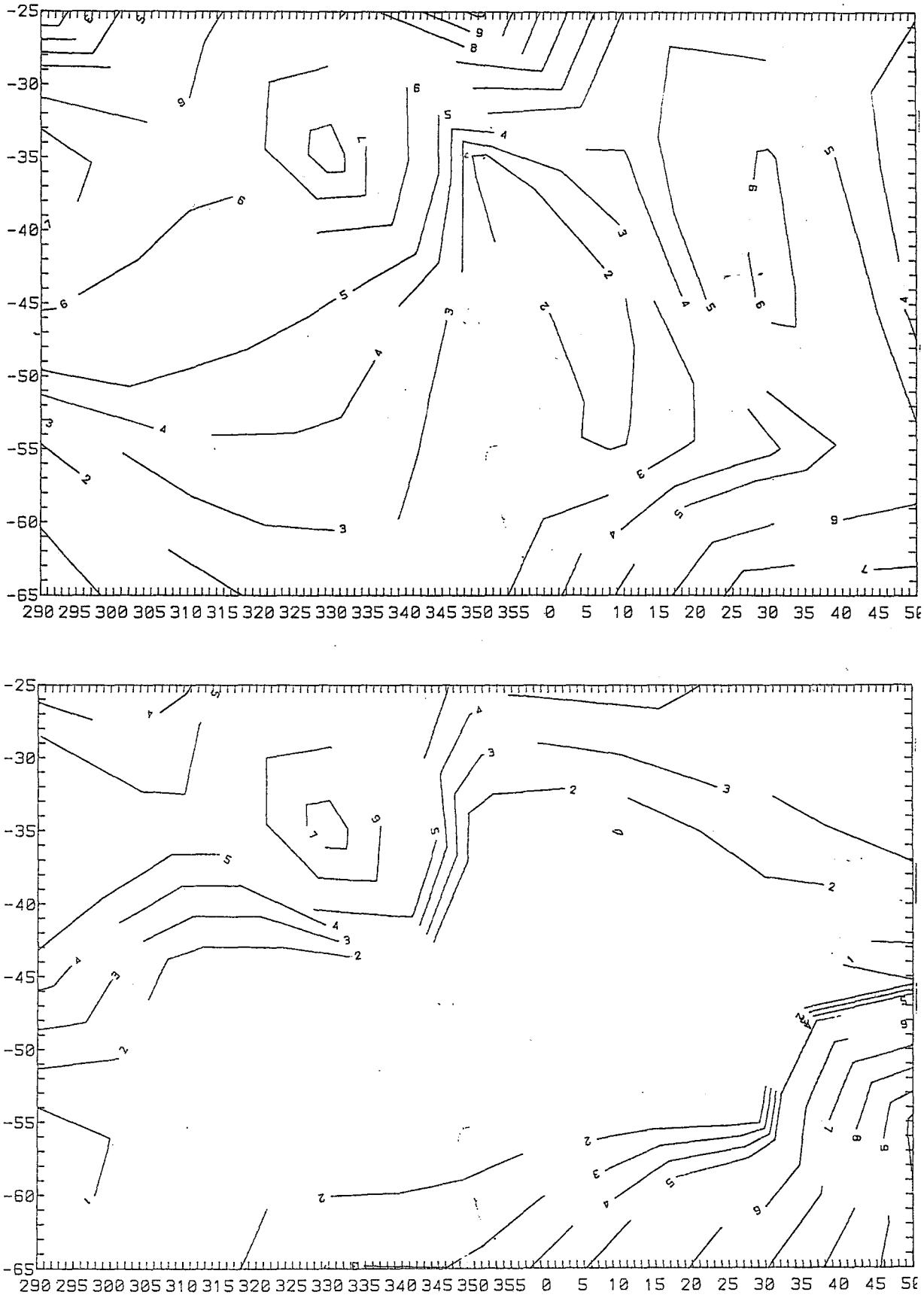

Figure 4.16: Contours of nighttime corrected precipitated electron energy fluxes at 300 km in the range 0.2 to 26 keV in units of 10^{-3} erg $cm^{-2}s^{-1}$ for the 6 winter months. The upper panel is for $K_p \leq 3$ and the lower panel is for $3< K_p \leq 6$.

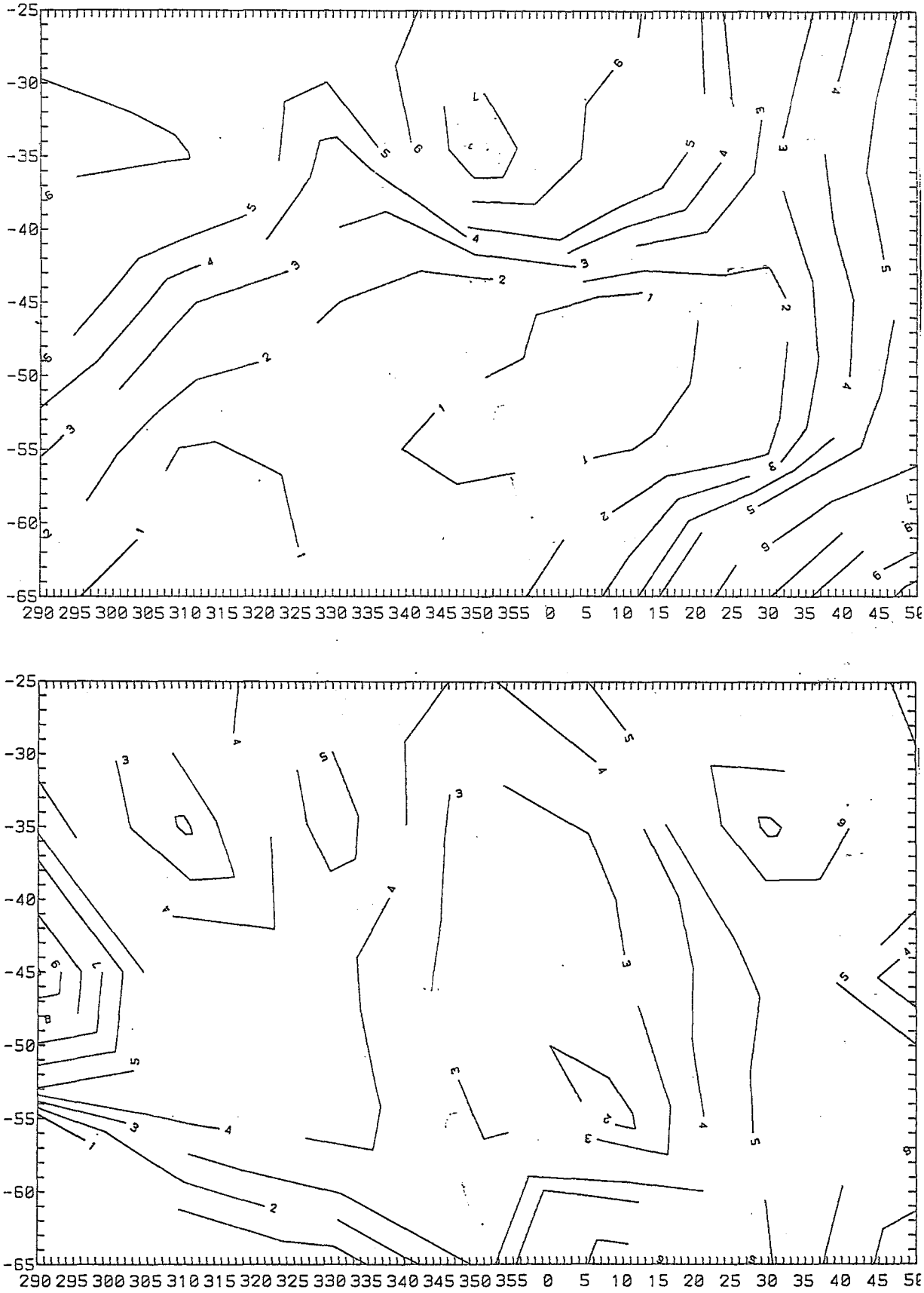

Figure 4.17: Contours of daytime corrected precipitated electron energy fluxes at 300 km in the range 0.2 to 26 keV in units of 10^{-3} erg $cm^{-2}s^{-1}$ for the 3 summer months. The upper panel is for $K_p \leq 3$ and the lower panel is for $3 < K_p \leq 6$.

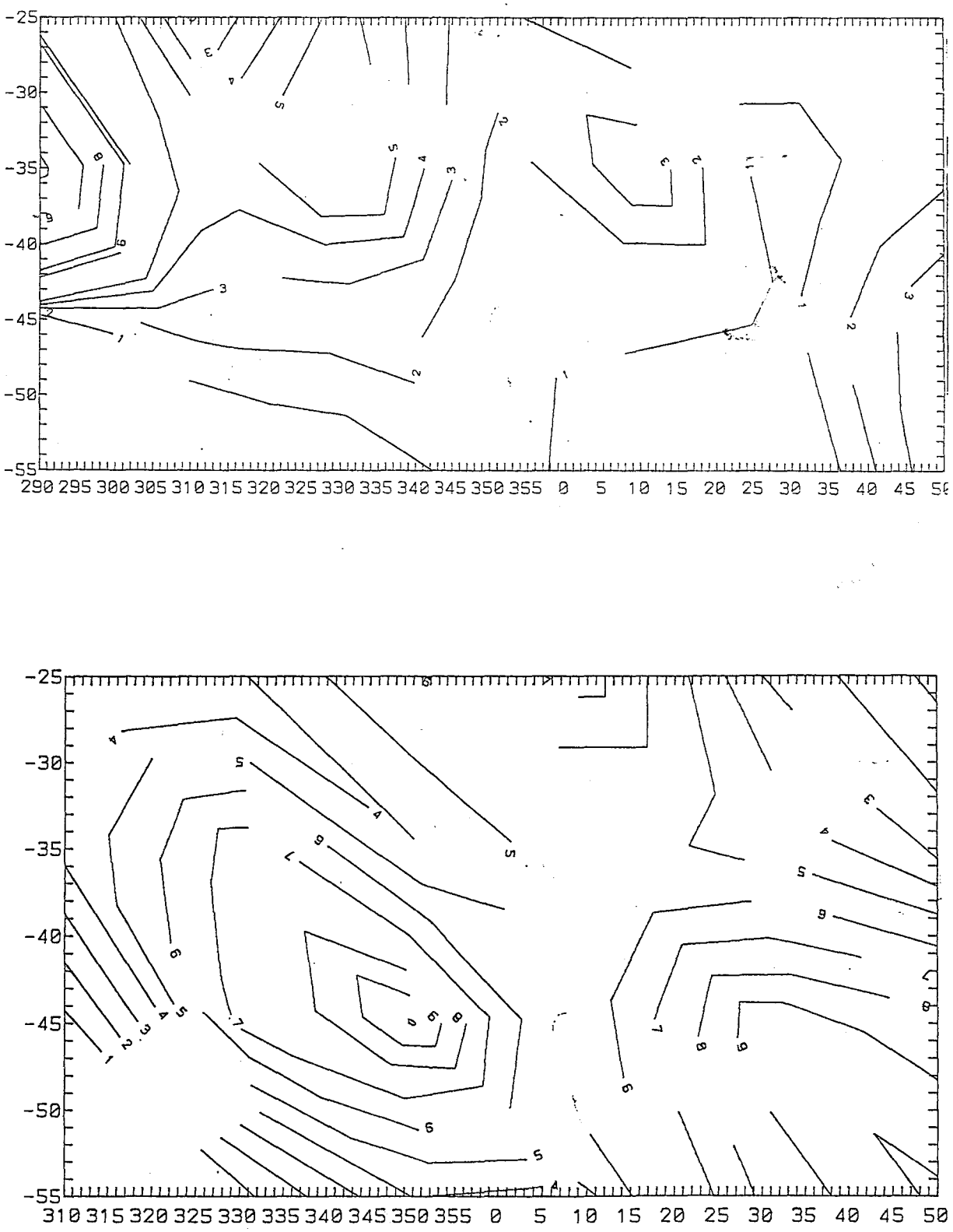

Figure 4.18: Contours of nighttime corrected precipitated electron energy fluxes at 300 km in the range 0.2 to 26 keV in units of 10^{-3} erg $cm^{-2}s^{-1}$ for the 3 summer months. The upper panel is for $K_p \leq 3$ and the lower panel is for $K_p \leq 3$ and the lower panel is for $3 < K_p \leq 6$.

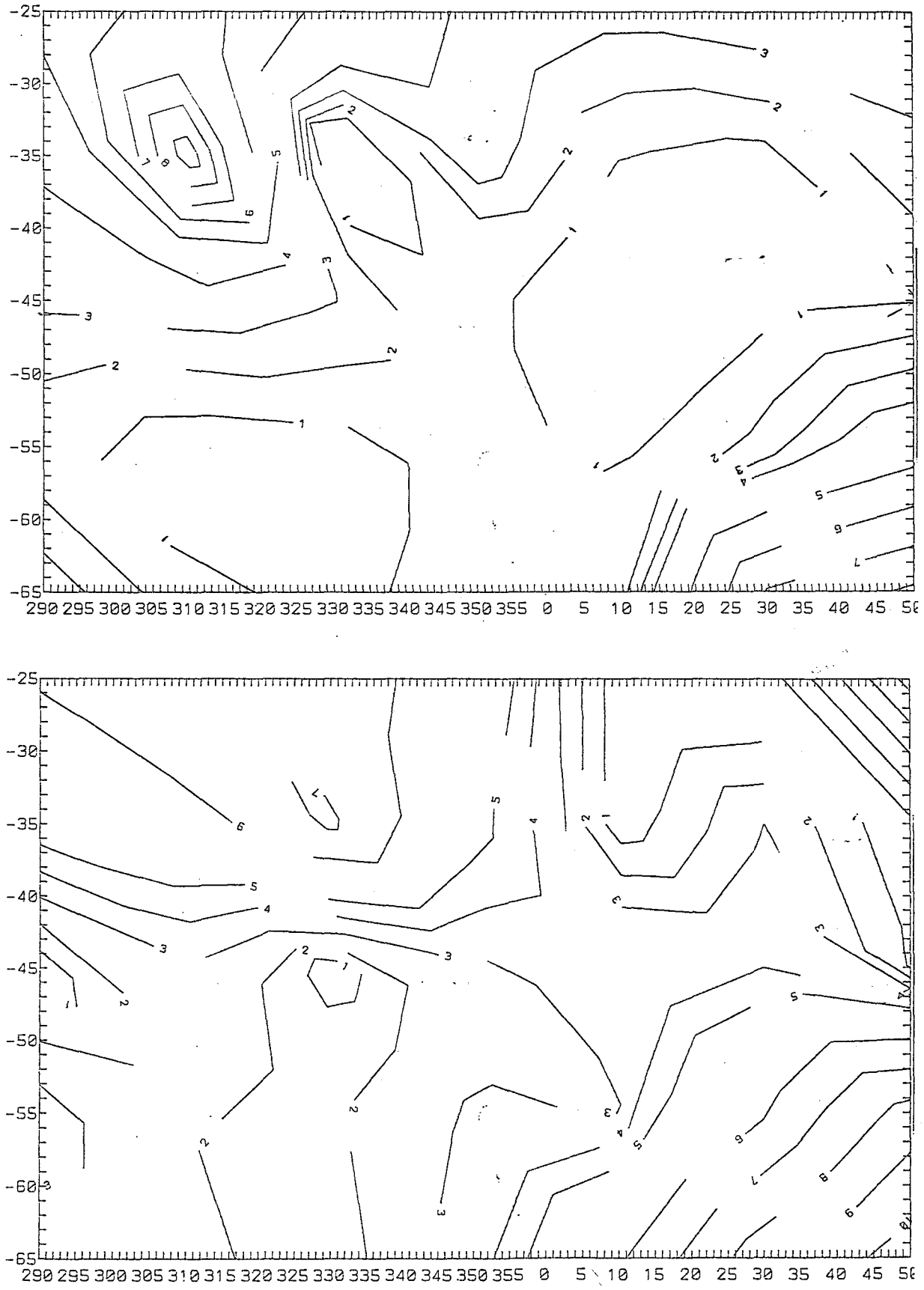

Figure 4.19: Contours of daytime corrected precipitated electron energy fluxes at 300 km in the range 0.2 to 26 keV in units of 10^{-3} erg $cm^{-2}s^{-1}$ for the 3 autumn (fall) months. The upper panel is for $K_p \leq 3$ and the lower panel is for $3 < K_p \leq 6$.

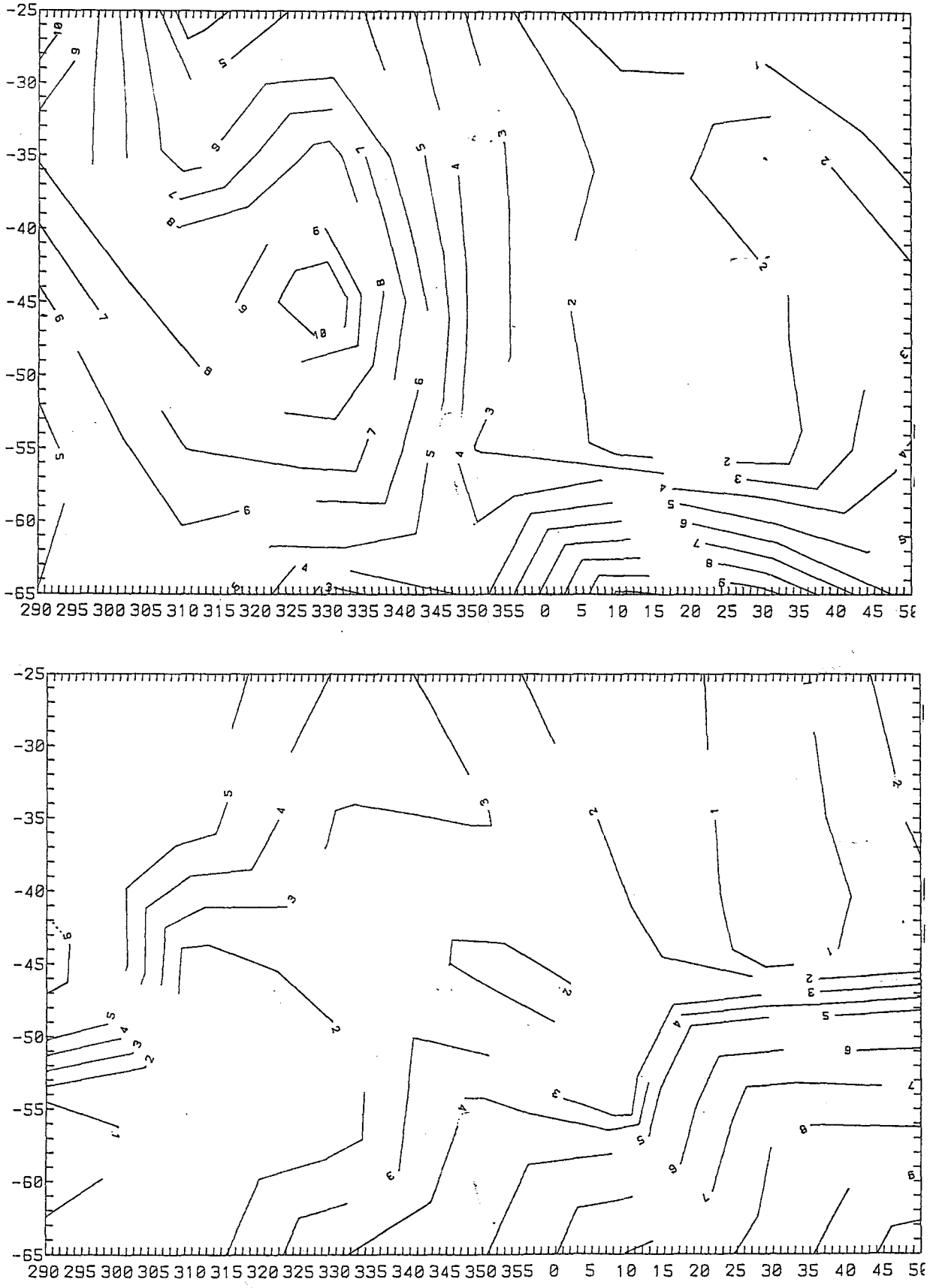

Figure 4.20: Contours of nighttime corrected precipitated electron energy fluxes at 300 km in the range 0.2 to 26 keV in units of 10^{-3} erg $cm^{-2}s^{-1}$ for the 3 autumn (fall) months. The upper panel is for $K_p \leq 3$ and the lower panel is for $3< K_p \leq 6$.

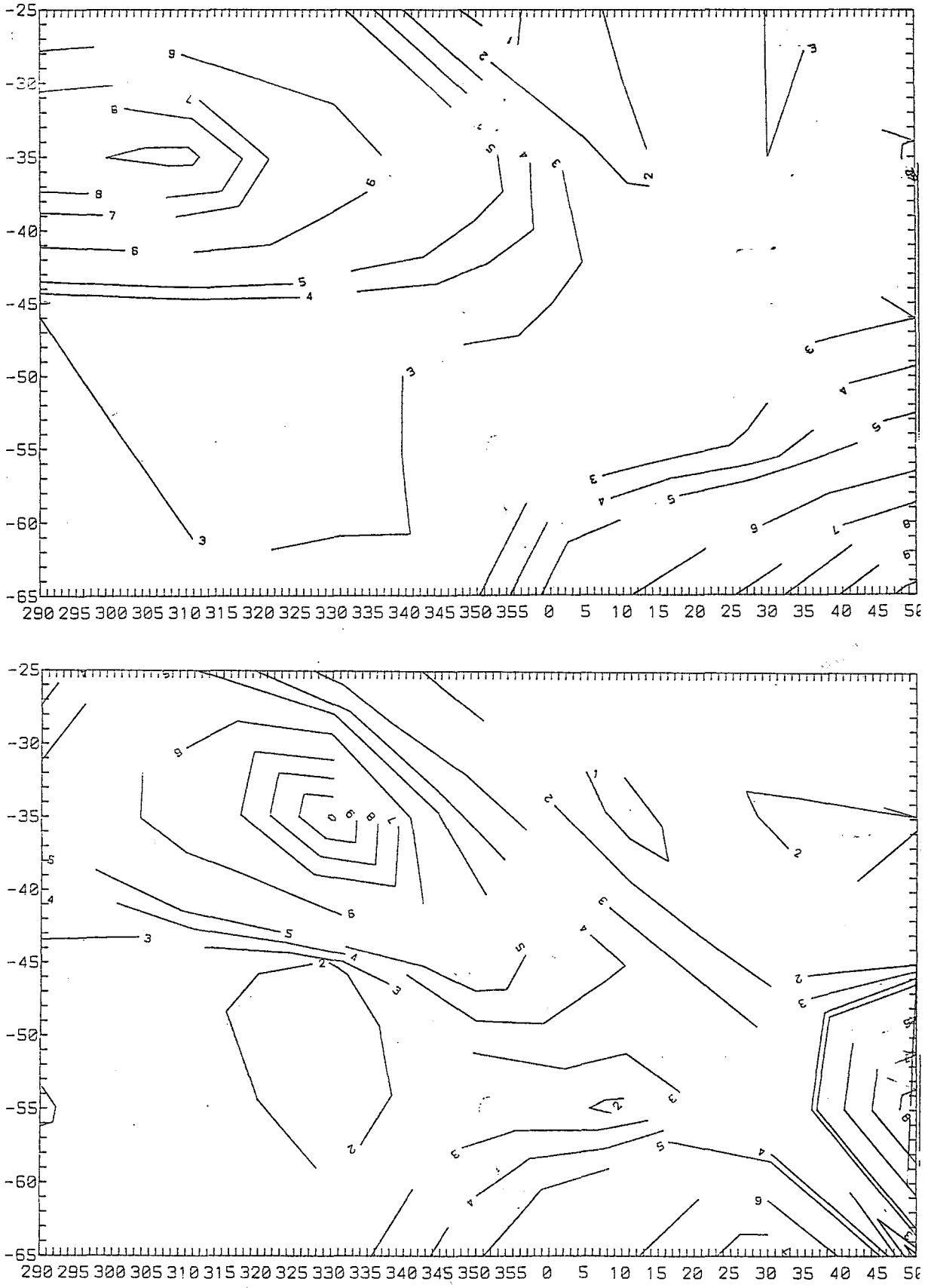

Figure 4.21: Contours fo daytime corrected precipitated electron energy fluxes at 300 km in the range 0.2 to 26 keV in units of 10^{-3} erg $cm^{-2}s^{-1}$ for the 3 winter months. The upper panel is for $K_p \leq 3$ and the lower panel is for $3< K_p \leq 6$.

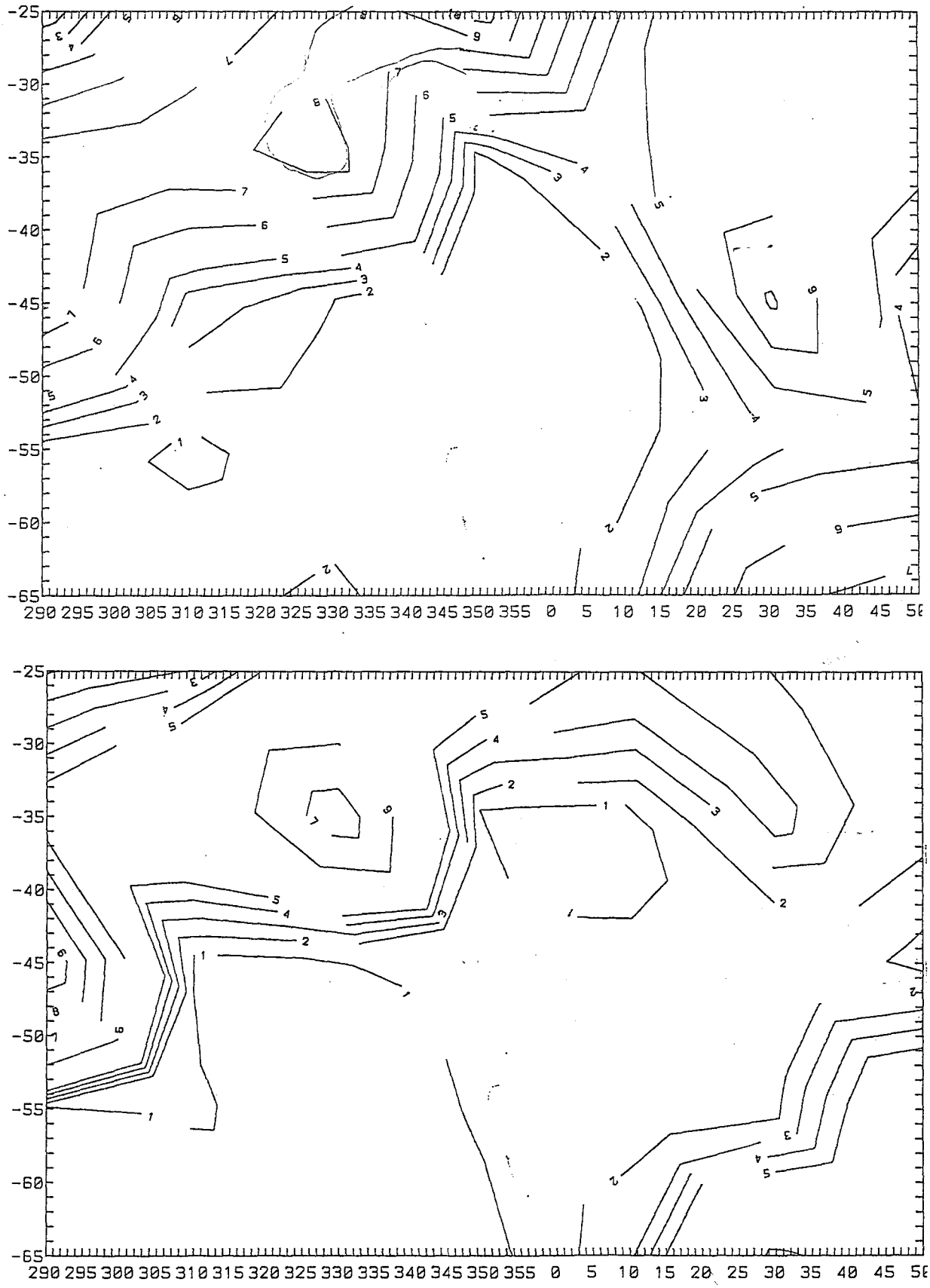

Figure 4.22: Contours of nighttime corrected precipitated electron energy fluxes at 300 km in the range 0.2 to 26 keV in units of 10^{-3} erg $cm^{-2}s^{-1}$ for the 3 winter months. The upper panel is for $K_p \leq 3$ and the lower panel is for $3< K_p \leq 6$.

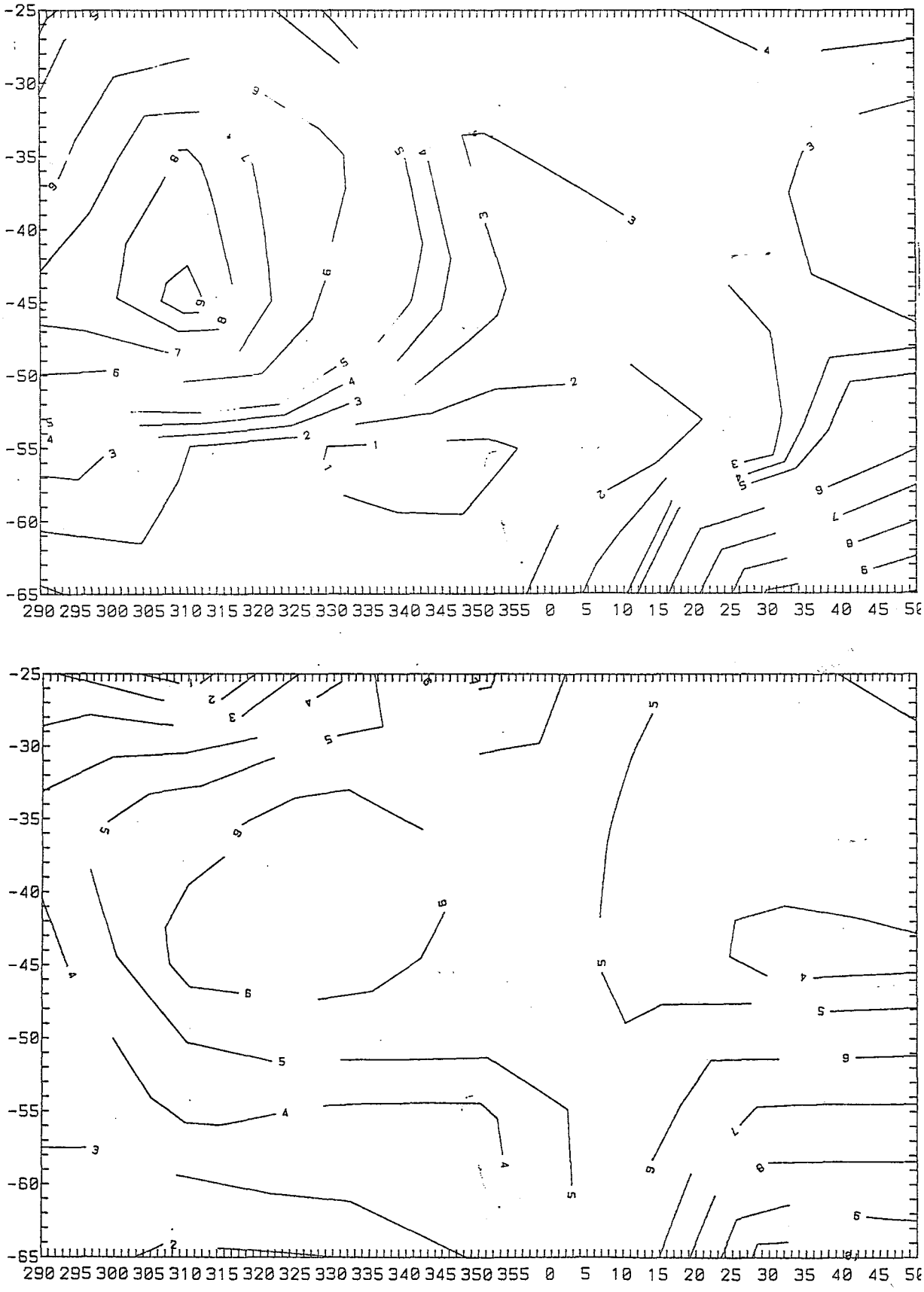

Figure 4.23: Contours of daytime corrected precipitated electron energy fluxes at 300 km in the range 0.2 to 26 keV in units of 10^{-3} erg $cm^{-2}s^{-1}$ for the 3 spring months. The upper panel is for $K_p \leq 3$ and the lower panel is for $3< K_p \leq 6$.

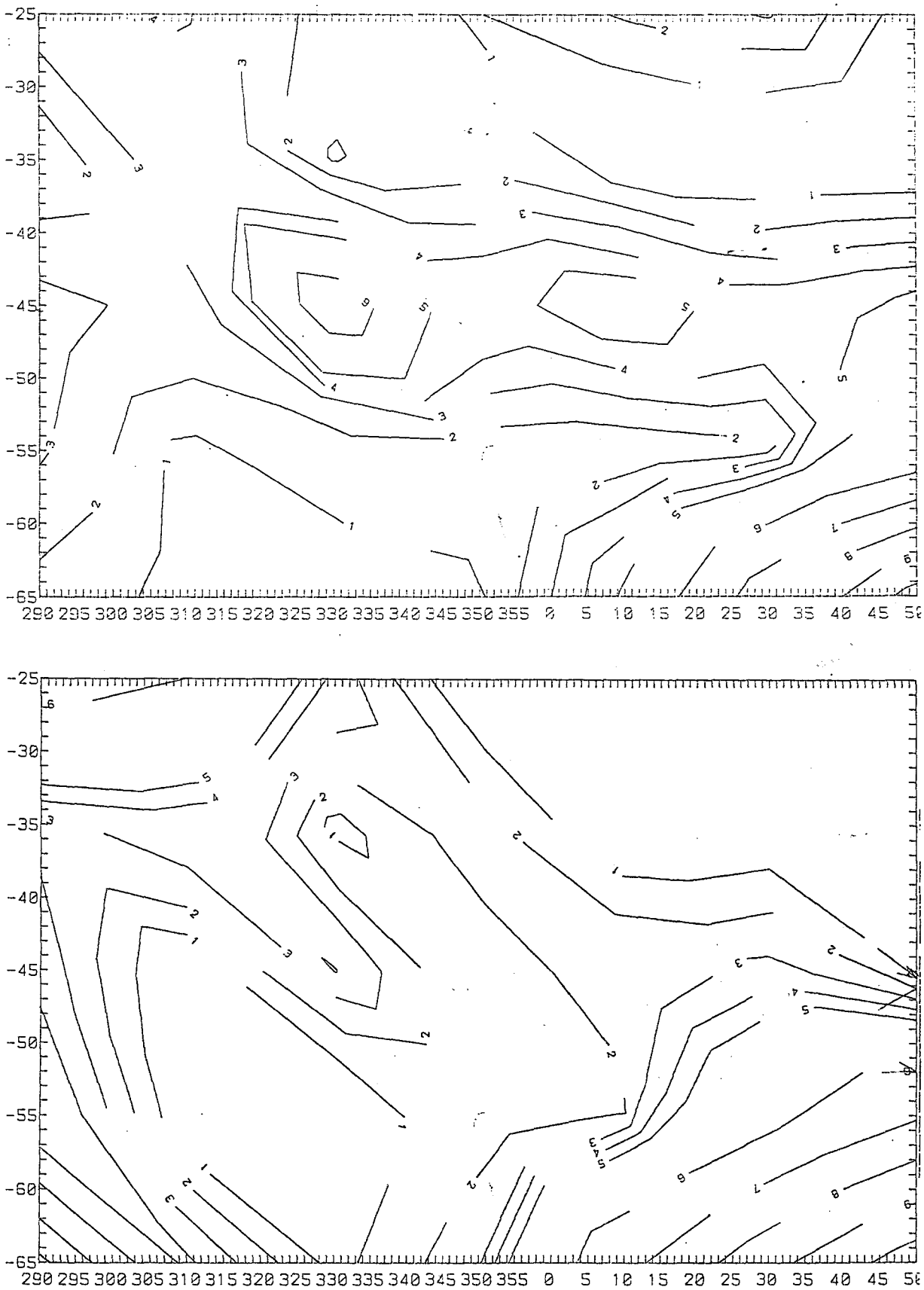

Figure 4.24: Contours of nighttime corrected precipitated electron energy fluxes at 300 km in the range 0.2 to 26 keV in units of 10^{-3} erg $cm^{-2}s^{-1}$ for the 3 spring months. The upper panel is for $K_p \leq 3$ and the lower panel is for $3 < K_p \leq 6$.

Chapter 5

The ISAAC Campaign

5.1 The Project ISAAC Cruise

As the foregoing chapters show, the South Atlantic Anomaly region is extremely interesting from an aeronomic point of view. Unfortunately, due to its inaccessibility, only satellite data exist, which clearly shows that electron precipitation is far more intense than positive ion precipitation. Accordingly, a research voyage through the region, where the rate of energy precipitation was greatest, was planned. On board would be instruments that were suitable for detecting and measuring the expected aeronomic effects. This research voyage became known as the Project ISAAC (International South Atlantic Anomaly Campaign). Because both the extra E-region ionization and the airglow could be conveniently observed at night, the expedition was organized for the mid-southern-winter of 1983 and centred on new moon, to give the longest possible observation periods.

The low-energy electrons discussed in the previous two chapters would be expected to produce their main effects in the E-and F-regions of the ionosphere, in the form of increased ionization density during both day and night and emission of the 391.4 nm radiation of the N_2^+ ion, excited by electron impact. The higher energy particles previously observed would show their main effect as an increase in absorption of radio waves passing through the D- and lower E-regions. Accordingly the ship carried an ionosonde, three tilting-filter airglow photometers and a riometer.

5.2 Instrumentation

To investigate the ionosphere a Barry Research VOS-1 Vertichirp ionosonde modified for microcomputer control as described by Poole (1985) and Poole and Evans (1985), was installed on board the research vessel, SA Agulhas. It was set in the vertical incidence mode to record an ionogramme on 35 mm film on the hour and every 15 minutes thereafter. The mean output power was about 3W and the instrument covered the range from 0.6 to 15 MHz in about 5 minutes. During most of the nights the microcomputer was programmed to produce one ionogramme from 0.6 to 7.5 MHz in 2.5 minutes, immediately followed by a similar one in which the height scale was expanded by a factor of two to show sporadic-E structure more clearly. During the voyage 2128 out of a possible 2184 ionogrammes were recorded. The missing ones were due to the necessity of lowering the transmitting antenna during loading and unloading at Gough Island and Tristan da Cunha, and to allow the ship's radio to be used for urgent communication purposes. The transmitting antenna was an inverted V fed at the apex and terminated with 300 ohms at each end. It was supported from the yardarm on the mainmast of the ship and ran to the bow and the stern on the starboard side. The receiving antenna was a dipole on the port side of the ship. The overall length of the SA Agulhas is just over 100 m and the yardarm is about 30 m above sea level.

For measuring the airglow intensities three airglow photometers of the tilting-filter type, modelled after the design of Eather and Reasoner (1969), were employed. They were mounted in the roof of the ionosphere laboratory. A collimator tube was mounted above each photometer to prevent scattered light from the ship from reaching the photomultiplier. During observations the ship carried as few lights as possible. The field of view of each photometer was about 5° wide. Although nominally directed at the zenith the photometers naturally moved with the ship as it rolled and pitched; in general observations were within 10° of the zenith. These instruments depended for their action on a narrow-band filter which was tilted through an angle of about 15° in steps under the control of a microcomputer. The filters were chosen so that the wavelength to be measured was passed when the filter was tilted through about 5°, so that the instrument swept through this wavelength during each cycle. The maximum response was then taken as the reading on the line and the response at maximum tilt as a measure of the background intensity. Below each filter was a photomultiplier tube operated in the photon counting mode. The wavelengths at which the intensities were measured were the oxygen red line at 630.0 nm and its green line at 557.7 nm, together with the N_2^+ band head at 391.4 nm.

The latter is diagnostic for particle precipitation, since it requires about 18.75 eV to excite its upper level from the ground state of neutral N_2 and there are no significant sources of such a large amount of energy at night other than energetic particles. The temperatures of the photometer filters were controlled to keep the wavelengths measured in the appropriate positions of filter tilt.

A riometer (Relative Ionospheric Opacity METER) is a radio receiver that receives cosmic radio noise and compares the intensity with a standard source. It thus gives a measure of the amount of absorption of radio waves from cosmic sources caused by their passage through the ionosphere and thus of the precipitation of higher-energy particles. A La Jolla 30 MHz riometer was installed on board the SA Agulhas, together with a twin-dipole antenna. Unfortunately, the ambient noise level due to other equipment on the ship was so high that the records obtained could not be used to detect D-region absorption variations in the course of the campaign.

A second riometer was however operated on Gough Island and performed very well. Surprisingly, it showed the period of the cruise to be very quiet, with no large absorption events and very few small ones. This suggests that the ionospheric effects described in the following sections, observed by the ionosonde and the airglow photometers on the ship, were due to low-energy electrons which were not accompanied by significant fluxes of higher energy particles. The higher energy particles would have been precipitated in the D-region, which would then have manifested themselves in the form of absorption events.

Fluxgate and pulsation magnetometers were set up on Gough Island during the campaign by the Magnetic Observatory of the CSIR, Hermanus. Good records were obtained but the fluxgate magnetometer showed very little activity at any time. Some pulsations were however recorded (Sutcliffe *et al.*, 1987).

5.3 The Itinerary of Project ISAAC

The SA Agulhas departed from Cape Town on 29 June 1983 and proceeded to Gough Island (40°S; 10°W) arriving there on 4 July 1983. A day later the ship sailed towards the first turning point (30°S;45°W), following a course that lay along the band of maximum energy precipitation, arriving on 11 July 1983. From this position the cruise continued to 42°S; 40°W, thus moving towards the south side of the region of most intense precipitation, arriving there 2 days later. The ship then made for the Tristan da Cunha group of islands (37°S; 13°W) arriving on 17 July

1983. After a brief sojourn, the return voyage to Cape Town commenced via Gough Island and following a slightly more southern route than on the outward voyage. The ship finally returned to port on 22 July after a cruise lasting 23 days. The route followed by the ship is shown in Fig. 5.1 where the crosses indicate the ship's position at midday UT on the dates indicated on the diagram. The diagram also shows the regions of high energy electron precipitation observed by Ginzburg *et al.* (1962) and of the lower energy electron precipitation delineated by Gledhill and Hoffman (1981).

The voyage took place during a period that was in general geomagnetically quiet. In fact, eight of the days are among the quietest of their months. The K_p indices are given in Table 5.1 (Coffey, 1983, 1984). There were two periods of increased magnetic activity, 12 and 13 July and 16-19 July. K_p did not exceed 5 at any time during the campaign.

5.4 The F-region of the Ionosphere

Fig. 5.2 shows the variation of foF2, and foF throughout the voyage. Gaps in the line indicate times when no data were available. A visual inspection of the ionogrammes revealed that there were travelling ionospheric disturbances (TIDs) on everyday of the voyage and this is evident in the jagged nature of the daytime maxima in Fig. 5.2. The maximum daily value of foF2 is thus elevated above its undisturbed value by these TIDs. The hourly foF2 values from Hermanus (34°S; 19°E), which lies at roughly the mean latitude of the cruise, are also shown in Fig. 5.2. There are clear signs of TIDs on the Hermanus ionogrammes as well. The difference appears to be that their amplitudes are generally smaller than those in the Anomaly. It is not known whether these TIDs originate in the Anomaly and propagate outwards from it, or whether they are the common type originating in the auroral zones and propagating equatorwards. It is not possible to decide on this issue from the data available here. The diurnal variation of foF2 at Concepcion (36.6°S; 73°W) also shows very pronounced peaks due to TIDs. The location of an advanced ionosonde on Gough Island, could be used to investigate the characteristics of the TIDs, including their velocity vectors and thus solve this problem.

The minimum values in the Anomaly are seen to be smaller than those at Hermanus. This may possibly be connected with the observations of elevated electron temperatures in the Anomaly region by Willmore (1964,1965) and more recently by Oyama and Schlegel (1984). The effects of this would include an increase in the recombination rate and therefore lower values of foF at

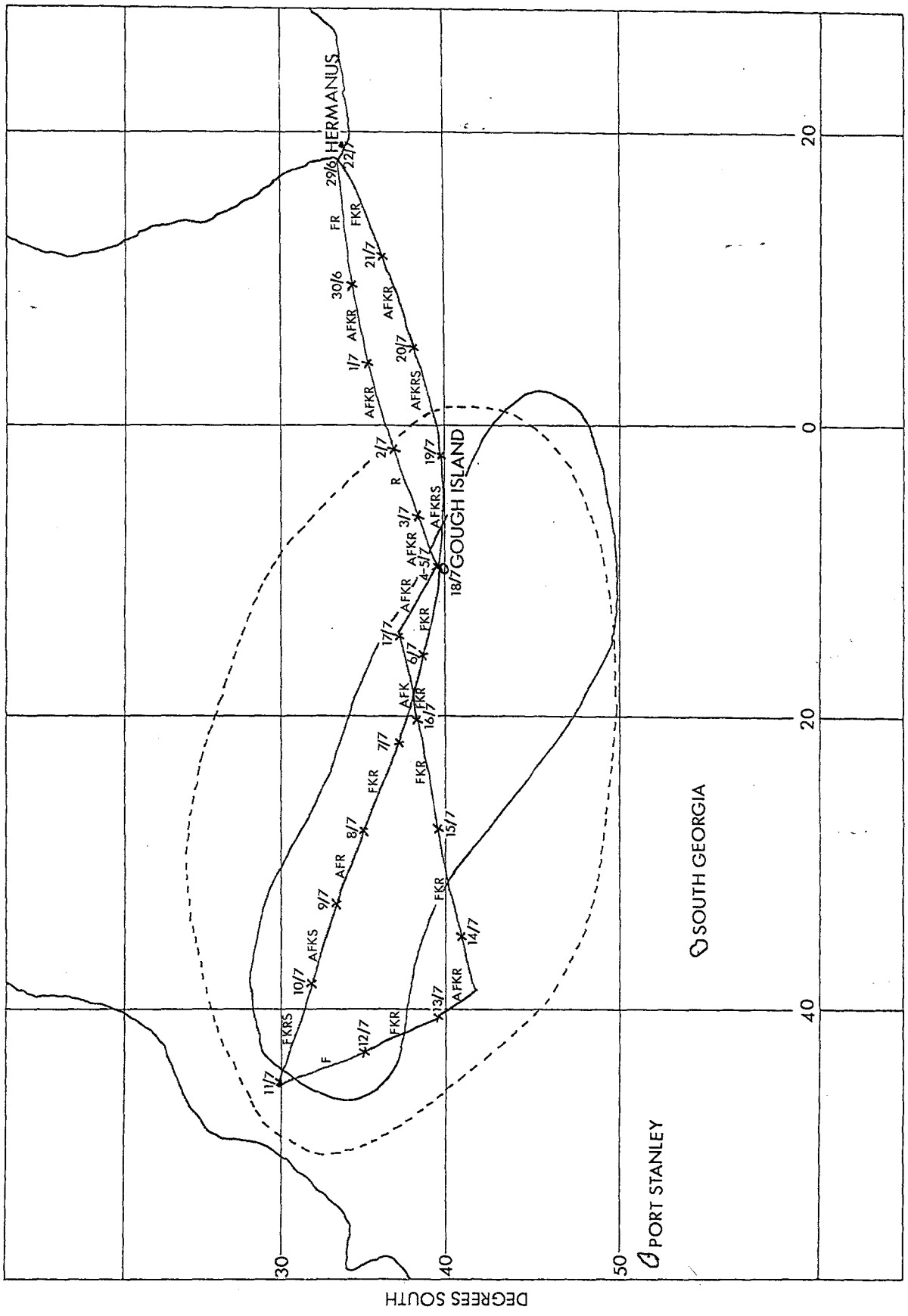

Figure 5.1: The South Atlantic Ocean, showing the contours indicating regions of precipitation of high energy (- - -) and low energy (—) electrons previously reported and the route taken by the SA Agulhas during Project ISAAC. The nighttime sporadic E types encountered are also shown.

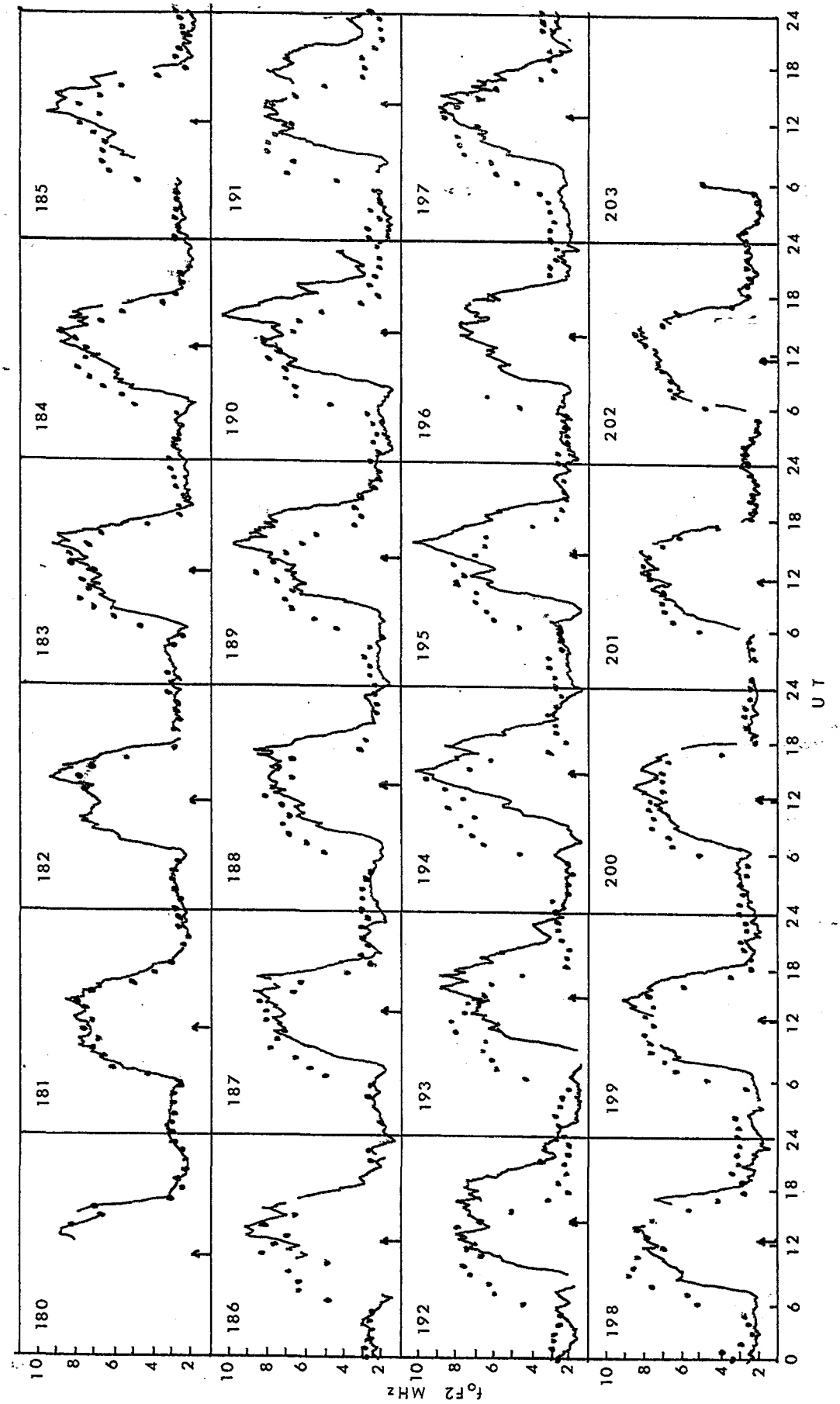

Figure 5.2: The variation of foF2 and foF throughout the voyage, where the solid line represents the quarter-hourly values as recorded on board the SA Agulhas and the closed circles the hourly values as recorded at Hermanus. Day number 180 corresponds to 29 June 1983 and day number 203 corresponds to 22 July 1983.

night, as appear in Fig. 5.2.

The behaviour of the F-region critical frequency on the night of 11-12 July (Day 192-193) is notable in that it shows the lowest sustained values of foF of any night of the voyage. This was also the night on which no evidence of electron precipitation effects was observed in the E-region. On the other hand, the night of 13-14 July (Day 194-195), which showed very definite particle-produced E-region ionization and 391.4 nm airglow emission, does not seem to differ significantly from the nights on either side of it or, indeed, any other night of the campaign.

Fig. 5.3 reproduced in the paper by Dore *et al.* (1985), shows the maximum and minimum values of foF2 recorded on each day of the cruise (circles) and, for comparison, the corresponding values for Hermanus (crosses). As can be seen, the maximum foF2, near noon is practically always greater than that at Hermanus, the average being 8.95 ± 0.15 MHz for the ISAAC cruise values and 8.29 ± 0.08 MHz for Hermanus. The lowest foF2 recorded, in the early morning, shows the opposite behaviour, with the ISAAC cruise values being consistently lower than those for Hermanus. The low early-morning values observed on board the SA Agulhas, often well below 1.5 MHz, were one of the most striking features of the F-region as observed during the cruise. The mean value of these minimum foF2 readings was 1.70 ± 0.06 MHz during the ISAAC campaign, whilst the value for Hermanus was 2.24 ± 0.05 MHz.

The higher values of foF2 during the daytime are in accordance with the expectation that the precipitating electrons would leave some energy in the F-region as they pass through (Kane, 1982). However, this is not what is shown by the minimum nighttime values. Perhaps, the precipitating electrons cause heating of the ambient electrons in the Anomaly hence raising the recombination rate and thus decrease the electron density below that observed at Hermanus.

The F-region of the ionosphere is controlled to a large extent by winds (Rishbeth, 1972) which blow the ionized gases up or down the lines of force of the geomagnetic field and so profoundly affect the loss rate. This effect and those of the TIDs must redistribute the F-region plasma to such an extent that any extra ionization due to the precipitation of electrons is negligible in comparison and so would remain undetectable. These effects may also be related to the very low values of foF observed at night in the Anomaly. In the absence of any data on upper atmospheric winds it is pointless to speculate further here.

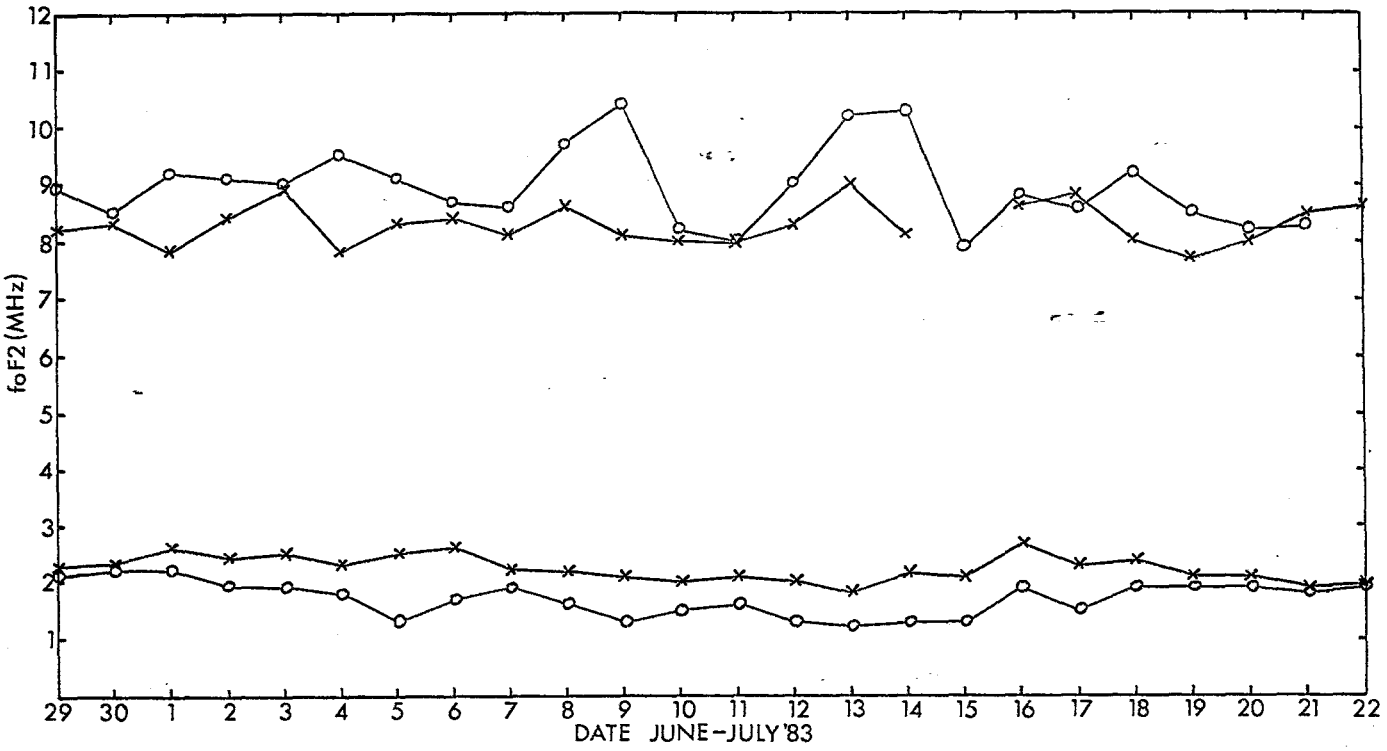

Figure 5.3: The maximum and minimum values of foF2 recorded on each day of the cruise (circles) and the corresponding values for Hermanus (crosses).

5.5 Daytime Effects in the E-region

The E-region is the part of the ionosphere most significantly affected by precipitating electrons in the energy range above 1 keV and is more amenable to quantitative treatment than the more irregular F-region. Good ionogrammes were available from the ISAAC voyage during the daytime periods, from which the ordinary ray critical frequency foE could be determined with satisfactory precision. It was therefore decided to examine these ionogrammes for anomalous variation of the daytime foE with solar zenith angle in order to look for any extra ionization which might be attributed to the precipitating electrons.

In Chapter 2 a method has been described which is able to show that there is good evidence for such ionization at Gough Island during a 25 day period in 1975. The method depends on plotting log foE versus log Ch(x,χ), where Ch(x,χ) is the Chapman grazing incidence function (Chapman, 1931 and Wilkes, 1954). This normally gives a straight line with a slope that is usually in the vicinity of -0.35. As has been shown earlier the slopes of the nine comparison stations outside the South Atlantic Anomaly all lie within one standard deviation of a straight line when plotted against a suitable function of latitude, the slope for Gough Island, which lies in the Anomaly was less than the expected value by more than five times its standard deviation.

Where it was shown that an extra source of ionization must be operative at Gough Island and that its magnitude (of the order of 150 $cm^{-3}s^{-1}$) was consistent with its identification with precipitating electrons from the magnetosphere.

Using the method described by Haggard and Gledhill (1985), the project ISAAC data were analysed, with the additional refinement that the solar zenith angles were computed for each quarter hour using the actual ship's position for use in the log foE versus log Ch(x,χ) plots. This was done for all times for which the solar zenith angle was less than 80°.

The slopes of the best fitting straight lines of the log foE versus log Ch(x,χ) plots for each day were found by the least squares method, together with estimates of their standard deviations. By comparison with the slopes appropriate for the ship's mean latitude during the day, as determined from Fig. 2.35, the ISAAC values were found to be significantly smaller than the expected slopes for places outside the Anomaly at the same latitudes. Since precipitating electron energy fluxes had previously been binned in bins of 10° longitude, it was again decided to average the values found for the slopes each day in bins of 10° longitude for comparison purposes. Fig. 5.4 shows a plot of slope versus longitude for the outward and return voyages of the ship. Fig. 5.4 exhibits a minimum value centred about 20°W.

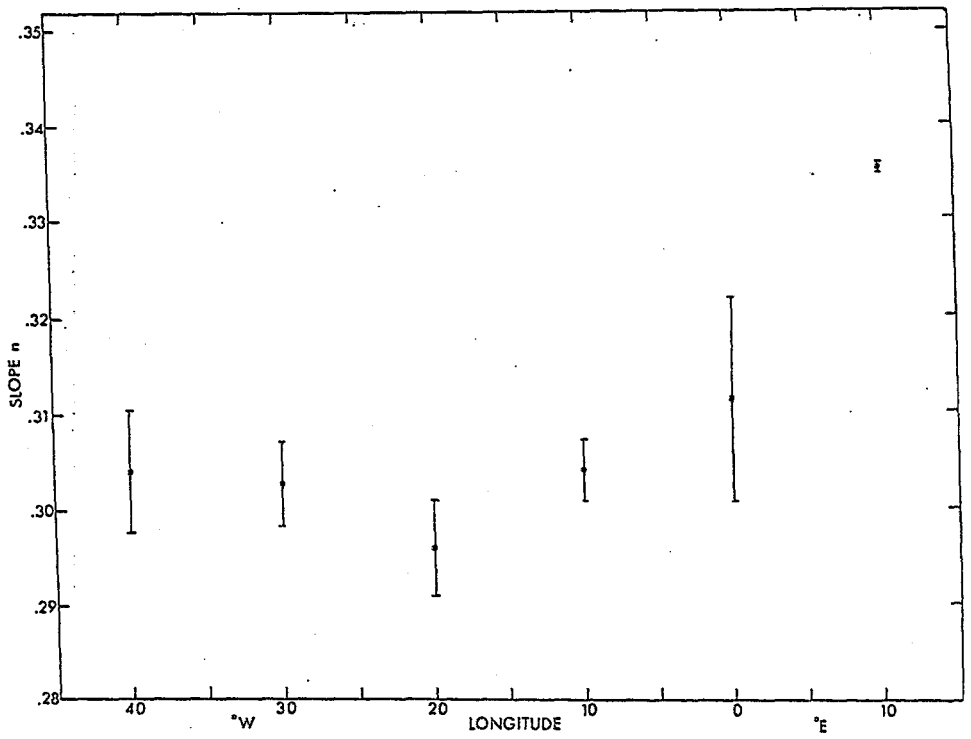

Figure 5.4: The slopes of log foE versus log Ch(800, χ) are plotted against the ship's longitude during the ISAAC voyage. The error bars denote the maxima and minima values for the 10° bins.

Using the same method as was employed in Chapter 2 to calculate values of the unperturbed E-layer critical frequency foE_u for each quarter hour and thus q_u, the unperturbed rate of production of electron-ion pairs per cm^3 per second from the expression $q_u = \alpha N_u^2$, where $N_u = 1.24 \times 10^4 (foE_u)^2$. For the effective recombination coefficient α, the true height of the E-layer maximum was calculated from N(h) profiles derived from the ionogrammes and substituted into the expression (Gledhill, 1986)

$$\alpha = 0.501 \exp(-0.165h) + 4.30 \times 10^{-6} \exp(-2.42 \times 10^{-2} h)$$

where α is in cm^3 per second and h in km.

The observed values of foE were converted to the corresponding ionization rate q_0 in a similar way. The extra production rates could then be found for each quarter hour as $\Delta q = q_0 - q_u$ $cm^{-3}s^{-1}$ as in the paper by Haggard and Gledhill (1985). The daily means of Δq, which are all significantly positive, and their standard deviations, are plotted versus longitude in Fig. 5.5. The closed circles refer to the outward voyage from Cape Town and the open circles to the return voyage.

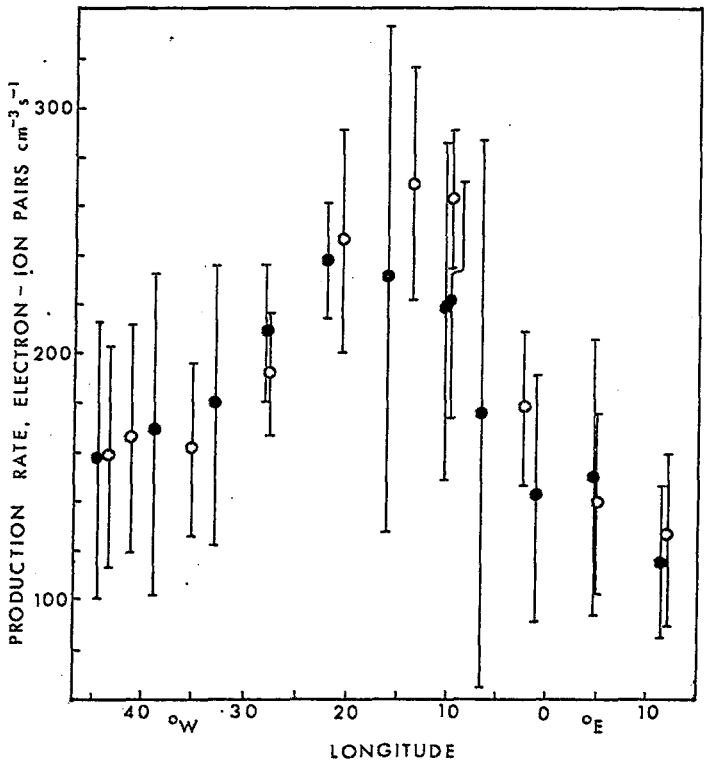

Figure 5.5: The daily means of the extra production values across the South Atlantic. The closed circles denote the outward voyage from Cape Town, whilst the open circles denote the return voyage.

Assuming that the most obvious source of the extra ionization is electron precipitation and that the energy spectrum varies inversely with energy, the average ionization rate profiles

were calculated for each longitude bin. The energy fluxes carried by precipitating electrons determined in the previous chapter were used. The CIRA (1972) mean model atmosphere was used and the mean magnetic dip angle appropriate for each day to calculate the maximum ionization rate. MSIS83 (Hedin, 1983) and CIRA (1986) were used as alternative models to obtain the ionization rates; the results were similar for all three methods. Thus, the theoretical ionization rates due to the precipitating electrons at the height of maximum precipitation could be calculated.

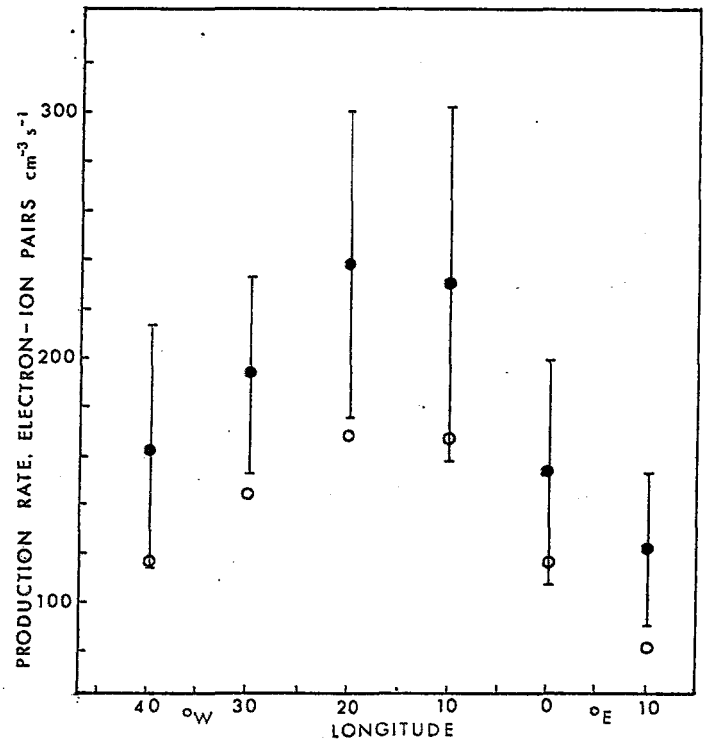

Figure 5.6: Variation of the extra daytime ionization rate across the Anomaly. Error bars are 1 standard deviation above and below the points denoted by closed circles obtained from the ISAAC data. The open circles indicate the ionization rate as calculated using Atmosphere Explorer-C measurements.

Fig. 5.6 shows the maximum production rate of electron-ion pairs $cm^{-3}s^{-1}$ versus longitude obtained by the above method, denoted by open circles. Also shown is the extra production rates calculated from the project ISAAC data, which are denoted by closed circles, taken from Fig. 5.5 and averaged. The data has once again been gathered in 10° bins. The similarity of the variation across the Anomaly is striking using the two different sets of data. As can be seen the observed production rates are consistently higher than the theoretically calculated production rates by a factor of about 1.4, though this is probably not significant in view of the approximations involved in both sets of calculations. What is highly significant is that all the values obtained from the ISAAC ionogrammes are definitely all positive and that their

variation across the Anomaly, with a maximum at about 20°W, is almost exactly parallel to that of the estimates made from Atmosphere Explorer-C data.

This leads to the conclusion that there is good evidence of a significant source of extra ionization, in addition to solar ultraviolet and X-radiation, in the South Atlantic Anomaly E-region. A further conclusion is that the observations are consistent with the identification of electrons in the energy range below 30 keV, precipitating from the magnetosphere, as this source.

5.6 Nighttime Effects in the E-region

There are three types of E-region traces on nighttime ionogrammes that are generally accepted as being due to ionization of that region by precipitating charged particles. These are auroral- (a-type), retardation- (r-type) and particle- (k-type) E traces. The characteristics of these records and their recognition and interpretation are discussed in the URSI sponsored books by Piggott and Rawer (1972) and the supplement thereto [Piggott (1975)].

All three types were encountered during the ISAAC campaign. At the end of the cruise it was found that there was only one night during which none of the particle-produced E-region traces was observed. This is indicated in Fig. 5.1 along the route taken by the SA Agulhas during the ISAAC campaign and are indicated by the letters A,R, or K. This in itself is good evidence that there are indeed observable aeronomic effects of particle precipitation in the South Atlantic Anomaly.

5.7 Auroral-type Sporadic-E Ionization

Fig. 5.7 (a) shows two typical examples of auroral-type (a-type) sporadic-E (Es) traces observed during the ISAAC cruise. They show the typical range-spreading characteristic of this type of record and the "layered" structure often observed. In the ionogramme taken at 23:15 UT on 13 July (day number 194) the top frequency exceeds 7 MHz. There can be no doubt that these are genuine auroral-type E traces; they differ completely from the diffuse type of E record sometimes observed in the equatorial region, as reference to Piggott and Rawer (1972) will confirm.

Figure 5.8 (a) shows all the occasions on which a-type Es traces were observed on the iono-

grammes. Each line corresponds to 24 hours, from midday to midday universal time UT. The dashed lines show the UT of local sunset and sunrise at the ship's position at sea level and the dotted lines show these times at the 100 km level. A dot appears at the time of each quarter-hourly ionogramme on which an a-type trace appeared. As the figure shows, a-type sporadic-E ionization was observed on 12 of the 23 nights of the cruise, though sometimes on only one ionogramme. It was mostly confined to the hours of darkness, though it once occurred when the solar zenith angle was about 75° (day 182 - 1 July).

As Fig. 5.1 shows, this type of sporadic-E trace was observed at scattered places throughout the voyage and was by no means confined to the region of most intense electron precipitation observed by previous researchers and this study. In particular, the points between 0° and 12°E are of interest. The ionogrammes taken simultaneously at the CSIR Magnetic Observatory at Hermanus (34°S; 19°E, Fig. 5.1) by the National Institute for Telecommunications Research were examined very closely. No trace of a-type sporadic-E could be found on any of them or, indeed, on any of the ionogrammes recorded at Hermanus during the whole voyage. The only type of sporadic-E trace found on the Hermanus ionogrammes was the normal flat (f-)type of sporadic-E commonly observed at mid-latitude stations. It should also be noted that the times of occurrence of f-type Es at Hermanus showed no correlation with those of a-, r- or k-type Es, or even of f-type, observed on the ship.

5.8 Retardation-type Sporadic-E Ionization

As is shown in the URSI Handbook (Piggott and Rawer, 1972), r-type sporadic-E traces usually look very much like normal daytime E-layer ionogrammes, with definite retardation cusps at the ordinary and extraordinary critical frequencies. They occur, however, during the night, when the normal E-layer critical frequencies are of the order of 0.5 MHz, whereas the r-type traces can reach critical frequencies of several MHz. They blanket the higher F-region traces over part of the frequency range but do not produce any retardation on the observable part of the F-region trace.

Fig. 5.7(b) shows two typical examples of this type of ionogramme recorded during the ISAAC cruise. Fig. 5.8(b) shows that such traces were observed on 20 of the 23 nights of the campaign. Their confinement to the hours of darkness is perhaps not as remarkable as in the case of a-type Es, since the r-type rapidly merges with the normal E-layer produced by solar photoionization

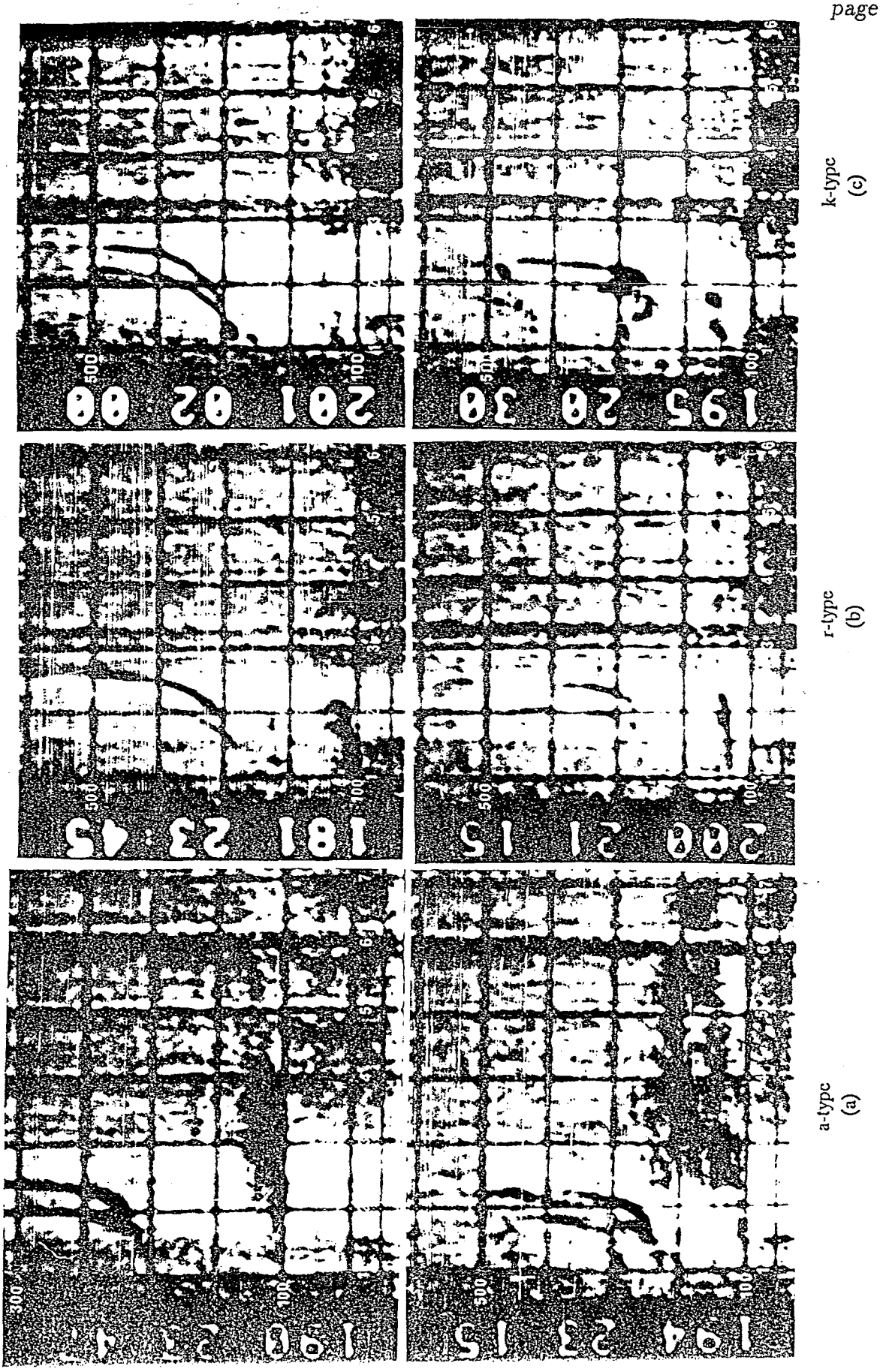

Figure 5.7: Ionogrammes showing ionization of the E-region during the nighttime. (a) Auroral type sporadic-E. (b) Retardation type sporadic-E. (c) Particle type sporadic-E.

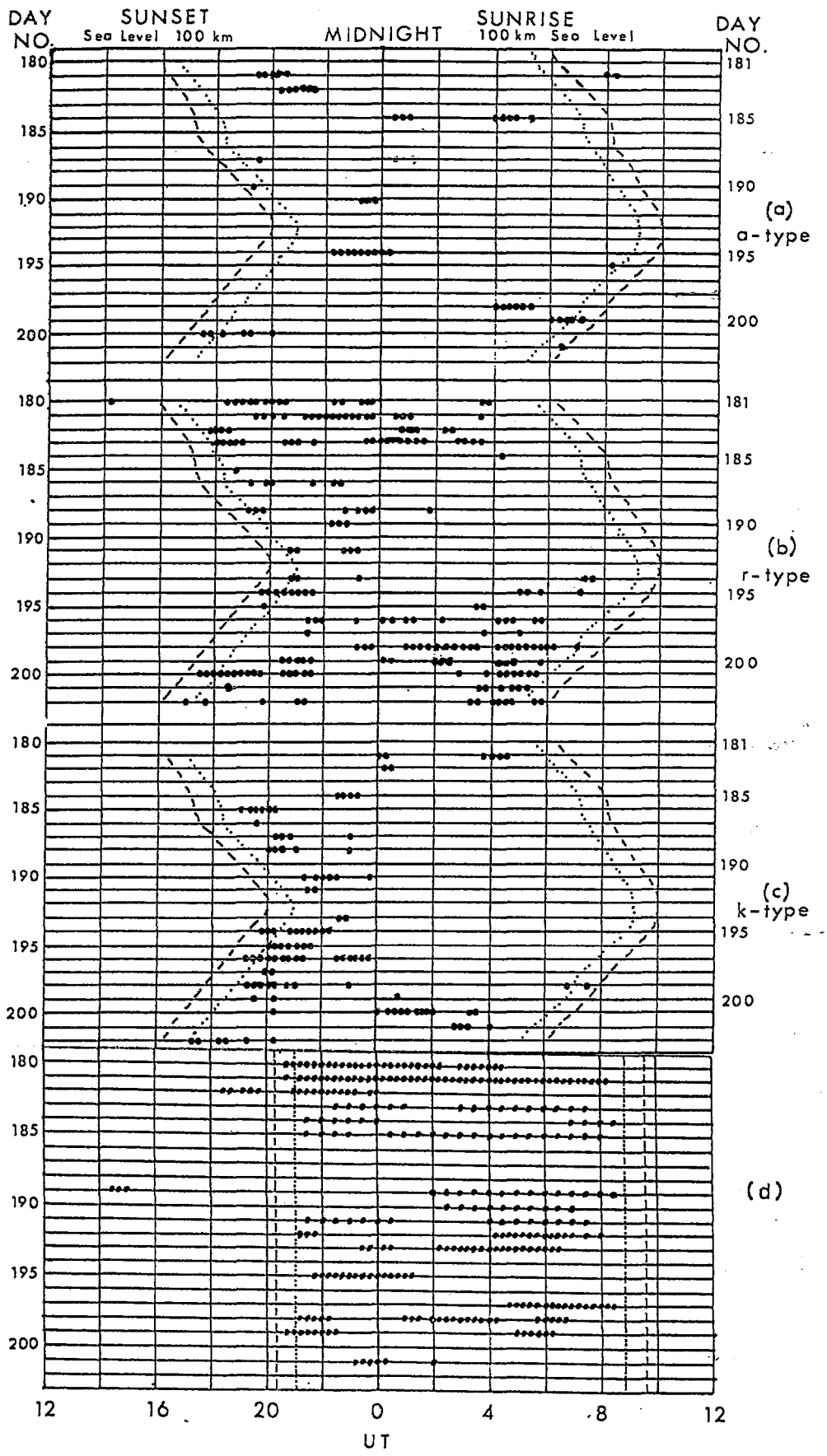

Figure 5.8: Times of occurrence of sporadic-E ionization attributed to ionization by electron precipitation. (a) Auroral type. (b) Retardation type. (c) Particle type. (d) Spread Es traces observed at Echoeira Paulista. Day No 180 = 29 June and Day No 202 = 21 July.

as the sun rises and thus becomes the extra source of ionization discussed earlier in this chapter.

As Fig. 5.1 shows, r-type Es traces were observed over the whole path of the cruise, and were found to occur even closer to Cape Town than the a-type Es. Nevertheless, no r-type traces were observed at Hermanus.

5.9 Particle-type Sporadic-E Ionization

The particle (k-) type of Es trace differs from the r-type mainly in that, while showing retardation at the ordinary and extraordinary critical frequencies, it does not blanket the F-region trace and shows the usual retardation on the upper layer traces above the E critical frequencies (Piggott and Rawer, 1972).

Two typical k-type ionogrammes from the ISAAC cruise are shown in Fig. 5.7(c), while Fig. 5.8(c) shows that k-type Es was observed on 19 of the 23 nights concerned. Again, the phenomenon is limited to solar zenith angles near to or greater than 90°, though, like the r-type, it no doubt merges with the normal E trace after sunrise. It is noticeable that k-type Es is confined to the premidnight hours during most of the cruise. The exceptions occur when the ship was east of Gough Island (10°W). Fig. 5.1 demonstrates that k-type Es, like the a- and r-types, was not limited to any particular area of the South Atlantic.

5.10 Sporadic-E Ionization at Cachoeira Paulista

Coordinated ionospheric sounding during the ISAAC cruise was conducted at Cachoeira Paulista, Brazil (22.6°S; 45°W). Cachoeira Paulista is close to the north-western turning point of the cruise and is very close to the region of lowest total magnetic field intensity that characterises the Anomaly. Quarter-hourly ionogrammes were recorded on all days of the campaign except 2-11 July, when only half-hourly observations were possible.

Abdu and Batista (1977) and Batista and Abdu (1977) have described nighttime sporadic-E records from Cachoeira Paulista which show marked spreading on the upper side of a level trace resembling the flat type of sporadic-E. There are often multiple reflections present, which is not common with the usual auroral type of spreading. Nevertheless Abdu *et al.* (1981) have shown by means of VLF phase measurements that the effects can be detected in the D-region

at 70 to 90 km. So it does seem that these unusual records are accompanied by precipitation of penetrating particles. They are often observed, even during magnetically quiet periods. In view of the differences between these traces and the a-type records observed on the ship, they shall be referred to as spread Es traces.

During magnetic disturbances increases in the altitude range of the spread Es echoes and in the blanketing frequency of the sporadic-E ionization were invariably observed. Similar enhancements, though to a minor degree, took place during the period of the ISAAC cruise on the nights of 16 and 17 July, when the K_p index was somewhat higher than the average for the rest of the period. Fig. 5.8(d) shows the occurrence of spread Es traces on the majority of nights during the campaign. Some rare cases of daytime events are also shown. No clear cases of r- or k-type Es were identified. In light of the paper by Abdu *et al.* (1981) these spread Es type traces shall be taken as evidence for particle precipitation over Cachoeira Paulista during the ISAAC cruise.

5.11 Sporadic-E Ionization at Concepcion

At Concepcion, Chile (36.8°S; 73°W), quarter-hourly ionogrammes were also recorded throughout the campaign. Although some spreading was seen on some of the E-layer traces, which could conceivably have been weak auroral-type Es, it was not clear enough or sufficiently sustained to be convincingly so. It rather resembled the spreading observed at Cachoeira Paulista. The ionogramme for 23:45 UT (18:15 LST) on 13 July shows this (Fig. 5.9). It has a similarity to the equatorial type of spreading and it should be remembered that the magnetic equator reaches its most southernly point in this longitude region.

High (h-) and cusp (c-) types of Es traces were recorded on every day of the campaign except for 29 and 30 June. These occurrences were limited to the period 12-22 UT, the latter being the approximate time of local sunset. During the night hours these types of Es were replaced by flat (f-) and low (l-) types, the former sometimes showing spreading. These were observed on every night of the cruise, often together.

Since no definite a-, r- or k-type traces were noted, the details of the other types of sporadic-E ionization shall not be pursued further here. However, it should be noted that, as with the f-type at Hermanus, they show no correlation with the occurrences observed from the ship.

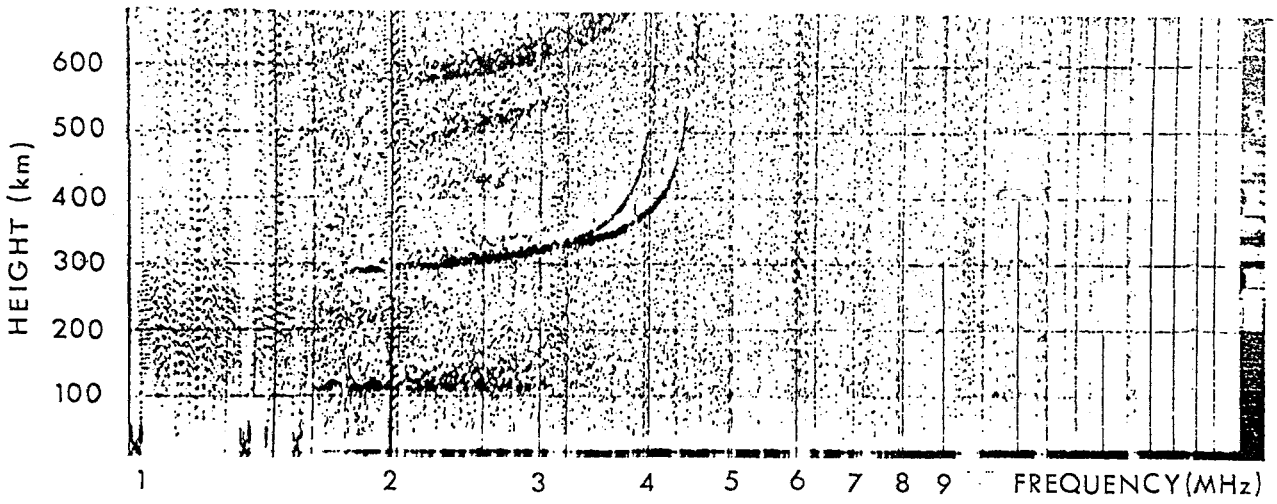

Figure 5.9: Ionogramme from Concepcion recorded at 23:45 UT (18:45 LST) on 13 July, showing spreading of the E-layer trace.

5.12 Comparison of Sporadic-E Ionization

The presence of particle-produced sporadic-E ionization on so many nights of the cruise was unexpected, in view of the variability of the energy carried by precipitating electrons as shown in Fig. 4.8 from Gledhill and Hoffman (1981). Comparison of the first three parts of Fig. 5.8 shows that there was only one night during the whole campaign, that of 11 July, when no particle-related E-layer ionization of any type was recorded. This was the night when the ship reached the extreme westerly part of the cruise, at 30°S; 45°W, the nearest to Brazil during the campaign. But, if the findings of Abdu *et al.* (1981) are accepted, that the flat type sporadic-E is often, though not necessarily, due to particle precipitation then particle type induced sporadic-E was recorded every night.

Comparing the shipboard observations with those at Cachoeira Paulista, it is noted that spread Es was absent at both locations on four nights, viz 5-6, 7-8, 15-16 and 21-22 July. On three nights spread Es was present over the ship but absent at Cachoeira Paulista, viz 6-7, 13-14 and 19-20 July. Whilst on eight nights spread Es was absent over the ship, but present at Cachoeira Paulista. On eight nights spread Es was present at both locations viz, 30 June - 1 July, 1-2, 3-4, 9-10, 11-12, 14-15, 17-18 and 18-19 July.

However, what is noteworthy is the presence of f-type sporadic-E over the ship on the night of 11-12 July, when it was closest to the Brazilian coast, and the presence of spread E-region traces at Cachoeira Paulista, (f-type Es), about 700 km north. As can be seen from Fig. 5.1 f-type sporadic-E was the only Es traces found over the ship. Another particularly striking feature is the very intense a-type Es over the ship on the night of 13-14 July and the absence of spreading at Cachoeira Paulista, about 1500 km NW of the ship. These results suggest that the intense particle produced ionization is very variable in both space and time. The absence of a-type particle produced sporadic-E at Concepcion at any time during the campaign presumably indicates that the South Atlantic Anomaly does not normally extend much beyond 70°W.

The average intensity of nighttime electron precipitation reported by Gledhill and Hoffman (1981) would produce a sporadic-E with a critical frequency for the ordinary ray of about 1 MHz. The maximum intensities they observed would raise this to perhaps 3 MHz on occasions. The average intensities of nighttime electron precipitation presented in Chapter 4 would yield similar results, but these values are the minimum possible values as explained in Chapter 4 and indeed if the selection criteria were not so stringent larger values would have resulted and hence larger foEs values. During the voyage, nighttime foEs values of the order 1-2 MHz were very common, though on occasions the a-type Es reached 6 or 7 MHz. Thus it appears that there is often a nighttime sporadic-E layer, of one or more of the particle induced types, viz a-, r- or k-types, over the South Atlantic Anomaly region. The ordinary ray critical frequencies would be of the order of 1-2 MHz, but very variable in character and certainly extending well beyond the region of maximum energy precipitation delineated by Gledhill and Hoffman (1981). The general average intensity nighttime electron precipitation map shown in Fig. 4.10, shows a peak of intensity centred on 35°S; 30°W but with a large high intensity spread out region more in keeping with the observed sporadic-E traces recorded over the ship during the ISAAC campaign. Similar conclusions have been reached by Abdu and Batista (1977) at Cachoeira Paulista.

Another rather remarkable feature of the sporadic-E types seen over the ship is the occurrence of auroral-type sporadic-E traces seen over the ship so close to Cape Town and their absence from the ionosphere over Hermanus. This may be due to the area of minimum intensity of electron energy deposition in the vicinity of Cape Town as shown by Fig. 4.10. A steep decrease in intensity is noticed as Cape Town is approached and this may account for the rapid change in sporadic-E types and occurrence between the ship and Hermanus.

5.13 Airglow Observations

Due to early moonrise times and general cloudiness during the ISAAC campaign, only 5 nights of usable data were obtained from the airglow photometers on board ship. The period for which photometric data is available is from the early morning (00:00) of 12 July to the early morning (07:19) of 16 July. The intensities of 630.0, 557.7 and 391.4 nm radiation during the three cloudless nights are shown in Fig. 5.10. If it is wished to measure the effects of electron precipitation, then particular attention should be paid to the N_2^+ emission at 391.4 nm. The upper level of this radiation has a high excitation energy above the ground state of neutral N_2 of 18.75 eV. This is very unlikely to be produced by any nocturnal process other than the precipitation of energetic particles. It may therefore be regarded as diagnostic for particle precipitation.

Figure 5.10 shows the variations during the early morning of 12 July, when the ship was near the western most point. The graph shows practically no activity at 391.4 nm and this is in agreement with the absence of any particle-related sporadic-E ionization during this period as indicated in Fig. 5.8. Panel (b) of Fig. 5.10 illustrates the values of 391.4 nm radiation for the night of 12-13 July and shows activity reaching 4 R at times. In Fig. 5.10(c) the intensity of 391.4 nm radiation reaches 16 R. This was the most active night of the voyage, 13-14 July, which coincided with the sustained appearance of ionogramme traces showing a-, r- and k-types of sporadic-E ionization, as indicated in Fig. 5.8, all of which are attributed to particle precipitation.

Simultaneous airglow observations made at Cachoeira Paulista are shown in Fig. 5.11. No significant intensity of radiation at 391.4 nm occurred on any of the three nights considered here. It is especially interesting to note that on the night of 13-14 July when the intensity of the 391.4 nm emission was observed from the ship to reach 16 R on two occasions and to record values above 10 R on three occasions, there was no evidence of corresponding activity at Cachoeira Paulista. In fact the intensity as observed from the ship did not fall below 2 R. This supports the previous conclusion from the sporadic-E observations, that the electron precipitation in the Anomaly region is spatially rather patchy and intermittent.

The intensities of 630.0 and 557.7 nm radiation shown in Fig. 5.10 are remarkably low. In panel (a) the maxima are about 8 R and 20 R for 630.0 nm and 557.7 nm respectively; in panel (b) the 630.0 nm trace reaches about 20 R and that for 557.7 nm nearly 30 R; and finally in

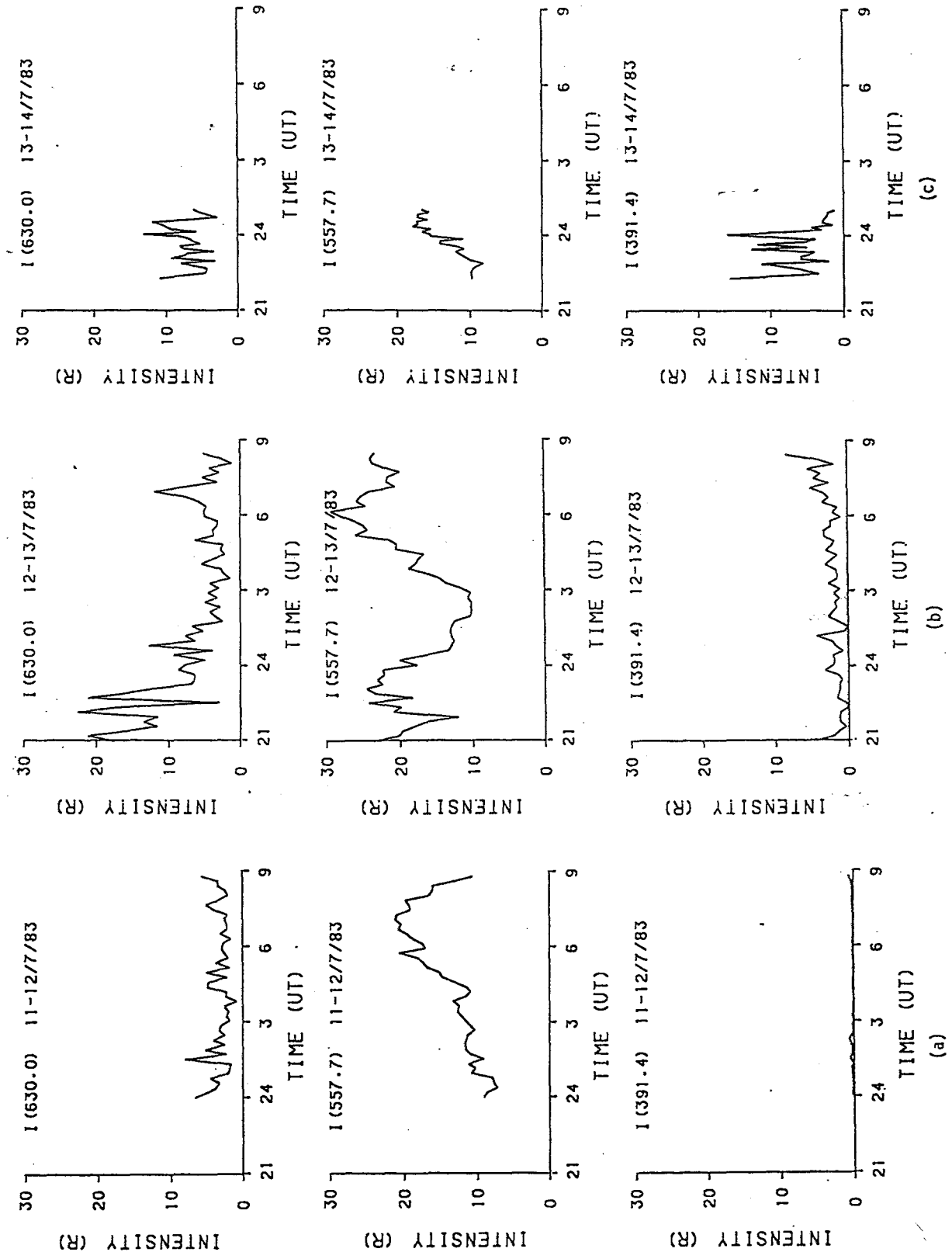

Figure 5.10: Intensities of airglow observed on three nights of the ISAAC voyage. (a) 11-12 July. (b) 12-13 July. (c) 13-14 July.

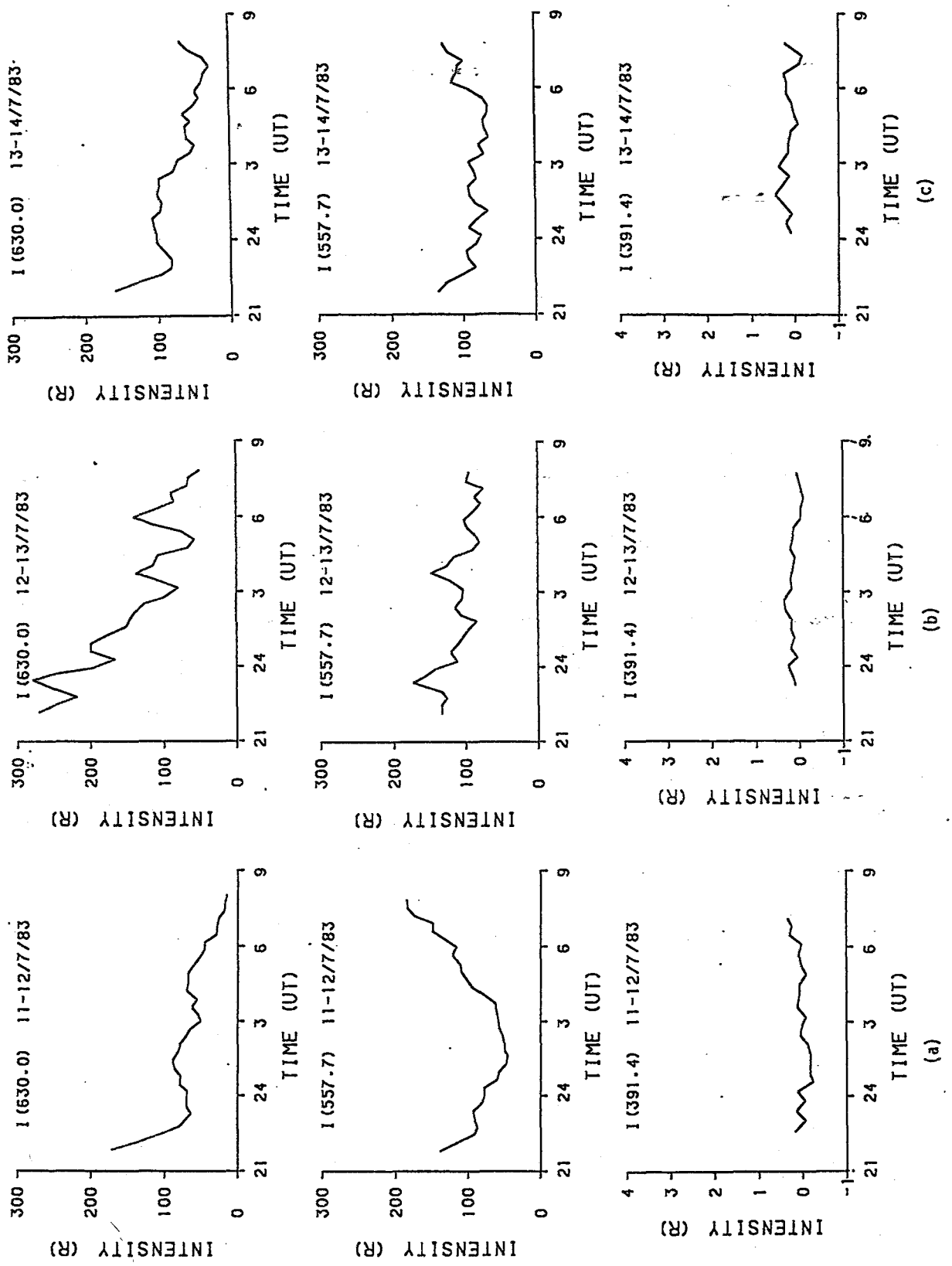

Figure 5.11: Intensities of airglow observed on the same three nights as those in Fig. 5.10, but at Cachoeira Paulista, Brazil.

panel (c) these intensities rise only to 14 R and 17 R respectively.

As Fig. 5.11 shows, the intensities of 630.0 nm and 557.7 nm radiation observed at Cachoeira Paulista are considerably greater than those measured simultaneously in the Anomaly region. The intensities of both these OI lines as recorded on the SA Agulhas are very small and Dore, (1991) goes to great lengths to verify these results as genuine, doing several cross calibration tests.

The usual values observed at mid-latitude outside the Anomaly are of the order of 100-150 R for 630.0 nm and 200-300 R for 557.7 nm (Sandford, 1964). Greenspan and Stone (1964) measured 70-150 R of 630.0 nm radiation between Cape Town and Gough Island and 200-300 R of 557.7 nm emission, with a curious maximum in between which they attributed to particle precipitation. Markham and Anctil (1966) flew close to the region during January and February 1964 and observed values of 630.0 nm intensity in the range 60-150 R and 557.7 nm in the range 90-260 R. Sahai *et al.* (1981) have observed values of 630.0 nm emission in the range 200-300 R on many occasions at Cachoeira Paulista. If the calibration of the photometers was correct, then the low intensities measured in the Anomaly can be considered to be the true values. These low values of 630.0 nm and 557.7 nm are not inconsistent with the low values of foF recorded at night in the Anomaly region. These airglow observations thus suggest that dissociative recombination may be the main excitation process.

If the average level of the 391.4 nm emission observed during the night of 13-14 July is taken to be about 2 R. Then, applying Torr and Torr's (1984) modification of Kasting and Hays's (1977) expression relating precipitation energy density to N_2^+ emission, a value of 2.4 $\times 10^{-3}$ erg $cm^{-2}s^{-1}$ is obtained, which is identical to the 3 winter month nighttime average maximum value observed by Atmosphere Explorer-C in the Anomaly region as per Table 4.1 and Fig. 4.22, for magnetically quiet days, i.e., $K_p \leq 3$. Fortuitous, but nevertheless very interesting!

5.14 Auroral type Es and Airglow

Fig. 5.12 shows the main traces on the ionogramme taken at 22:17 UT on 13 July. It is almost the same ionogramme shown in Fig. 5.7(a), but taken 2 minutes later, using the expanded height scale.

If it is assumed that all the patchy traces in the diagram represent portions of an ionogramme

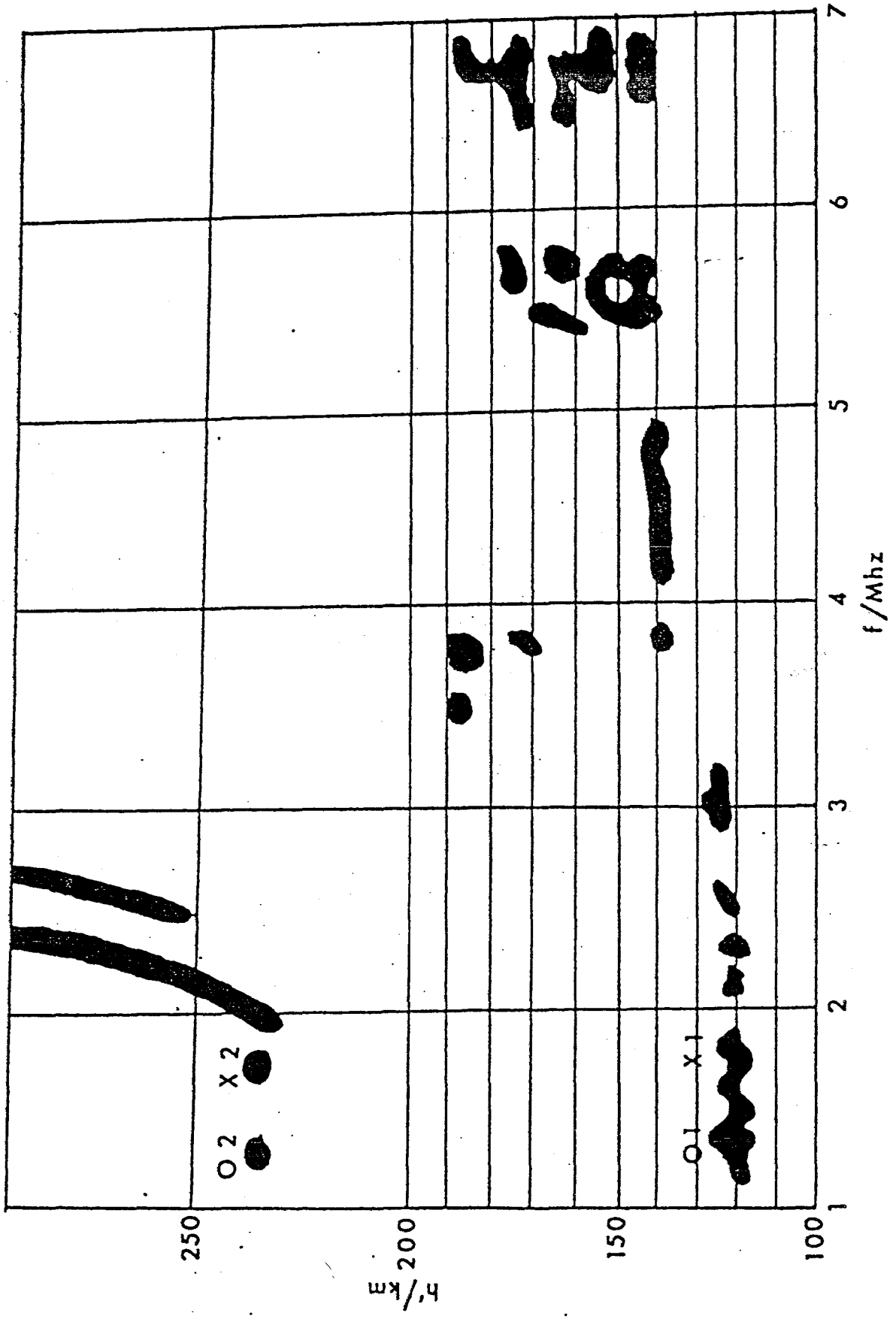

Figure 5.12: Drawing showing the main features of the ionogramme recorded at 22:17 UT on 13 July during the ISAAC cruise. Full particulars are given in text.

which all come from overhead, the critical frequency foEs would be about 6 MHz. This would correspond to an electron density of the order of 5×10^5 cm^{-3}. We may use the method described by Gledhill (1984), to estimate that this would require an energy flux, carried by precipitating electrons, of about 17 erg $cm^{-2}s^{-1}$. This energy flux would produce about 5 kR of 391.4 nm radiation and an associated visible aurora!

On the night in question, or any night for that matter during the campaign, no visible phenomena were noticed. As Fig. 5.10 shows, the intensities of 630.0 nm, 557.7 nm and 391.4 nm radiation were about 11 R, 10 R and 16 R respectively at the time under consideration. Clearly the interpretation that the ionization producing the ionogramme is all overhead is incompatible with these figures. The electron flux that would produce 16 R of 391.4 nm emission may be estimated, assuming the energy spectrum to vary like E^{-1} as found by Gledhill and Hoffman (1981). This value is found to correspond to a value of foEs of about 1.3 MHz.

The point labelled O1 in Fig. 5.12 lies at 1.40 MHz and that labelled X1 at 1.84 MHz. The difference, 0.44 MHz, is reasonably close to the difference of the ordinary and extraordinary critical frequencies calculated for this geographical position and height, 0.41 MHz, especially if it is taken into consideration that the points O1 and X1 are probably on the cusps of the E traces but not at the critical frequencies themselves. This interpretation, that O1 and X1 are close to the ordinary and extraordinary Es critical frequencies overhead, is strengthened by the presence of the two spots O2 and X2. These are separated by 0.44 MHz and lie at a virtual height of 230 km. The corresponding points on the first order trace should thus lie at 115 km. In fact, the two points O1 and X1 can be seen on the original ionogramme to lie at about 116 km. It can be concluded that the critical frequency foEs was near to, and probably slightly greater than, 1.40 MHz.

With the short portion of Es trace leading up to the patch labelled O1 it is not possible to deduce the N(h) distribution of the electrons in the sporadic-E layer. However, it is reasonable to assume a true height of the Es maximum, say 118 km, and ask what monoenergetic flux would produce a peak electron density of 2.4×10^4 cm^{-3}, corresponding to the foEs of 1.4 MHz. It is found that a flux of 2.4×10^6 electrons $cm^{-2}s^{-1}$, of energy 5.6 keV, would do this. This amount of energy would produce about 11 R of 391.4 nm radiation. Despite the numerous approximations made in this deduction, it is in much more satisfactory agreement with the observed value of 16 R than the original assumption which yielded 5 kR. Hence it can be concluded that the value of foEs is indeed just about 1.4 MHz and this represents the overhead

ionization density responsible for the O1 trace on the ionogrammes.

The remaining patchy traces on the ionogramme must then be oblique reflections, possibly from field-aligned ionization patches. This is in accordance with their greater range. The dip angle at the ship's position at this time was 45°. Thus the range of reflections from field-aligned ionization at about 120 km heights should be about $\sqrt{2} \times 120$ or 170 km. This lies in the middle of the reflections in the frequency range 3-7 MHz and suggests that this interpretation may well be correct. Dudeney and Rodger (1985) use similar arguments in their discussion of the spatial structure of sporadic-E traces at high latitude stations.

5.15 Retardation and Particle type Es and Precipitating Electrons

From 19:45 to 22:00 UT on 13 July both r- and k-types of Es were present as shown in Fig. 5.8. These took the form of two separate traces on the ionogrammes, a lower trace typically at virtual heights between 100 and 110 km and the upper one at 125-140 km. Agreement between the heights of multiple reflections confirms on some of the ionogrammes that the reflections come from vertically overhead and are not obliquely reflected. With this evidence, it is worthwhile to produce N(h) profiles in the usual way, as described by Haggard (1984), from scaled virtual heights and frequencies. This has been done for the period 21:00 to 21:45 UT. Using these N(h) profiles as starting data, it is then possible to deduce the energy spectra of the electrons presumed to produce the ionization, assuming that the flux is isotropic over the downward hemisphere.

The resulting N(h) curves are shown in the upper row of Fig. 5.13, together with the corresponding electron energy spectra in the lower row. The two-layered structure is evident in the N(h) profiles, with the lower layer at a real height of about 105 km and the upper one peaking in the range 115-125 km. The electron spectra show two parts with different slopes. The lower-energy parts are mainly responsible for the upper layers and the higher-energy, more penetrating electrons, for the lower layers. The development of the peak at 7 keV at 21:30 UT is interesting in that it is reminiscent of spectra observed in the auroral zones, though the fluxes observed in the South Atlantic Anomaly are two or three orders of magnitude less (cf Gledhill *et al.*, 1987). The crosses in the upper part of Fig. 5.13 are the electron densities calculated

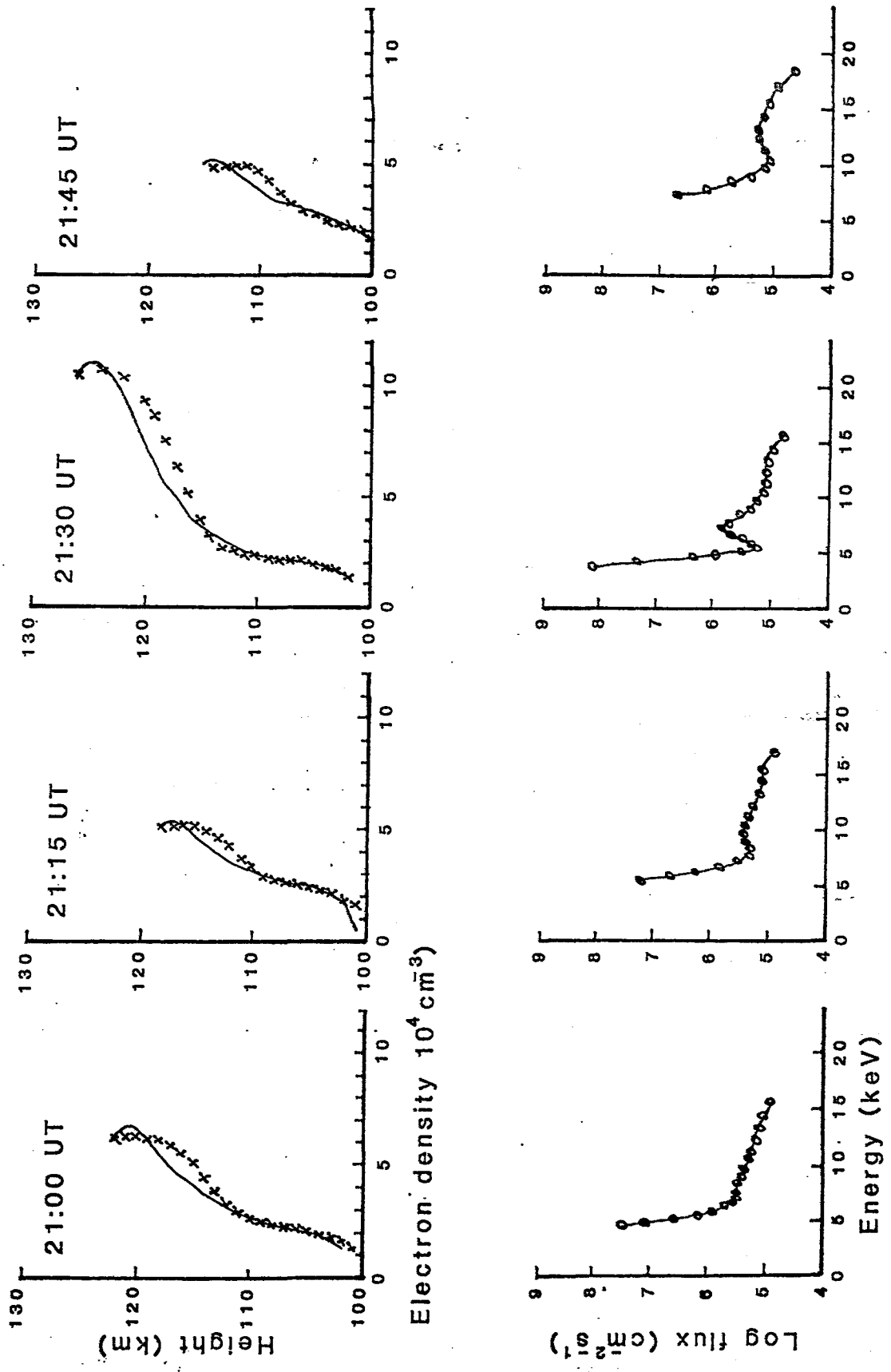

Figure 5.13: The upper panel shows the electron density versus true height curves for four times during the night of 13 July. The lower panel shows the corresponding electron energy spectra deduced from the curves of the upper panel. The crosses in the upper panel represent the electron densities calculated from the spectra.

from the spectra in the lower row. The deviations near the maximum of the upper layer in each case suggest that electron precipitation alone does not account for the distribution of ionization there. The upper layer peak is too narrow to be built up from a continuous electron energy spectrum, or even a monoenergetic electron stream. Winds may play a part in redistributing the plasma.

No significant absorption events were observed on the riometer at Gough Island during the night of 13 July. Calculation based on the electron energy spectra shown in Fig. 5.13 shows that the accompanying absorption should be about 4×10^{-2} dB. However, if a table of Hourly equatorial Dst values for the night of 13 July from 20:00 to 23:00 is consulted, values of - 29, - 30, - 31 and - 29 gammas are found. The hourly equatorial Dst values provide an index of geomagnetic activity as a function of Universal Time (UT). Large negative variations in Dst are produced by low-energy particles in the magnetosphere, which would be deposited in the higher ionospheric layers and not in the D-layer (Sugiura and Chapman, 1966 and Frank 1968).

5.16 Spread Sporadic-E at Cachoeira Paulista

The spread Es traces recorded at Cachoeira Paulista differ from the normal auroral-type Es in several important respects. Reference to Fig. 5 of the paper by Batista and Abdu (1977) will illustrate these.

(a) There is a very definite flat lower edge to the traces. This is not usual with a-type Es, though it is sometimes seen. Generally, a-type Es has a sloping lower edge.

(b) Several higher order traces often occur. These are found at integral multiples of the base virtual height of the first reflection, showing that they come from the zenith. This is also true of the spread echoes on the upper side of the traces. Thus, these traces do not seem to be typical auroral-type Es where the spread traces appear to be obliquely reflected.

(c) On the night of 12-13 July spread Es is recorded from 02:15 to 06:30 UT (See Fig. 5.8(d)), whereas the simultaneous records of 391.4 nm emission at the same location (Fig. 5) show no significant intensity. Thus, on this occasion at least, it seems that the spread Es trace was not due to electron precipitation.

(d) Nevertheless, the VLF phase observations of Abdu *et al.*, (1981) show clearly that particle precipitation does indeed take place at Cachoeira Paulista, at least during times of

greater magnetic activity, and that these particles are capable of reaching the D-region and producing ionization there. Possibly, these are higher energy particles.

(e) The type of spreading and the occurrence of a similar, though less pronounced, effect at Concepcion (Fig. 5.9) suggest a connection with the type of E-trace spreading associated with the equatorial anomaly.

With these considerations in mind the times have been recorded of observation of spread Es at Cachoeira Paulista, but the lack of correlation with particle Es types observed from the ship, the different type of spreading and the lack of coincidence with 391.4 nm emission leads to the believe that one may be dealing with a rather different phenomenon here and that the auroral-type Es region in the Anomaly may indeed stop short of the Brazilian coast.

It would be instructive to undertake an examination of the geographic and temporal distribution of this spread Es phenomenon over South America, including the Argentinian stations at Buenos Aires and, in particular, Tucuman. This should help to elucidate the parts played by equatorial anomaly effects and by particle precipitation in the production of these spread Es traces and would be very useful in delineating the western limits of the precipitation region itself.

5.17 Geomagnetic Field Correlation

In their preliminary analysis of the results of Project ISAAC, Dore *et al.* (1985) stated that these supported the conclusion of Gledhill and Hoffman (1981) that the intensity of electron precipitation in the Anomaly is less during magnetically disturbed periods than it is when K_p is low. This is borne out by the more detailed consideration of the measurements made during the cruise in this section. This conclusion is also supported by the findings, after detailed analysis of Atmosphere Explorer-C data as Table 4.1 for $K_p \leq 3$ and Table 4.2 for $3 < K_p \leq 6$ show, especially the 3 month winter seasonal grouping.

The most active night, with all three types of particle-produced sporadic-E ionization was that of 13-14 July. From Table 5.1 it is noted that the K_p values from 18:00 UT on 13 July to 03:00 UT on 14 July, which covers the period of activity, were 1, 2 and 1- respectively. On the other hand, the single night that showed no particle-related E-region ionization, 11-12 July, had K_p values from 18:00 UT to 06:00 UT of 1-, 2, 2- and 1-, so that there appears to be no relation between K_p and the occurrence of particle precipitation. This is in contra distinction to the

correlation between particle precipitation and magnetic activity reported at Cachoeira Paulista by Batista and Abdu (1977). A fluxgate magnetometer operated on Gough Island during the cruise showed no significant magnetic activity at any time. A pulsation magnetometer showed pulsations, but at times that do not appear to correlate with the observed E-region effects reported here (Sutcliffe 1987).

It may be significant, however, that the period of maximum particle activity, 13-14 July, was preceded by a period of greater magnetic activity. As shown in Table 5.1, the K_p values for the period 12:00 UT on 12 July to 15:00 UT on 13 July were 4-, 4-, 5-, 4-, 5, 4, 4, 3+ and 3. The particle effects followed this by about 20 hours. Another period of greater magnetic activity (Table 5.1) from 09:00 UT on 16 July to 06:00 UT on 18 July, was also followed by an active night from the particle point of view, from 17:00 UT to 22:00 UT on 19 July, again with about 20 hours delay. On the other hand, the active period from 09:00 UT to 24:00 UT on 6 July was followed by only slight activity in the E-region, with some r-type some k-type sporadic-E between 18:00 UT and 00:00 UT on 7 July. Here again, the delay is of the order of 20 hours.

These observations can be taken as mere indications of a possible connection and are certainly not statistically significant.

The project ISAAC campaign certainly showed that there are aeronomic effects in the South Atlantic Anomaly that are easily detectable and more prevalent and intense than expected on the basis of the earlier satellite observations of precipitating electron energy spectra.

The occurrence of auroral-type sporadic-E ionization was unexpected and more intense than would have been anticipated on the basis of earlier work. This extra ionization at nighttime will have significant effects on communications across the Anomaly especially at the higher frequencies. Clearly, the limited time interval of 23 days of the campaign was far too short to provide answers to many of the questions that may be raised on consideration of its results.

Thus the direction of motion of the travelling ionospheric disturbances discussed briefly here and the question of whether the auroral-type sporadic-E traces really arise from field aligned ionization and the reason for the absence of more intense 391.4 nm emission when the field aligned. The more closely ionized regions overhead and the absence of large riometer absorption effects, require more study.

Date	1	2	3	4	5	6	7	8	SUM
29 June	2	3−	4−	4−	3+	2+	2−	2	21+
30 June	2−	1+	2	2+	2	2	2−	2	15
1 July	2+	2	1	1+	2−	1+	2	1+	13
2 July	1	2−	1+	1+	2+	3−	3+	3−	16+
3 July	3−	2−	2	2+	1+	2	3−	2+	17
4 July	2−	2−	1+	1	2+	3−	3	2	16−
5 July	2−	1	1	2+	2−	2+	1	1	12
6 July	2−	2	2+	5−	3+	3−	2+	3−	22−
7 July	1+	2−	2−	3+	4−	3−	3−	4	21
8 July	2	2+	3+	2+	2−	2+	2+	3−	19
9 July	3	4−	1+	3+	2	2+	3−	3−	21
10 July	2−	2	2−	1+	1−	1−	1	1−	10−
11 July	1−	1−	1−	2−	1	1	1−	2	8+
12 July	2−	1−	1+	2+	4−	4−	5−	4−	22−
13 July	5	4	4	3+	3	1+	1	2	24−
14 July	1−	2	2+	2	2	2	2−	1	14−
15 July	1+	2−	1−	1−	1	1	2−	2	10
16 July	3−	3+	2	4+	4+	3	4+	4	28−
17 July	4	4	4−	4+	4−	4−	4	4+	32−
18 July	5−	4	3	3	3+	3+	3−	3	27
19 July	3−	2	2+	2+	2−	3	2+	2	18+
20 July	2+	+2	3−	1+	1	1+	2−	2	15−
21 July	1+	2+	2−	2	2−	2	2−	2−	14+

Table 5.1 Geomagnetic three-hourly range indices K_p during the ISAAC campaign.

Chapter 6

Conclusions

6.1 Brief Resumé

The region of very low magnetic field intensity B in the South Atlantic region was viewed after the discovery of the radiation belts as the Rosetta stone of magnetospheric physics. It was envisaged that the zone of trapped radiation would interact strongly with the upper atmosphere. This interaction was in fact proposed by Dessler (1959). In his proposal he envisaged a two zone structure of energetic radiation. This magnetosphere-atmosphere interaction was expected to produce optical and ionospheric effects in the South Atlantic similar to those observed in the auroral zones.

Greenspan and Stone (1962) searched for the optical effects and observed a maximum intensity of about 20 R at 427,8 nm, although the "Starfish" and high altitude nuclear explosions cast some doubt on their findings. Later, Eather and O'Brien (1967) failed to detect enhancements of optical radiation during quiet magnetic conditions. Paulikas (1975), reports that significant optical effects are apparently never generated as a result of particle precipitation in the Anomaly Region, but that the fluxes of precipitating electrons are sufficiently strong to produce localized enhancements of ionization in the D- and E-regions of the ionosphere.

These effects were first predicted by Zmuda (1966), drawing on the results of various researchers such as Forbush *et al.*, 1962; Paulikas and Freden, 1964; Imhof and Smith, 1965; Williams and Kohl, 1965. Martin *et al.* (1973) presented evidence of particle precipitation into the Anomaly Region during a sudden commencement of a magnetic storm, although only a small flux of energetic electrons precipitating into the atmosphere were detected in the energy range of

about 7.5 MeV. Earlier, Ghielmetti *et al.* (1964) had reported high X-ray flux in the 20-60 keV interval at about 30 km above the South Atlantic.

Roederer *et al.* (1971) carefully looked at the question of eastward drifting electrons interacting with the atmosphere in the South Atlantic Anomaly as their mirror points dip deeper and deeper into the atmosphere and reached the conclusion that their effects would be localized in the immediate vicinity of the Anomaly Region.

Torr *et al.* (1975) presented a model of the rates and locations of particle precipitation in the South Atlantic Anomaly and the resulting aeronomic effects. Fig. 6.1 summarizes their results, which predicts a mean airglow intensity of about 20 R at 391,4 nm for a narrow longitude interval near 30°W at L = 2.

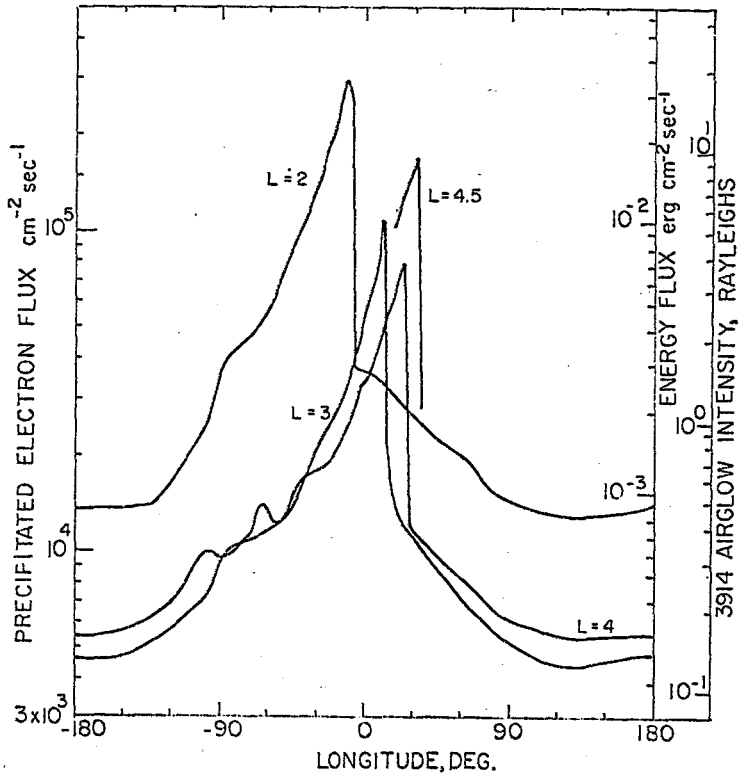

Figure 6.1: Longitudinal variation of precipitated electron flux in the southern hemisphere. Also shown is the energy flux as well as the 391.4 nm optical radiation resulting from this input. From Torr *et al.* (1975).

As anyone familiar with the literature on the South Atlantic Anomaly knows, the aeronomic effects of particle precipitation into the Anomaly are not well established and considerable controversy abounds. This is mainly because the effects that have been monitored are considerably weaker than was initially predicted due to over optimistic estimates of particle fluxes precipitating into the Anomaly Region. The inaccessibility of the Region has made direct measurements of particle precipitation and their effects difficult to measure. What is known, is

that the effects would be most noticeable in the region 60 km to 150 km. Technologically it is difficult to operate satellites near this region, although Atmosphere Explorer-C and Dynamics Explorer, later on, have managed to operate at about 300 km altitude successfully.

6.2 Results of Bottomside Soundings

In many respects the results of this dissertation represent the first "bottomside" observations of the ionosphere and the associated aeronomic effects in the South Atlantic Anomaly Region.

The Gough Island voyages as well as the observations at Gough Island and the ISAAC cruise results all reflect the enhancement of the F2- region of the ionosphere in the South Atlantic Anomaly Region as opposed to the surrounding permanent observatories. Travelling Ionospheric Disturbances were also noticed every day during the project ISAAC campaign.

The daytime E-region analysis during the stay at Gough Island in 1975 as well as the Project ISAAC campaign revealed that the slope of the straight line graph of log foE versus log $\mathrm{Ch}(x, \chi)$ is anomalously low, up to 5 standard deviations lower. These results show that there is a significant source of extra ionization in addition to Solar UV and X-radiation in the South Atlantic Anomaly daytime E-region. These results are also consistent with the identification of electrons in the energy range below 30 keV precipitating from the magnetosphere as the source of ionization.

The nighttime sporadic-E ionization encountered during the Project ISAAC campaign, as illustrated in Fig. 5.8, is overwhelmingly in favour of particle precipitation produced Es ionization, viz a-, k- and r-type sporadic-E.

On three of the five days that it was possible to operate the airglow photometers N_2^+, 391.4 nm, airglow between 10 R and 16 R was measured, which is entirely consistent with what would be expected from values predicted in the previous section.

One thing is certain, the ISAAC cruise has definitely established that electrons, precipitating into the upper atmosphere in the South Atlantic Anomaly, produce measurable effects in the ionosphere. Whilst the increase in ionization in the daytime is relatively small, that at night raises the critical frequency of the E-region from about 0.5 MHz to 1 or 2 MHz on average and sometimes to more than 7 MHz. The precipitation is irregular in time and space and possibly, at least as far as auroral-type ionization is concerned, aligned along the lines of force

of the geomagnetic field. Travelling ionospheric disturbances are observed every day in the Anomaly and are responsible for unusually large daily maxima of ionization density in the F-region. It is however, not clear what their direction of propagation is. During the nights, the ionization in the F-region is unusually sparse compared to the E-region. Unusually low values of 630.0 nm and 557.7 nm airglow values were observed. During periods of intense nighttime ionization easily measurable intensities of 391.4 nm radiation were observed, confirming particle precipitation as the cause.

The question as to the field alignment of the auroral-type ionization and the direction of motion of the TIDs could be answered by the installation of an advanced digital ionosonde, with direction-of-arrival capabilities, on Gough Island. The deployment of riometers, operating at several frequencies, on Gough Island would give information on the higher-energy electron precipitation into the D-region, whereas the installation of tilting-filter photometers would complete the array of monitoring equipment for the detection of particle precipitation in the South Atlantic Anomaly Region.

6.3 Results of Topside Measurements

The results of the nighttime precipitated electron energy fluxes exhibit maxima at about 33°S; 47°W and 57°S; 23°E, whereas the minimum electron density occurs at these positions. Electron temperatures show a minimum in the South Atlantic Anomaly Region increasing in magnitude towards the auroral zone.

In general, the maximum NO^+ ion concentrations coincide with minimum precipitated electron energy fluxes and vice versa. Likewise, the same is true for NO^+ ion concentrations and electron densities, but the O^+ ion concentrations exhibit similar maxima and minima as the electron densities. Since the increase in NO^+ ion concentrations is far greater than the increase in O^+ ion concentrations for large values of K_p, the ratio of NO^+/O^+ is markedly affected by an increase in magnetic activity.

The occurrence of ionization minima close to electron precipitation maxima and the rapid fluctuations observed by other researchers, tend to suggest that electric fields play an important role in determining the configuration of the ionosphere in the South Atlantic Anomaly.

The analysis of the 5 year period of Atmosphere Explorer-C data for both daytime and nighttime

precipitated electron energy fluxes is lower (1.4) for moderately disturbed magnetic conditions as opposed to 5 for quiet conditions. However, the daytime precipitated electron energy fluxes is less during moderately active periods, whereas the nighttime values are far greater. The inference can be drawn that the magnetic disturbances tend to increase the nighttime precipitated electron fluxes and do not affect the daytime values too much. The winter months also exhibit greater ratios of fluxes inside the Anomaly to fluxes outside the Anomaly.

The average nocturnally precipitated electron energy fluxes for quiet and moderately disturbed magnetic conditions was found to be between 1×10^{-4} and 38×10^{-4} erg $cm^{-2}s^{-1}$. The daytime electron energy fluxes tended to vary between 1×10^{-3} and 8×10^{-3} erg $cm^{-2}s^{-1}$ and decreases with increasing magnetic activity.

Finally, it is seen that precipitating electrons provide a significant and sometimes dominant source of ionization in the lower ionosphere in the South Atlantic Anomaly Region, although no significant optical radiation is excited by this precipitation of energetic electrons with the possible exception of the N_2^+ band head at 391.4 nm.

References

Abdu, M.A., Ananthakrishnan, S., Coutinho, E.F., Krishnan, B.A. and Reis, E.M. da S., Azimuthal drift and precipitation of electrons into the South Atlantic geomagnetic anomaly during an SC magnetic storm, J. Geophys. Res., **78**, 5830-5836, 1973.

Abdu, M.A. and Batista, I.S., Sporadic E-layer phenomena in the Brazilian geomagnetic anomaly: Evidence for a regular particle ionization source, J. Atmospheric Terrest. Phys., **39**, 723-731, 1977.

Abdu, M.A., Batista, I.S., Piazzo, L.R. and Massambani, O., Magnetic storm associated enhanced particle precipitation in the South Atlantic Anomaly: evidence from VLF phase measurements, J. Geophys. Res., **86**, 7533-7542, 1981.

Abdu, M.A., Batista, I.S. and Sorbral, J.H.A., Particle ionization rates from total solar eclipse rocket ion composition results in the South Atlantic Geomagnetic Anomaly, J. Geophys. Res. **84**, 4328-4334, 1979.

Abdu, M.A. and Rai, D.B., Night time ionization by particle precipitation in the South Atlantic Anomaly, Int. Symp. on Solar Terr. Phys., Saõ Paulo, Brazil, **3** 178-188, 1974.

Armstrong, T. Morphology of the center zone electron distribution at low altitudes from January through July and September 1963 from Injun 3, J. Geophys. Res., **70**, 2077-2110, 1965.

Batista, I.S. and Abdu, M.A., Magnetic storm associated delayed sporadic E enhancements in the Brazilian Geomagnetic Anomaly, J. Geophys. Res., **82**, 4777-4783, 1977.

Birkeland, K. The Norwegian Aurora polaris expedition, 1902-1903., Vol 1, H Aschehauz and Co, Oslo, 1908.

Brace, L.H., Theis, R.F. and Dalgarno, A. The cylindrical electrostatic probes for Atmosphere Explorer-C, -D and -E, Radio Sci., **8**, 341-348, 1973.

Beynon, W.J.G. and Brown, G.M., IGY Instruction Manual Volume III - The Ionosphere, Pergamon Press, London, 1957.

Cavalieri, D.J., Roland, R.J., Potemra, T.A. and Gavin, R.F., The correlation of VLF propagation variations with atmospheric planetary-scale waves, J. Atmospheric Terrest. Phys., **36**, 561-574, 1974.

Chapman, S. The absorption and dissociative or ionizing effect of monochromatic radiation in an atmosphere on a rotating earth. II Grazing incidence, Proc. Phys. Soc., **43**, 483-501, 1931.

Chapman, S. and Bartels, J., Geomagnetism, Clarendon Press, Oxford, 1940.

CIRA, Cospar International Reference Atmosphere, Akademie-Verlag, Berlin, 1972.

CIRA86, Cospar International Reference Atmosphere: 1986 Part 1: Thermosphere Models, Ed. Rees, D., Oxford, Pergamon, 1988.

CIRA86, Cospar International Reference Atmosphere: 1986 Part II Middle Atmosphere Models, Ed-

Rees, D., Oxford, Pergamon, 1990.

Coffey, H., Geomagnetic and Solar data,J. Geophys. Res., **88**, 9290, 1983.

Coffey, H., Geomagnetic and Solar data,J. Geophys. Res., **89**, 1029-1030, 1984.

Dachev, T.P., Peculiarities in ion concentration distribution in the Brazilian magnetic anomaly region, Dokl. Bolg. Akad. Nauk, **29**, 987-989, 1976.

Dalgarno, A., Hanson, W.B., Spencer, N.W., and Schmerling, E.R., The Atmosphere Explorer mission, Radio Sci., **8**, 263-266, 1973.

De Mendonca, F., Ionospheric electron content measurement in regions of low magnetic dip and through the Brazilian magnetic anomaly, Space Res., V, 687-701, 1965.

Dessler, A.J., Effect of magnetic anomaly on particle radiation trapped in geomagnetic field, J. Geophys. Res, **64**, 713-715, 1959.

Doherty, R.H., Observations suggesting particle precipitation at latitudes below 40°N,

Radio Sci., **6**, 639-646, 1971.

Dore, I.S., The utilization of tilting-filter photometry in airglow and auroral research, M.Sc. Thesis, Rhodes University, 1991.

Dore, I.S., Evans, G.P., Gledhill, J.A., and Haggard, R., Preliminary ionospheric and airglow results of project ISAAC, Mem. Nat. Inst. Polar Res., **38**, 146-153, 1985.

Dudeney, J.R. and Rodger, A.S., Spatial structure of high latitude sporadic E, J. Atmospheric Terrest. Phys., **47**, 529-535, 1985.

Eather, R.H. and O'Brien, B.J., Photometric observations in South America and their relation to trapped radiation, J. Atmospheric Terrest. Phys., **30**, 1585-1590, 1968.

Eather, R.H. and Reasoner, D.L., Spectrophotometry of faint light sources with a tilting-filter photometer, Appl. Opt., **8**, 227-241, 1969.

Forbush, S.E., Pizzella, G. and Venkateson, P., The morphology and temporaral variations of the Van Allen radiation belt, October 1959 to December 1960, J. Geophys. Res., **67**, 3651-3668, 1962.

Frank, L.A., Recent observations of low-energy charged particles in the earth's magnetosphere, Physics of the Magnetosphere, Carovillano, R.L. (Ed), Reidel, Dordrecht, Holland, 271-289, 1968.

Ghielmetti, H.S., Becerra, N., Godel, N.M., Heredia, H. and Roederer, J.G., Enhancement of the X-ray intensity at balloon altitudes in the South American Anomaly, Phys. Res. Lett., **12**, 388-390, 1964.

Ginzburg, V.L., Kurnosova, L.V., Logachev, V.I., Razorenov, L.A., Sirotkin, I.A. and Fradkin, M.I., Investigation of charged particle intensity during the flights of the second and third space ships, Planet. Space Sci., **9**, 845-854, 1962.

Gledhill, J.A., Aeronomic effects of the South Atlantic Anomaly, Rev. Geophys. Space Phys. **14**, 173-187, 1976.

Gledhill, J.A., Electron precipitation during the magetospheric substorm on 27 July 1979, S. Afr. J. Phys., 7, 33-38, 1984.

Gledhill, J.A., The effective recombination coefficient of electrons in the ionosphere between 50 and 150 km, Radio Sci., 21, 399-408, 1986.

Gledhill, J.A., Dore, I.S., Goertz, C.K., Haggard, R., Hughes, W.J., Scourfield, M.W.J., Smits, D.P., Stoker, P.H., Sutcliffe, P.R., Wakerley, P.A. and Walker, A.D.M., A magnetospheric substorm observed at Sanae, Antarctica, J. Geophys. Res., 92, 2461-2475, 1987.

Gledhill, J.A., and Hoffman R.A., Nighttime observations of 0.2- to 26-keV Electrons in the South Atlantic Anomaly made by Atmosphere Explorer C, J. Geophys. Res., 86, 6739-6744, 1981.

Gledhill, J.A. and Torr, D.G., Ionospheric effects of precipitated electrons in the South Radiation Anomaly, Space Res., VI, 222-229, 1966.

Gledhill, J.A., Torr, D.G. and Torr, M.R., Ionospheric disturbance and electron precipitation from the outer radiation belt, J. Geophys. Res., 72, 209-214, 1966.

Gledhill, J.A. and van Rooyen, H.O., The South Atlantic geomagnetic anomaly and the radiation belts, Proc. 5th Intern. Symp. Space Technol. Sci., Tokyo, 1003-1010, 1963.

Gough, M.P., Particle precipitation in the South Atlantic Anomaly deduced from VLF propagation path measurements, J. Atmospheric Terrest. Phys., 37, 1379-1383, 1975.

Greenspan, J.A. and Stone, C.A., The longitudinal variation of night airglow intensity in the region of the South Atlantic magnetic anomaly, J. Geophys. Res., 69, 465-469, 1964.

Haggard, R., The E-layer ionization over SANAE during the substorm of 27 July 1979, S.Afr. J. Phys., 7, 28-32, 1984.

Haggard, R. and Gledhill, J.A., Observations of the ionosphere over the South Atlantic Ocean, S.Afr. J. Antarct. Res., 6, 14-18, 1976.

Haggard, R. and Gledhill, J.A., Evidence for ionization of the E- region of the ionosphere by electron precipitation at Gough Island, in the South Atlantic Anomaly,J. Atmospheric Terrest. Phys., 47, 581-585, 1985.

Hedin, A.E., The atmospheric model in the region 90 to 2000 km, Adv. Space Res., 8, 9-25, 1988.

Hedin, A.E., Solah, J.E., Evans, J.V., Reber, C.A., Newton, G.P., Spencer, N.W., Kayser, D.C., Alcayde, S., Bauer, P., Cogger, L. and McClure, J.P., A global thermospheric model based on mass spectrometer and incoherent scatter data, MSIS 1, N_2 density and temperature, J. Geophys. Res., 82, 2139-2147, 1977.

Hoffman, J.H., Hanson, W.B. and Lippincott, C.R., The magnetic ion-mass spectrometer on Atmosphere Explorer, Radio Sci., 8, 315-322, 1973.

Hoffman, R.A., Burch, J.L. and Janetske, R.W., AE-LEE measurements at low and mid-latitude, Proceedings of the Workshop of electron contamination in X-ray Astronomy Experiments, (Ed.,

Holt, S.S.), Goddard Space Flight Center Report X-661-74-130, 1974.

Hoffman, R.A., Burch, J.L., Janetzke, R.W., Mc Chesney, J.F., Way, S.H. and Evans, D.S., Low-energy electron experiment for Atmosphere Explorer-C and -D, Radio Sci., 8, 393-400, 1973.

Holmes, J.C., Johnson, C.Y. and Young, J.M., Ionospheric Chemistry, Space Res., 5, 756-766, 1965.

Holt, S.S., Proceedings of the workshop on electron contamination in X-ray astronomy experiments, Doc. X-661-74-130, Goddard Space Flight Center, 1974.

Imhof, W.L. and Smith, R.V., Longitudinal variations of high-energy electrons at low altitudes, J. Geophys. Res., **70**, 569-577, 1965.

Kane, R.P., Particle precipitation in the ionospheric F2 region at locations in the vicinity of the South Atlantic magnetic anomaly, Ann. Geophys., **38**, 841-848, 1982.

Kasting, J.F. and Hays, R.B., A comparison between N_2^+ 4278 Å emission and electron flux in the auroral zone., J. Geophys. Res., **82**, 3319-3323, 1977.

Kaufmann, P., Rizzo Piazza, L., Massambani, O., Diniz Borges, V.N. and Koppe, E.H., Longitudinal dependence of ionospheric total electron content in the South Atlantic Geomagnetic Anomaly, Nature, **261**, 677-679, 1976.

Kelley, M.C., Swartz, W.E., Tayon, Y. and Tobert, R., On the relationship between the plasma density profile measured in the equatorial E- and F-regions and simultaneous energetic particle and spread-F observations, J. Atmospheric Terrest. Phys., **39**, 1263-1268, 1977.

King, J.W., Smith, P.A., Eccles, D., Fooks, G.F. and Helm, H., Preliminary investigation of the structure of the upper atmosphere as observed by the topside sounder satellite, Alouette, Proc. Roy. Soc., **A281**, 464-487, 1964.

Knudsen, W.C., Geographic distribution of F-region electrons with about 10eV energy, J. Geophys. Res., **73**, 841-856, 1968.

Knudsen, W.C. and Sharp, G.W., F2-region electron concentration enhancements from inner radiation belt particles, J. Geophys. Res., **73**, 6275-6283, 1968.

Kurnosova, L.V., Flux of charged particles at heights 200-300 km above the earth, Trud. Ordera. Lenin. Fiz. Inst. Im. P.N. Lebedeva, **88**, 143-171, 1976.

Maeda, K., Diffusion of low energy auroral electrons in the atmosphere, J. Atmospheric Terrest. Phys., **27**, 259-275, 1965.

Markham, T. and Anctil, C., Airborne night airglow measurements in the South Atlantic magnetic anomaly, J. Geophys. Res., **71**, 997-999, 1966.

Martin, I.M., Rai, D.B., Da Costa, J.M., Palmeira, R. and Trivedi, N.B., Enhanced electron precipitation in the Brazilian magnetic anomaly in association with sudden commencements, Nature, **240**, 84-86, 1972.

Massambani, O., The east-west asymmetry of the ionospheric electron context in the South Atlantic

geomagnetic anomaly region, J. Atmospheric Terrest. Phys., 40, 1143-1146, 1978.

McIlwain, C.E., Co-ordinates for mapping the distribution of magnetically trapped particles, J. Geophys. Res., 66, 3681-3691, 1961.

Mendes, A.M., Ananthakrishnan, S. and Paes de Barros, M.H., Phase and amplitude changes of VLF signals associated with PCA events, with reference to the South Atlantic geomagnetic anomaly, Ann. Geophys., 26, 483-492, 1970.

Meyer, S.L., Data Analysis for Scientists and Engineers, John Wiley and Sons, New York, 1975.

Muggleton, L.M., A describing function of the diurnal variation of $N_m(E)$ for solar zenith angles from 0° to 90°, J. Atmospheric Terrest. Phys., 34, 1379-1384, 1972.

Muzzio, J.L.R., Raminez Pardo, P. and de Mendonca, F., Measurements of the earth's total magnetic field at heights of 1000 km in the Brazilian Anomaly, Space Res., VI, 217-221, 1966.

Northrop, T.G., The adiabatic motion of charged particles, Interscience, New York, 1963.

O'Brien, B.J., High-latitude geophysical studies with satellite Injun 3.3. Precipitation of electrons into the atmosphere, J. Geophys. Res., 69, 13-43, 1964.

Oya, H., Takahashi, T. and Morioka, A., Electron density distribution and particle precipitation in South Atlantic Anomaly: Report on gyro-plasma probe observation installed in Taiyo, J. Geomag. Geoelectr., 31, Suppl., S95-S112, 1979.

Oyama, K.I. and Schlegel, K., Anomalous electron temperatures above the South American magnetic field anomaly, Planet. Space. Sci., 32, 1513-1522, 1984.

Paulikas, G.A. Precipitation of particles at low and middle latitudes. Rev. Geophys., 13, 709-734, 1975.

Paulikas, G.A. and Freden, S.C., Precipitation of energetic electrons into the atmosphere, J. Geophys. Res., 69, 1239-1249, 1964.

Prange, R., Energetic (keV) ions of ionospheric origin in the magnetosphere, A review, Ann. Geophys., 34, 187-214, 1978.

Prange, R. and Crifo, J-F., Suprathermal particle observations in the nighttime ionosphere at low latitudes, Geophysics. Res. Lett., 4, 141-144, 1977.

Poole, A.W.V., Advanced Sounding 1, The FMCW alternative, Radio Sci., 20, 1609-1616, 1985.

Poole, A.W.V. and Evans, G.P., Advanced Sounding 2. First results from an advanced chirp ionosonde, Radio Sci., 20, 1617-1623, 1985.

Piggott, W.R., High Latitude Supplement to the URSI Handbook on Ionogram Interpretation and Reduction, WDC-A for STP, Boulder Colo., USA, 1975.

Piggott, W.R. and Rawer, K., URSI Handbook of Ionogram Interpretation and Reduction, WDC-A for STP, Boulder Colo., USA, 1972.

Raitt, W.J., Laflin, S. and Boyd, R.L.F., A synoptic view of ionic constitution above the F-layer

maximum, Space Res., 5, 629-634, 1965.

Rees, M.H., Auroral ionization and excitation by incident energetic electrons, Planet. Space Sci., 11, 1209-1218, 1963.

Rees, D. and Fuller-Rowell, T.J., The CIRA theoretical thermosphere model, Adv. Space Res., 8, 27-106, 1988.

Rishbeth, H., Thermospheric winds and the F-region: A review, J. Atmospheric Terrest. Phys., 34, 1-47, 1972.

Rishbeth, H. and Garriott, O.K., Introduction to Ionospheric Physics, Academic Press, NY and London, 1959.

Roederer, J.G., Welch, J.A. and Herod, J.V., Longitude dependence of geomagnetically trapped electrons, J. Geophys. Res., 72, 4431-4447, 1967.

Rothwell, P., Electron density distribution in the topside ionosphere at medium and high magnetic latitudes and during magnetic disturbances, Space Res., IV, 480-487, 1964.

Sandford, B.P., Aurora and airglow intensity variations with time and magnetic activity at southern high latitudes, J. Atmospheric Terrest. Phys., 26, 747-769, 1964.

Sharp, G.W., Imhof, W.C. and Johnson, R.G., Direct evidence for corpuscular radiation effects on the ionosphere in the Southern anomaly region, Space Res., VI, 203-216, 1966.

Spenner, K. and Plugge, R., Electron temperature model derived from AEROS-A, Space Res., 18, 241-244, 1978.

Stassinopoulos, E.G., World maps of constant B, L and flux contours, NASA, SP-3054, 1970.

Störmer, C., The polar aurora, Clarendon Press, Oxford, 1955.

Sugiura, M. and Chapman, S., Tables and figures related to the geomagnetic dipole field, Goddard Space Flight Center, NASA Report X612-66-546, 1966.

Sutcliffe, P.R., Hattingh, S.K.F. and Boshoff, H.F.V., Longitudinal effects on the eigenfrequencies of low-latitude Pc3 pulsations, J. Geophys. Res., 92, 2535-2543, 1987.

Svennesson, J. and Westerlund, S., Stellar X-ray effects on VLF radio wave propagation, J. Atmospheric Terrest. Phys., 41, 361-365, 1979.

Torr, D.G. and Torr, M.R., Ionospheric effects caused by electrons from the outer radiation belt, Nature, 216, 1193-1194, 1967.

Torr, D.G., Torr, M.R., Hoffman, R.A. and Walker, J.C.G., Global Characteristics of 0.2 to 26 keV Charged Particles at F region Altitudes, Geophys. Res. Lett., 3, 305-308, 1976.

Torr, D.G., Torr, M.R., Walker, J.C.G. and Hoffman, R.A., Particle precipitation in the South Atlantic Geomagnetic Anomaly, Planet. Space Sci., 23, 15-26, 1975.

Torr, M.R. and Torr, D.G., Energetic oxygen in a mid-latitude aurora, J. Geophys. Res., 89, 5547-5553, 1984.

Trivedi, N.B., Rai, D.B., Martin, I.M. and Da Costa, J.M., Particle precipitation in Brazilian geomagnetic anomaly during magnetic storms, Planet. Space. Sci., **21**, 1699-1704, 1973.

Vampola, A.C. and Gorney, D.J., Electron energy deposition in the middle atmosphere, J. Geophys. Res., **88**, 6267-6274, 1983.

Van Allen, J.A., Ludwig, G.H., Ray, E.C. and McIlwain, C.E., Observation of high intensity radiation by Satellites 1958 α and γ, Jet propulsion, **28**, 588-592, 1958.

Van Allen, J.A., McIlwain, C.E. and Ludwig, G.H., Radiation observations with Satellite 1958ϵ, J. Geophys. Res., **64**, 271-286, 1959.

Van der Walt, A.J., Stoker, P.H., Maree, J.P., Zeeman, P.B. and Hamm, F.M., Airglow and enhanced penetrating electromagnetic radiation in the southern radiation anomaly, Space Res., **VI**, 189-202, 1966.

Vernov, S.N., Gorchakov, E.V., Shavrin, P.I. and Sharvina, K.N., Radiation belts in the region of the South Atlantic Magnetic Anomaly, Space Sci. Rev., **7**, 490-533, 1967.

Voss, H.D. and Smith, L.G., Energetic particles and ionization in the nighttime middle and low latitude ionosphere, Aeronomy Rep., **78**, Univ. Ill. Urbana., 1977.

Voss, H.D., and Smith, L.G., Global zone of energetic particle precipitation, J. Atmospheric Terrest. Phys., **42**, 227-239, 1980.

Westerlund, S., Reder, F.H. and Åbom, C., Effects of polar cap absorption events on VLF transmissions, Planet, Space Sci., **17**, 1329-1374, 1969.

Wilkes, M.V., A table of Chapman's grazing incidence Integral Ch(x, χ), Proc. Phys. Soc., **67B**, 304-308, 1954.

Williams, D.J. and Kohl, J.W., Loss and replenishment of electrons at middle latitudes and high B values, J. Geophys. Res., **70**, 4139-4150, 1965.

Willmore, A.P., Ionospheric heating in the F-region, Proc. Roy. Soc., **A281**, 140-149, 1964.

Willmore, A.P., Geographical and solar activity variations in the electron temperatures of the upper F-region, Proc. Roy. Soc., **A286**, 537-558, 1965.

Willmore, A.P., and Henderson, C.L., Magnetic shell enhancements during magnetic disturbances, Space Res., **V**, 241-249, 1965.

Wulff, A. and Gledhill, J.A., Atmospheric ionization by precipitated electrons, J. Atmospheric Terrest. Phys., **36**, 79-91, 1974.

Zmuda, A.J., Ionization enhancement from van Allen electrons in the South Atlantic magnetic anomaly, J. Geophys. Res., **71**, 1911-1917, 1966.